BNL - 52624
Formal Report

Proceeding of Workshop on Photo-injector for Energy Recovery Linac

X.J. Wang
National Synchrotron Light Source
Brookhaven National Laboratory
Upton, New York 11973

January 2002

National Synchrotron Light Source

Brookhaven National Laboratory
Operated by
Brookhaven Science Associates
Upton, NY 11973

Under Contract with the United States Department of Energy
Contract Number DE-AC02-98CH10886

DISCLAIMER

This report was prepared as an account of work sponsored by an agency of the United States Government. Neither the United States Government nor any agency thereof, nor any of their employees, nor any of their contractors, subcontractors or their employees, makes any warranty, express or implied, or assumes any legal liability or responsibility for the accuracy, completeness, or any third party's use or the results of such use of any information, apparatus, product, or process disclosed, or represents that its use would not infringe privately owned rights. Reference herein to any specific commercial product, process, or service by trade name, trademark, manufacturer, or otherwise, does not necessary constitute or imply its endorsement, recommendation, or favoring by the United States Government or any agency thereof or its contractors or subcontractors. The views and opinions of authors expresses herein do not necessarily state to reflect those of the United States Government or any agency thereof.

National Synchrotron Light Source

Proceeding of Workshop on Photo-injector For Energy Recovery Linac

January 22 – 23, 2001

Edited by X.J. Wang

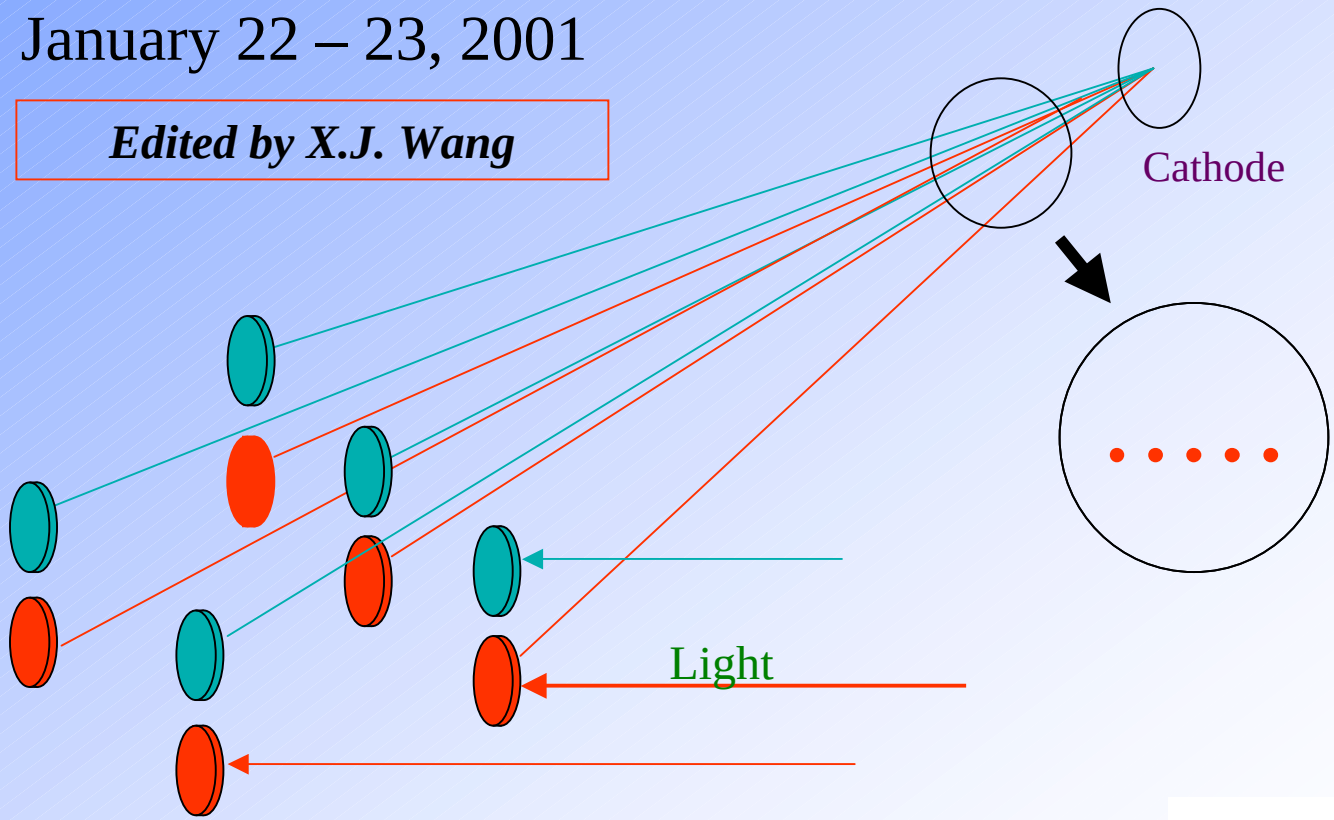

Brookhaven Science Associates
U.S. Department of Energy

BROOKHAVEN NATIONAL LABORATORY

Almost 50 people attended the workshop, it is the first time a workshop covered all major aspects of photoinjector, from DC to RF.

Introduction

Workshop on Photo-injectors for Energy Recovery Linac was held at National Synchrotron Light Source (NSLS) of Brookhaven National Laboratory (BNL) on January 22 and 23, 2001. Fifty people attended the workshop; they came from three countries, representing universities, industries and national laboratories.

This is the first workshop ever held on photo-injectors for CW operation, and for the first time, both DC and RF photo-injectors were discussed at the workshop. Workshop covered almost all major issues of photo-injectors, photocathode, laser system, vacuum, DC, 433 MHz/B-factory cavities based RF gun, 1.3 GHz RF gun and beam instrumentation. High quantum efficiency and long live time photocathode is the issue discussed during the workshop. Four working group leaders have done great jobs summarizing the workshop discussion, and identifying the major issues for future R&D.

The support provided by BNL and NSLS made it possible for this workshop. Service and help from A. Bowden, K. Loverro and E. Morello made this workshop successful. I would like to express my gratitude to Drs J. Marburger, R. Osgood and S. Krinsky for their support. The workshop attendee and all my BNL colleague, who made this workshop productive, thank you.

X.J. Wang

Workshop Chairman

Workshop On Photo-injector For Energy Recovery Linac

Monday, January 22, 2001 NSLS Seminar Room
8:00 – 8:30 Continental breakfast
Chair ***J.B.Murphy/BNL***
8:30 – 8:40 AM: Welcome ***S. Krinsky / BNL***
8:40 – 9:00 AM: Overview of PERL ***I. Ben-Zvi / BNL***
9:00 – 9:20 AM: Workshop Charge ***W. Graves/BNL***
9:20 – 9:40 AM: Beam Dynamics issues in Energy Recovery Linac
V. Yakimenko / BNL
9:40-10:00 AM: Coffee Break
Chair ***K.J. Kim/APS***
10:00 – 10:45 AM: Issues in Low Emittance, High Average Current DC Photoemission Guns ***C. Sinclair / JLAB***
10:45-11:30 AM: Laser Systems for DC and RF guns ***T. Rao / BNL***
11:45-12:15 Recent results of the high-current Advanced FEL photoinjector operating with surface-passivated cesium telluride photocathodes
Dinh Nguyen /LANL
12:15 – 1:15 PM: Working lunch provided by NSLS

Afternoon Session NSLS Seminar Room
Chair ***D. Robin /ALS***
1:15 PM – 2:00PM: Boeing High Duty Photocathode RF Gun Experiments
D. Dowell / Boeing
2:00 – 2:15: The new L-band 1 1/2 cell photocathode RF gun at Argonne
Manoel Conde / ANL
2:15- 2:30: Ultra-stable Laser system for Photocathode RF gun Applications
Katsuyuki Kobayashi / SHI
2:30 – 2:45 A regenerative electron source for a high average current energy recovery linacs ***Alexander Zholents /LBNL***
2:45- 3:05: Working groups Organization Babzien, Sinclair, Dowell, Gai

3:05-3:20 Coffee Break

3:20 – 6:00 Working group presentation and discussion
1. Laser system for PERL (NSLS Conference room A) Chair: M. Babzien /BNL
   A. Femto-second and Picosecond lasers for accelerator applications
   Katsuyuki Kobayashi / SHI

2. DC Gun working group (NSLS Chairman's office) Chair: C. Sinclair / JLAB
   A. DC Photoinjector for PERL T. Shaftan and F. Zhou/ BNL

3. 433 Hz RF gun working group (NSLS Conference room B) Chair: D. Dowell / Boeing
   A. 433 MHz Cavity based photocathode RF Gun Injector for PERL
   D. Dowell/Boeing
   B. Possible use of PEP-II cavity technology for a photocathode RF gun

R. Rimmer of LBNL

4. L-band RF gun working group (NSLS Seminar Room) Chair: W. Gai /ANL

A. Results of the Fermilab High-Brightness Photo-Injecto Jean-Paul Carneiro of Fermilab

B. TESLA X-Ray FEL and TTF Injector P. Piot /DESY

C. L-band LN_2 Cooled Photoinjector for PERL X.Y.Chang/BNL

D. Beam Dynamics Issues at PERL Injector X.J. Wang/BNL

6:30 PM ***Working Dinner (Berkner Hall Room A.) Courtesy of BNL director office***

Tuesday, January 23, 2001

8:00 AM-8:30 AM Continental Breakfast at NSLS Seminar room

8:30 AM – 9:30 AM: NSLS Seminar room Chair: H. Edward/FNAL

1. 8:30 – 8:50 Beam instrumentation Consideration for PERL Injector X.J. Wang

2. 8:50 – 9:00 Energy Compression Optimization at JLab IR-DEMO Recirc. FEL P. Piot /DESY

2. 8: 50 – 9:30 Discussion on beam instrumentation and PERL injector configuration

9:30 – 9:45 Coffee Break

9:45 – 12:15 Working group discussions and Report Preparation

12:15 – 1:30 PM Lunch

1:30 – 3:30 PM Working group report and Discussion at NSLS Seminar Room
Chair: M. Cornacchia / SSRL

1. Laser system for PERL M. Babzien

2. DC Gun option for PERL C. Sinclair

3. 433 MHz /B-factory cavity based RF gun D. Dowell

4. L-band RF gun for PERL W. Gai

4:00 PM Adjourn

Photoinjected Energy Recovery Linac R&D at Brookhaven National Laboratory

- PERL - Promising technology: High-brightness, high-power electron beams.
- Three PERL projects at BNL:
  - Electron cooler for RHIC
  - Electron Ion Collider (eRHIC)
  - PERL based light source
- Work started nearly two years ago on eRHIC
- Workshop on NSLS upgrade, October 23, 2000.
- Essential element: The photoinjector

Electron Cooling of Ions

Electron cooling is established at low energy, but:

- High-energy - New technology
- Operation in a collider
- Bunched beam

Invented by G.I. Budker (INP, Novosibirsk) 1966

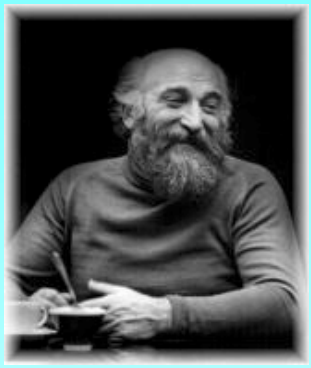

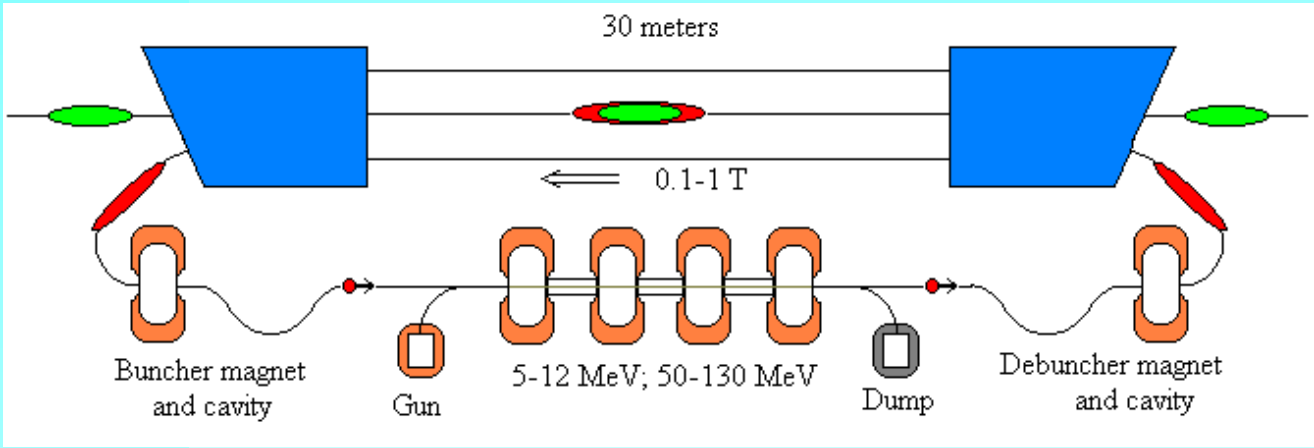

Electron cooling will provide a factor of 10 increase in the integrated luminosity of RHIC, as well as better accumulation of rare species.

eRHIC – a Polarized Electron on Ion or Polarized Proton in RHIC

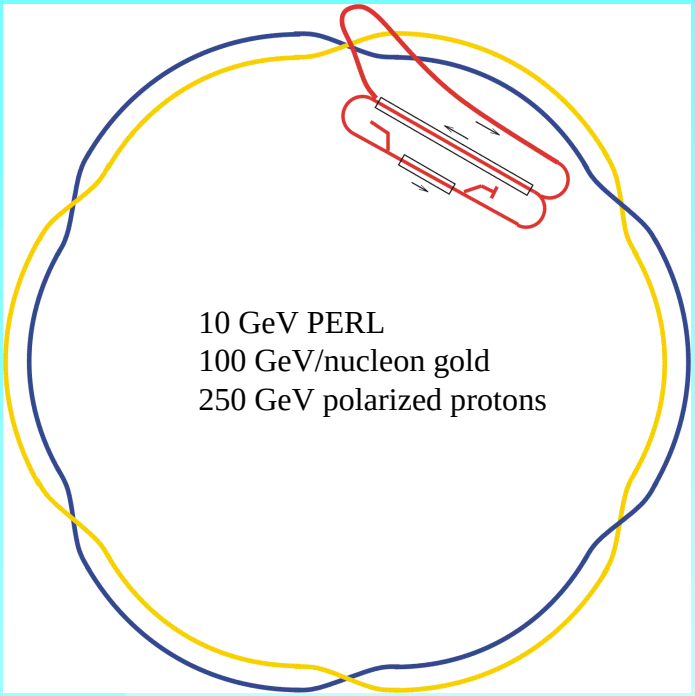

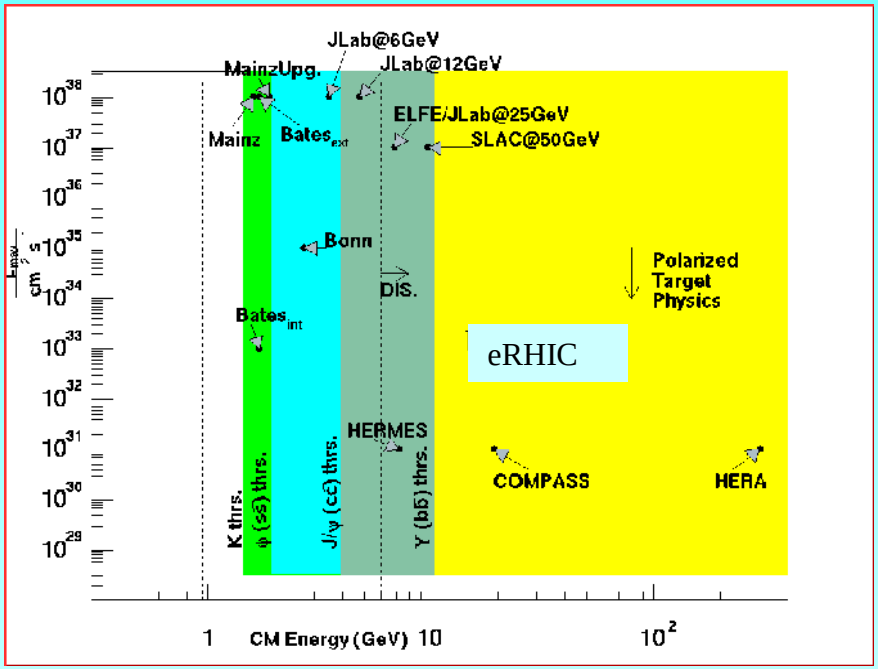

The Electron-Ion Collider is proposed as an essential tool for research into the fundamental structure of matter:

- What is the *structure* of hadrons in terms of their quark and gluon constituents?
- How do quarks and gluons *evolve* into hadrons via the dynamics of confinement?
- How do the quarks and gluons *reveal* themselves in the structure of atomic nuclei?

Ilan Ben-Zvi
PERL Photoinjector Workshop,
BNL, January 22-23, 2001

Brookhaven Science Associates

BROOKHAVEN NATIONAL LABORATORY

Synchrotron Radiation: Where are we going?

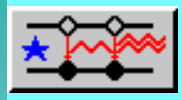

Laser revolutions:

- **High resolution spectroscopy**
- **Short pulse (dynamics)**

- X-rays due next!
- How do we do it?
  The answer may be linac based sources.

Large Ribosomal Subunit at 2.4 Å resolution, N. Ban et al. Science, 289, 905 (2000)

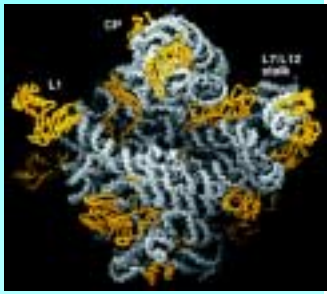

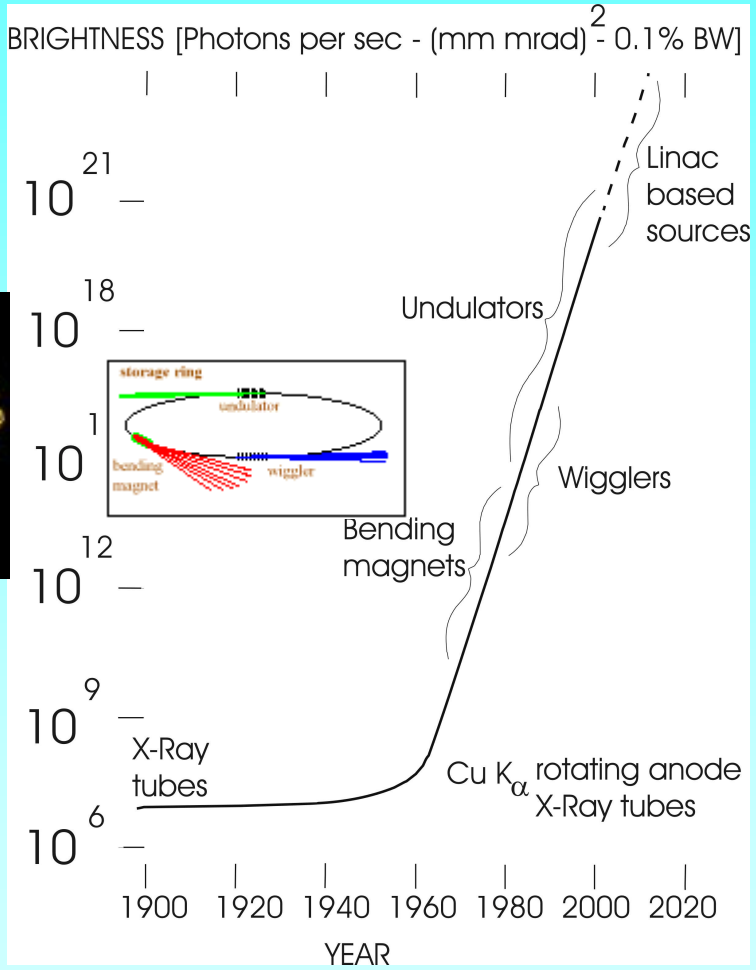

- Ultrafast Structural Dynamics
- Ultrafast Processes & Time-Dependent Measurements
- Ultrahigh Spatial Resolution
- Microscopy
- Coherent X-ray Scattering
- Ultrasmall Membrane Proteins

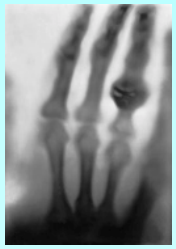

Electron beam brightness

$$B_{und} \cong \frac{2\times 10^{18}}{\varepsilon_x \varepsilon_y} \frac{N_W K^2}{1+K^2/2} \quad \varepsilon \text{ in mm-mrad}$$

- **In a storage ring emittance is the result of an equilibrium:**

$$\varepsilon_x = \left(7.7\times 10^{-4}\, nm - rad\right) \frac{\gamma^2}{N_{cell}^{\ 3}}$$

(Chasman-Green Lattice)

- **In a linac, no equilibrium: "Normalized Emittance" is a conserved quantity.**

$$\varepsilon_x = \frac{\varepsilon_n}{\gamma}$$

Short pulses, peak brightness:

Storage rings can not produce a very short pulse due to Touschek lifetime!

Ring	E [GeV]	σ_L [ps]
ALS	1.5	14
SLS	2.4	13
SOLEIL	2.5	12
DIAMOND	3	10
ESRF	6	16
LCLS (Linac)	15	0.28

Various linac tools:

- Photoinjector
  - Small emittance
  - High charge
- SRF linac
  - CW operation
  - Preserve emittance
- Energy recovery
  - High current
- Bunch compression
  - Short pulse

BNL gun IV

TESLA 1.3 GHz
Nb structure

JLAB high power
FEL PERL

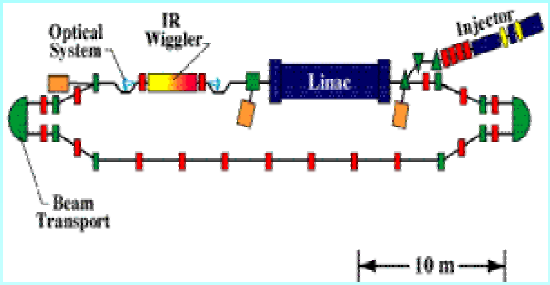

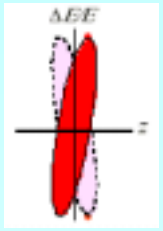

Linac Beam Parameters

Parameter	Units	Value
Energy, single pass	GeV	3
Average current	Amperes	0.2
Bunch repetition frequency	GHz	0.433 / 1.3
Bunch charge	nC	0.45 / 0.15
rms emittance: Normalized - Geometrical -	 μm Å	 1 / 0.5 1.7 / 0.8

PERL Brightness

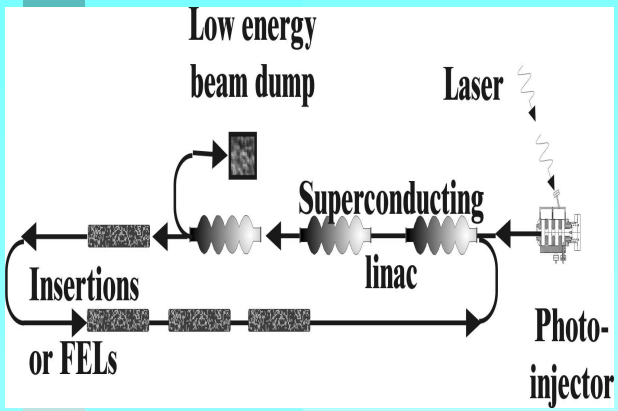

Even the spontaneous emission is outstanding!

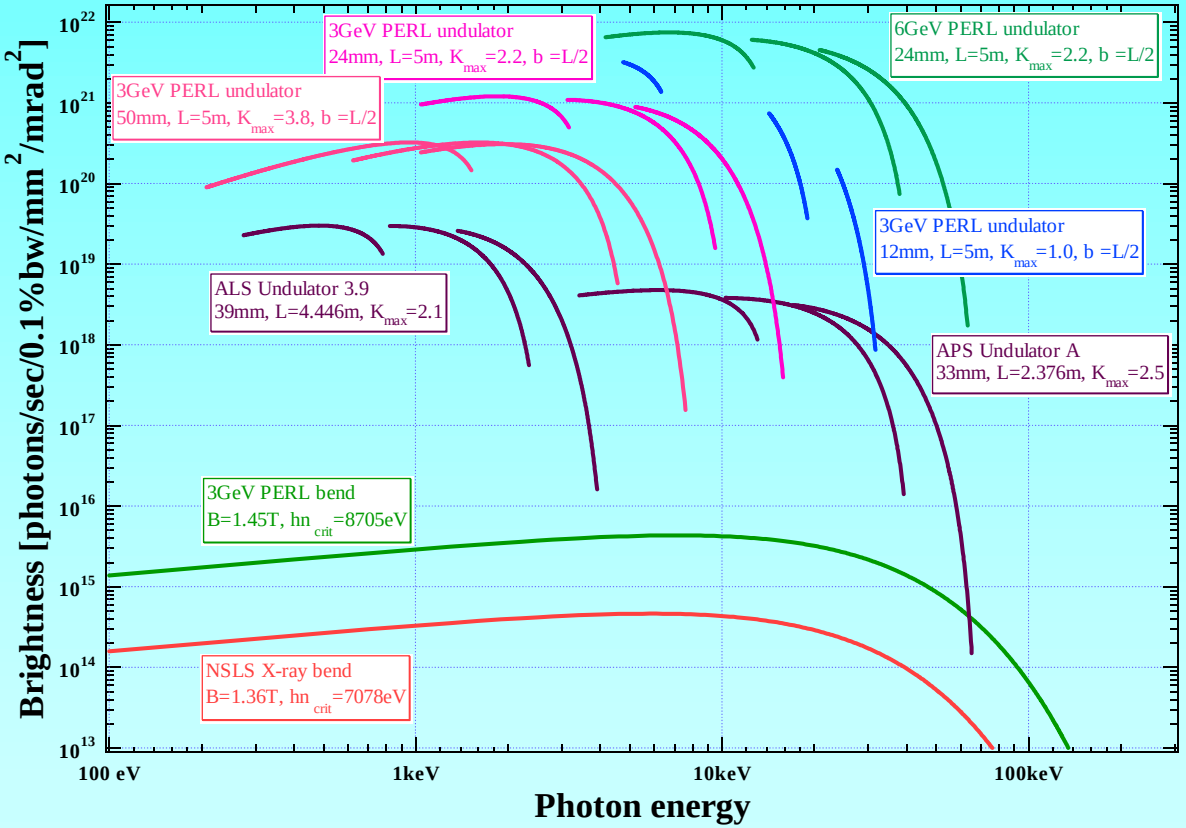

Ilan Ben-Zvi
PERL Photoinjector Workshop,
BNL, January 22-23, 2001

Layout of a Light-Source PERL

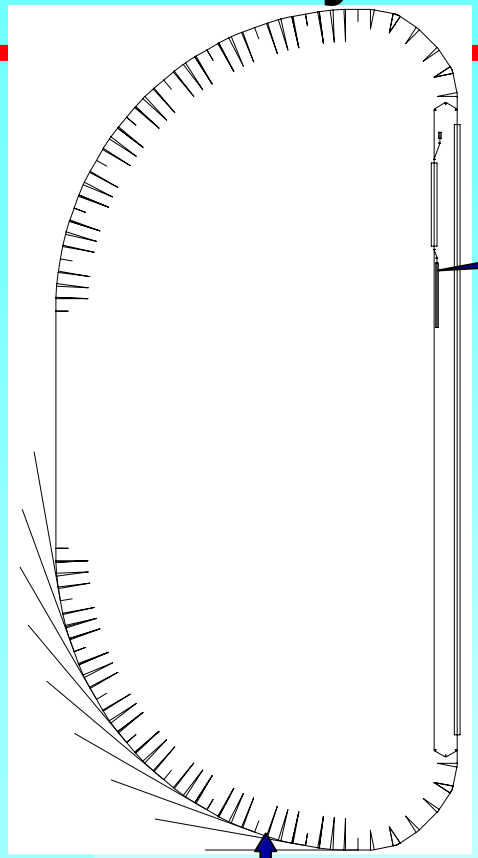

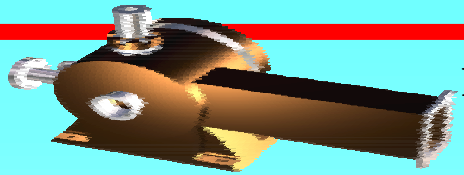

Photoinjector

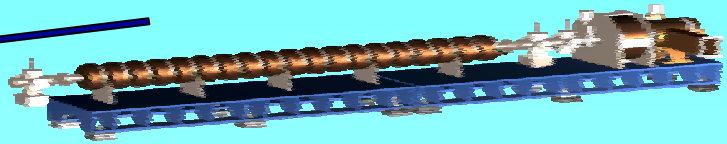

Injection linac

9-cell cavity

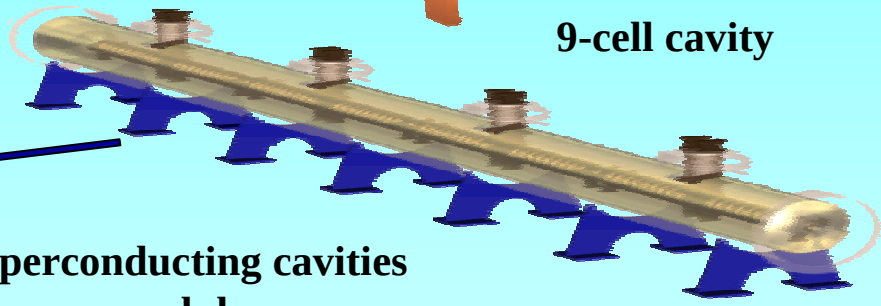

Superconducting cavities module

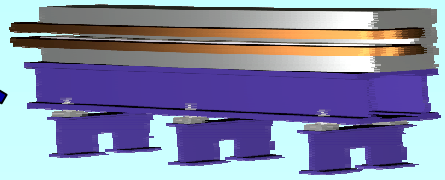

Dipole magnet

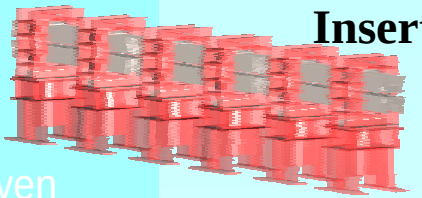

Insertion device

Ilan Ben-Zvi
PERL Photoinjector Workshop,
BNL, January 22-23, 2001

Promise of a PERL Light Source

- Diffraction-limited source to:
  - 10~20Å in BOTH planes, $\varepsilon_x\varepsilon_y$~ (1-3Å)^2 at 3-GeV.
  - 5~10Å in BOTH planes, $\varepsilon_x\varepsilon_y$~ (0.25-0.75Å)^2 at 6-GeV.
- Variable ε_x /ε_y emittance ratio, (at a constant product $\varepsilon_x\varepsilon_y$) allowing an extremely small vertical emittance (with larger horizontal emittance) on demand.
- Sub-picosecond in the range of 100 fs.
- Virtual 'top-off' yielding a constant heat load on chambers, optics - high long-term stability.
- Electro-optical control of the pulse-format through the laser (spacing, pseudo-random sequences of arbitrary length, variable charge, variable pulse length).

Performance Goals for the PERL Photoinjector

Presented by William S. Graves at
the PERL Photoinjector Workshop

NSLS/BNL

Jan. 22, 2001

Overview

- Workshop goals and key issues
- Desired parameters at injector end
- Laser system
- Cathode
- Gun: DC, 433 MHz, 1.3 GHz
- Booster accelerator to 25 MeV
- Beam diagnostics

Key Issues for PERL Injector

- Compare all approaches at 25 MeV final energy.
- Charge per bunch: 0.15 nC or 0.45 nC
- High rep rate: 1300 or 433 MHz
- Normalized RMS emittance: ~1 mm-mrad
- Longitudinal RMS emittance: 3 ps * 23.2 KeV @ 25 MeV
- Uptime: 24 hrs/day, 25 days/month, 11 months/year

Beam Parameters at end of Photoinjector

- Average current ~ 200 mA
- RMS Pulse length < 3 ps.
- Normalized RMS emittance ~ 1 mm-mrad
- Energy ~ 25 MeV
- Uncorrelated RMS energy spread < 23 keV at 25 MeV

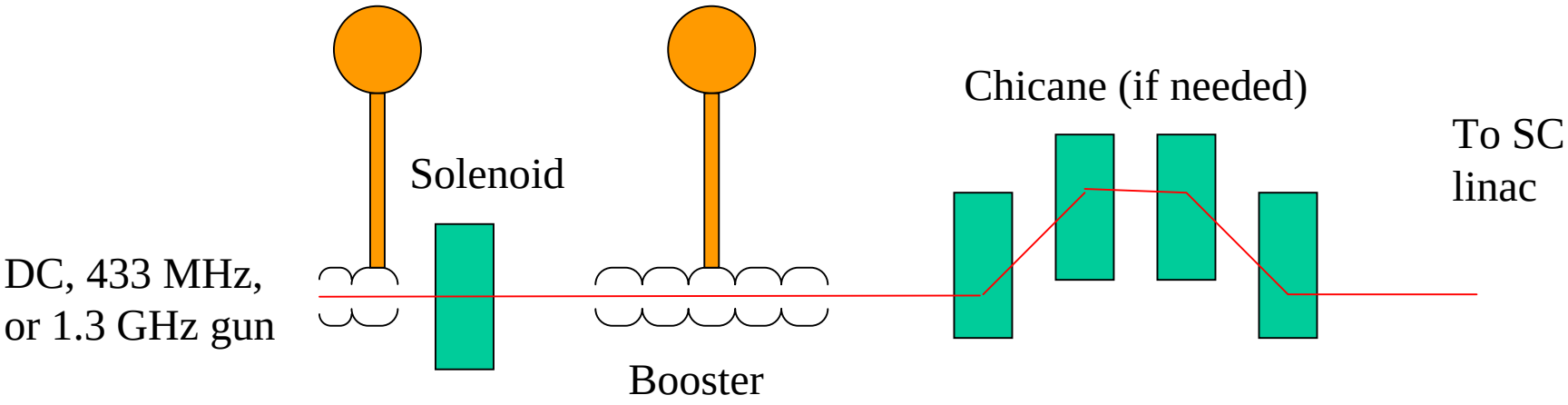

Laser System

Laser system and cathode are closely related and must be considered together.

Laser must operate at either 433 MHz or 1.3 GHz.

Laser

- Performance goals are:
  - Amplitude stability: 1.0e-3 peak-to-peak at 10 MHz
  - Pointing stability: 1.0e-3 RMS
  - Timing stability: 0.2 ps RMS at frequencies greater than 1 MHz
  - Uniformity: 5% peak-to-peak (including cathode emission)
- Show block diagram of system from oscillator through transport to cathode.
- Estimate power losses in transverse and longitudinal pulse shaping and mode cleanup.
- Average power required in IR, visible, UV. Show assumptions for losses and Q.E.
- Address heating and peak power effects.
- Identify measured results for existing components. Compare with requirements.
- Strategy for 24 hour uninterrupted operation.
- Identify major technical challenges to meet PERL requirements.

Cathode Material

Cathode

- Identify material.
- Plot quantum efficiency vs time for life of cathode.
- Strategy for 24 hour operation including redundancy/changeout requirements for planned and unplanned cathode replacement.
- Address reproducibility of performance: Q.E., uniformity, lifetime.
- Limitations in bunch length (prompt emission?) and average charge emitted.
- Cathode production and handling equipment required.
- Describe existing performance and enhancements needed.
- Identify major technical challenges.
- If considering cryogenic cooling, identify special requirements, e.g. load-lock mechanism, and cathode change procedure.

Gun Performance

RF System

- Average beam current required is 200 mA (0.45 nC at 433 MHz or 0.15 nC at 1.3 GHz).
- Address average power requirements: CW power source, thermal loading, acceleration.
- System must run 24 hours/day, 7 days/week.
- Phase and amplitude stability.
- State existing measured results for high average power operation.
- Limitations in average current (variable beam loading)?
- Identify major technical challenges.

Beam Dynamics

- Simulations should indicate optimized performance including effects of space-charge, RF, thermal emittance, and emittance correction. Indicate peak current, bunch length, energy, energy spread, emittance, charge. Note correlated and uncorrelated quantities.
- Show scaling of performance with charge per bunch.
- State self-consistent measured results for energy gain, emittance, bunch length, charge, average current, energy spread.
- Indicate performance tradeoffs used in optimization.
- Identify major technical challenges to achieving predicted performance.
- Provide phase space plots for each plane at final energy of 25 MeV.

Booster Accelerator Performance

RF System

- Average beam current required is 200 mA.
- Address average power requirements: CW power source, thermal loading, acceleration.
- Phase and amplitude stability.
- State existing measured results for high average power operation.
- Limitations in average current (variable beam loading)?
- Identify major technical challenges.

Beam Dynamics

- Simulations should indicate optimized performance including effects of space-charge, wakefields, CSR, and emittance correction. Indicate peak current, bunch length, energy, energy spread, emittance, charge. Note correlated and uncorrelated quantities.
- State self-consistent measured results for energy gain, emittance, bunch length, charge, average current, energy spread.
- Address bunch compression if necessary.
- State energy spread, emittance, charge, pulse length at final energy.
- Indicate performance tradeoffs used in optimization.
- Identify major technical challenges.
- Provide phase space plots for each plane at final energy of 25 MeV.

Electron Beam Diagnostics

For high average current beams, identify methods to measure:

- Vertical and horizontal emittance.
- Energy and energy spread.
- Bunch length.
- Charge.
- Peak and average current.
- Bunch-to-bunch timing jitter.

Identify feedback systems required for laser and RF.

Beam Dynamics Issues in Photoinjected Energy Recovery Linac

Vitaly Yakimenko
PERL Beam Dynamics & Optics Working Group

January 22, 2001

Beam Dynamics Issues

Key Question: Can we preserve the "bright" beam from the injector which must then pass through the compressors and the insertion devices before being returned to the linac for energy recovery?

Issues of Concern: Wakes, CSR, BBU, Errors, Stability …

Electron Beam Requirements for PERL

1. Transverse Normalized RMS Emittance:

   0.5-1 mm-mrad

2. Longitudinal Emittance (RMS σ_L x σ_E):

   3 ps x 0.09% at 25 MeV
   100 fs x 0.1% at 3 GeV

3. Average Current: 200 mA

$$\sigma_{RMS} = FWHM / 2.35$$

Average Current

$$\overline{I} = 200 \quad mA$$

Mode	Charge per bunch [nC]	Spacing [cm]
Each bucket of 1.3 GHz	0.15	23
Every 3rd bucket or 433MHz	0.45	70

7 orders magnitude higher repetition rate then for similar beam in LCLS at 120 Hz

Electron Bunch Length/Pulse Duration

Ring	E [GeV]	σ_L [ps]
ALS	1.5	14
SLS	2.4	13
SOLEIL	2.5	12
NSLS XRAY	2.8	158
DIAMOND	3	10
ESRF	6	16

- 3rd generations ring sources have σ_L ~12 ps.
- Goal of PERL to have σ_L ~100 fs!

Synchrotron Radiation

Incoherent Spontaneous Emission
in the 2π of dipoles (ρ=7m and 3GeV):

$$U_{[KeV]} = 88.5 \frac{E^4_{[GeV]}}{\rho_{[m]}}$$

$$U = 1\,MeV$$

Coherent enhancement of SR
(*J.B. Murphy et al. PA, 1997*)

$$k = \frac{3}{2} \frac{N_e}{\gamma^4} \cdot \left(\frac{\rho}{2\sigma_z} \right)^{\frac{4}{3}}$$

Charge [nC]	Bunch σ_L [ps]	Enhancement factor	SR Power [MW]
0.45	0.1	20	4.2
0.45	0.5	2.4	0.68
0.15	0.1	7	1.6
0.15	0.2	2.7	0.74

CSR

Problems: Emittance growth, Energy spread, Radiated power

Energy spread due to CSR (no shielding) Derbenev et. al. TESLA FEL 95-055

$$\Delta E \approx 0.22 \frac{N r_0 L_d mc^2}{(R\sigma_s^2)^{2/3}}$$

in the 2π of dipoles (0.15 nC, 100 fs bunches, ρ=7m and 3GeV):

$$\sigma_E \approx 1.3 \cdot 10^{-3}$$

We are using Elegant and TraFiC4 codes to calculate emittance growth due to CSR.

CSR shielding

CSR reduction by parallel plate shielding
(*J.B. Murphy et al. PA, 1997*)

$$gap \propto \left(\rho\sigma_z^2\right)^{1/3}$$

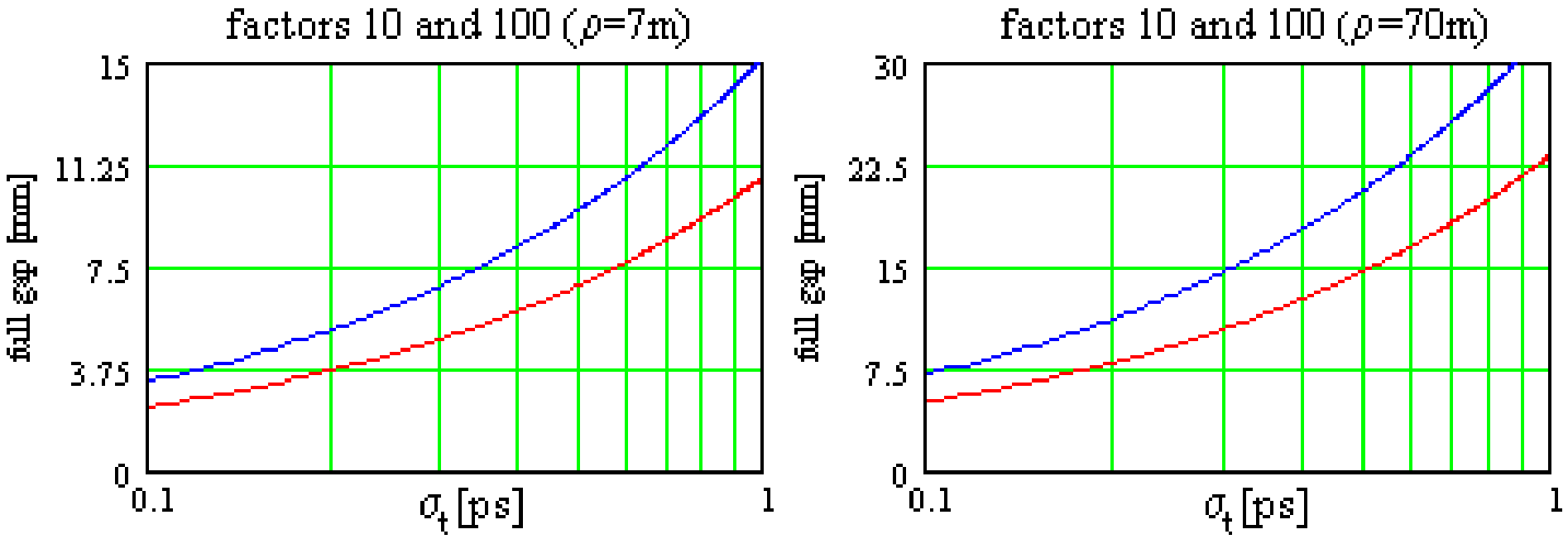

Shielding might be possible and is under study

Resistive Heating

Simple heating from resistive wall for small gap chambers

$$P_{[W/m]} = k_{loss} Q^2 f_L = k_{loss} I_{ave}^2 / f_L$$

High rep rate is preferable

$$k_{loss} = \frac{c}{\pi a} \frac{\Gamma\left(\frac{3}{4}\right)}{4} \sqrt{\frac{Z_0}{2\sigma\sigma_z^3}}$$

Charge per bunch [nC]	Bunch length σ_L [ps]	Full gap 2a [mm]	$P_{[kW/m]}$ for Cu	$P_{[kW/m]}$ for Al
0.45	0.1	5	3.6	5.4
0.15	0.1	5	1.2	1.8

Surface roughness, geometric wakes, etc. are under consideration.

Scaled Layout

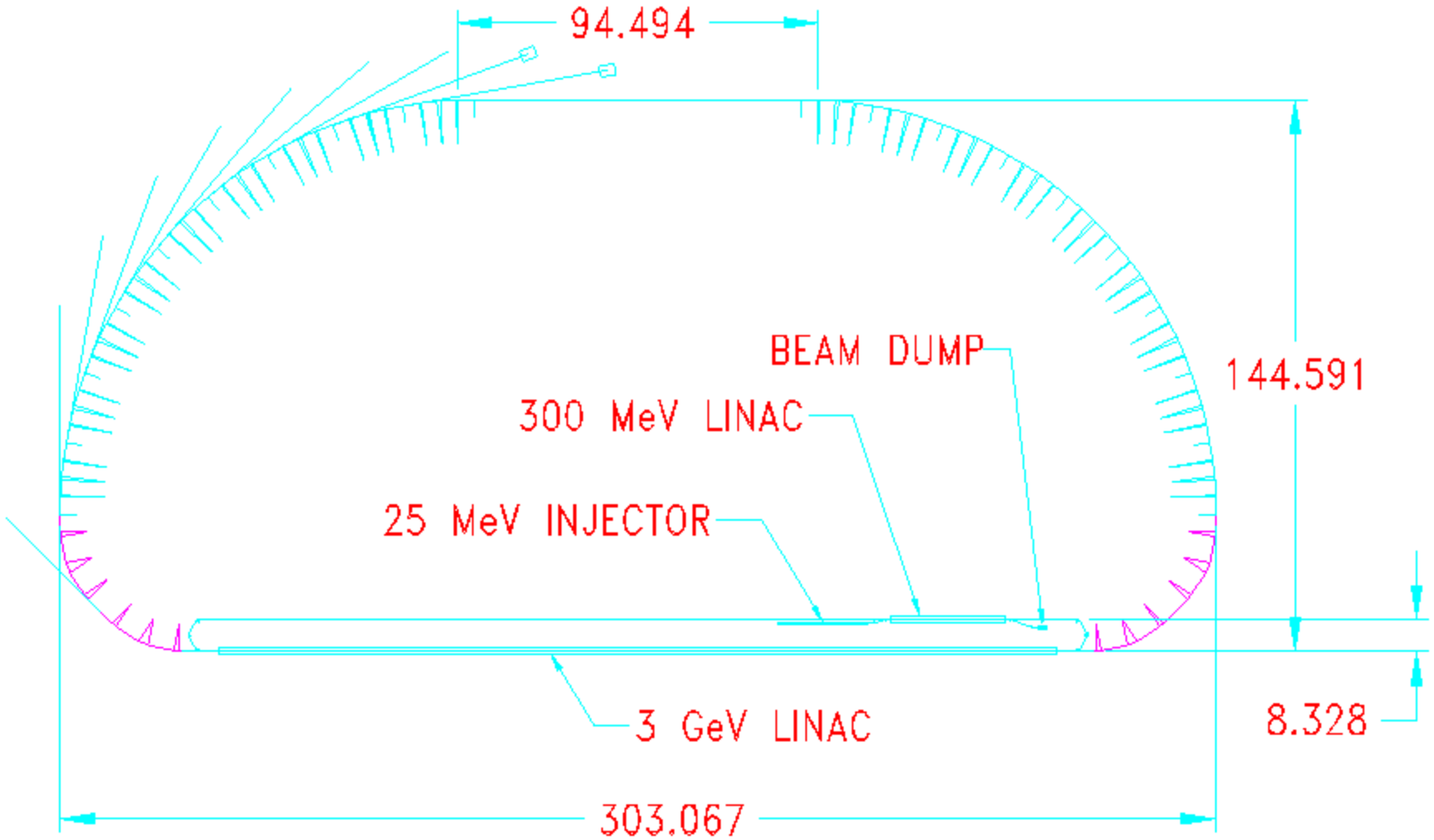

There are 24 straight sections for insertion devices

Basic Arc Cell Optics for Return Leg and Bunch Compression

Extended triple bend achromat optics offers ability to tune R_{56} by changing dispersion in the middle dipole

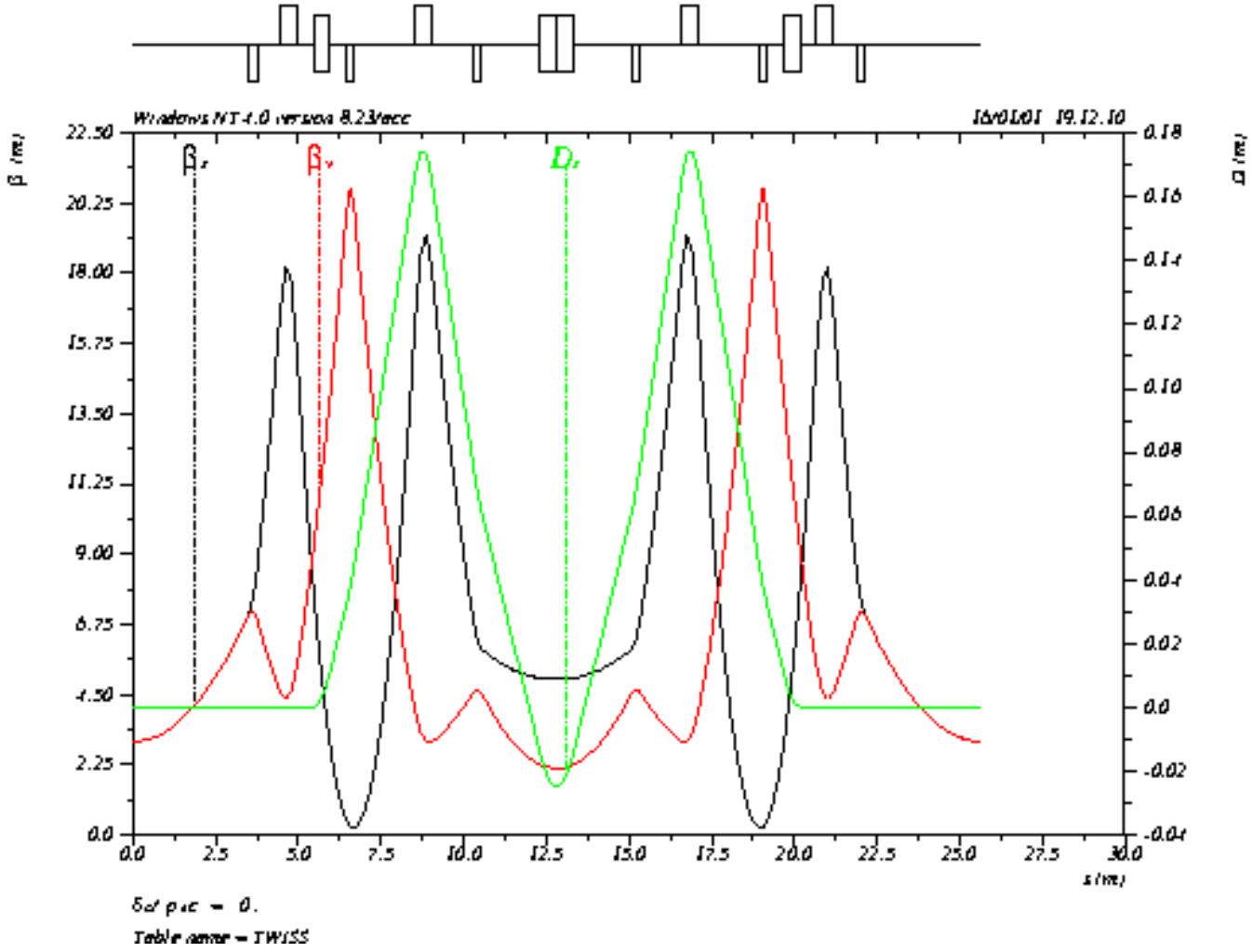

Schematic Layout

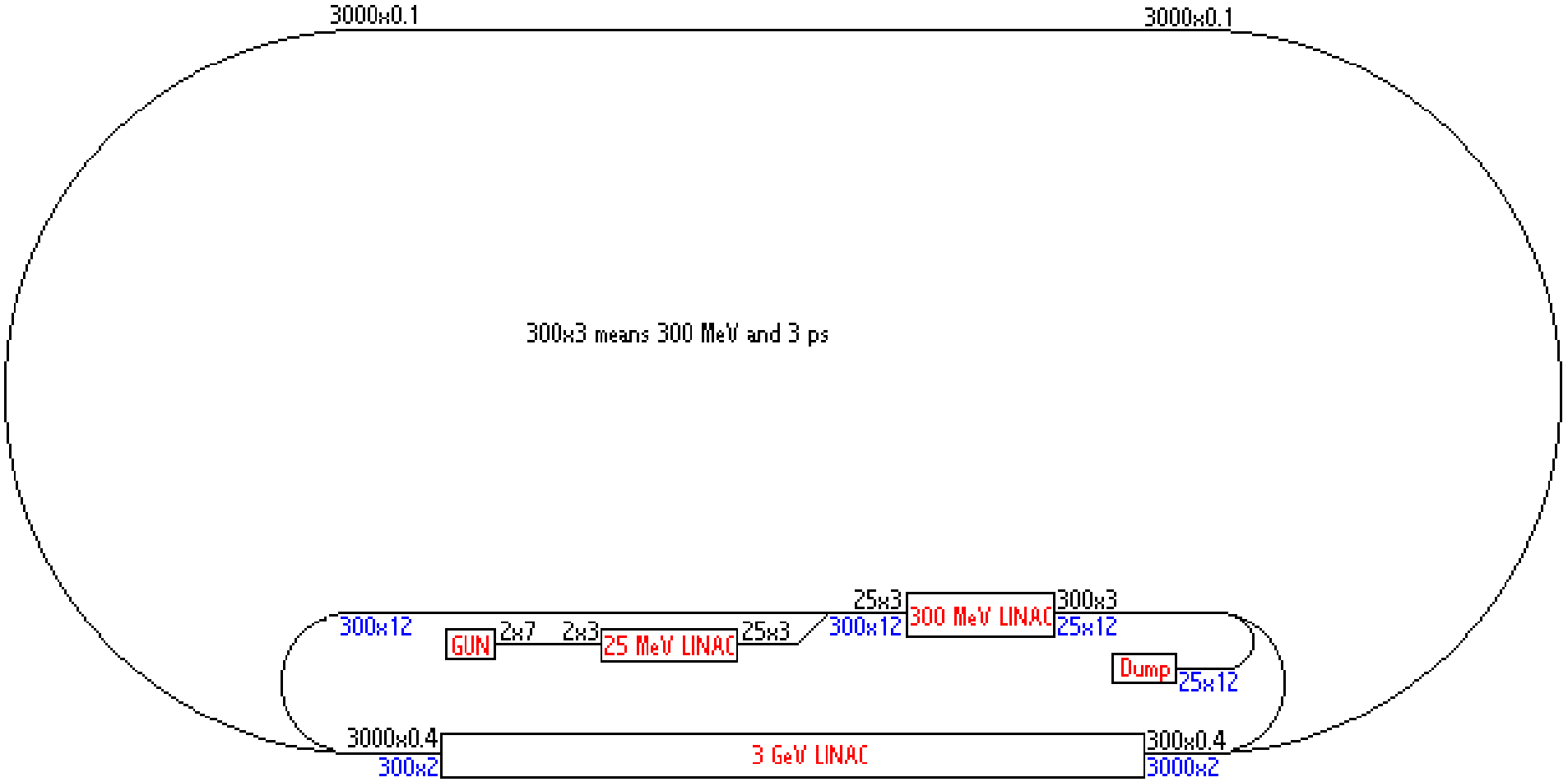

Longitudinal Phase-Space

ID line width: $\frac{\Delta\lambda}{\lambda} = \frac{1}{nN_p} \oplus 2\frac{\Delta E}{E}$

$$F(s,\delta) \propto \exp\left(-\frac{1}{2(1-r^2)}\left[\frac{s^2}{\sigma_L^2} - \frac{2r\,s\,\delta}{\sigma_L\sigma_\delta} + \frac{\delta^2}{\sigma_\delta^2}\right]\right)$$

requires $\frac{\Delta E}{E} < 10^{-3}$

$$\sigma_u = \sqrt{1-r^2}\,\sigma_\delta \qquad \sigma_c = r\sigma_\delta$$

	Beam energy [MeV]	Bunch length σ_t[ps]	Uncorrelated energy spread σ_u[%]	Correlated energy spread σ_c [%]	R[5,6] [cm]
Gun	2	7	0.500	-1.054	
Ballistic compr. (1.6m dri	2	3	1.167	0.000	-16.3
Low energy linac	25	3	0.093	0.000	
Small ER LINAC	300	3	0.008	0.778	
Small arc compressor	300	0.4	0.058	0.776	12.9
Large ER LINAC	3000	0.4	0.006	0.078	
Arc-compressor	3000	0.1	0.023	0.074	15.4
X-ray compressor	3000	0.03	0.078	0.000	3.7

We need to budget for some degradation of the longitudinal emittance due to compression and RF curvature effect (**no degradation in the table**)

HGHG-based X-ray Device

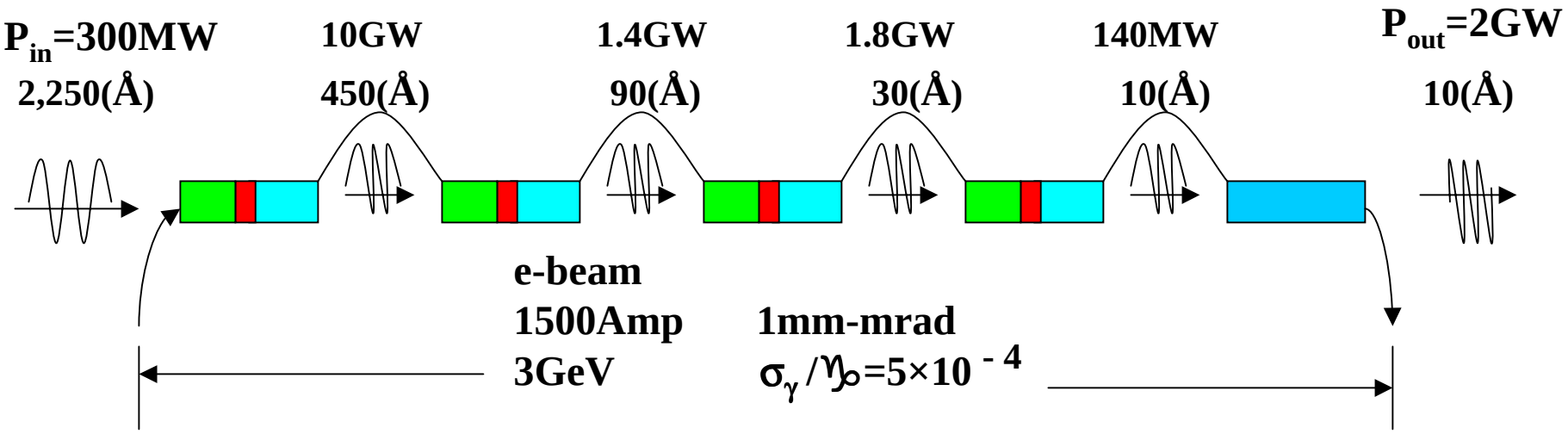

I_{pk} (Amp)	ε_n(mm-mrad)	L_W (m)	λ_{final} (Å)	P_{out} (GW)
1500	1	46	10	2
750	1	49	18	1
2500	2	35	18	4
2500	2	45	10	1

J.H. Wu & L.H. Yu

FEL mode

1. Larger charge is preferable for FEL

2. FEL operate at low repletion rate (reduces problem with average heat)

3. Possibly, FEL bunches would be produced by separate gun at low repetition rate.

Conclusions

1. The ability to produce and preserve short electron bunches, $\sigma_L < 1$ ps & $\sigma_E < 10^{-3}$, is a cornerstone of the PERL project.

2. Most of the potential problems are due to coherent effects, as a result lower charge per bunch and a higher repetition rate is preferable.

3. Work is in progress to assess the impact of all the beam dynamic effects on the performance of PERL.

ISSUES IN LOW EMITTANCE, HIGH AVERAGE CURRENT DC PHOTOEMISSION GUNS

Charles K. Sinclair
Jefferson Lab

HIGH QUANTUM EFFICIENCY CATHODES

There are three broad classes of high QE cathodes to consider:

- alkali antimonides – e.g: Cs_3Sb, K_2CsSb, etc.
  - visible light below ~ 600 nm required
- alkali tellurides – e.g. Cs_2Te, K-Te, Cs-K-Te, etc.
  - UV light below ~ 275 nm required
- NEA semiconductors – e.g GaAs, GaAsP
  - visible to near IR light below ~ 800 nm required

High Quantum Efficiency is Essential

For any linear photoemitter, the current is given by:

$$i(mA) = \frac{\lambda(nm)}{124} \bullet P_{laser}(W) \bullet QE(\%)$$

So, for example, to provide 200 mA average current for PERL:

Cathode Type	Wavelength (nm)	P x QE (W-%)
NEA GaAs	780	31.8
K_2CsSb (PEA)	532	46.6
KCsTe (PEA)	266	93.2

Note that this assumes that every laser photon and every emitted electron are used. Losses of either increase the required P x QE.

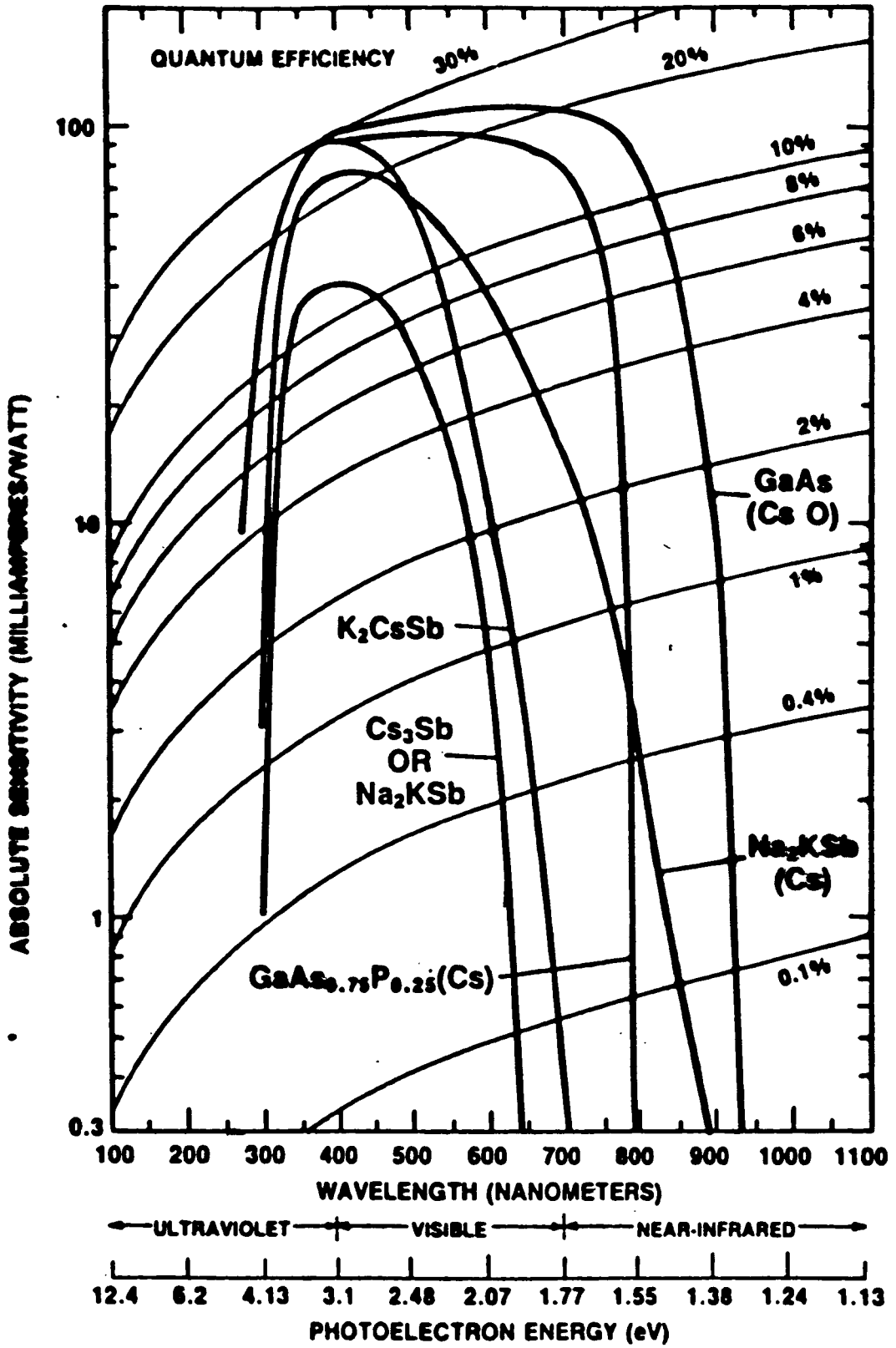
QUANTUM EFFICIENCY
30%
20%
10%
8%
6%
4%
2%
1%
0.4%
0.1%
GaAs (Cs O)
K2CsSb
Cs3Sb OR Na2KSb
Na2KSb (Cs)
GaAs0.75P0.25(Cs)
100
10
1
0.3
ABSOLUTE SENSITIVITY (MILLIAMPERES/WATT)
100 200 300 400 500 600 700 800 900 1000 1100
WAVELENGTH (NANOMETERS)
ULTRAVIOLET
VISIBLE
NEAR-INFRARED
12.4 6.2 4.13 3.1 2.48 2.07 1.77 1.55 1.38 1.24 1.13
PHOTOELECTRON ENERGY (eV)

THE THREE-STEP MODEL OF PHOTOEMISSION

- Optical absorption by electron
- Transport (diffusion) of electron to cathode surface
- Escape of electron through surface potential barrier

For alkali antimonide and alkali telluride photocathodes, the absorption coefficient is ~ 30/μ, while for negative electron affinity GaAs photocathodes, it is ~ 1.4/μ.

ELECTRON AFFINITY

Electron affinity is defined here as the energy difference between the bottom of the conduction band in a bulk semi-conductor, and the vacuum level well outside the semiconductor.

High quantum efficiency photoemitters are of two types – called positive electron affinity (PEA) (e.g. alkali antimonides and alkali tellurides) and negative electron affinity (NEA) (e.g. cesiated GaAs).

In a positive electron affinity photocathode, electrons MUST escape before they thermalize to the bottom of the conduction band, where they cannot escape, while in negative electron affinity cathodes, the electrons can escape from the bottom of the conduction band, and thus may thermalize before photoemission.

In an NEA photocathode illuminated reasonably close to the bandgap energy, the absorption coefficient is low. The electrons are absorbed over a considerable distance, and thermalize to the conduction band minimum, loosing the history of the wavelength of the illuminating photon.

EMITTANCE

$$\varepsilon_{geom,rms} = \sqrt{\langle x^2 \rangle \langle x'^2 \rangle - \langle xx' \rangle^2}\ ,\ \text{and}\ \ \varepsilon_{n,rms} = \beta\gamma\varepsilon_{geom,rms}$$

The "full" emittance, defined as four times the rms emittance above, includes 100% of the beam particles in a uniformly filled phase space, and about 90% of the particles in a beam with Gaussian profiles for x and x' (and about 90% of the particles in a K-V beam).

For a beam with a uniformly filled spot of radius r, and a Maxwell-Boltzmann distribution of velocities characterized by temperature T:

$$\varepsilon_{n,rms} = \frac{r}{2}\sqrt{\frac{kT}{mc^2}}\ ,\ \text{more generally,}\ \varepsilon_{n,rms} = \frac{r}{2}\sqrt{\frac{E_{th}}{mc^2}}$$

There are few high quality measurements of the thermal emittance from photoemission cathodes. The best measurements I know of were made by Bruce Dunham (Ph.D thesis, and PAC '95, p. 1031). He illuminated a NEA GaAs photocathode with a tophat profile laser beam of various wavelengths and spot diameters. His results determine the effective thermal energy, and show that at longer wavelengths, the effective temperature is close to room temperature.

BLACK – THESIS
RED – '95 PAC

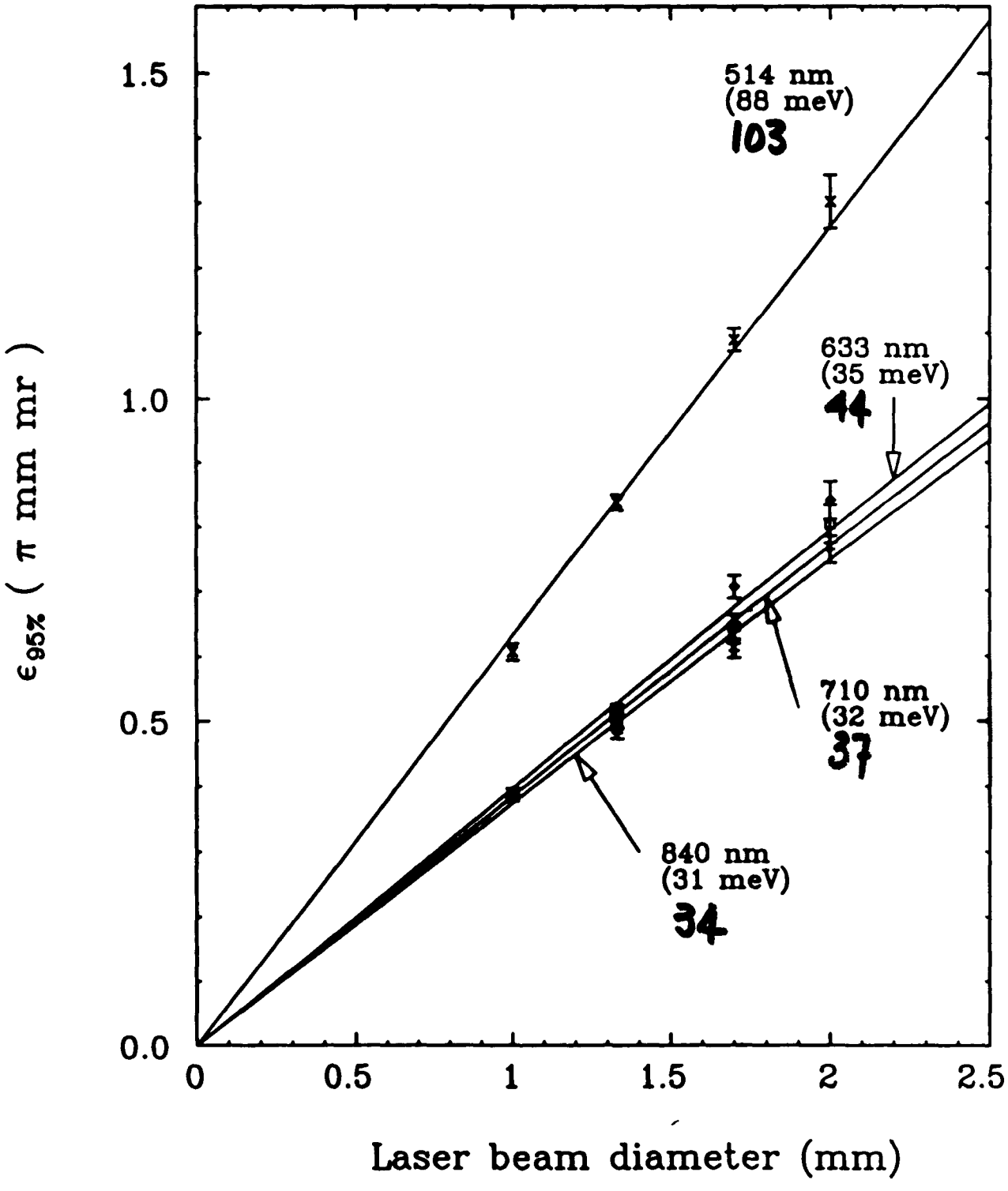

Measured 95% emittance versus laser beam spot diameter for various optical wavelengths.

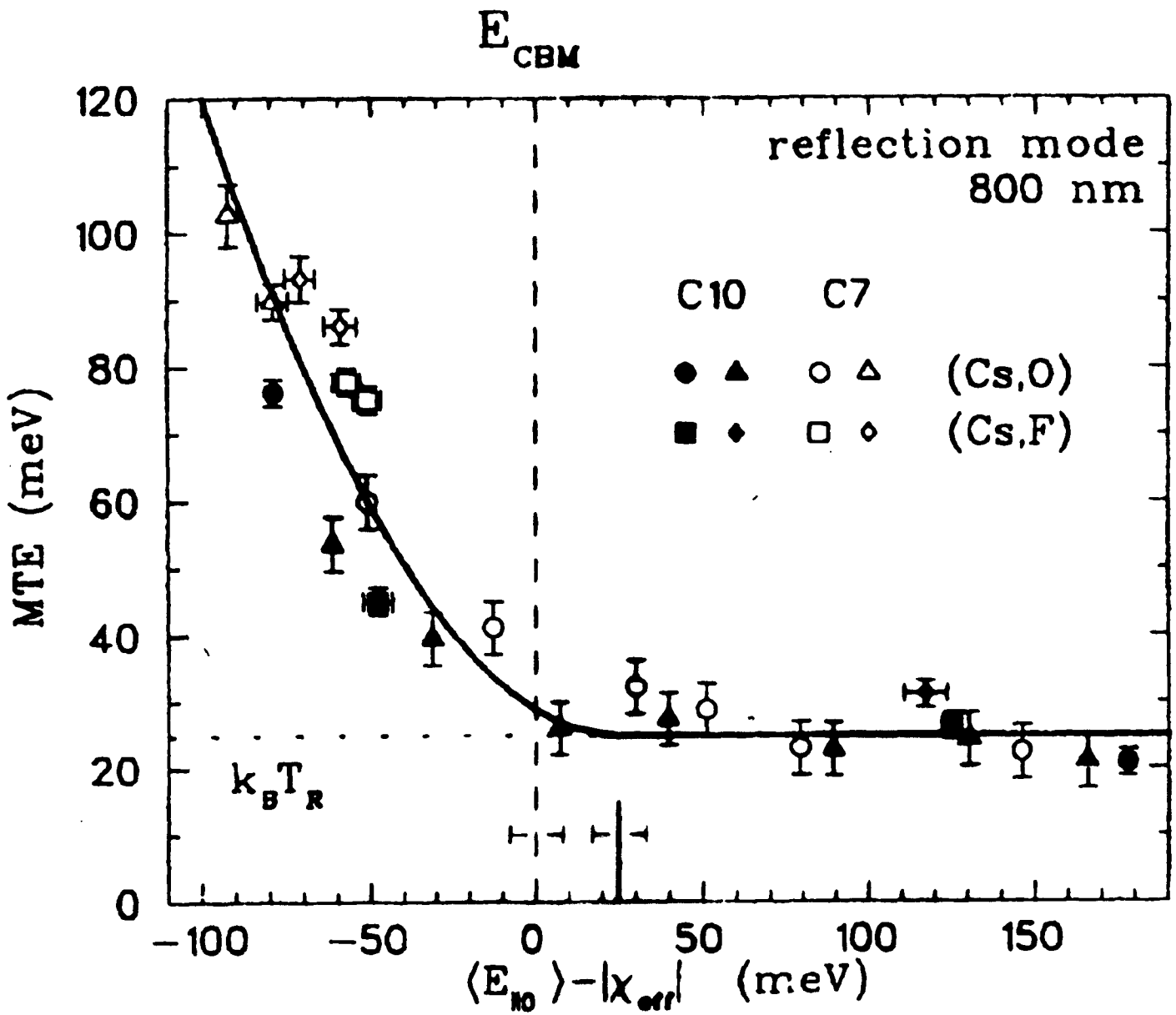
E_CBM
reflection mode
800 nm
C10 C7
(Cs,O)
(Cs,F)
MTE (meV)
k_B T_R
⟨E_no⟩ − |χ_eff| (meV)
120
100
80
60
40
20
0
−100
−50
0
50
100
150

EFFECTIVE TEMPERATURE SUMMARY

- Dunham obtains wavelength dependent effective cathode temperatures. Within about 0.3 eV of the bandgap, his effective temperature is about 1.5 times the physical temperature.

- Engwall quotes a larger effective temperature than Dunham. His measurements have a very large spread, with the smallest numbers consistent with the Dunham numbers, the largest a factor of two higher.

- In the JLab nuclear physics injector we have measured emittances very close to the Dunham values on a beam with RF structure (499 and 1497 MHz) and Gaussian laser profiles

- The effective temperature is dependent on the NEA activation

- Cooling the cathode has been demonstrated to reduce the energy spread of a photoemitted beam

THE IMPACT OF THE THERMAL ENERGY

- To avoid space charge problems, want:

$$Q_{bunch} \leq Q_{stored} / 10,$$

which leads to:

$$Q_{bunch}(pC) \leq 2.78 E_{cath}(MV/m)(r(mm))^2$$

- If we say $E_{thermal} = \beta(51\ meV)$, then we have:

$$r(mm) = 2\varepsilon_{n,rms}(mm-mrad)\sqrt{\frac{10}{\beta}}, \text{ so}$$

$$Q_{bunch}(pC) \leq 111 E_{cath}(MV/m)\frac{\varepsilon^2}{\beta}$$

EXAMPLES

- With $\beta \sim 6$ and $\varepsilon \sim ½$, for 154 pC/bunch, need $E_{cathode} \sim 33$ MV/m. These numbers are about OK for a Cs_2Te cathode, and the cathode field is OK for an RF gun.

- With $\beta \sim 1$ and $\varepsilon \sim ½$, for 154 pC/bunch, need $E_{cathode} \sim 5.5$ MV/m. These numbers are about OK for a GaAs cathode, and the cathode field is OK for a DC gun.

- A 433 MHz RF gun with a Cs_2Te cathode looks like it would require a cathode field too large to be practical.

CONCLUSION: the nature of the cathode will have a lot to do in determining the nature of the gun for these small emittances.

CATHODE LIFETIME ISSUES

- At JLab, we operate NEA GaAs cathodes on both the FEL and the nuclear physics accelerators, with total charge delivery from a cathode approaching 1 A-hr

- PERL will require about 1500 A-hr per operating year.

- JLab GaAs cathode operating lifetimes are limited only by ion back-bombardment. Thus the lifetime is best expressed in terms of delivered coulombs per unit illuminated area – not clock hours. The best results we have give 1/e operating lifetimes of 1.0 to 1.2 times 10^5 coulombs/cm^2.

- The use of multiple illuminated spots from a large area cathode, two readily interchangeable guns, and vacuum improvements may allow the PERL requirement to be met.

IMPROVING THE GUN VACUUM

- Massive NEG pump arrays surround the cathode-anode gap
- NEG coated beam tubes act as a pump, a diffusion barrier, and have very low ESD
- Elimination of electrons originating from large radius on the cathode is essential. We anodize a ring at large radius on the cathode wafer to eliminate emission from this region.
- Field emitted electrons degrade the vacuum through ESD, so field emission must be kept at extremely low levels
- Once established, our gun vacuums slowly improve in time, and require no maintenance

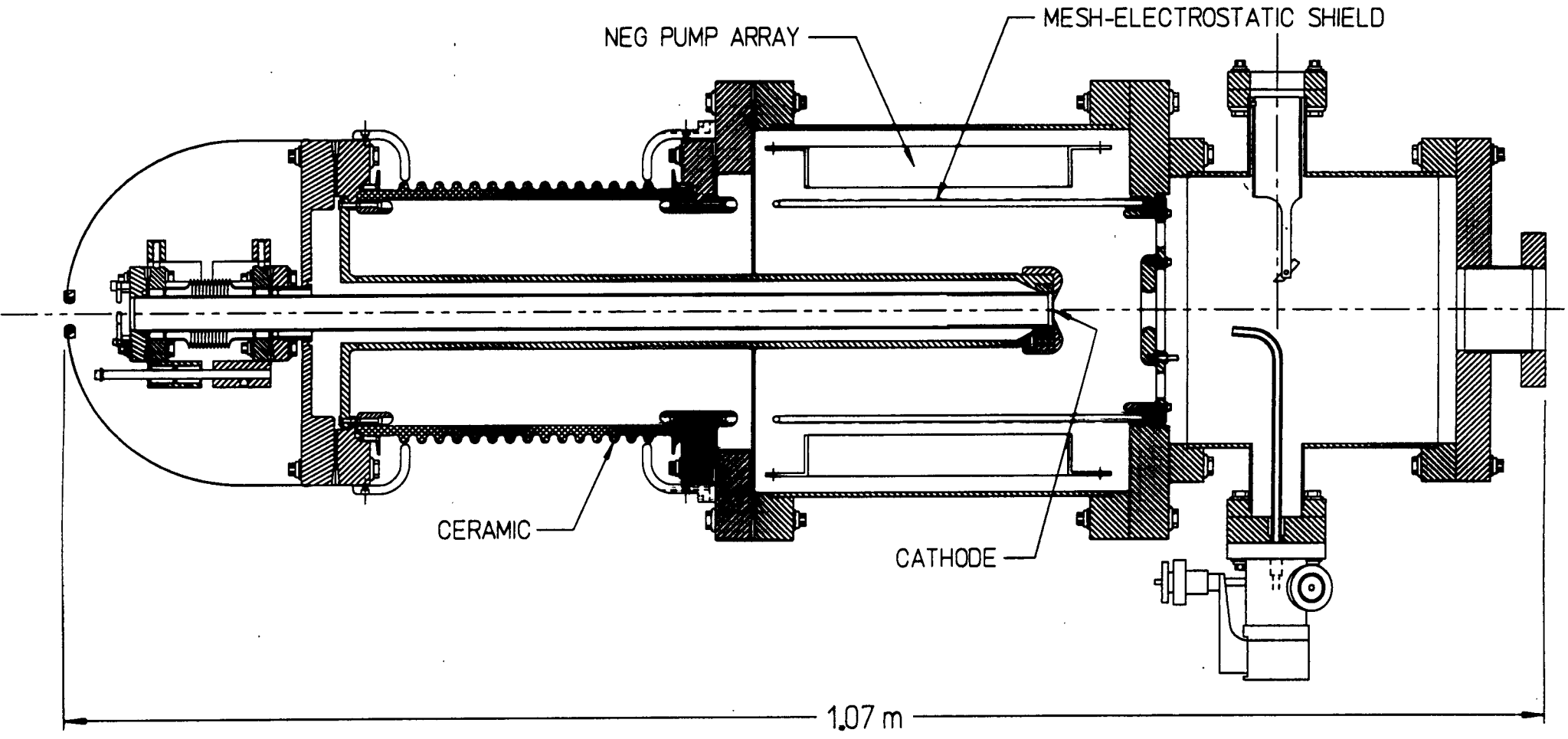
NEG PUMP ARRAY
MESH-ELECTROSTATIC SHIELD
CERAMIC
CATHODE
1.07 m

VACUUM – THE NEXT STEPS

- Develop chambers with reduced outgasing rate
- Develop species-specific pumping
- Investigate the use of diffusion barriers
- Employ impermeable chamber walls
- Develop improved vacuum diagnostics

We believe it should be practical to reach into the 10^{-13} torr range with careful work. This should dramatically reduce the ion back bombardment problem.

LASER ISSUES

High average power lasers operating at appropriate wavelengths, and with suitable RF time structure are not easy to come by.

We use a Ti:sapphire laser which is very stably mode locked to the accelerator RF (499 or 1497 MHz) by gain modulation. The gain modulation is provided by an RF gain switched diode laser.

This system has delivered up to 2 W output, and is in routine use on the accelerator.

The RF output frequency of the laser is readily variable over a huge range – we have operated between 233 MHz and 2.5 GHz. The output power is independent of the RF frequency.

We see no reason that this laser cannot be developed to provide at least 10 W

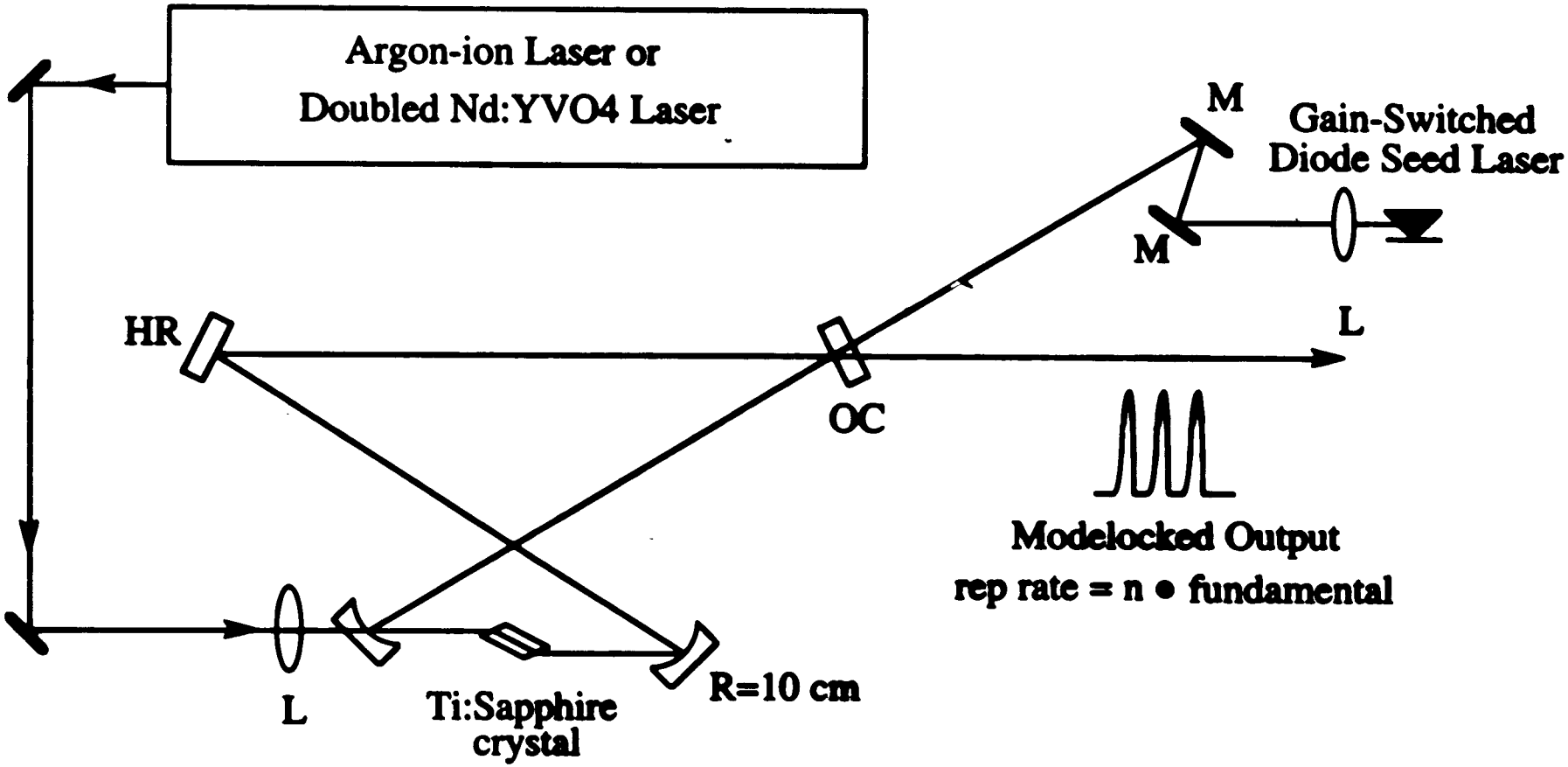

JLAB prototype laser; Alternative to 100 mW Diode Systems
high power, modelocked ti:sapphire

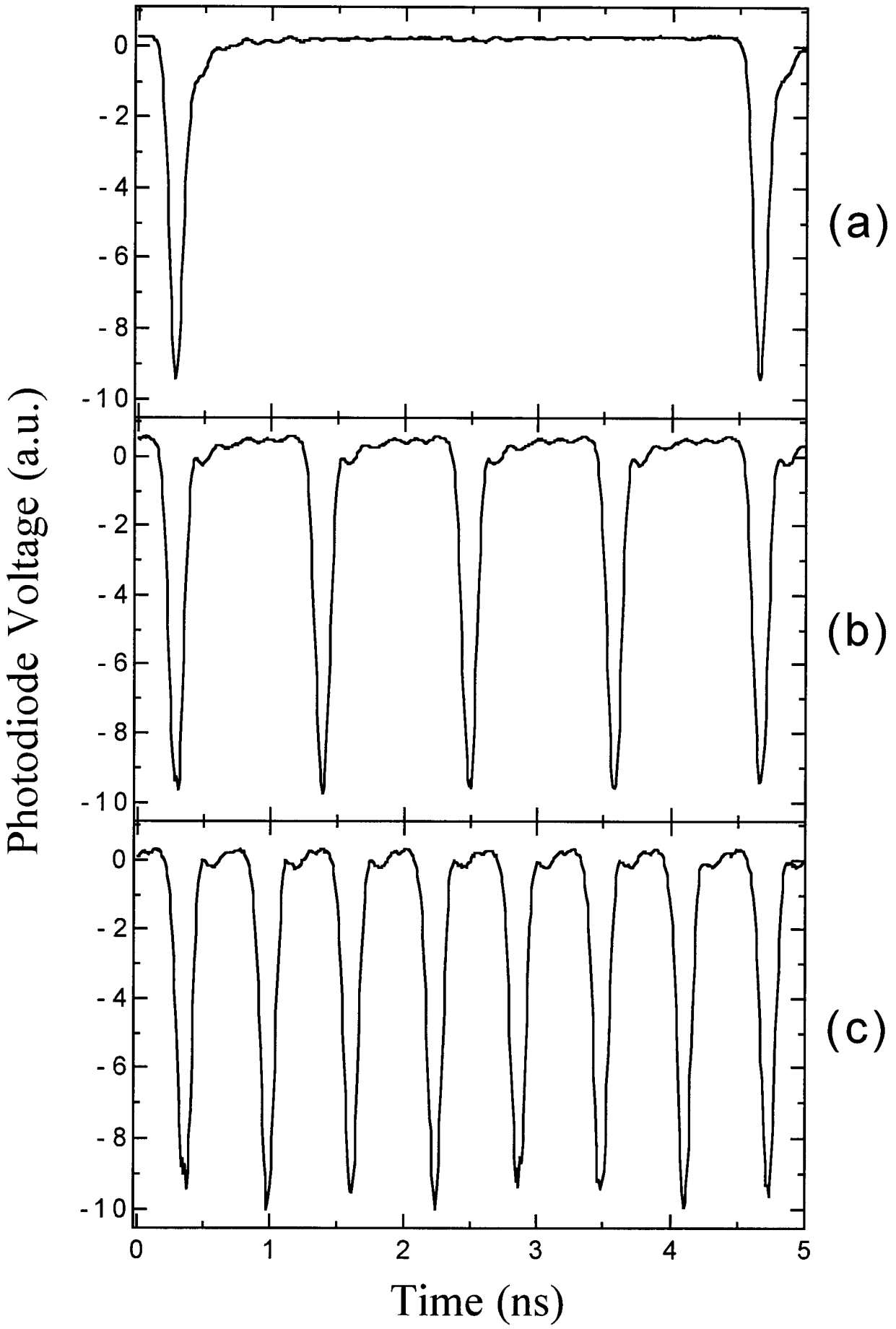
Photodiode Voltage (a.u.)
0
-2
-4
-6
-8
-10
(a)
(b)
(c)
0
1
2
3
4
5
Time (ns)

DC Gun issues

- High fields are necessary at the cathode (and therefore even higher fields elsewhere on the cathode electrode)

- Field emission from the cathode electrode and its support structure must be very low. Field emitted electrons degrade the vacuum through ESD, and may cause charging of the cathode insulator resulting in catastrophic vacuum failure.

- Ian Brown has developed an ion implantation process to make a uniform, high sheet resistance on a ceramic. We have adapted this to our 500 kV FEL gun with great success.

- We have treated conventional stainless steel electrodes with plasma-source ion implantation. This reduced the field emission from large area electrodes by over a factor of one thousand. We believe we can operate a DC gun at 20 to 25 MV/m cathode field.

VACUUM GAP VOLTAGE BREAKDOWN COMPARISON

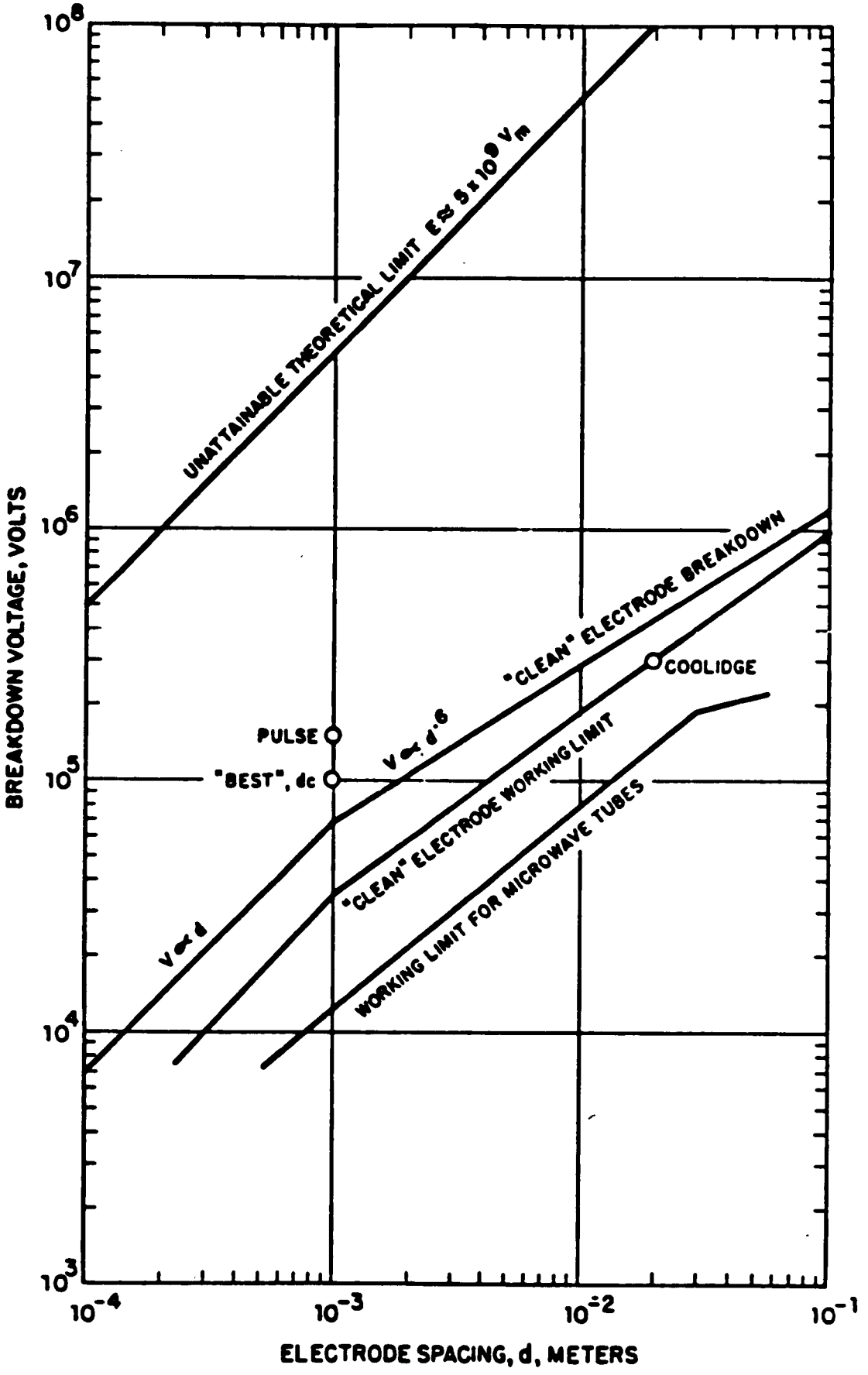

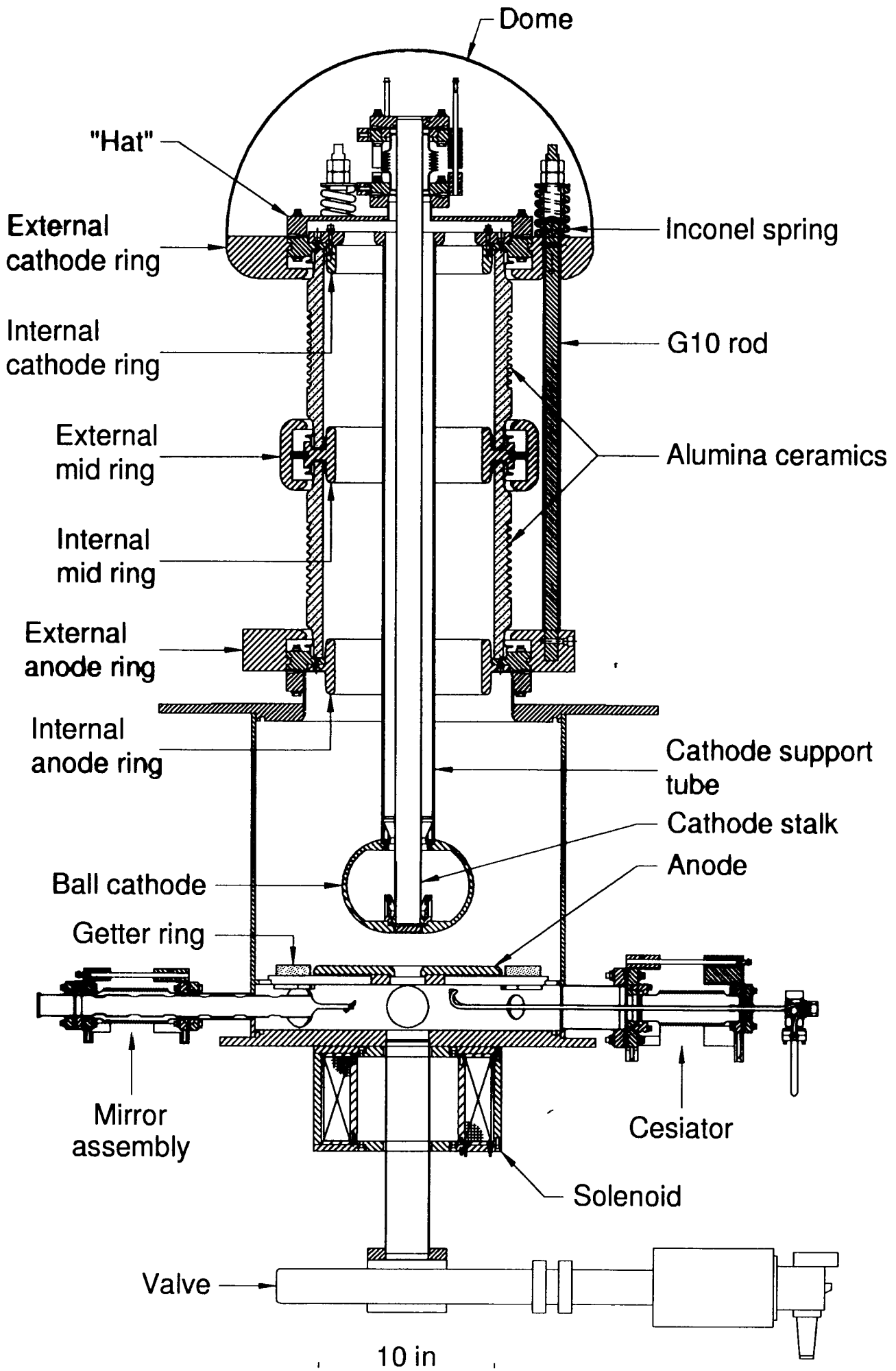
Dome
"Hat"
External cathode ring
Inconel spring
Internal cathode ring
G10 rod
External mid ring
Alumina ceramics
Internal mid ring
External anode ring
Internal anode ring
Cathode support tube
Cathode stalk
Anode
Ball cathode
Getter ring
Mirror assembly
Cesiator
Solenoid
Valve
10 in

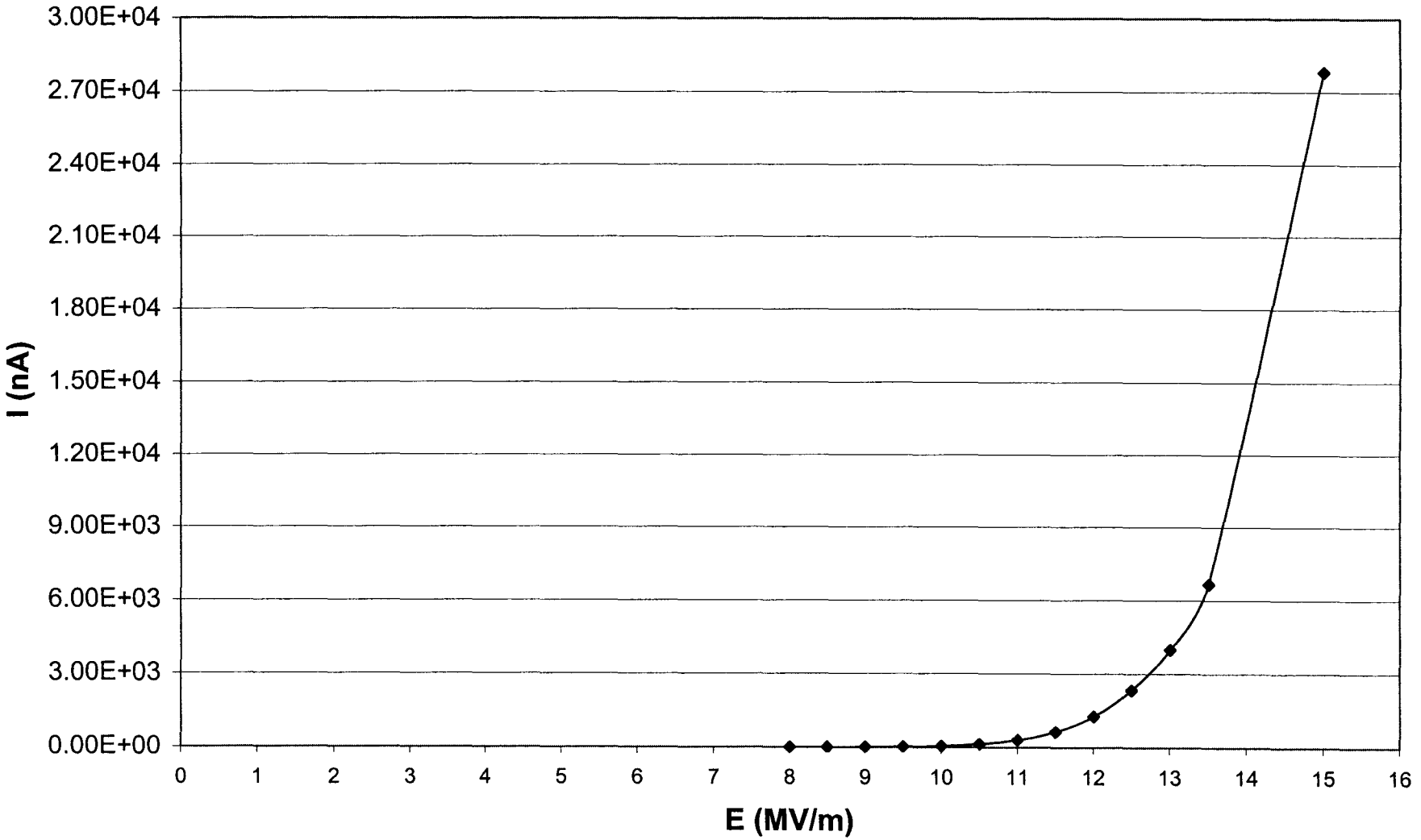
I vs E for 5mm gap 1um SST
3.00E+04
2.70E+04
2.40E+04
2.10E+04
1.80E+04
1.50E+04
1.20E+04
9.00E+03
6.00E+03
3.00E+03
0.00E+00
I (nA)
0
1
2
3
4
5
6
7
8
9
10
11
12
13
14
15
16
E (MV/m)

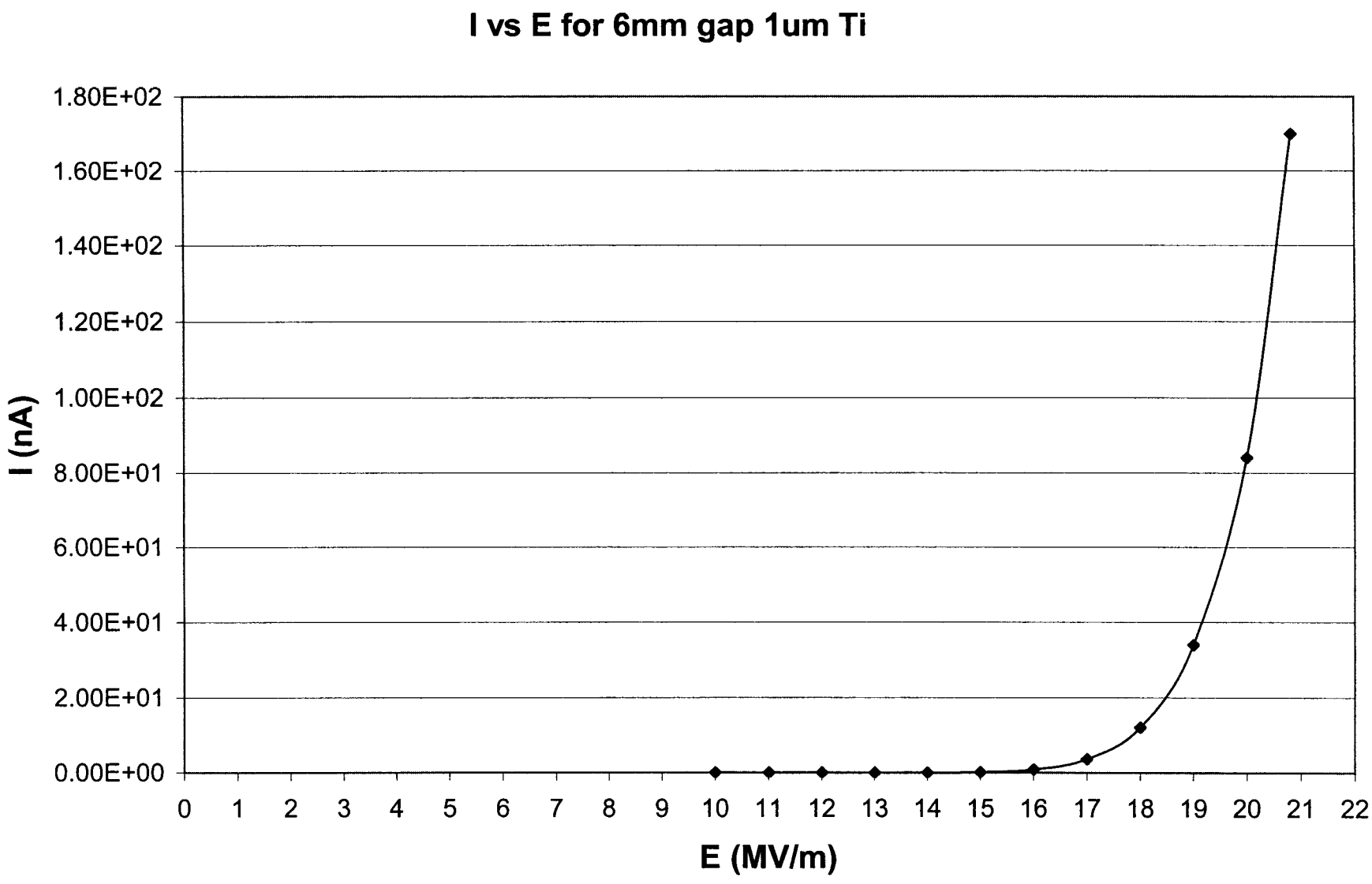
I vs E for 6mm gap 1um Ti
1.80E+02
1.60E+02
1.40E+02
1.20E+02
1.00E+02
8.00E+01
6.00E+01
4.00E+01
2.00E+01
0.00E+00
I (nA)
0 1 2 3 4 5 6 7 8 9 10 11 12 13 14 15 16 17 18 19 20 21 22
E (MV/m)

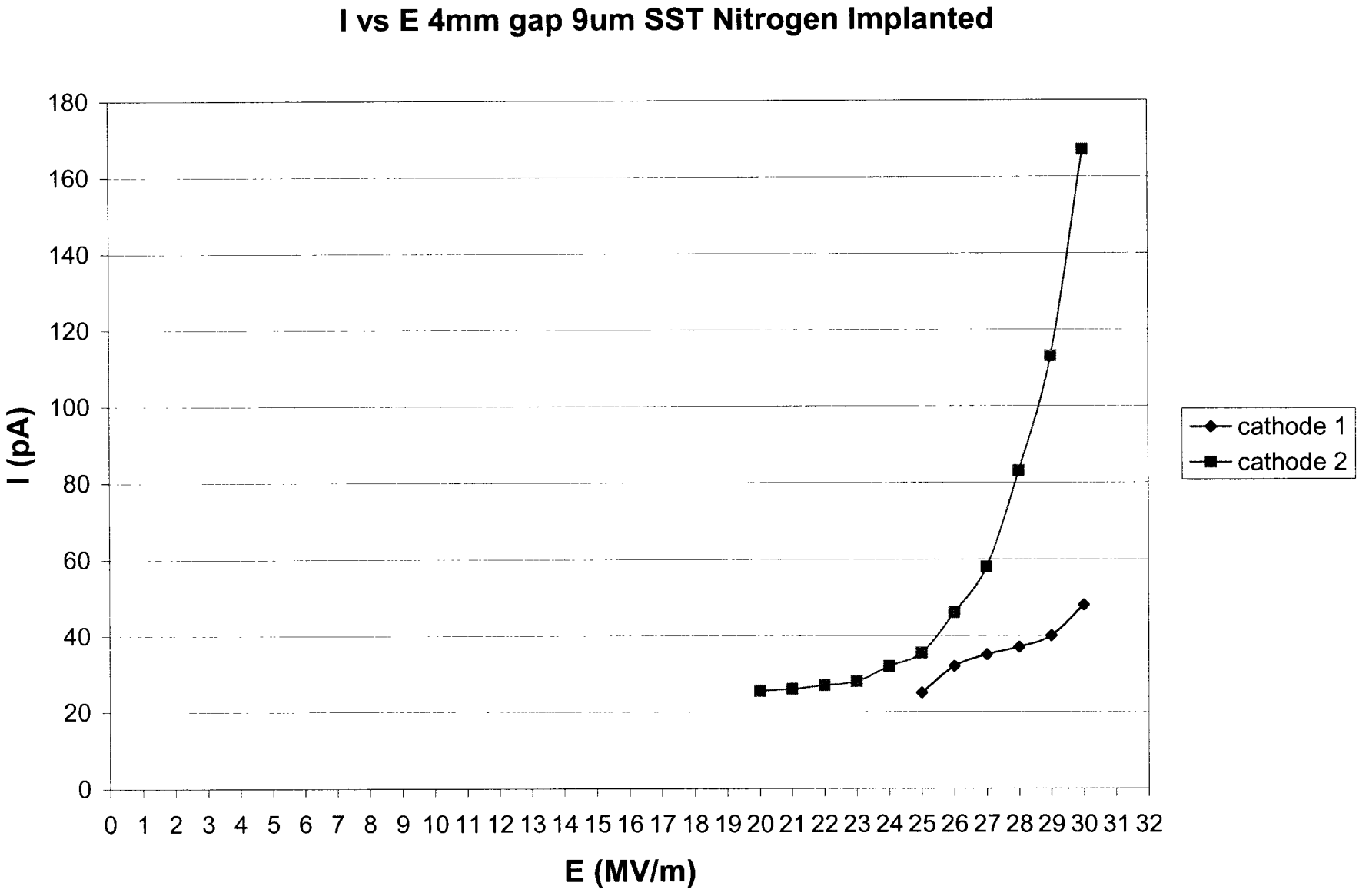
I vs E 4mm gap 9um SST Nitrogen Implanted
I (pA)
E (MV/m)
0
20
40
60
80
100
120
140
160
180
0 1 2 3 4 5 6 7 8 9 10 11 12 13 14 15 16 17 18 19 20 21 22 23 24 25 26 27 28 29 30 31 32
cathode 1
cathode 2

CONCLUSIONS

- The NEA cathode offers a very small thermal emittance, and the hope that lowering the cathode temperature would reduce this even further.

- Cathode lifetime is presently limited only by ion back bombardment, implying that improved vacuum (which is surely possible) will result in lifetime improvements.

- The primary issues in a DC gun – the cathode insulator and reduction of field emission – appear under control for guns operating up to ~750 kV with ~ 20 MV/m cathode field.

- Lasers for any 200 mA photoemission gun are a challenge. The GaAs cathode offers the advantage of using IR light, avoiding frequency doubling (or more), providing the highest current per watt of light, and using a laser which easily provides the RF structure.

LASER SYSTEMS FOR DC AND RF GUNS

M. BABZIEN, B. SHEEHY, T. SRINIVASAN-RAO, T.TSANG

Brookhaven National laboratory, Upton, NY 11973

Presented at the workshop on Photoinjector for energy recovery LINAC, Jan. 22-23, 2001

LASER SYSTEM REQUIREMENTS

POWER REQUIREMENT:

REQUIRED CURRENT * PHOTON ENERGY/ QE

FOR 200 mA CURRENT, 2 eV PHOTONS, AND 2% QE,

LASER POWER = 20 W ON CATHODE

~ 20 ps FWHM

FLAT TOP TRANSVERSE AND LONGITUDINAL PROFILE

PULSE TRAIN SHAPING

STABILITY

AMPLITUDE: 10^{-3} **pk-pk at 10 MHz**

TIMING: **0.2 ps RMS for freq. > 1 MHz**

TRANSVERSE, LONGITUDINAL PROFILE: 5% pk-pk

RELIABILITY

24/7 OPERATION

REDUNDANCY

SCALABILITY

BASIC LAY OUT OF LASER SYSTEM:

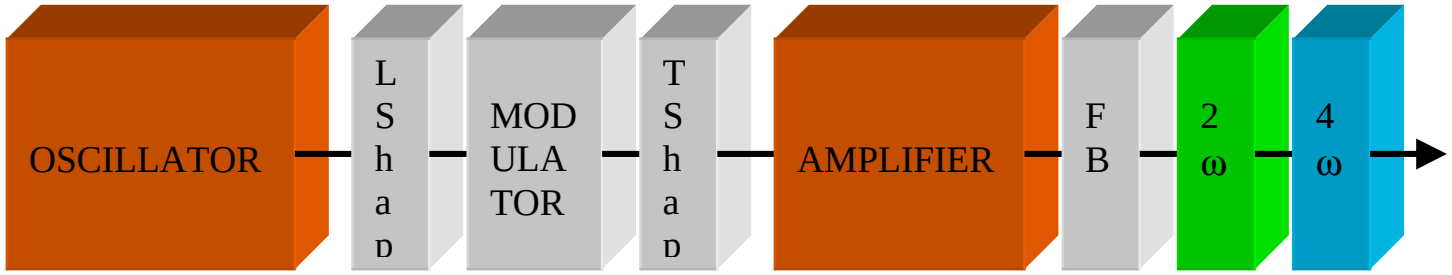

OSCILLATOR:

a) Single oscillator @1.06 μm, 1.3 GHz, < 7 ps, 0.5 W, Custom, commercial unit

Single unit to synchronize

No redundancy

b) Multiple oscillators, each at 1.5 μm, 1.3 GHz <5 ps, tens of mW, Commercial unit

Built in redundancy
Pulse stacking for temporal shaping and Mach-Zender interferometer for slicing
Fiber makes alignment relatively easy
Rapid advance due to Communications industry
Suitable for DC/RF gun

Multiple units to synchronize
Requires 3ω / frequency shifting for multi-alkali cathodes
Scaling to higher powers difficult and requires frequency shifting
May be expensive

LONGITUDINAL PULSE SHAPING:

a) Stretching

- **Conventional**
- **50% efficiency**
- **Arbitrary waveform using masks**

b) Stacking

- **Novel technique**
- **No loss**
- **Arbitrary waveform using different path length**
- **Interference effects**

AMPLIFIER:

Single Amplifier:

Commercial, diode pumped, high power amplifier modules available

Multiple Amplifiers:

Fiber Amplifiers with > 10 W possible

ISSUES:

Amplitude Stability:

Diode laser stability driven by current and temperature stability .01% possible

Saturated or unsaturated operation?

Saturated:	Better stability
	Gain changes with seed rep. rate
Unsaturated:	Gain indep. of rep.rate
	Lower stability

Simulations Indicate that ~ *5 -*7 degradation of input pulse, depending on the gain

Spatial and temporal uniformity of micropulses

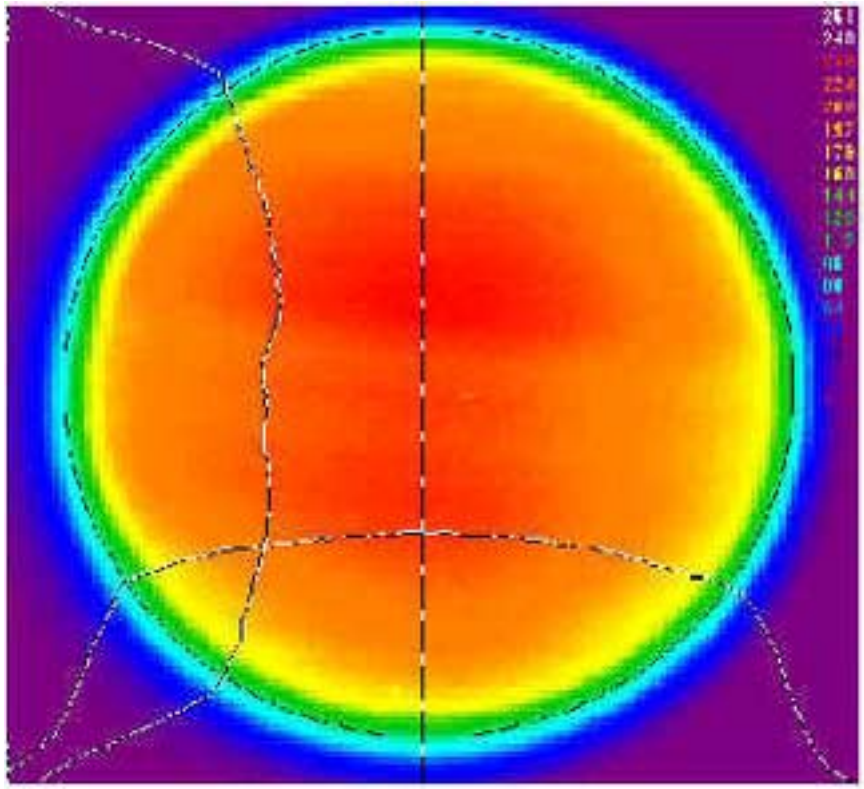

Relay Image of fluorescence of 6.3 mm diameter, 0.6% dopant Nd:YAG rod

FEEDBACK:

Amplitude

Timing

Spatial profile

Temporal profile

DOUBLING CRYSTAL:

Efficiency:Low peak power and high average power:

30% efficiency for the Boeing laser system

10 W by intracavity doubling in commercial, diode pumped, CW lasers

Crystal dimensions, Damage threshold to be determined

VARIOUS OPTIONS AVAILABLE:

SINGLE OR MULTIPLE HEADS FOR OSCILLATOR AND AMPLIFIERS

LONGITUDINAL SHAPING BY STACKING OR STRETCHING

BULK/MACH-ZENDER MODULATOR

AND MORE

BIGGEST ISSUE: CATHODE LIFETIME AND MAINTENANCE OF CONTINUOUS OPERATION

CATHODE LIFETIME VARIES FROM HOURS TO WEEK

Ultra high vacuum at cathode is a must

Laser power must be scalable

Quick switch from cathode

LASER SYSTEM MUST BE DESIGNED TO ACCOMMODATE THESE NEEDS

Recent Results of the High-Current Advanced FEL Photoinjectors

Dinh Nguyen

LANSCE-9
Los Alamos National Laboratory

PERL Photoinjector Workshop
NSLS, Brookhaven National Laboratory
January 22-23, 2001

Overview of the Advanced Free-Electron Laser (AFEL) Experiment

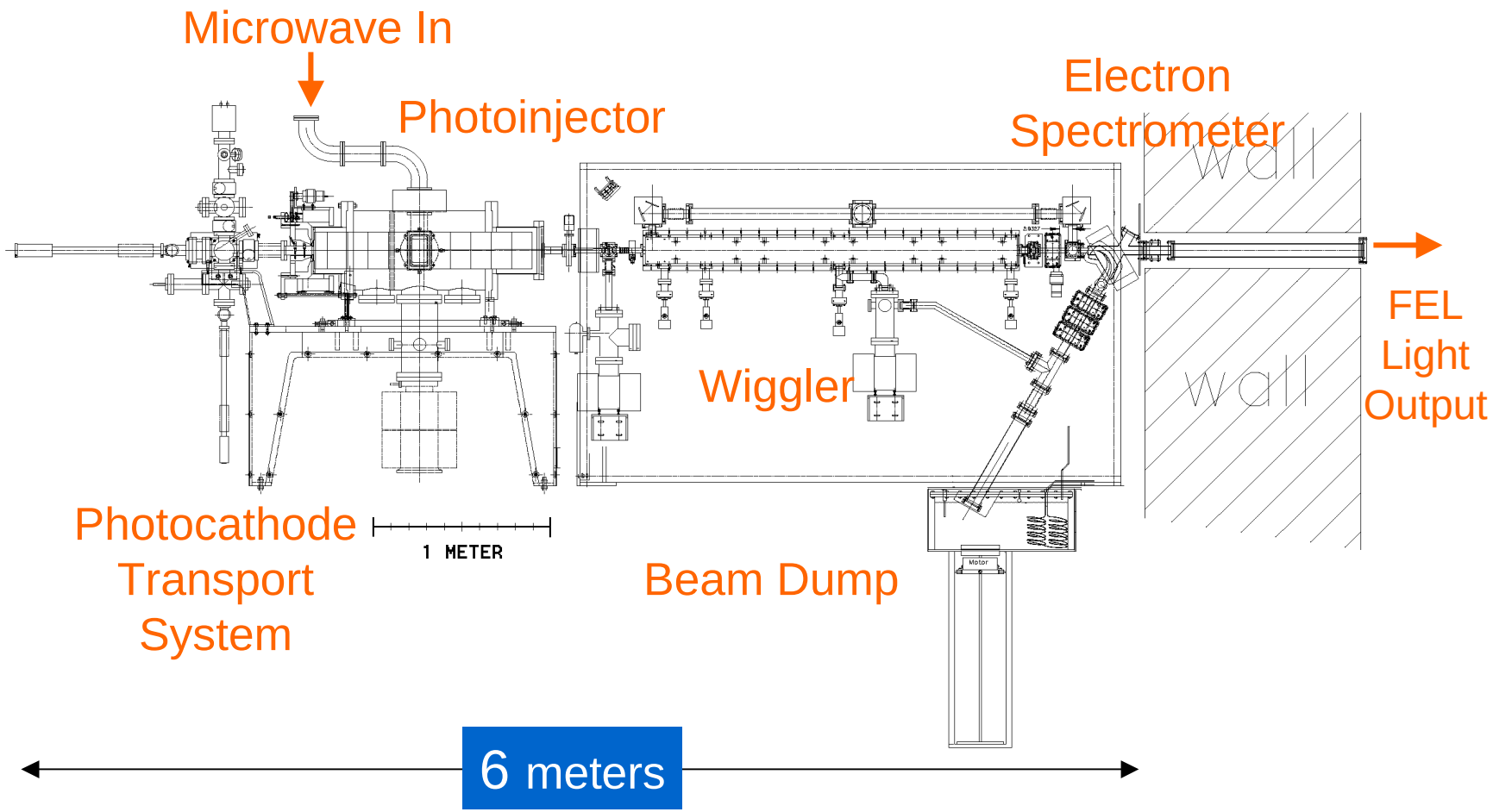

The Advanced FEL Photoinjector Operates at 20 MV/m Gradient and 200 mA Average Current

- 1300 MHz
- E_b = 15-20 MeV
- I_{macro} = 100-400 mA
- Q = 1-4 nC
- ε_{rms} = 1.6 mm-mrad
- $\Delta\gamma/\gamma$ = 0.2%
- Injection $\phi = 30^o$
- Solenoid = 300A
- Bucking Sol. = 310A

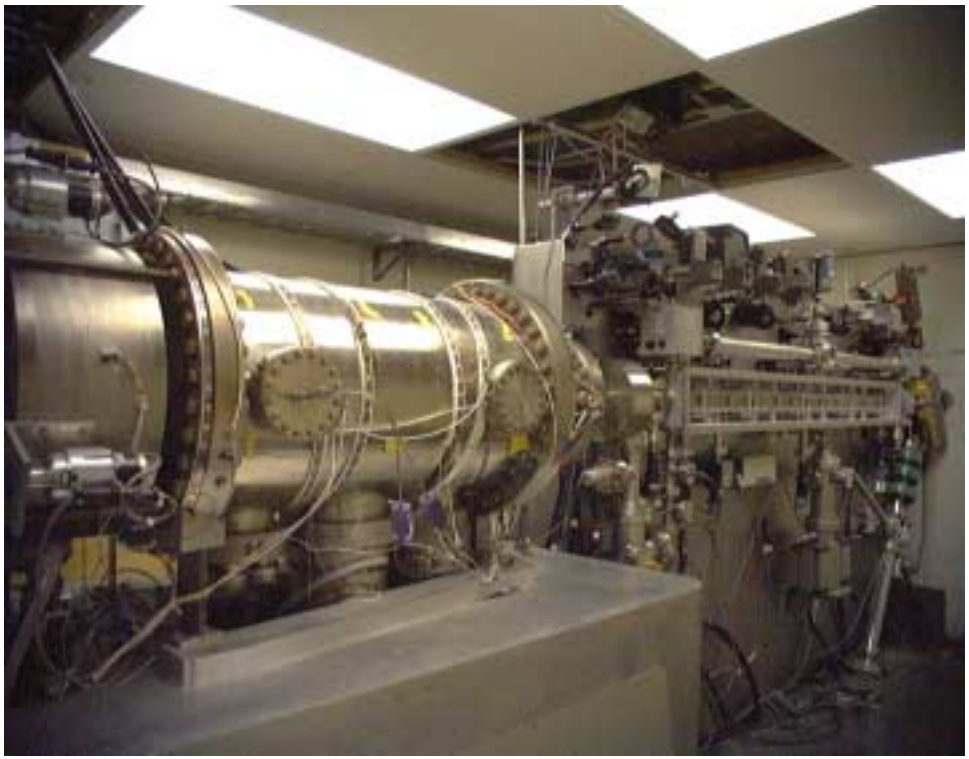

Schematic of the AFEL Photoinjector

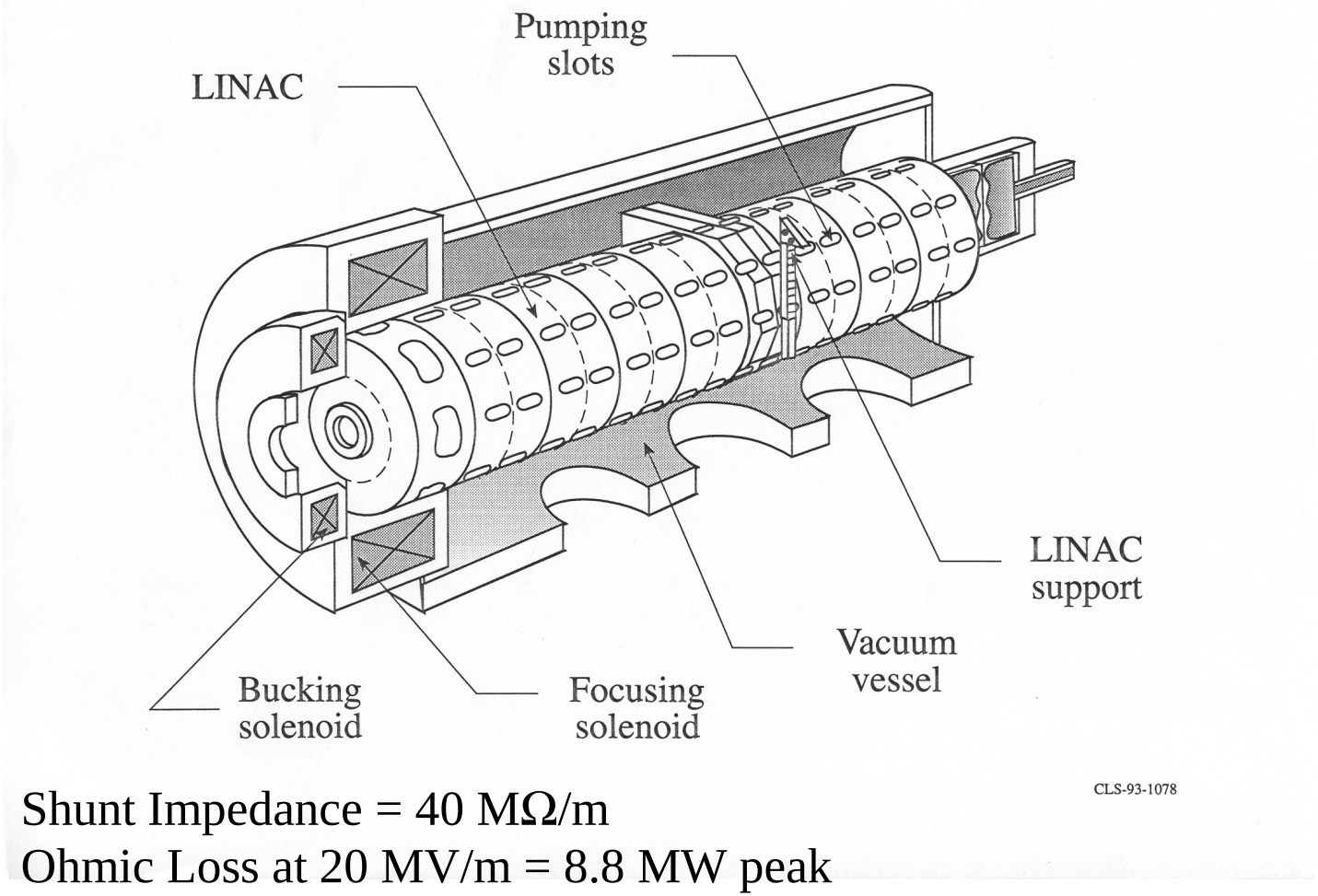

Shunt Impedance = 40 MΩ/m

Ohmic Loss at 20 MV/m = 8.8 MW peak

Cryogenic (77K) operation reduces ohmic loss by a factor 2.

Cs_2Te Energy Levels and Quantum Efficiency

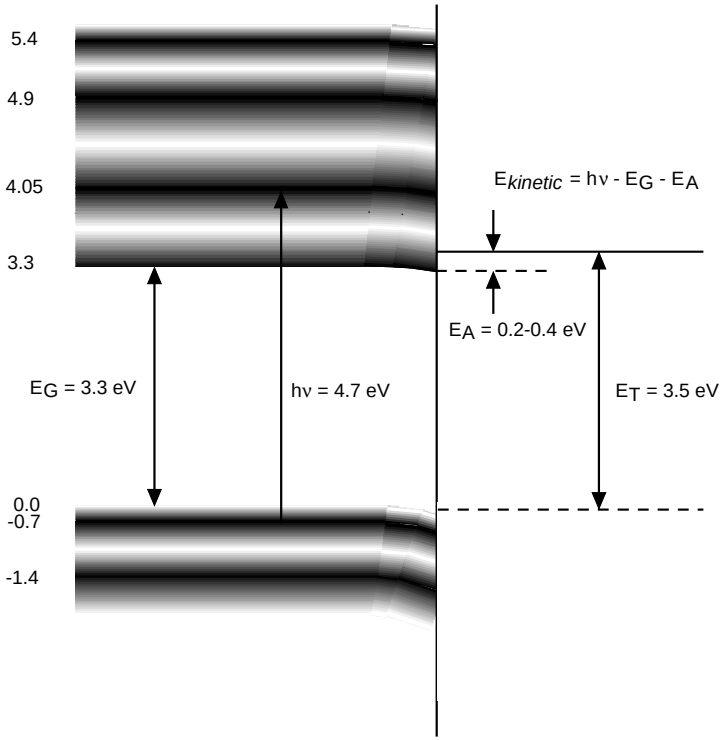

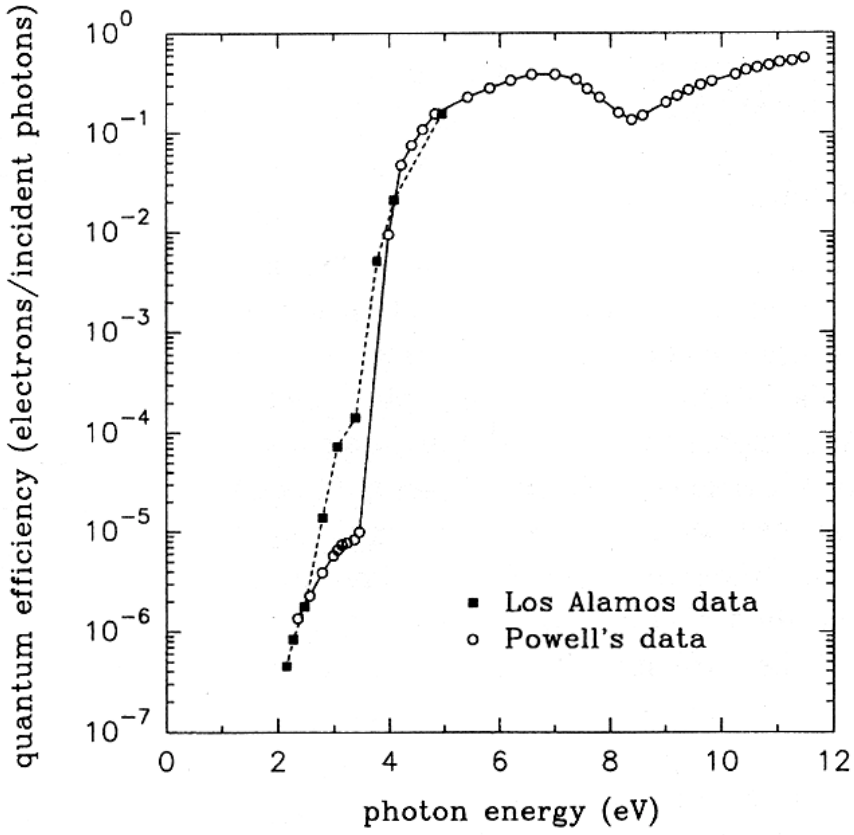

UV photons at 263 nm = 4.7 eV
Electron Affinity = 0.2-0.4 eV
Thermal energy of photoelectrons is ~ 0.2 eV
Estimated thermal emittance = 0.3 mm-mrad/mm photoemission radius.

Beam Measurements with 1 nC Charge and 2.6 mm Emission Radius

(Steve Gierman's Thesis)

Emittance measurements with a ps streak camera

Measured slice emittance 1.6 mm-mrad at 1 nC

PARMELA slice emittance 0.6 mm-mrad at 1 nC (thermal emittance not included)

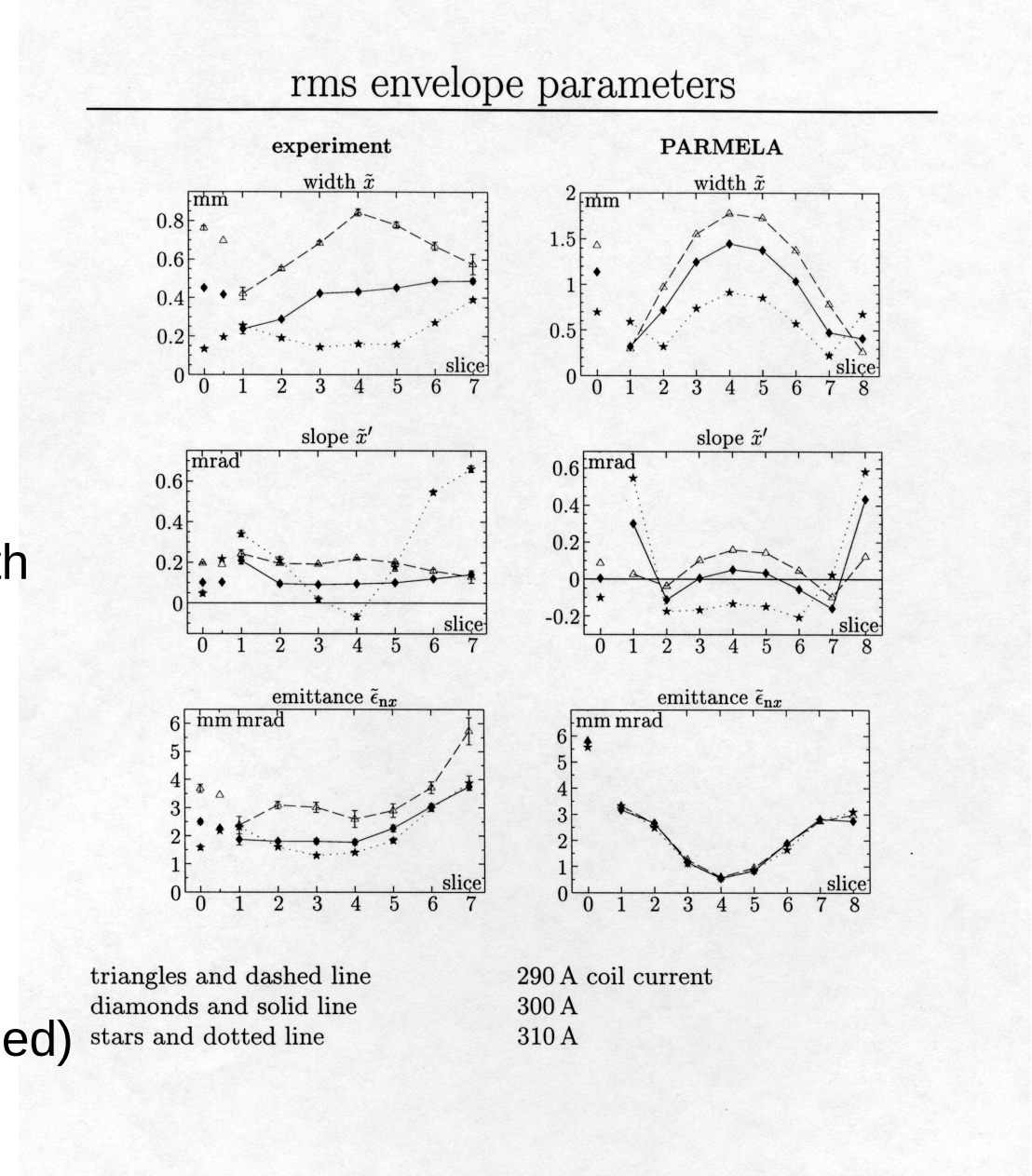

Beam Measurements with <5 nC Bunch Charge and 7 mm Emission Radius (SASE Experiment)

Measured rms radius and inferred normalized emittance vs charge

Measured FWHM pulse length and inferred peak current vs charge

The AFEL Drive Laser Consists of a Diode-pumped Oscillator and two Flashlamp-Pumped Amplifiers

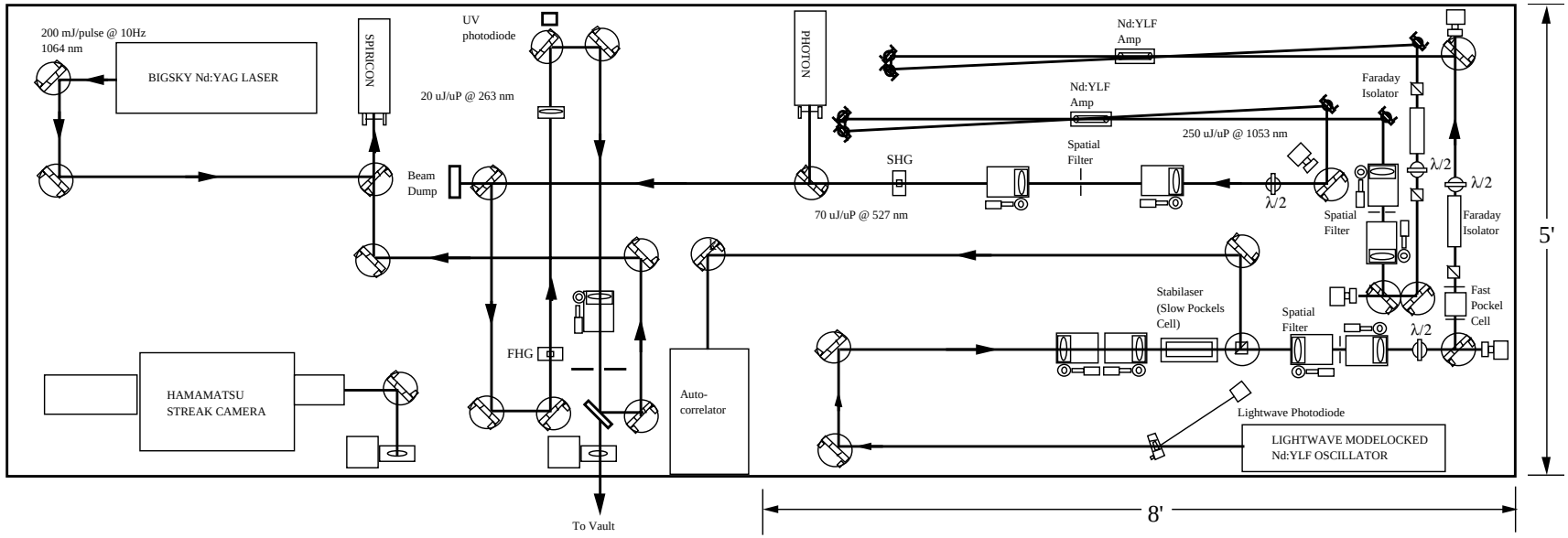

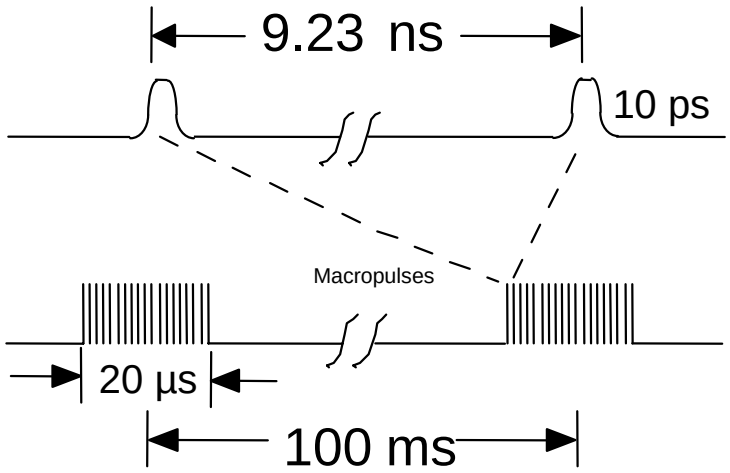

Drive Laser Characteristics

@1053 nm = 30 µJ
@527 nm = 15 µJ
@263 nm = 5 µJ (1 nC at 0.1%)
Macropulse = 2000 Micropulses
Macropulse Rep. Rate = 10 Hz
Diode-pumping to increase duty factor.

Stability Tests Show 1/e Lifetime of Cs_2Te Photocathode Is 40 Hours at J=60 A/cm^2

Measurements
in AFEL Linac
200 mA
Low duty

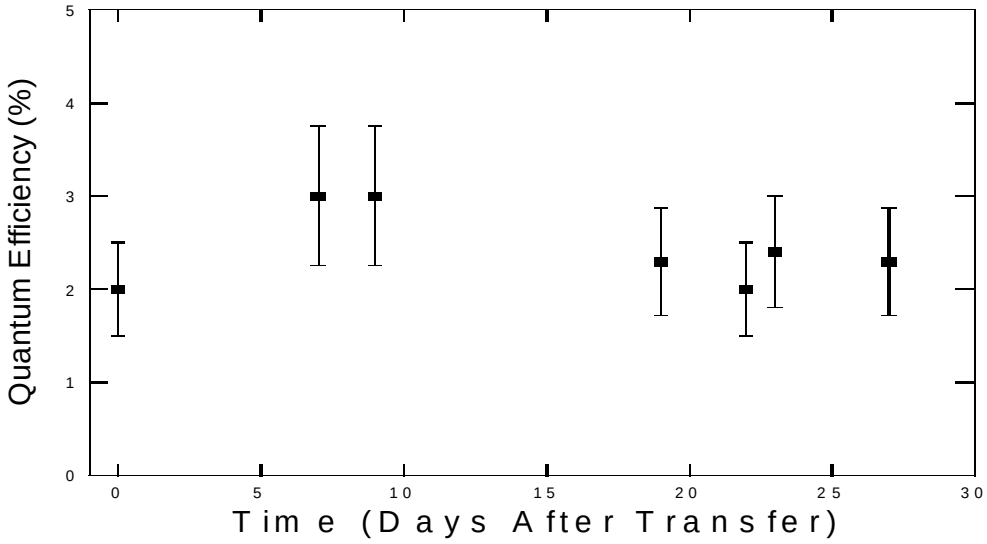

Measurements*
in DC Gun
1/e lifetime = 40 hours
at J=60 A/cm^2
Q=8 x 10^6 Coulomb/cm^2

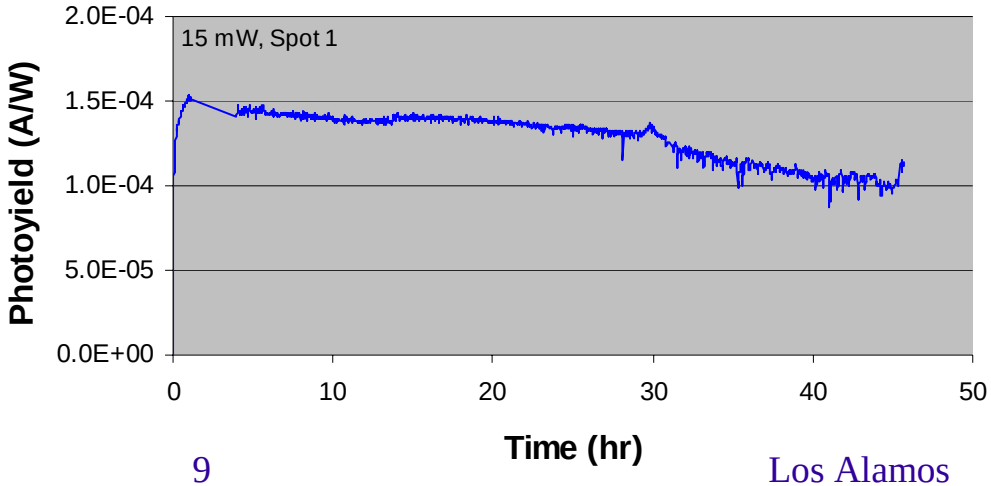

* Courtesy of Etec, Inc.
An Applied Materials Company

CsBr Coating Passivates Cs_2Te Photocathodes Against Contamination at the Expense of Q.E.

	Uncoated	Coated
	Cs2Te	CsBr:Cs2Te
Total thickness of Te (Angstroms)	150	150
Total thickness of Cs (Exposure minutes)	200	170
Reflective QE (@257 nm) before CsBr	5%	10%
Approximate CsBr thickness (Angstroms)	0	90
Reflective QE (@257 nm) after CsBr	NA	3%
Reflective QE after N2 exposure for 15 min	<0.0001%	0.11%
QE after N2 exposure & 150C/2-day heating	<0.0001%	0.09%

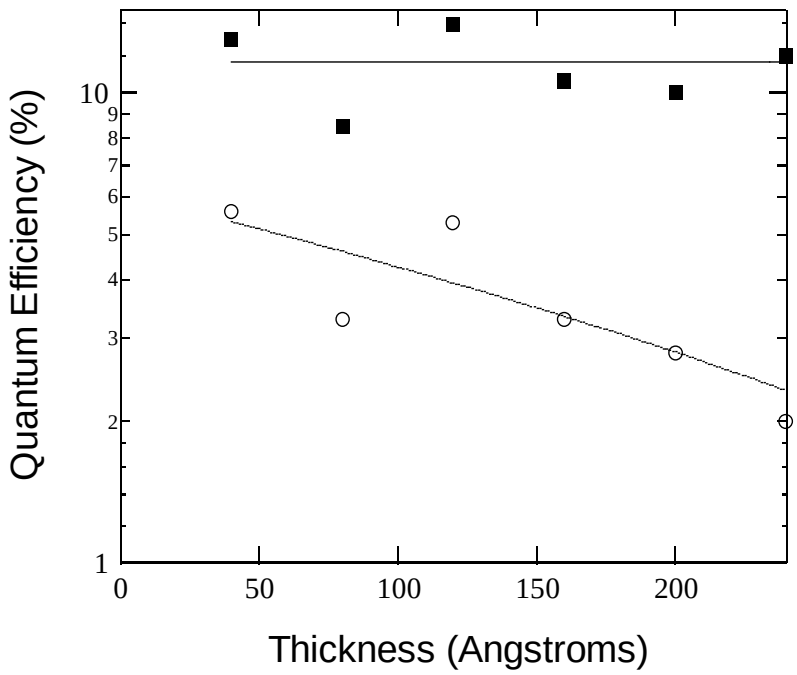

Removable Hexatriacontane Coating Offers Excellent Protection Against Nitrogen Exposure

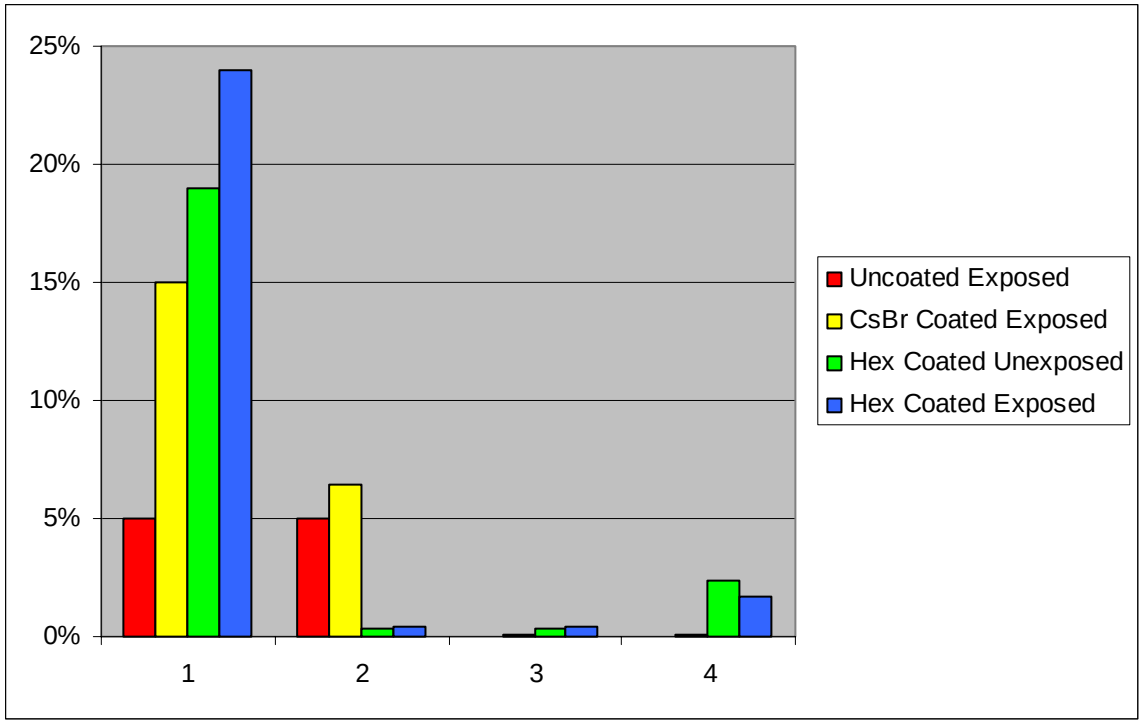

1: Before Coating 3: After Exposed

2: After Coating 4: After Stripping

Los Alamos Preparation Chamber Provides CVD for Making Semiconductor Photocathodes

- Cs_2Te, CsKTe
  CsK_2Sb, Cs_3Sb
- CsBr, NaI, CsI
  Hexatriacontane
- UHV, RGA
- Thickness Monitor
- Cathode transfer mechanism

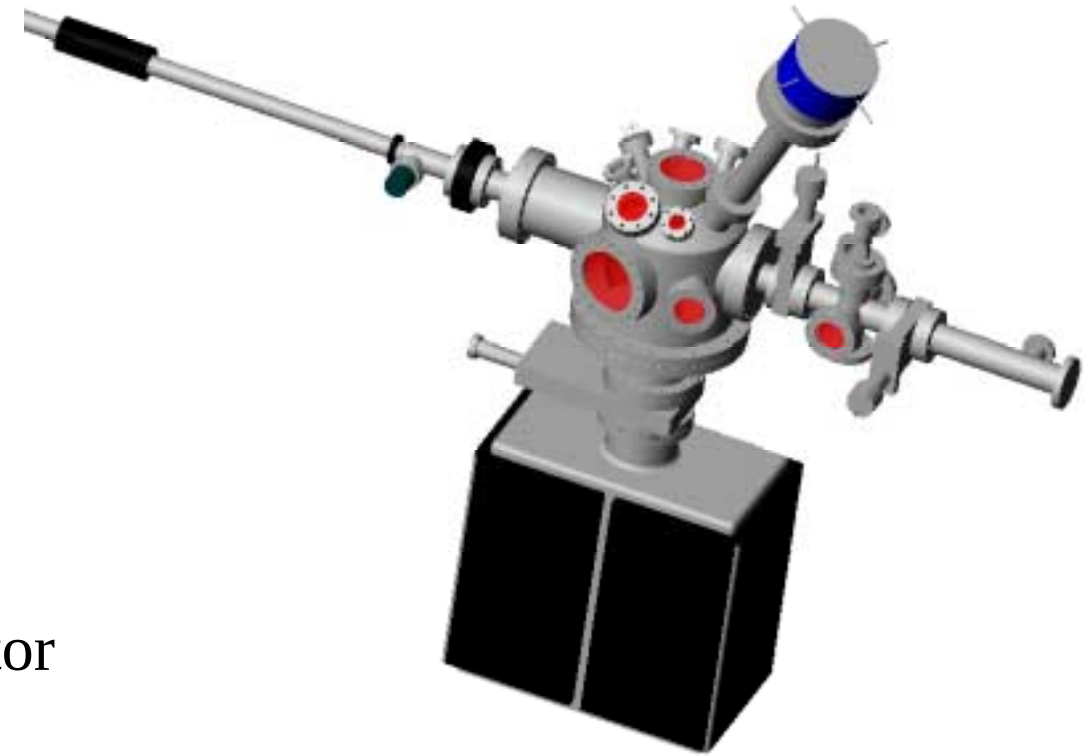

Sub-picosecond Accelerator (SPA) for Electron Beam-Pumped Plasma Wakefield

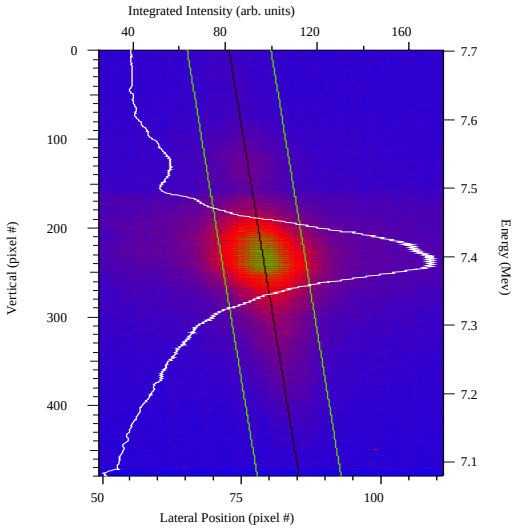

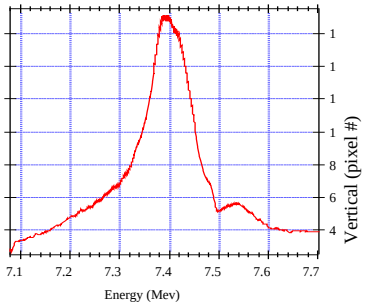

Gas plume off.

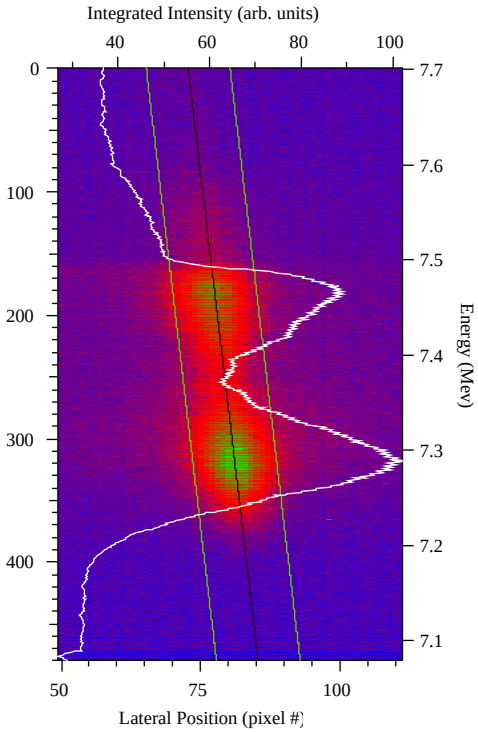

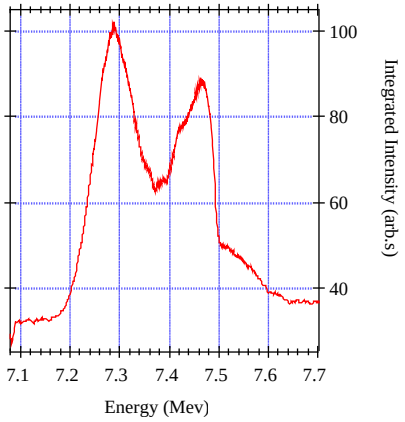

Gas plume on. Demonstrated deceleration gradient is about 60 MV/m.

Summary

• The Advanced FEL photoinjector at LANL offers several important capabilities:

- ✔ High average current (up to 400 mA)
- ✔ Excellent emittance at high charge
- ✔ High repetition rate
- ✔ Cryogenic operation (cut ohmic loss in half)

• Passivating Cs_2Te photocathode with CsBr protects against contamination in the linac but not to nitrogen exposure.

• Passivating Cs_2Te photocathode with removable hexatriacontane demonstrates excellent protection against exposure to 1 atmophere of nitrogen.

• A 1/e lifetime of 40 hrs for continuous operation at 60 A/cm^2 has been achieved.

• Sub-picosecond bunch compression has been demonstrated on the Los Alamos Sub-picosecond Accelerator.

433 MHz High Duty Photocathode RF Gun Experiments

David H. Dowell
Boeing Physical Sciences Research Center
Seattle, WA

Boeing
J. Adamski, FEL Program Manager
T. D. Hayward, Acc. Physics and Design
P. E. Johnson, Acc. HV, RF Systems and Operations
C. A. Lancaster, Controls
H. Mann, Mechanical Engineering
L. Milliman, Controls
C. D. Parazzoli, Theory and Simulation
A. M. Vetter, Acc. and RF Design

Collaborators
P.G. O'Shea, University of Maryland

CEA, Bruyeres-le-Chatel, France:
S. Joly
A. Loulergue
G. Haouat
J.P. de Brion

LANL

Gun Talk Outline

I. 433 MHz PhotoInjector Design Philosophy.

II. Review of 433 MHz RF Photocathode Gun Technology

- **A. Gun Design and Demonstrated Performance**
- **B. Cathode QE and Lifetime**
- **C. Drive Laser Performance**

III. Electron Beam Quality

- **A. Transverse Emittance**
- **B. Longitudinal Emittance**

IV. Summary and Conclusions

Historical Perspective

Motivation:

Design, build and test an RF photocathode gun capable of operating at high current and high duty factor for GBFEL.

Result:

A 1992 demonstration of a two-cell, 433 MHz photocathode gun at 32 mA of average current and 25% duty factor.

Photoinjector Design Philosophy

Use a CW low frequency photocathode gun to generate high charge (1-5 nC) and long (50 ps) micropulses.

Advantages:

Capable of CW operation
High charge
Long micropulses

→ **Excellent Beam Quality at High Beam Current**

Disadvantage:

Cathode field limited to 25-30 MV/m

Accelerate in Low frequency RF cavities.

Advantages:

Minimizes wakefields
CW operation

Disadvantage:

Accelerating gradient limited to 5 MV/m

Linearize and compress to high peak current at 20 MeV.

Advantages:

Linearizing improves compression
Reduces space charge emittance growth

Disadvantage:

Emittance growth due to coherence synchrotron radiation

Layout of the 433 MHz PhotoInjector

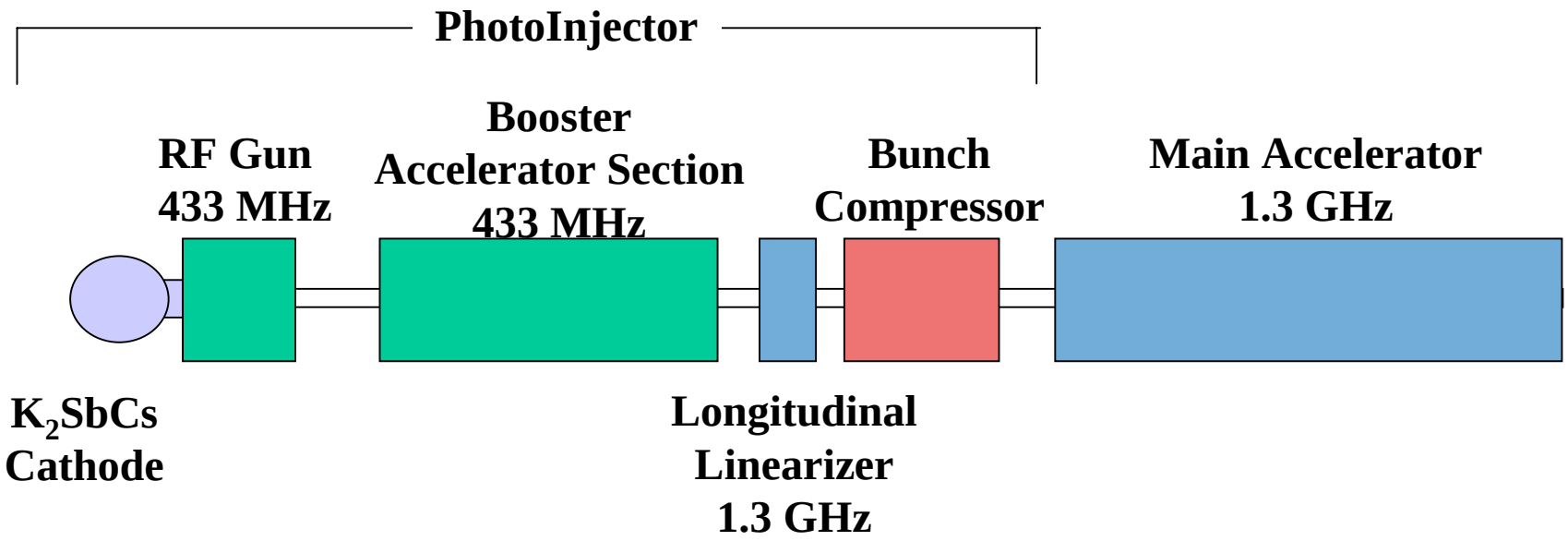

Electron Beam Optics of the 433 MHz Photocathode Gun

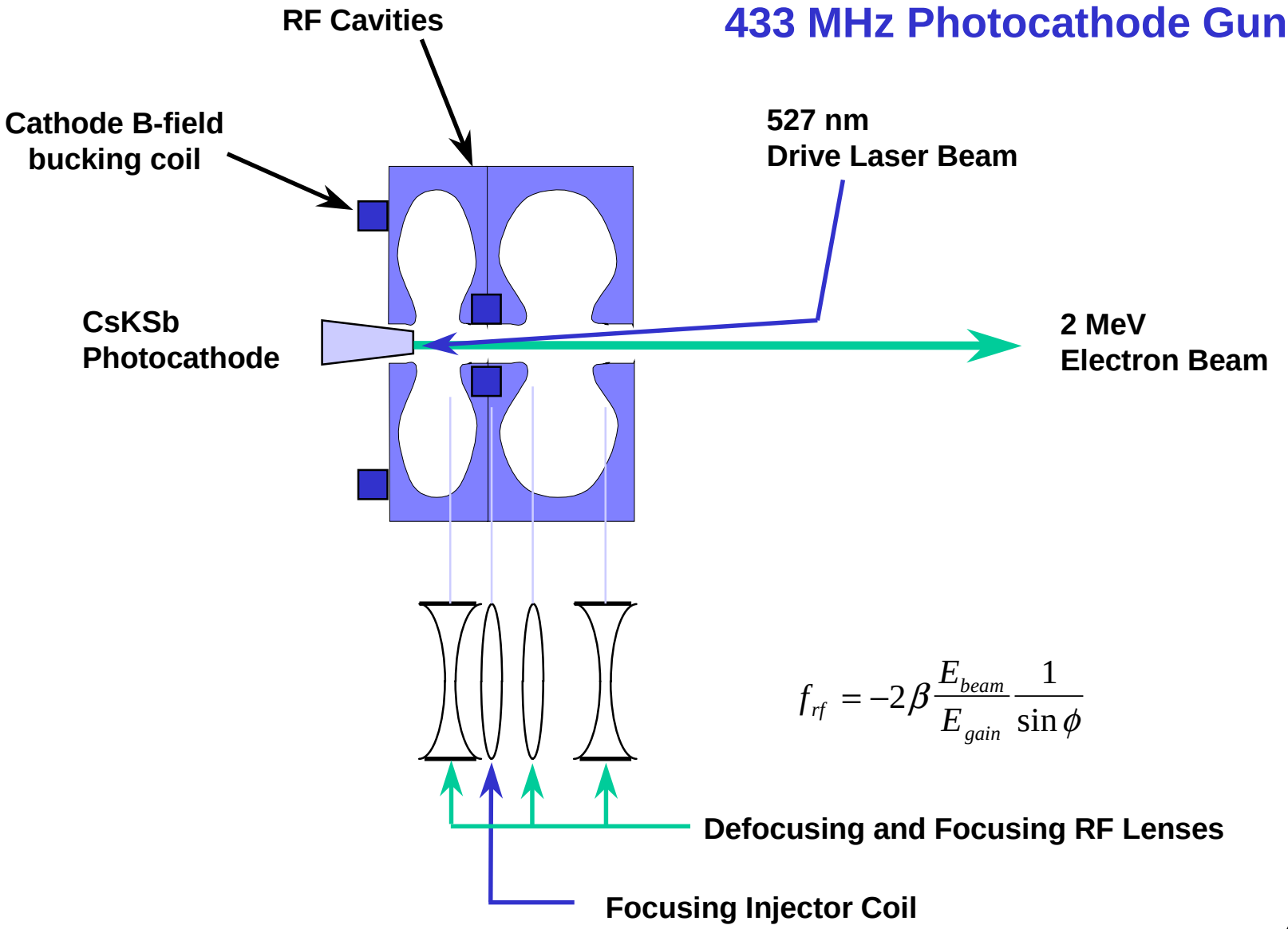

$$f_{rf} = -2\beta \frac{E_{beam}}{E_{gain}} \frac{1}{\sin\phi}$$

The Boeing 433 MHz RF Photocathode Gun

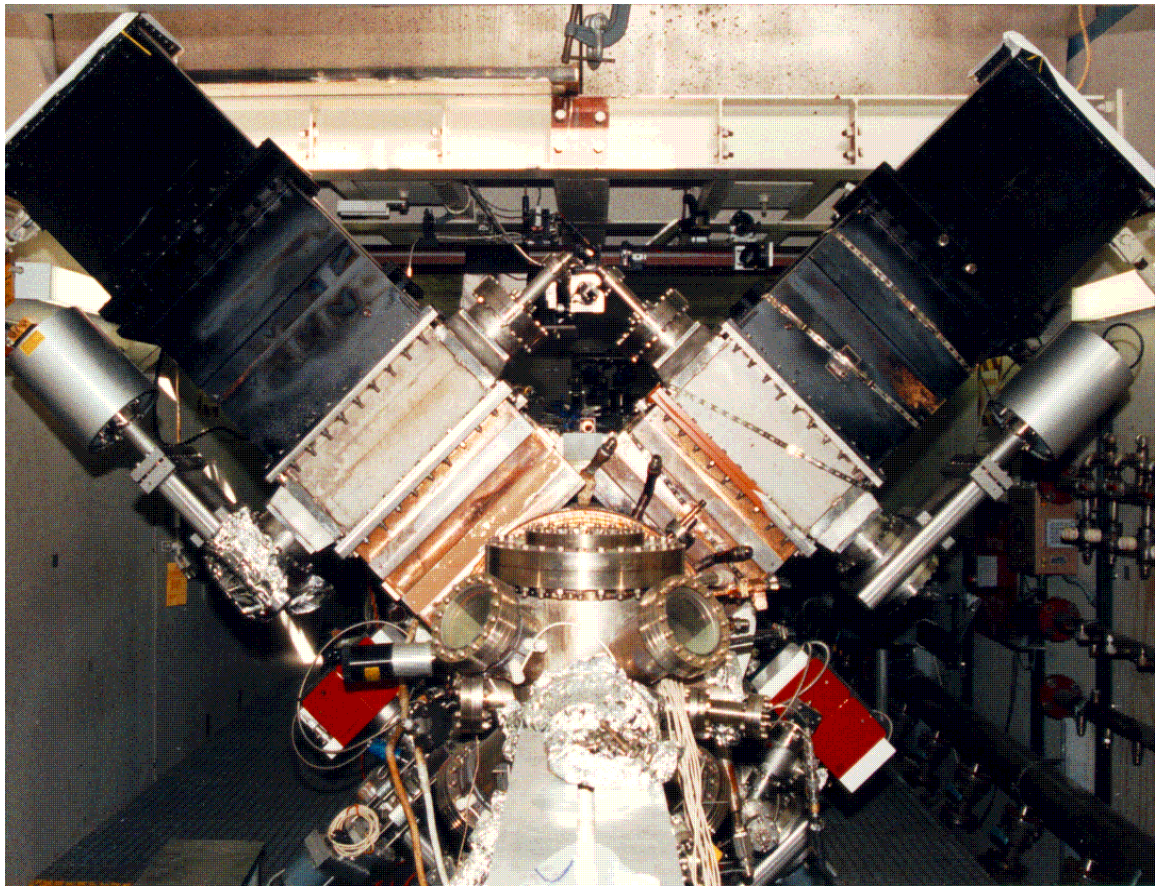

Demonstrated Performance of 433 MHz Photocathode Gun, 1992 H-D Test

Photocathode Performance:		
	Photosensitive Material:	K_2CsSb Multialkali
	Quantum Efficiency:	5% to 12%
	Peak Current:	45 to 132 amperes
	Cathode Lifetime:	1 to 10 hours
	Angle of Incidence:	near normal incidence
Gun Parameters:		
	Cathode Gradient:	26 MV/meter
	Cavity Type:	Water-cooled copper
	Number of cells:	4
	RF Frequency:	433 $x10^6$ Hertz
	Final Energy:	5 MeV(4-cells)
	RF Power:	600 $x10^3$ Watts
	Duty Factor:	25%, 30 Hertz and 8.3 ms
Laser Parameters:		
	Micropulse Length:	53 ps, FWHM
	Micropulse Frequency:	27 $x10^6$ Hertz
	Macropulse Length:	10 ms
	Macropulse frequency:	30 Hertz
	Wavelength:	527 nm
	Cathode Spot Size:	3-5 mm FWHM
	Temporal and Transverse Distribution:	gaussian, gaussian
	Micropulse Energy:	0.47 microjoule
	Energy Stability:	1% to 5%
	Pulse-to-pulse separation:	37 ns
	Micropulse Frequency:	27 $x10^6$ Hertz
Gun Performance:		
	Emittance (microns, RMS):	5 to 10 for 1 to 7 nCoulomb
	Charge:	1 to 7 nCoulomb
	Energy:	5 MeV
	Energy Spread:	100 to 150 keV

RF Characteristics of 433 MHz Gun Cavities

Measured Values

Measured Gun Cavity RF Characteristics

Parameter		L1	L2	Units
frequency	f	433.33	433.33	MHz
shunt impedance	$R=V^2/P_c$	2.86	4.28	MΩ
coupling coefficient	β	3.1	3.1	

Operating Parameters for Existing Gun Cavities
External Coupling Coefficient β=3.1

Parameter		L1	L2	Units
nominal accelerating voltage	V	0.9	1.1	MV
wall loss power	P_c	285	285	kW
beam power @ I_{avg}=200 mA	P_b	180	220	kW
forward power required	P_k	515	545	kW
reflected power	P_r	50	40	kW

Optimized for 200 Milliamperes

Operating Parameters for PERL-Optimized Gun Cavities
External Coupling Coefficient β=2.0

Parameter		L1	L2	Units
nominal accelerating voltage	V	0.9	1.1	MV
wall loss power	P_c	285	285	kW
beam power @ I_{avg}=200 mA	P_b	180	220	kW
forward power required	P_k	470	505	kW
reflected power	P_r	5	2	kW

Data supplied by A.M. Vetter.
See also:
J.L. Warren, T.L. Buller and A.M. Vetter,
"Design of MCTD Photoinjector Cavities",
Proc. 1989 IEEE PAC, Vol I, pp.420-422.
May 20-27, 1989, Chicago, Illinois,

Types of Photocathodes

Material	QE Range	Drive Laser Wavelength	Cathode Fab.	Vacuum Req.	Drive Laser
Metal (Cu, Mo…)	~0.02-0.06%	260 nm, UV	None	10^{-7} T	Difficult
CsK_2Sb	10-14%	527 nm	Difficult	10^{-10} T	Moderate
CsTe	10-14%	260 nm	Easy	10^{-9} T	Moderate to Difficult
LaB_6	~0.1%	355 nm	Easy	10^{-7} T	Difficult
Ga As (Cs)	1-5%	527 nm	Moderate	10^{-11} T	Moderate

Photocathode Fabrication Chamber

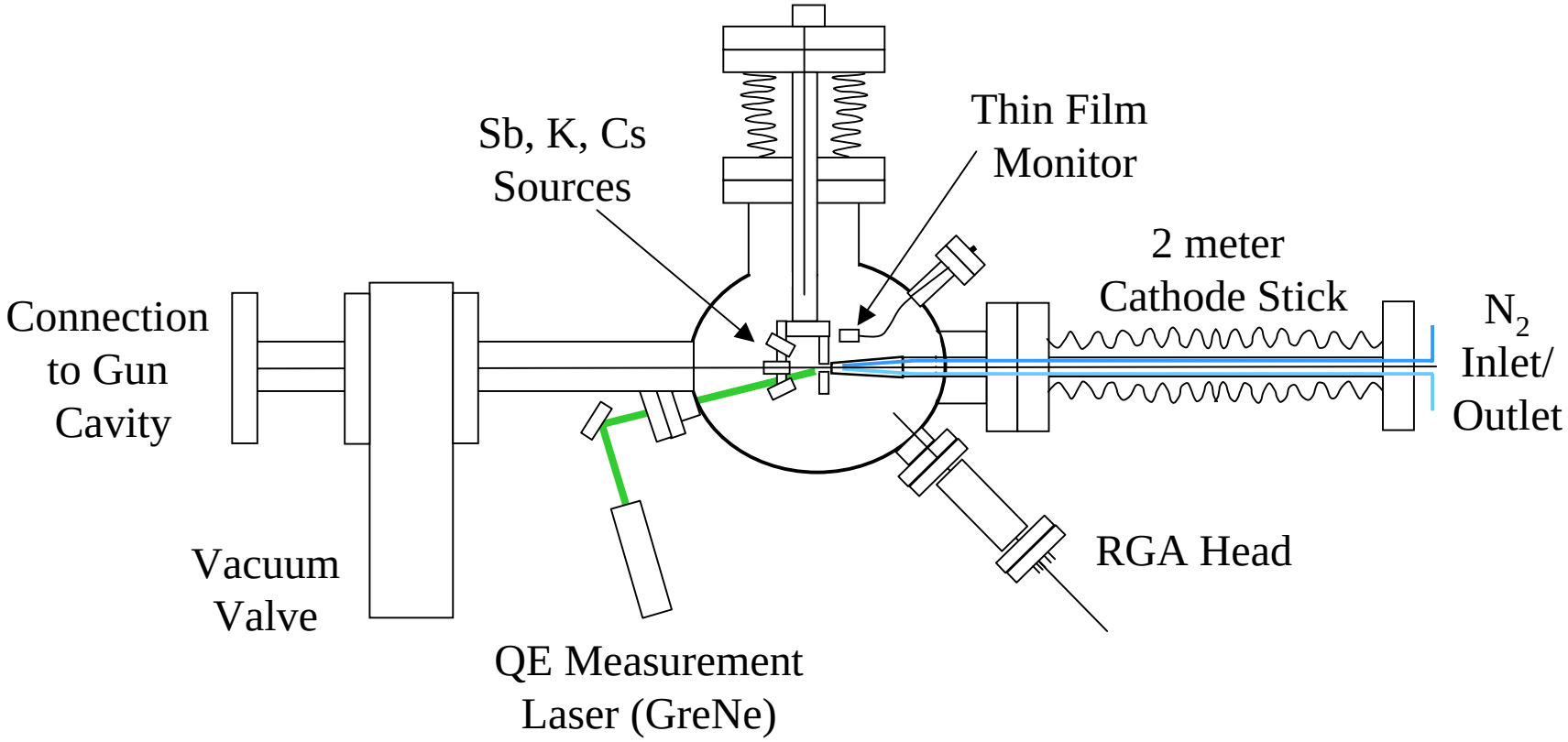

QE Fabrication History and Gun Space Charge Limits

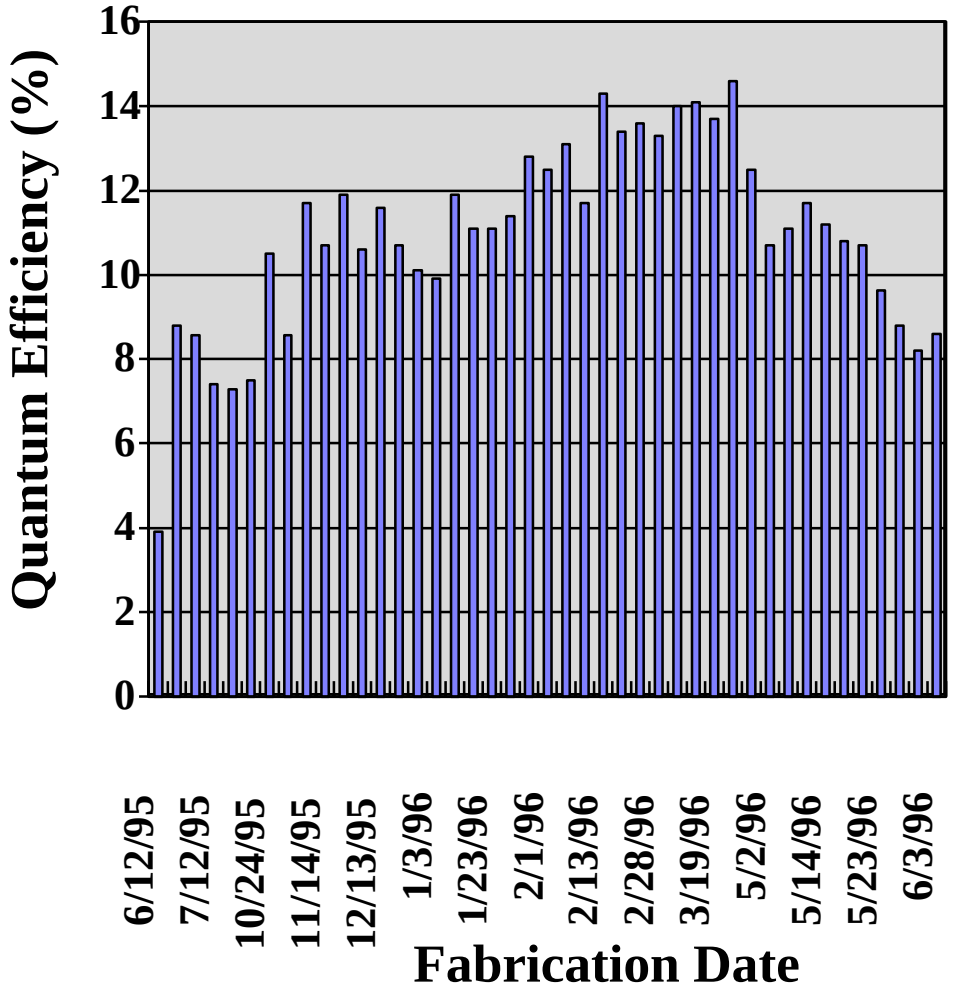

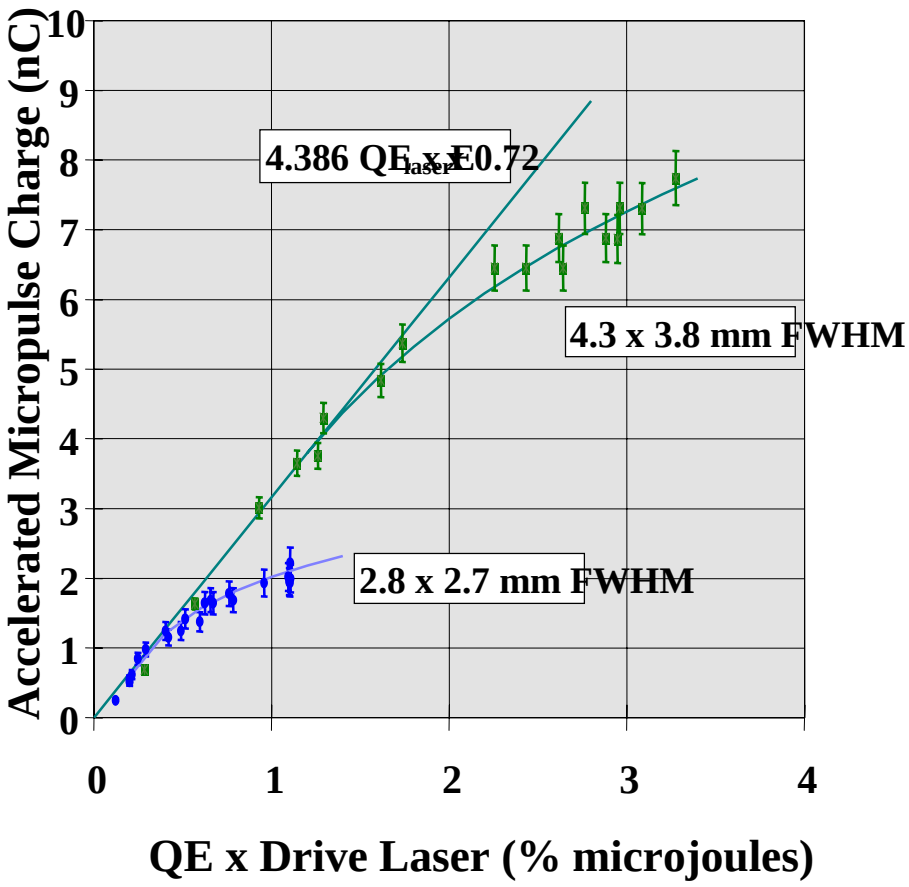

Cathode Lifetime Vs. H_2O Partial Pressure

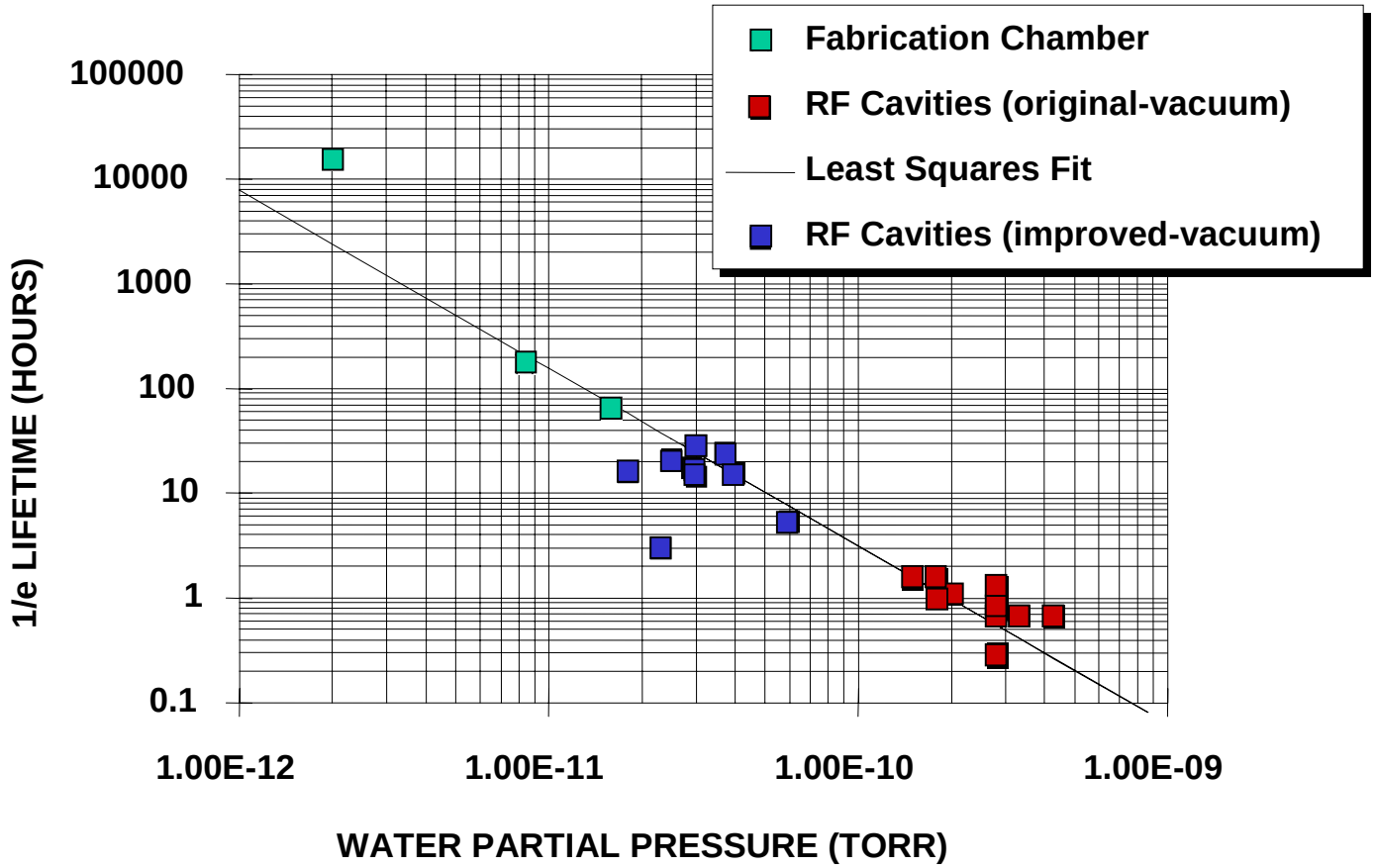

Photocathode 1/e Lifetime Vs. Duty Factor

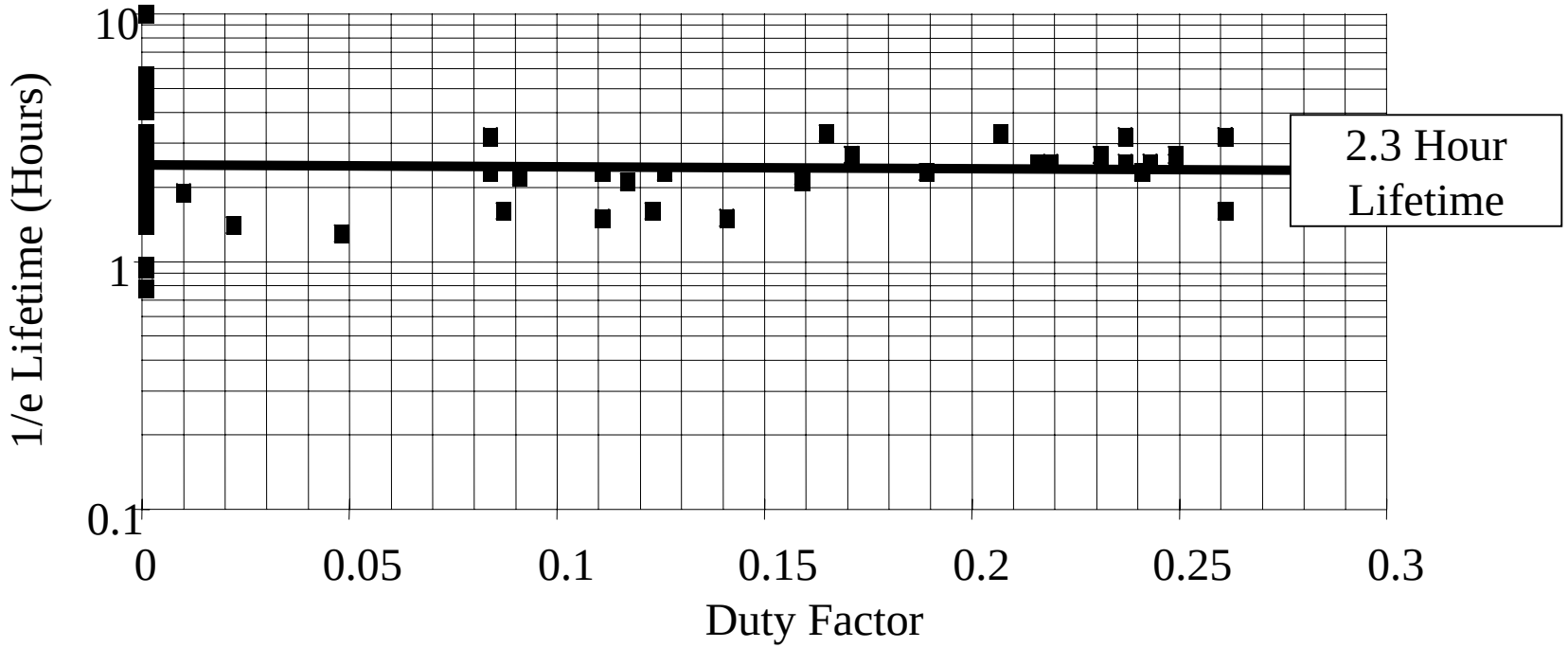

Cathode Rejuvenation and Improving Lifetime by Operating with Hot Cathode

Rejuvenating a used K_2CsSb cathode by heating it to 120 degrees C. The quantum efficiency increases at the rate of 2.5% / hour

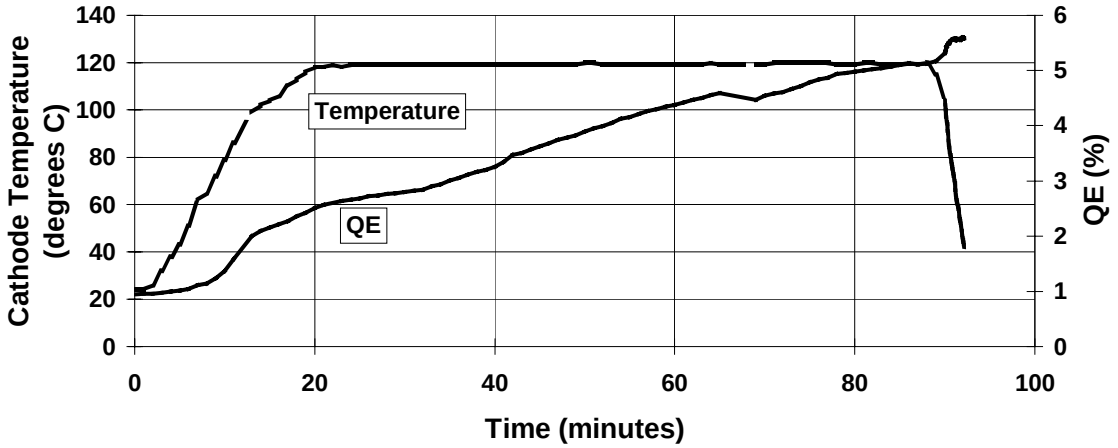

Photocathode quantum efficiency at elevated temperature in the RF cavity vacuum

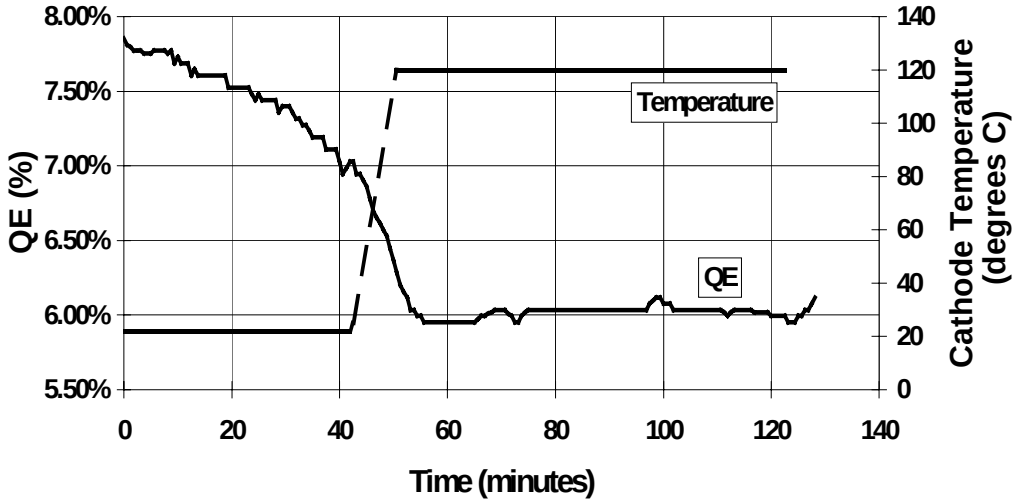

Heating the Cathode With a High Power Diode Laser

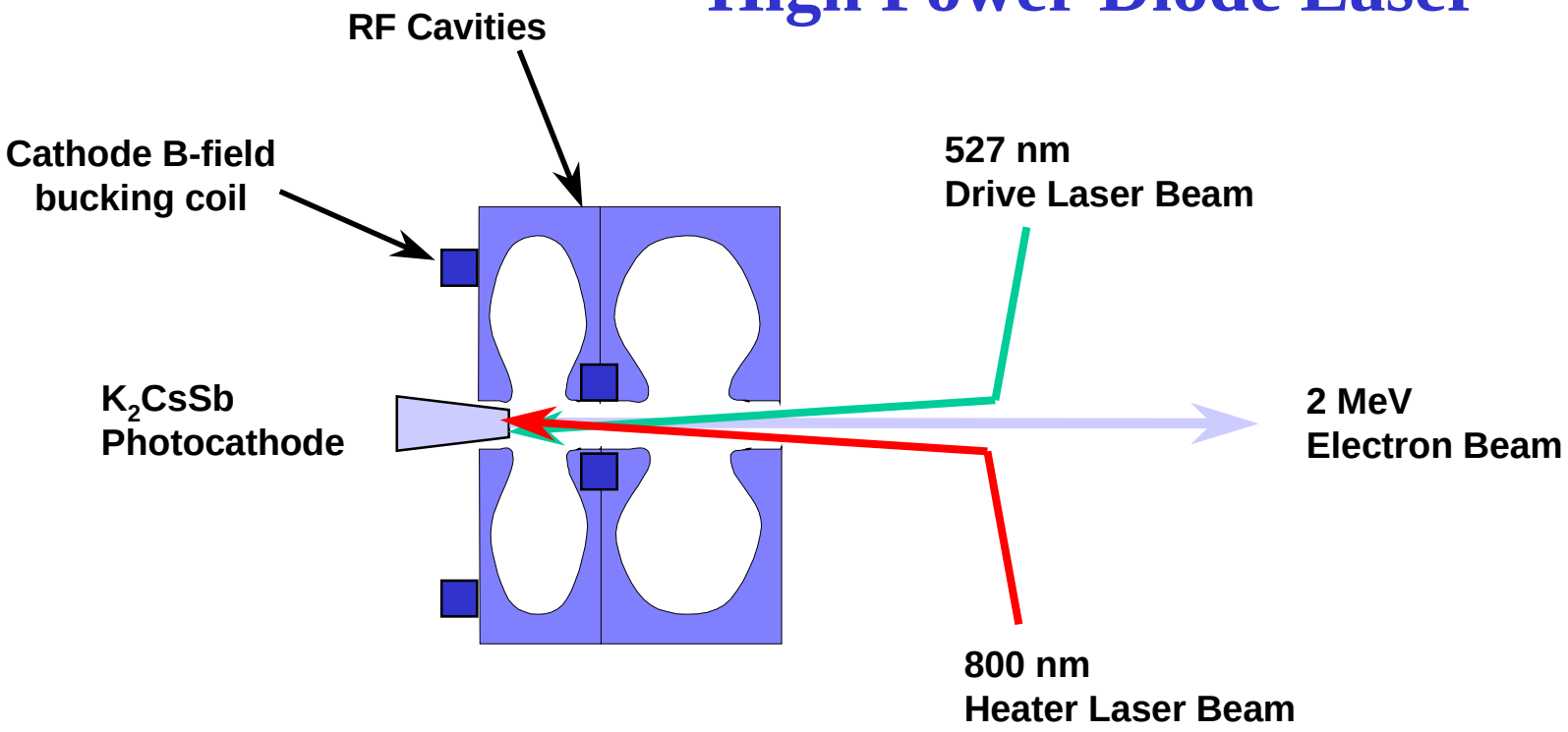

Drive Laser Configuration
Used in 1992 High Duty Test

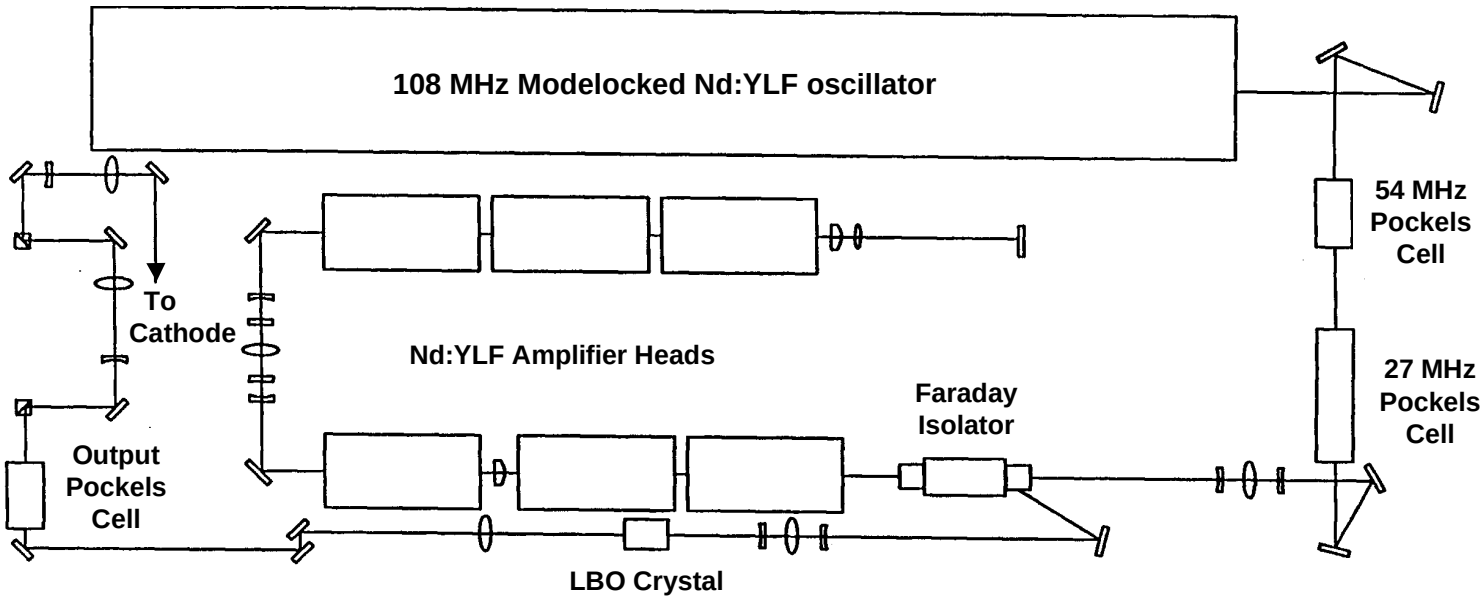

433 MHz Gun Transverse Beam Quality Measurements
1992 and 1994-1996 Test Results

Gun Emittance Vs. Microbunch Charge

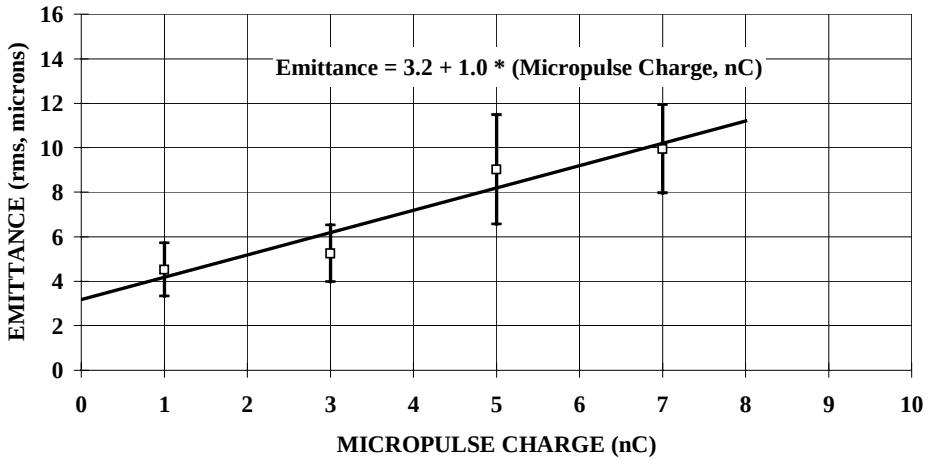

Beam Emittance at 3 nC Gaussian-Gaussian Distributions

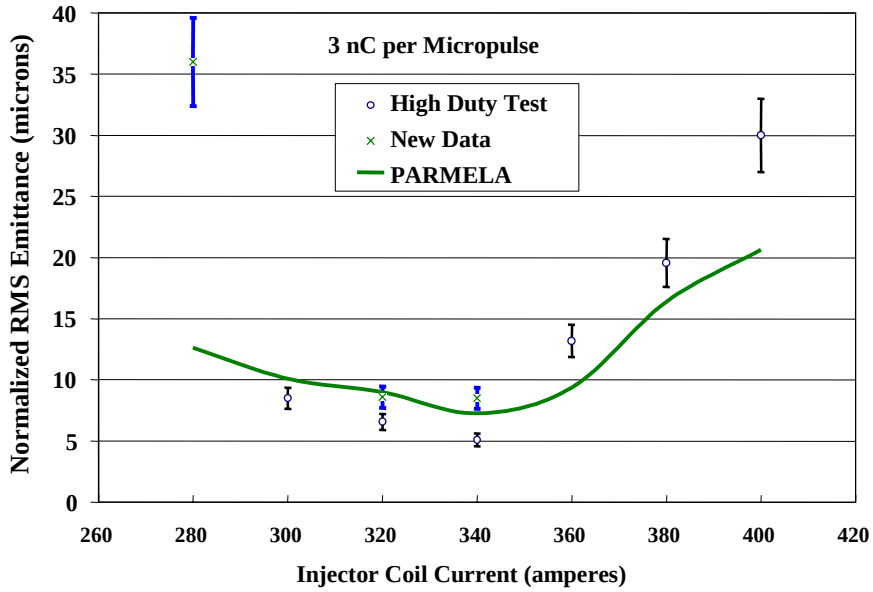

PARMELA_B Simulations at 0.5 nC

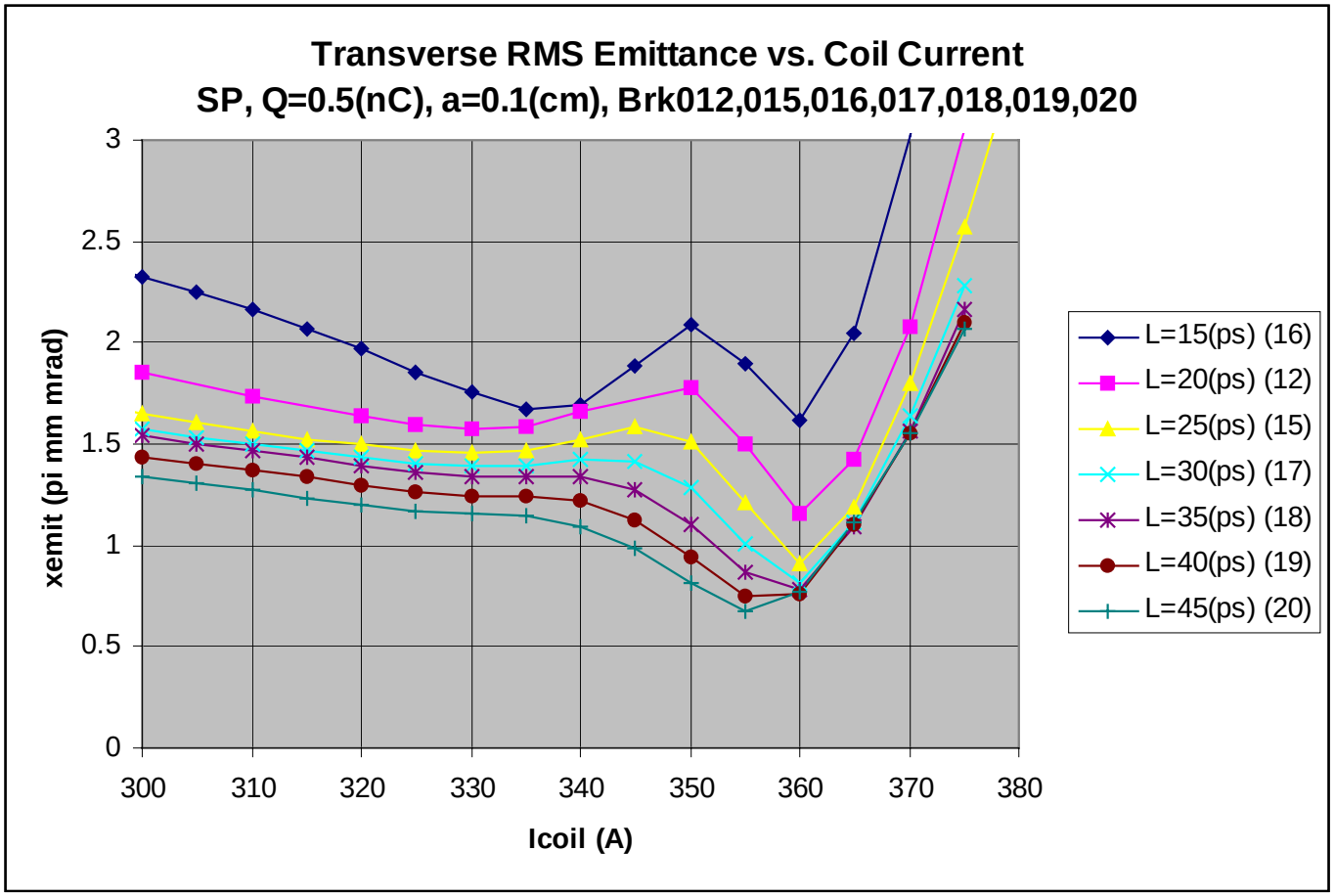

PARMELA_B calculations provided by B. Koltenbah, Boeing

Longitudinal Emittance

Components of the ELSA Accelerator Used to Make the Longitudinal Phase Space Measurements

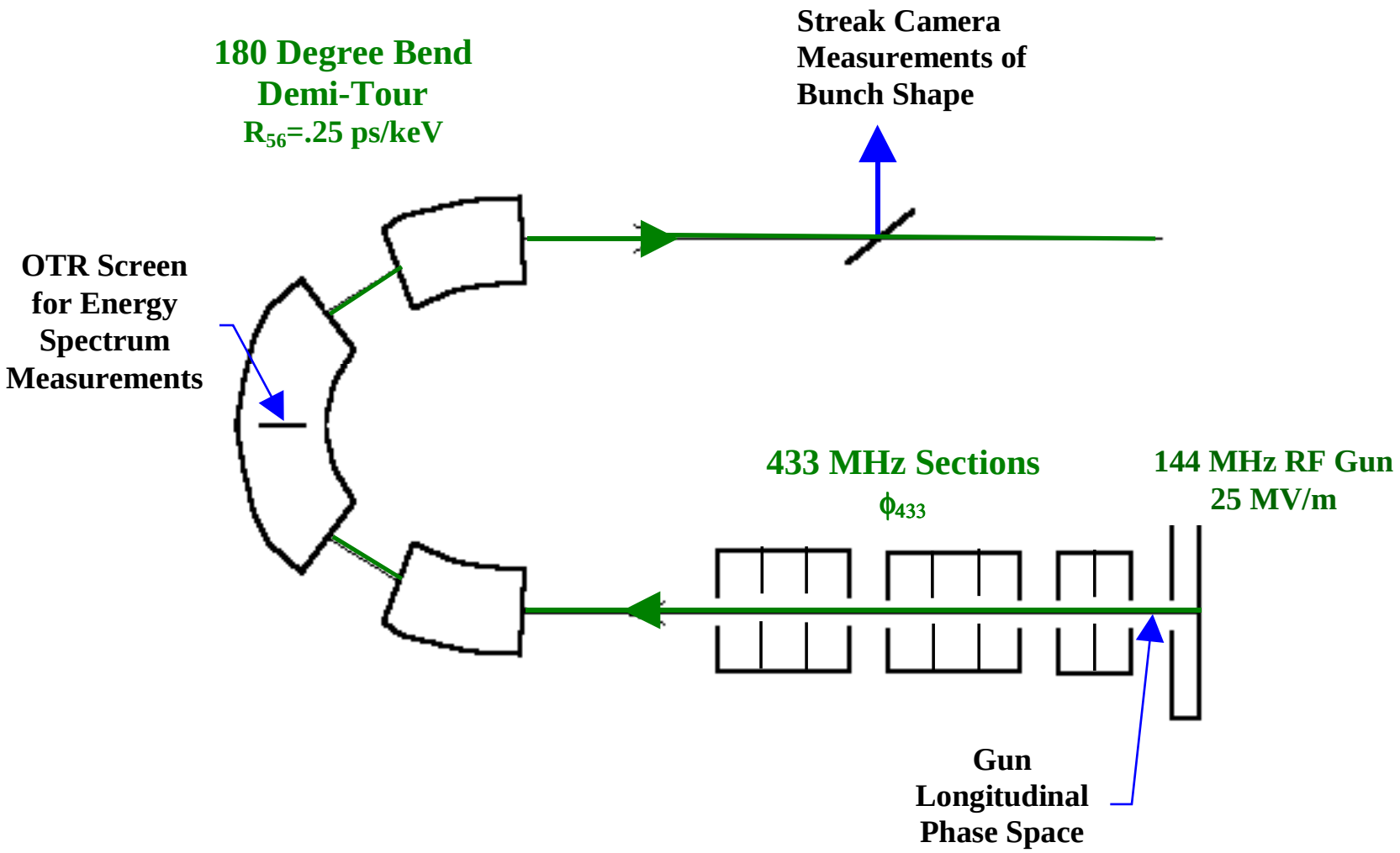

Definition of Phase Space Parameters, Including Correlations

Longitudinal Beam Ellipse:

$$\gamma\Delta t^2 + 2\alpha\Delta t\Delta E + \beta\Delta E^2 = \frac{\varepsilon_\ell}{\pi}$$

Longitudinal Beam Matrix:

$$\tau = \begin{pmatrix} \tau_{11} & \tau_{12} \\ \tau_{12} & \tau_{22} \end{pmatrix} = \varepsilon_\ell \begin{pmatrix} \beta & \alpha \\ \alpha & \gamma \end{pmatrix}$$

$\sqrt{\tau_{11}}$ = **Uncorrelated Bunch Length**

$\sqrt{\tau_{22}}$ = **Uncorrelated Energy Spread**

Include correlated emittance by distorting the ellipse boundary using quadratic and cubic terms:

$$\Delta E = -\frac{\alpha}{\beta}\Delta t \pm \sqrt{\left(\frac{\alpha}{\beta}\Delta t\right)^2 - \frac{\gamma\Delta t^2 - \frac{\varepsilon_\ell}{\pi}}{\beta}} + a\Delta t^2 + b\Delta t^3$$

Distortions of the Longitudinal Phase Space Ellipse

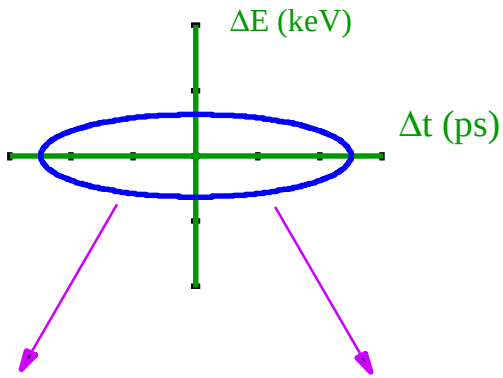

Undistorted Phase Space
$\tau_{12} = 0$
a = 0, b = 0

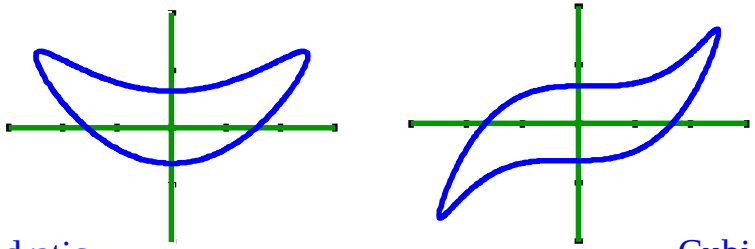

Quadratic Distortion
$\tau_{12} = 0$
a > 0, b = 0

Cubic Distortion
$\tau_{12} = 0$
a = 0, b > 0

Fits to 1 nC per Microbunch Data

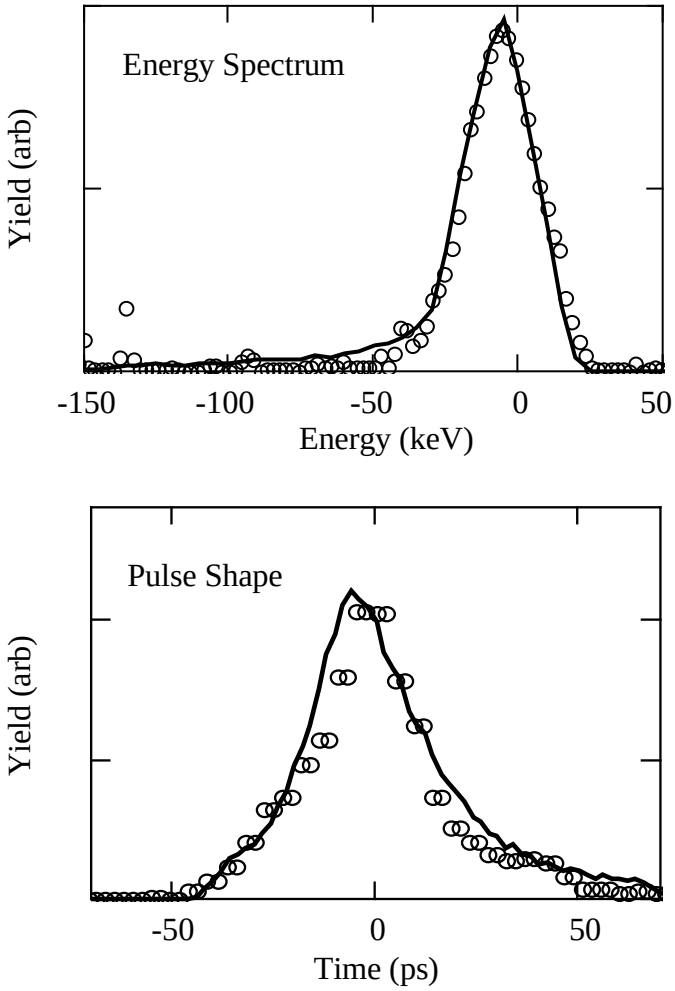

Longitudinal Phase Space Distributions Obtained from the Data Analysis

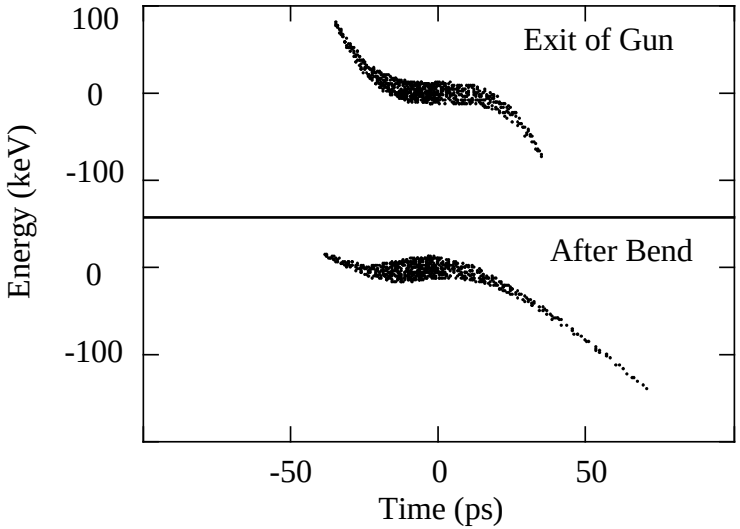

Ref: S. Joly et al.,...

The Uncorrelated Emittance Grows Linearly with Surface Charge Densities Below the Space Charge Limit

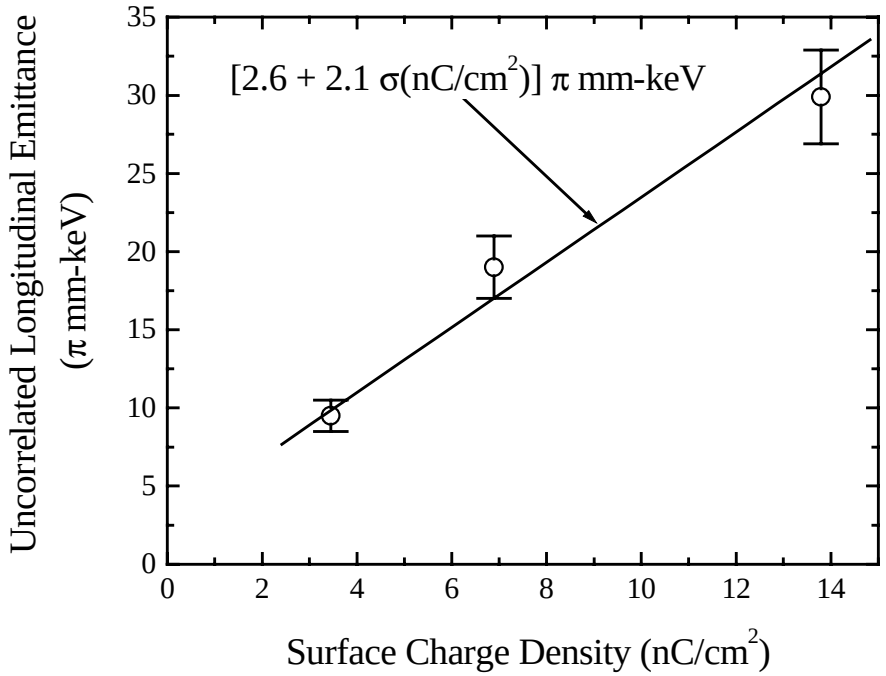

In These Experiments Most of the Emittance Growth Was due to Increased Energy Spread

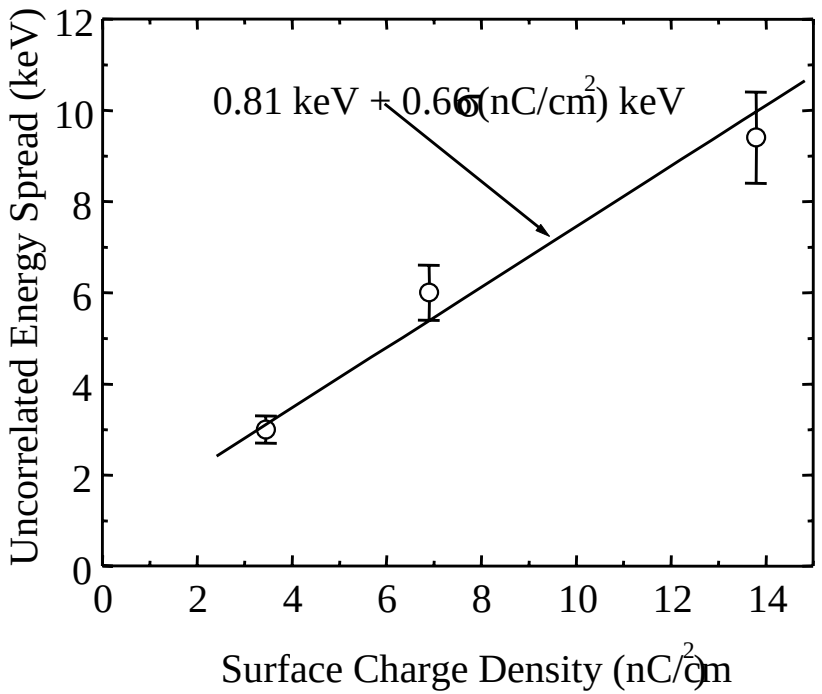

Pulse length a constant 11 ps(rms)

10 nC/cm² corresponds to 11 MV/m

Ref: D.H. Dowell et al., PAC97.

Summary and Conclusions

433 MHz PhotoIjnector Design Philosophy/Approach:
- **Gun, Booster, Linearizer and Compressor**

433 MHz Gun has Demonstrated Most of the PERL Requirements:
- **Duty Factor**
- **Beam Quality:**
  - **Transverse and Longitudinal Emittance**

Problems and Unfinished Business:
- **Cathode Lifetime**
- **Cathode Fabrication**
- **Drive Laser**
- **RF Design and Controls**
- **Experimental Verification of Low Emittance at 0.5 nC**
- **Start-to-End Simulations**
- **CSR Experiments**

The New L-Band 1 ½ Cell Photocathode RF Gun at Argonne*

M.E. Conde, W. Gai, R. Konecny, J.G. Power, P. Schoessow, X. Sun, ANL, Argonne, IL 60439, USA

Abstract

We report on the status of the new short bunch, high intensity electron gun at the Argonne Wakefield Accelerator. The 1-1/2 cell L-band photocathode RF gun is expected to produce 10 – 100 nC bunches with 2 – 5 ps rms pulse length and normalized emittance less than 100 mm mrad. The beam energy at the exit of the gun cavity will be in the range 7.5 – 10 MeV. A standing-wave linac structure operating at the same frequency (1.3 GHz) will increase the beam energy to about 15 MeV. This beam will be used in wakefield acceleration experiments with dielectric loaded structures. These travelling-wave dielectric loaded structures, operating at 7.8 and 15.6 GHz, will be excited by the propagation of single bunches or by trains of up to 32 electron bunches.

1 INTRODUCTION

High current short electron beams have been a subject of intensive studies [1]. One of the particular uses for this type of beam is in wakefield acceleration applications. High current (kA) short electron beam generation and acceleration did not materialize until the advent of RF photoinjector technology[2]. Although most photocathode RF gun development has been concentrated on high brightness, low charge applications such as free electron laser injectors, there have been several relatively high charge RF photocathode based electron sources built and operated[3,4,5]. In general, there are two approaches to attaining high peak current. One approach is to generate an initially long electron bunch with a linear head-tail energy variation that is subsequently compressed using magnetic pulse compression. The advantage of magnetic compression is that it is a well-known technology and can produce sub-picosecond bunch lengths. However, due to strong longitudinal space charge effects, this technology is limited to relatively low charges (<10 nC).

Another approach is to directly generate short intense electron bunches at the photocathode and then accelerate them to relativistic energies rapidly using high axial electric fields in the gun [3]. The advantage of this approach is that it can deliver very high charges, for example, 100 nC if one uses an L-band gun. This would satisfy the requirements of most electron driven wakefield experiments for both plasma and dielectric structures, if the pulse length is short enough (< 10 ps FWHM). So far, the Argonne Wakefield Accelerator (AWA) has demonstrated the capability of producing 100 nC, 25 — 35 ps (FWHM) electron beams at 14 MeV. This unprecedented performance was obtained using a half cell photocathode gun cavity and two standing wave iris-loaded linac sections [6]. The AWA machine has reached its design goal and has been used for dielectric wakefield [7] and plasma [8] experiments. The initial results are encouraging [9]. Achieving higher gradients in wakefield experiments would require the drive electron pulse to be even shorter and have a lower emittance. In this paper, we discuss the design of a new RF photocathode gun with the capability of producing 10 - 100 nC with 2 - 5 ps (rms) pulse lengths.

2 DESIGN CONSIDERATIONS

In order to generate high charge and short bunch lengths from a photocathode RF gun, the electric field on the cathode surface has to be very intense. In this way the electrons leaving the cathode surface are quickly accelerated to relativistic velocities, minimizing the bunch lengthening and the emittance growth that the space charge forces produce [10,11]. There is also bunch lengthening and transverse emittance growth at the exit iris of the gun cavity due to the defocusing forces of the RF fields. Thus, this effect also calls for high accelerating gradient and high beam energy at the exit of the gun. It is therefore desirable to have a multicell gun with high accelerating gradient. Practical considerations (mainly a finite amount of RF power) limit the design to 1 – 1/2 cells. The choice for our new gun design is a Brookhaven type 1– 1/2 cell cavity [12] scaled up to L band operation. This gun will be followed by one of the present linac tanks that exist at the AWA facility.

A detailed numerical study [13, 14] of this gun was performed with the codes SUPERFISH and PARMELA [15]. Table 1 summarizes the parameters used in the simulations. These extensive numerical simulations showed a strong dependence of bunch length and emittance with respect to the accelerating gradient in the gun cavity (Fig. 1). Based on these studies, it was decided that an accelerating gradient of 80 MV/m on the cathode

* This work is supported by the Department of Energy, High Energy Physics Division, Advanced Technology Branch under the Contract No. W-31-109-ENG-38.

surface was a good operating point. This requires 10 MW of RF power to be coupled into the gun cavity, which still leaves enough power to run one of the linac tanks. This accelerating gradient yields good values of emittance and bunch length, while still not high enough to make the RF conditioning of the gun a challenging task. (In fact, we recently conditioned a duplicate of the present AWA gun up to a gradient of 125 MV/m [16].)

Table 1. The gun design parameters as calculated using SUPERFISH.

Inner Radius of the Cell, b (cm)	9.03
Radius of the iris, a (cm)	2.75
Width of the iris, d (cm)	1.5
Aperture of the exit (cm)	2.5
Operating frequency (GHz)	1.3
Initial beam radius (cm)	1
Quality factor, Q	26008

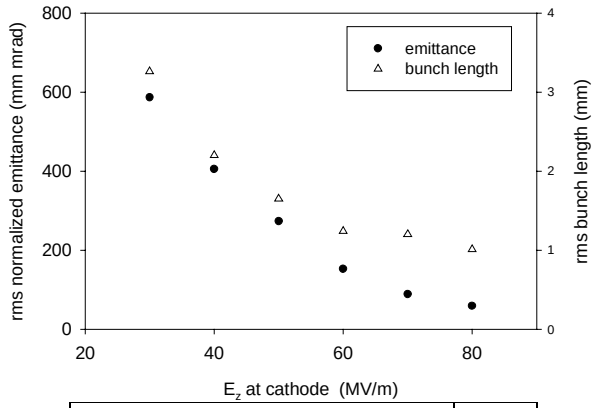

Shunt impedance (MΩ/m)	36.47

Figure 1: Emittance and bunch length as a function of the accelerating gradient on the cathode surface, for a 40 nC bunch.

3 CONSTRUCTION AND RF MEASUREMENTS

The RF gun will be operated with a focusing solenoid and a bucking solenoid to cancel the magnetic field on the plane of the cathode. These two solenoids are exactly next to each other, with the photocathode plane as their plane of symmetry. This maximizes the space available for the RF power coupler over the full cell of the gun. There is a vacuum pumping port in the full cell, located diametrically opposite to the RF coupler, both being at the equator line of the full cell. An RF pickup probe is placed near the vacuum pumping port, relying on the evanescent RF fields present in that location. An RF tuning plunger is located half way along the circumference of the full cell between the RF coupler and the vacuum pumping port. This breaks the symmetry of the full cell, but it is acceptable in our L-band size cavity. The perturbation of the field lines near the axis of the cavity is negligible. In the half cell, the cathode holder can also function as a tuning plunger, allowing us to adjust the parameters of the two cells, in order to achieve the right resonance frequency for the π mode and field balance in the cavity. The cooling channels are drilled along the cylindrical wall of the gun, and also run over part of the back and front plates of the cavity.

Numerical simulations of this final design yield values for the emittance and bunch length that are slightly worse than the ones obtained in reference [13, 14]. This results from the fact that the location and dimensions of the solenoids are not dictated only by the optimization of the beam parameters, but also by other physical constraints. The degradation is however very small, and the gun is still expected to generate very short bunches with low emittance. Results of numerical simulations with PARMELA are shown in Fig. 2. These plots show emittance, bunch length, energy and radial coordinate as a function of the longitudinal coordinate along the accelerator for a bunch charge of 40 nC. At the exit of the linac the code predicts a normalized rms emittance of 66 mm mrad and an rms bunch length of 3.7 ps.

Figure 2: Numerical simulations of a 40 nC electron

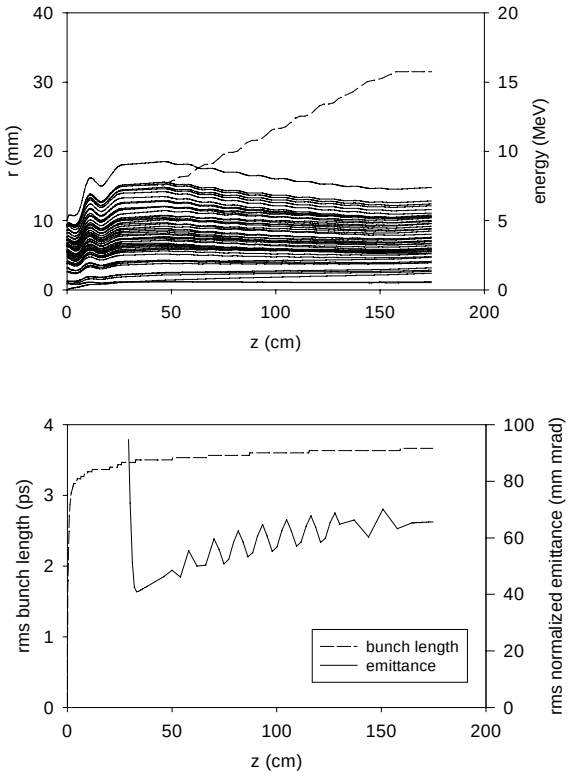

bunch as it propagates along the gun and linac structures: (a) energy and trajectories in the transverse plane; (b) bunch length and emittance.

The gun (Fig. 3) is presently being installed in a test area for RF conditioning and commissioning. The value of the unloaded quality factor (Q_0) of the gun is presently

21000, but this number will increase slightly when the final cathode holder (with better electric contact) is installed. Figure 4 shows the profile of the axial electric field along the axis of the cavity measured by the usual bead-pulling technique. After the final brazing cycle the gun cavity became somewhat overcoupled (S_{11} = −10 dB); a tuning post in the waveguide will improve the coupling.

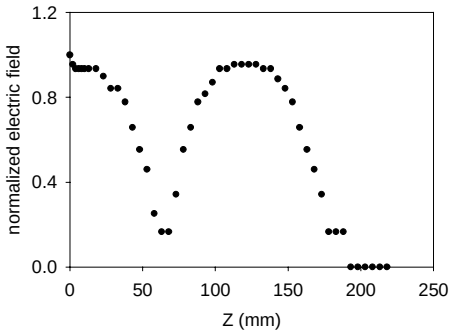

Figure 3: Gun before final brazing cycle.
Figure 4: Profile of axial electric field along the axis of the cavity.

4 CONCLUSION

The new AWA photocathode RF gun will dramatically improve the capabilities of our program to study wakefield acceleration in dielectric loaded structures and plasmas. The electron beam produced by this gun is expected to excite wakefields in plasmas with accelerating gradients in excess of 1 GeV/m with a plasma density of ~10^{14} /cm^3.

In dielectric loaded structures, this beam will also make a significant improvement over presently attainable gradients. One can use this beam to directly demonstrate collinear wakefield acceleration gradients in excess of 50 MV/m corresponding to 200 MW of RF power generated in 30 GHz dielectric structures.

It is worth pointing out that the present AWA photocathode RF gun has achieved unprecedented values of charge per bunch, and has allowed us to advance the understanding of wakefield acceleration in plasmas and in dielectric structures. However, the present gun was designed when only a very limited amount of RF power was available for the experiment (2 MW). Thus, the beam parameters, namely, bunch length and emittance, suffered serious limitations due to this relatively low level of RF power. The newly designed gun will take advantage of the higher level of RF power now available in the facility, yielding better beam parameters and, consequently, higher accelerating gradients in the wakefield acceleration experiments.

REFERENCES

[1] C. Travier, Proceedings of Advanced Acceleration Concepts Workshop, Edited by P. Schoessow, AIP Proceedings, No. **335**, p.57, 1994.
[2] J. Fraser *et al.*, IEEE Trans. Nucl. Sci., NS-32, p.1719 (1985).
[3] P. Schoessow *et al.*, Proceedings of Particle Accelerator Conference, p.976, 1995.
[4] B. Carlsten, *et al.*, Proceedings of Particle Accelerator Conference, p.985, 1995.
[5] E. Colby *et al.*, Proceedings of Particle Accelerator Conference, p.967, 1995.
[6] M.E. Conde *et al.*, Phys. Rev. ST Accel. Beams **1**, 041302 (1998); M.E. Conde *et al.*, Proceedings of Particle Accelerator Conference, p.1996, 1997.
[7] P. Schoessow *et al.*, Proceedings of Particle Accelerator Conference, p.639, 1997.
[8] N. Barov *et al.*, Phys. Rev. ST Accel. Beams **3**, 011301 (2000); N. Barov, M.E. Conde, W. Gai, J. Rosenzweig, Phys. Rev. Lett., Vol. 80, No. 1, p.81, 1998.
[9] P. Schoessow *et al.*, Journal of Applied Physics, Vol. 84, No. 2, p.663, 1998.
[10] K.J. Kim, Nuclear Instrumentation and Methods, **A275**, p.201, 1989.
[11] L.Serafini, J. Rosenzweig, Physical Review E, Vol. **55**, No. 6, p.7565, 1997.
[12] K. Batchelor *et al.*, Proceedings of European Particle Accelerator Conference, p.541, 1990.
[13] W. Gai *et al.*, Nucl. Instr. and Meth. A 410, p.431, 1998.
[14] W. Gai *et al.*, Proceedings of Advanced Acceleration Concepts Workshop, Baltimore, 1998.
[15] SUPERFISH and PARMELA, Las Alamos National Lab. Report LA-UR-96-1834, 1997 and LA-UR-96-1835, 1996.
[16] C.H. Ho *et al.*, Proceedings of Linac98 Conference, Chicago, 1998.

Ultra-stable Laser system for Photocathode RF gun Applications

Katsuyuki Kobayashi
Sumitomo Heavy Industries (USA), Inc
c/o Aculight Corporation
11805 North Creek Parkway S. Bothell, WA 98011
E-mail: kobayashi@aculight.com

A part of this work is performed under the management of the Femtosecond Technology Research Association , supported by New Energy and Industrial Technology Development Organization.

Contents

- Production
  - Pulrise
- Research & Development
  - Amplifier
  - Square pulse

Pulrise: Stable UV Laser for Photoinjector

Laser medium	Nd:YLF
Pulse width	12 ps @1047 nm, 8 ps @262 nm
Pulse energy	2 mJ @1047 nm, 0.2 mJ @262 nm
Jitter	<0.5 ps RMS
Dimension	600 mm(W)X900mm(D)X300mm(H)
Repetition rate	25 Hz (100 Hz available)

Stability of Pulrise

Energy stability (IR)

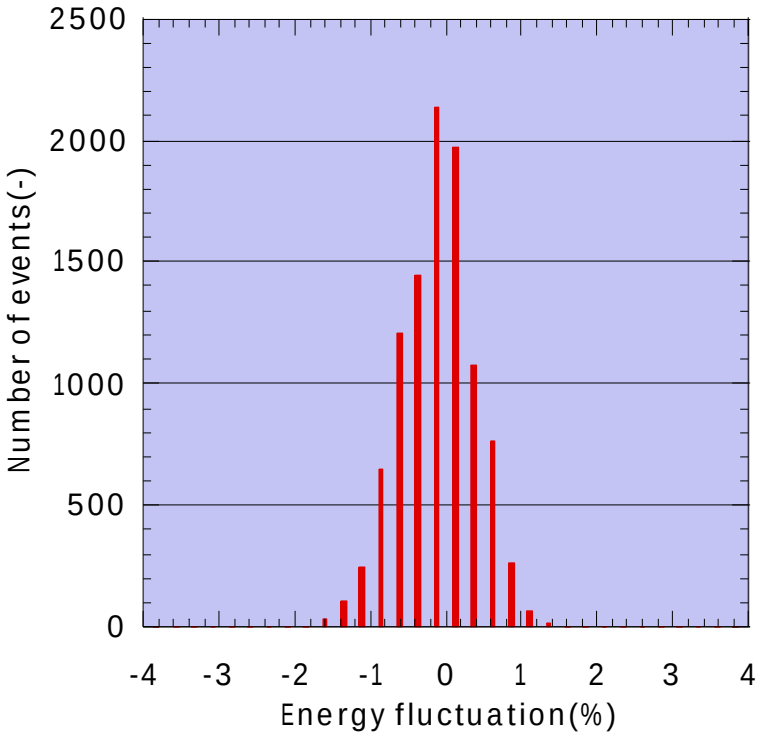

Total shot number 10000

Standard deviation 0.55%

Beam profile (IR)

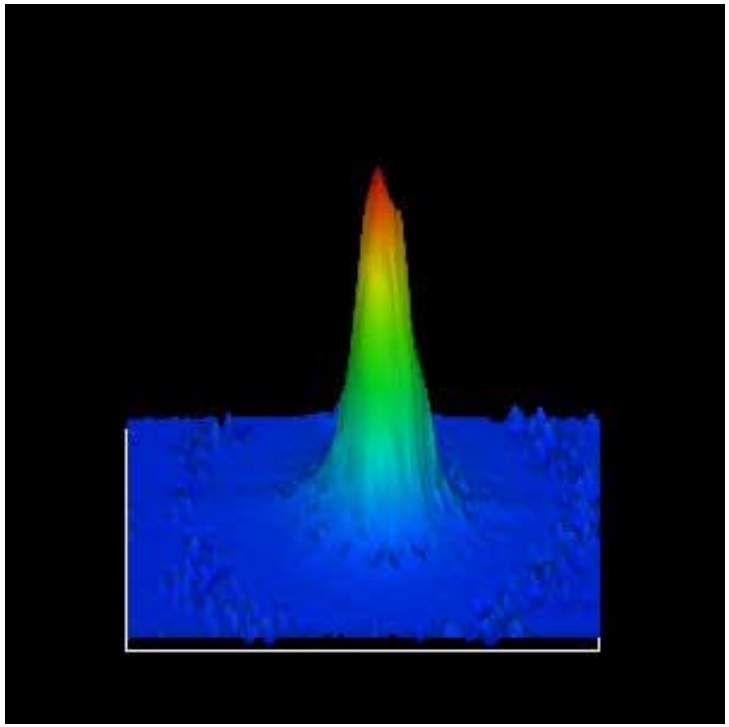

Pointing stability σ=5μrad

Electron Bunch Characteristics

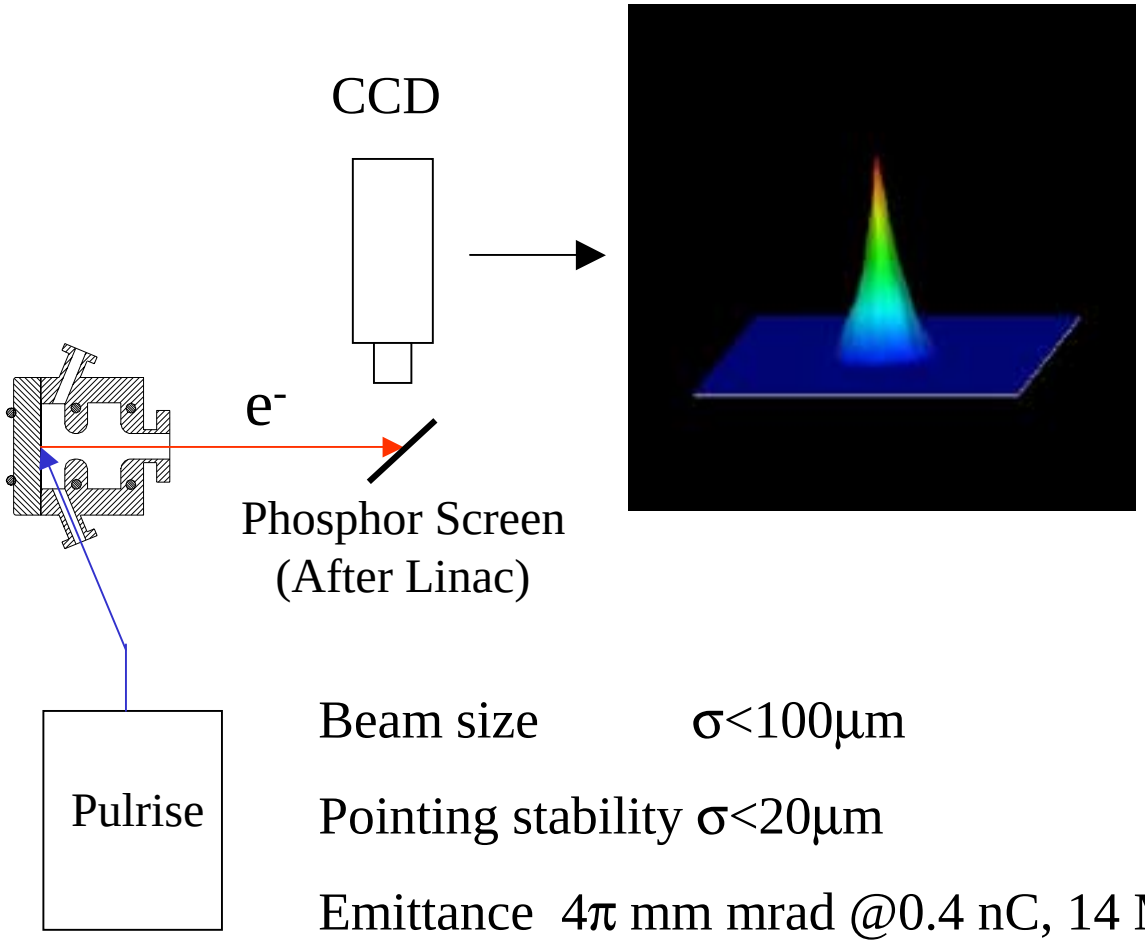

Beam size σ<100μm

Pointing stability σ<20μm

Emittance 4π mm mrad @0.4 nC, 14 MeV

Charge 4 nC (Max)

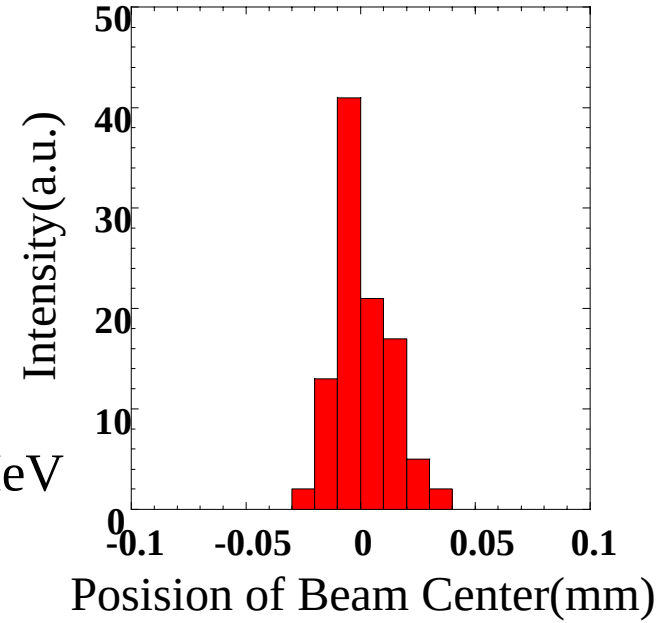

Nd:YLF Amplifier

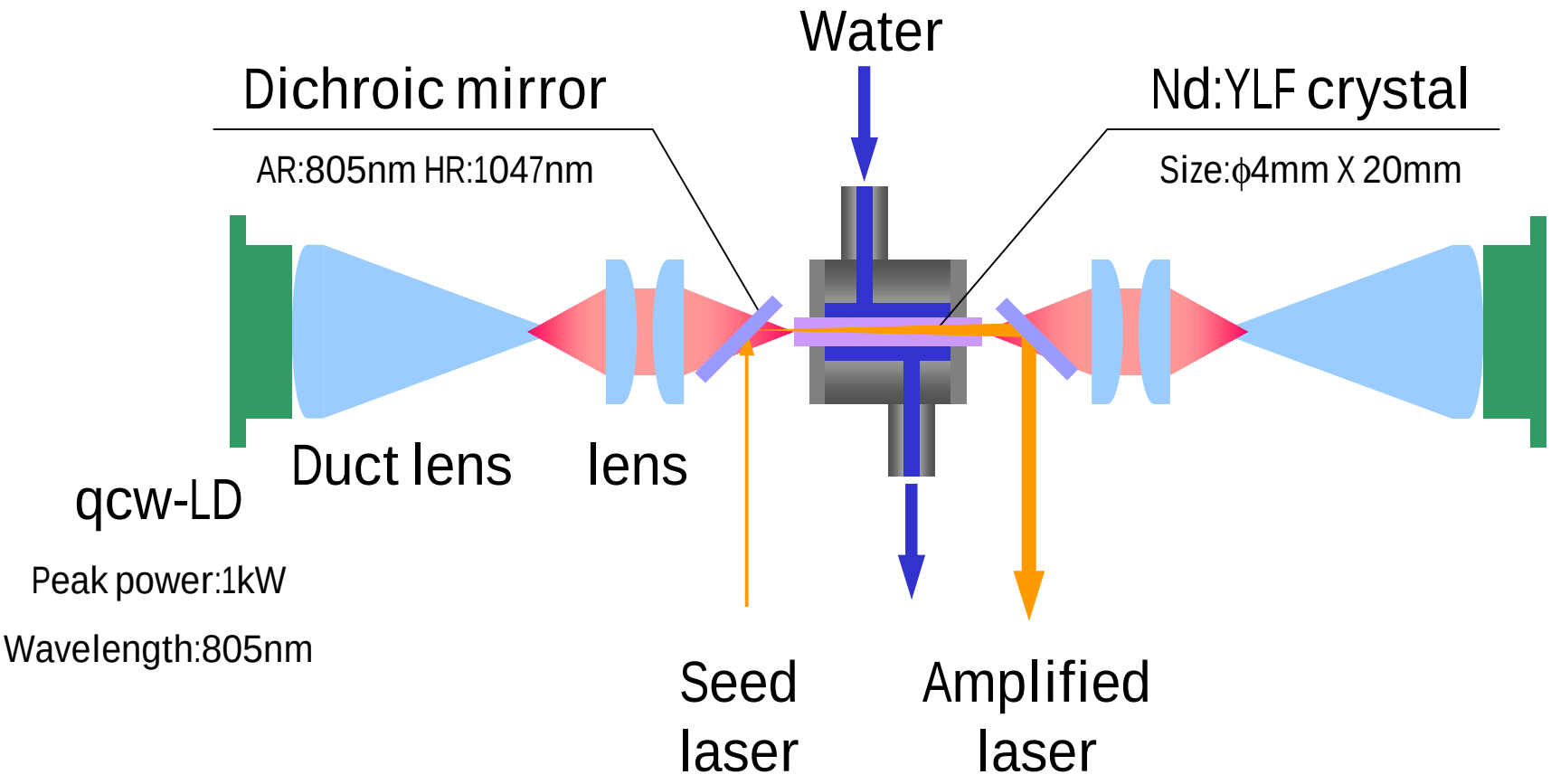

Nd:YLF Amplifier

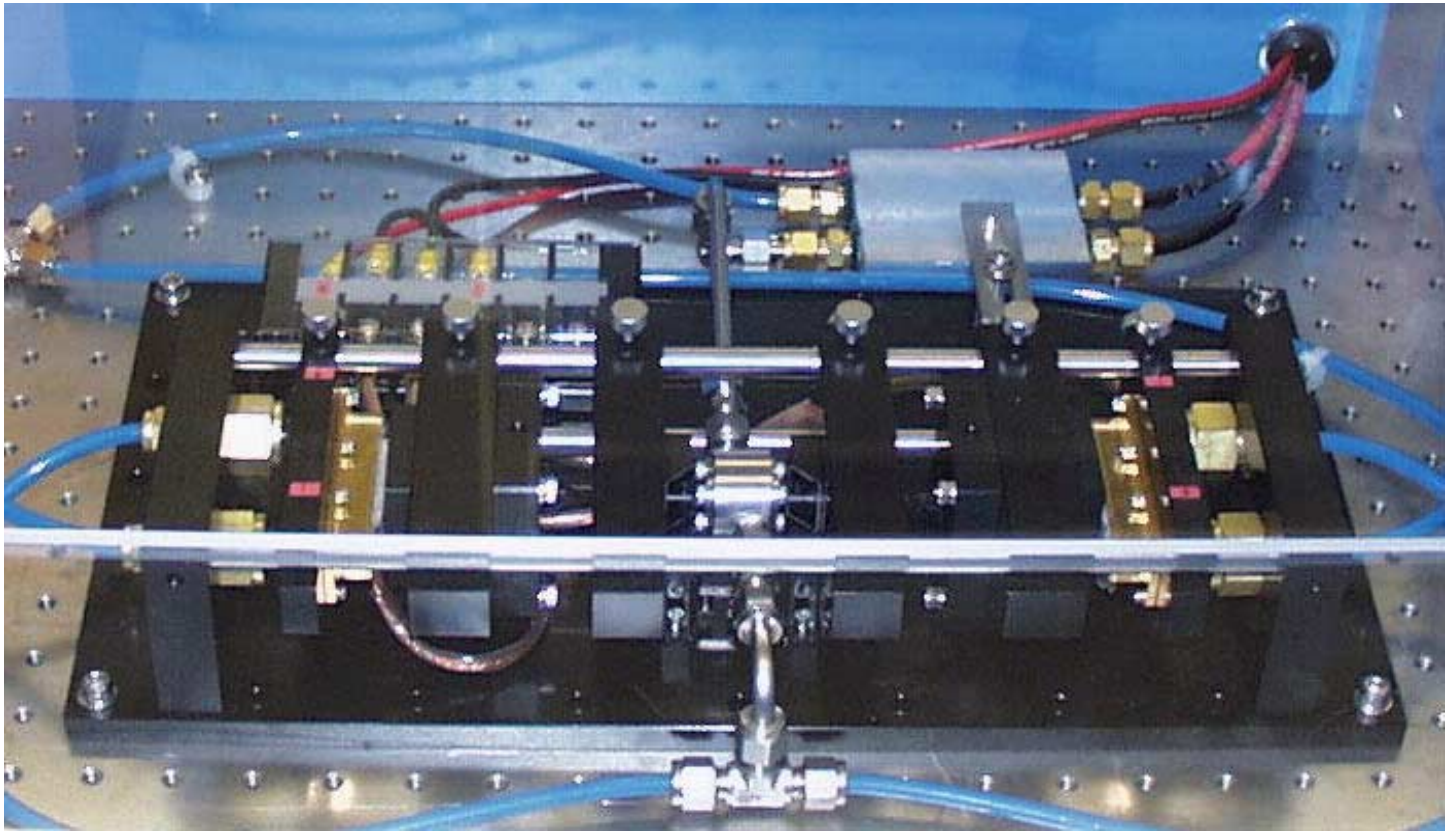

Amplification with 2-pass configuration

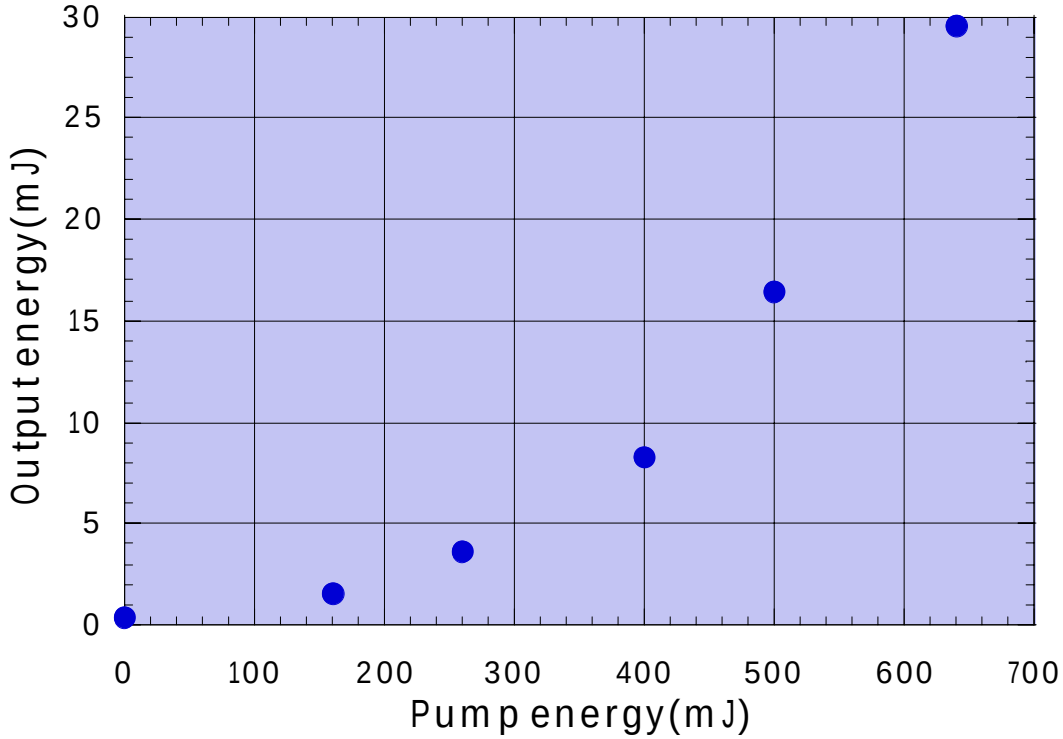

The amplifier was operated as double pass configuration. The seed laser energy was 0.4mJ. The pump laser pulse width was 400μs and the repetition rate was 10Hz .

Beam Profile and Focused Diameter

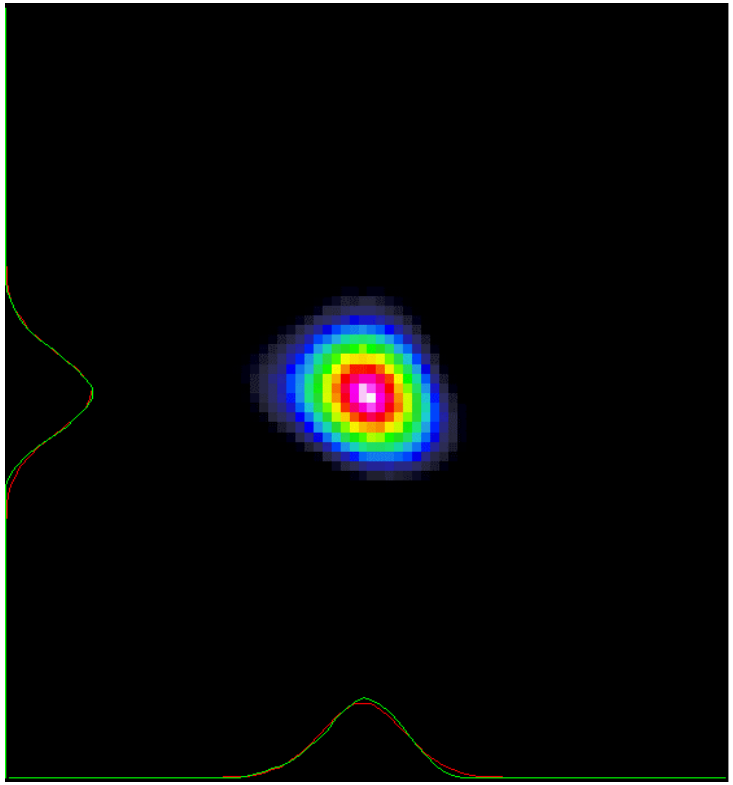

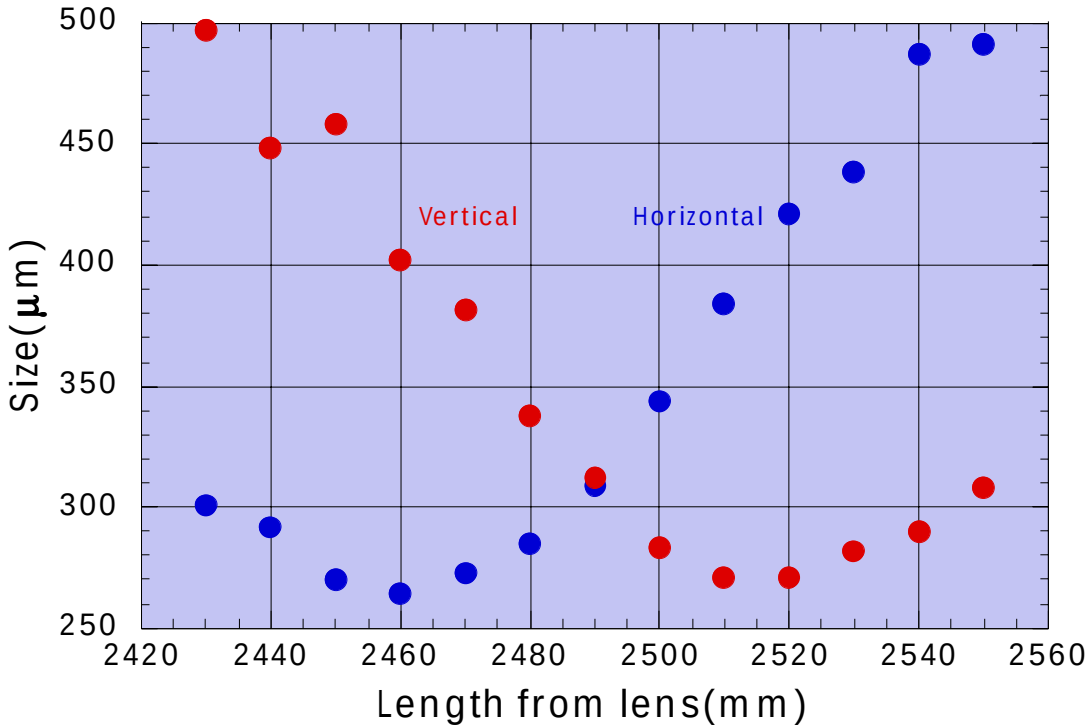

with 2500 mm lens

The beam diameter (the width of the 1/e^2 intensity level) was approximately 300μm.

Pulsewidth

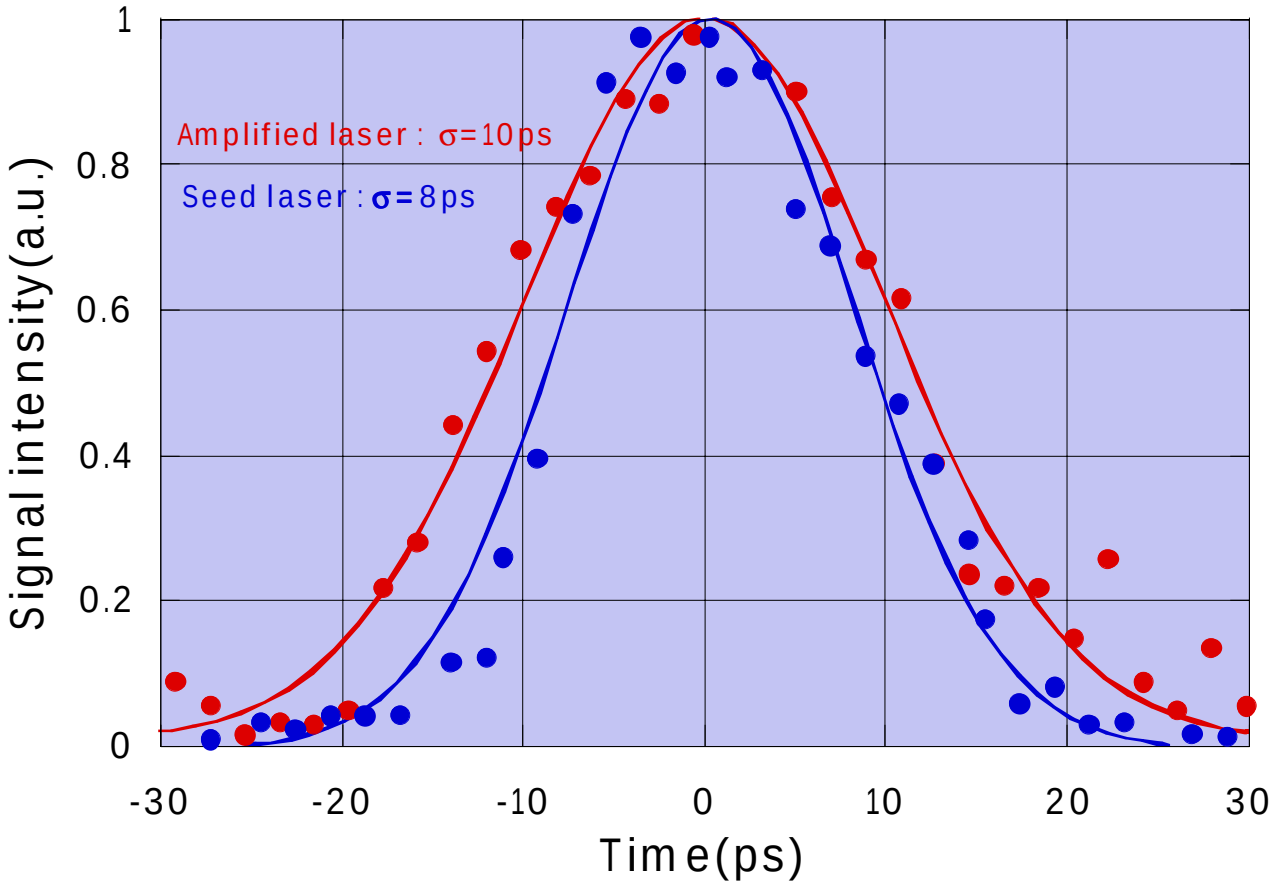
Amplified laser : σ=10ps
Seed laser : σ=8ps
Signal intensity(a.u.)
1
0.8
0.6
0.4
0.2
0
-30
-20
-10
0
10
20
30
Time(ps)

Square Pulse Shaping with a SLM

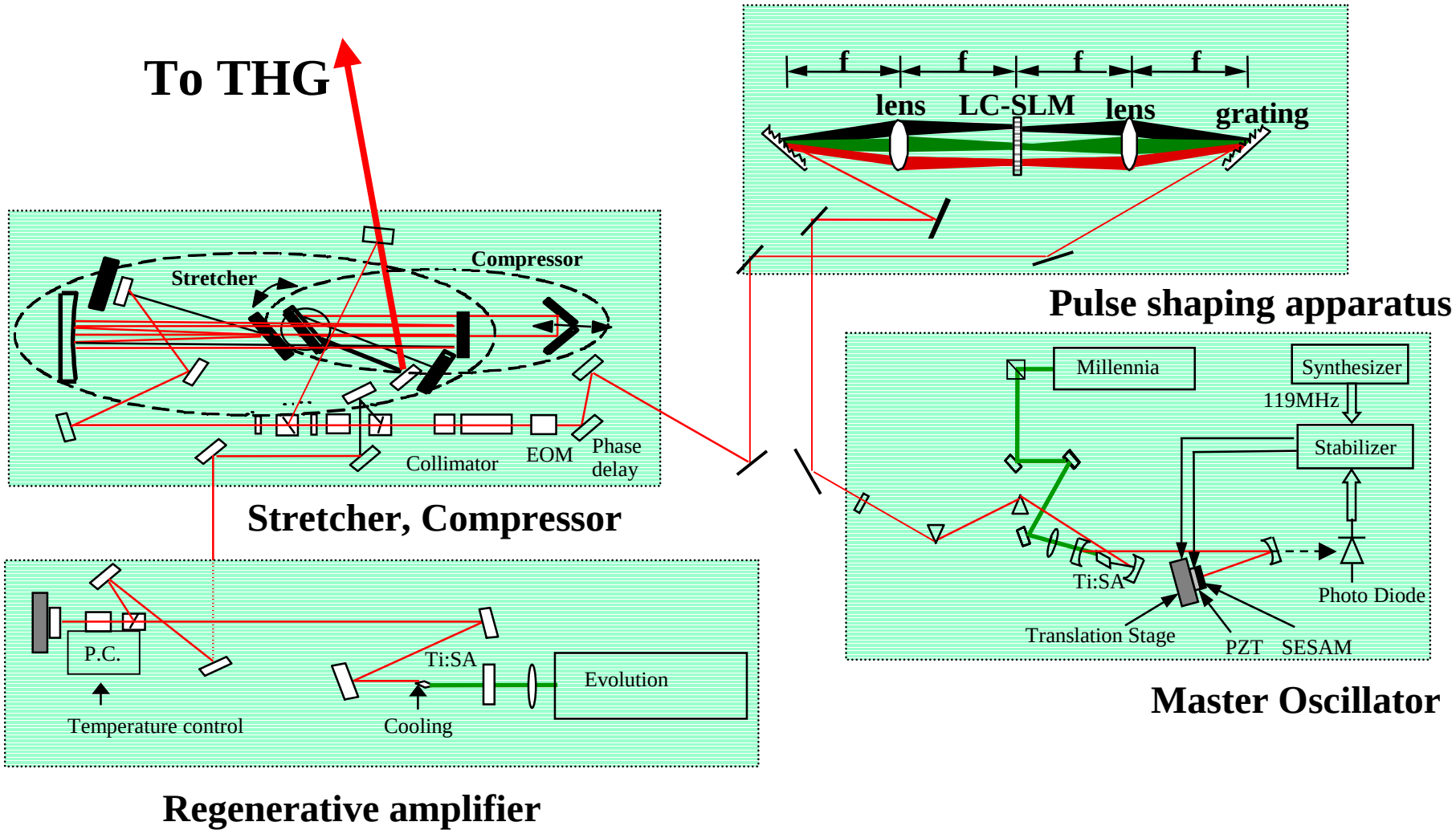

Autocorrelation Trace

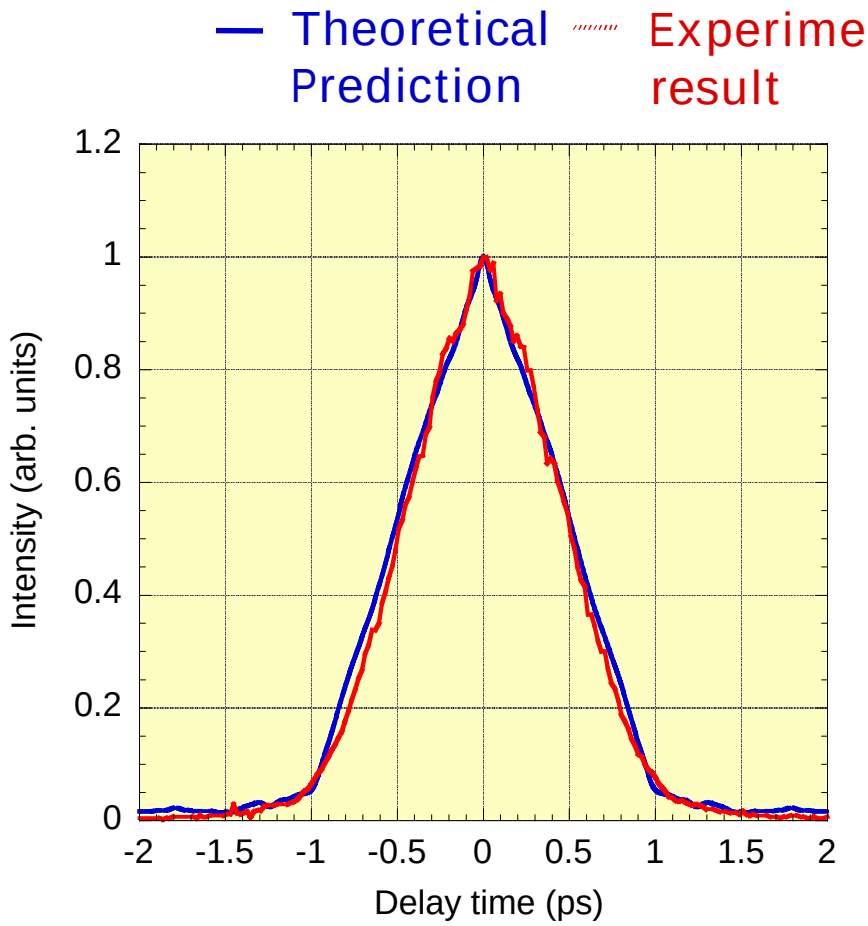

Pulsewidth	1 ps
Energy	0.3mJ (IR)
repetition	1 kHz

Triangle trace indicates square temporal profile.

Summery

Pulrise
- Stable UV laser for photo-injector
- Already open to the market

Amplifier
- Prototype model finished
- Continuing for production model
  - Please visit Photonics West at San Jose
  - Paper #4267-30
  - Poster session 5:30 to 7:00 PM on 1/24

Square Pulse
- Trying to generate THG

Katsuyuki Kobayashi: kobayashi@aculight.com

A Regenerative Source for a High Average Current Energy Recovery Linacs

Alexander Zholents and Max Zolotorev

Scylla and Charibdys of Photocathode guns with a high average current

Metal cathodes (Cu, Mg):	Semiconductor (K_2CsSb, Cs_2Te):
excellent lifetime	poor lifetime 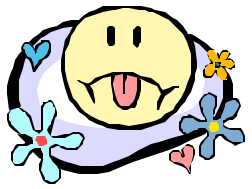
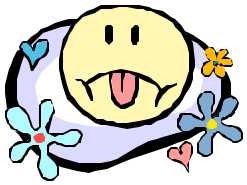 poor quantum efficiency; need ultraviolet laser	excellent quantum efficiency 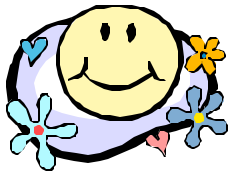

A Recirculating SR Source for Ultrafast X-Ray Science

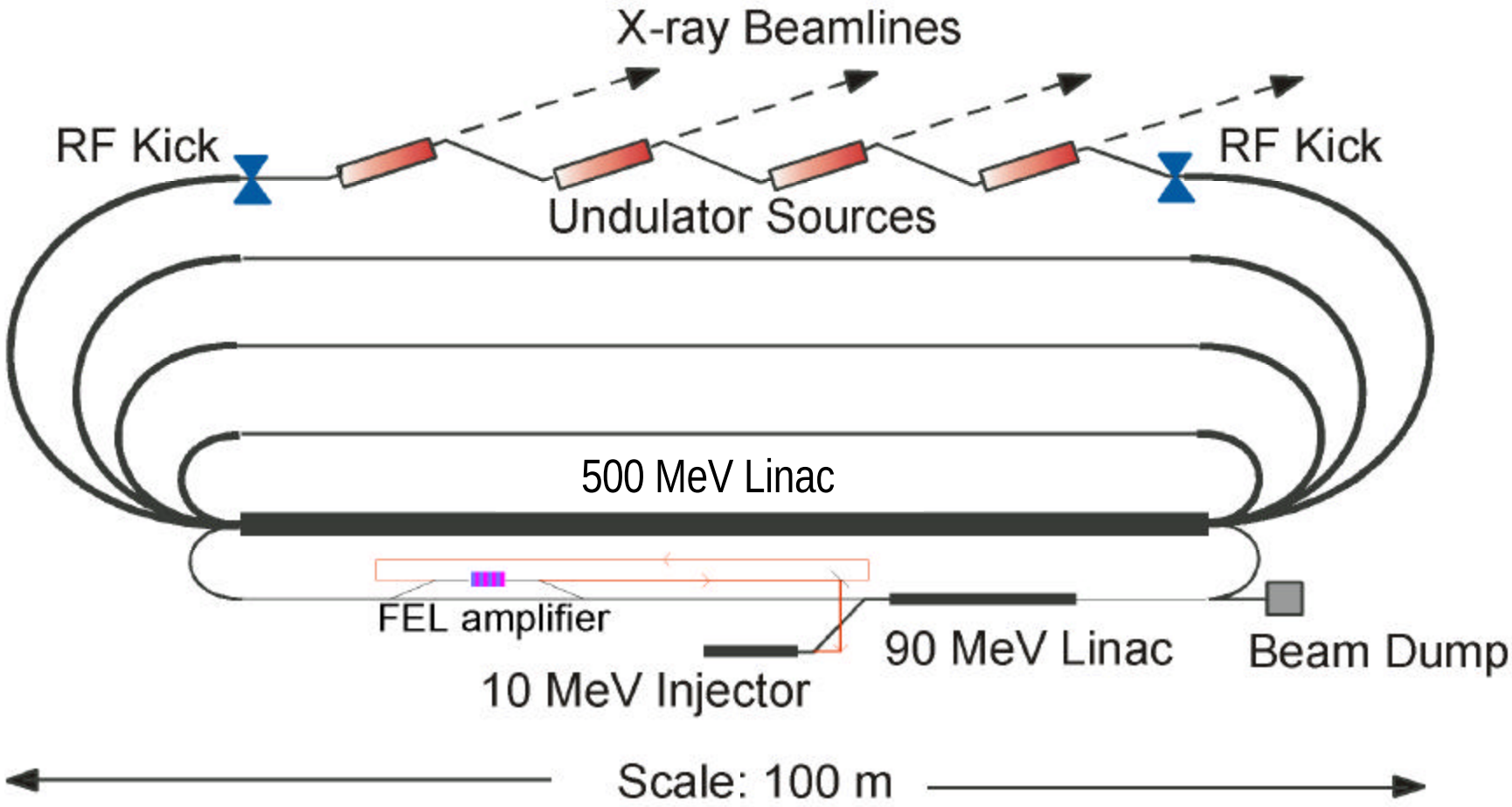

Two stages of pulse compression:

a) electron beam: 10 ps → 1 ps

b) x-rays: 1 ps → 100 fs

Compression of x-ray pulses

is possible due to a correlation between the longitudinal and transverse positions of electrons inside the electron bunch created by the RF orbit deflection in a cavity in the beginning of the final straight section.

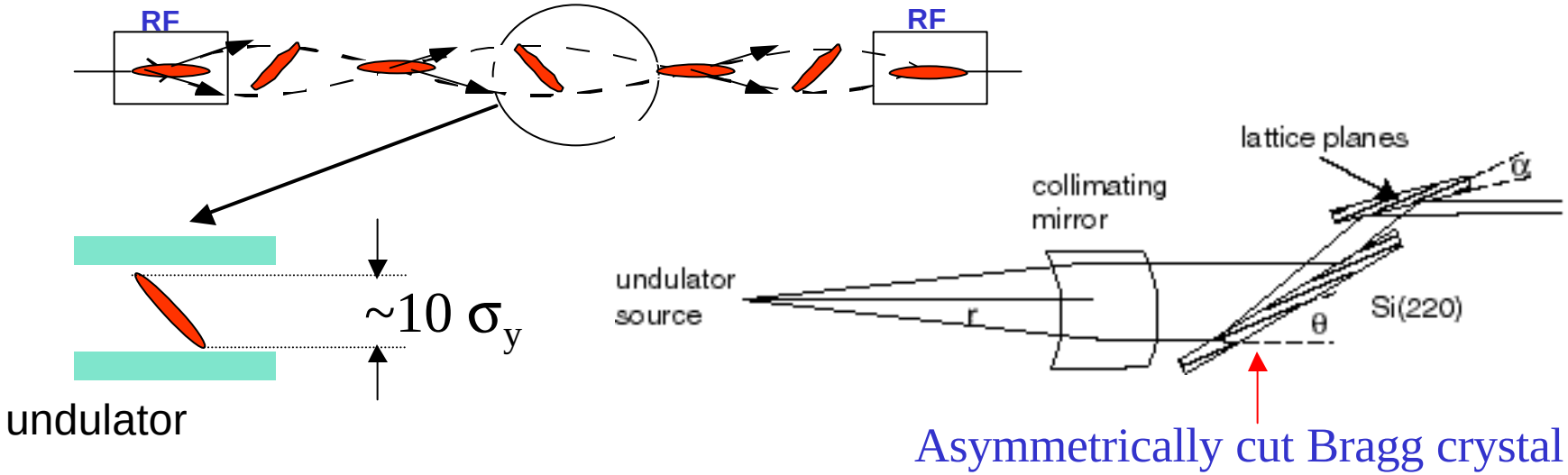

Diffraction limited size of a source at λ 1Å is 2 μm

Beam size at ε_n=0.4 mm-mrad is ~10 μm

Electron beam parameters out of the injector

Energy	20 MeV
Charge	1 nC
Normalized rms horizontal emittance	20 mm-mrad
Normalized rms vertical emittance	0.4 mm-mrad
Energy spread at 20 MeV	15 keV
Pulse length (uniform distribution)	10 ps

The RF gun parameters:

RF frequency	2.6 GHz
Peak electric field on a cathode	100 MV/m
Repetition rate of injection pulses	10-100 kHz

Laser parameters:

Wavelength (3-rd harmonic of Ti:sapphire laser)	267 nm
Pulse energy	100 μJ
Pulse length (FWHM)	10 ps
Repetition rate	10-100 kHz

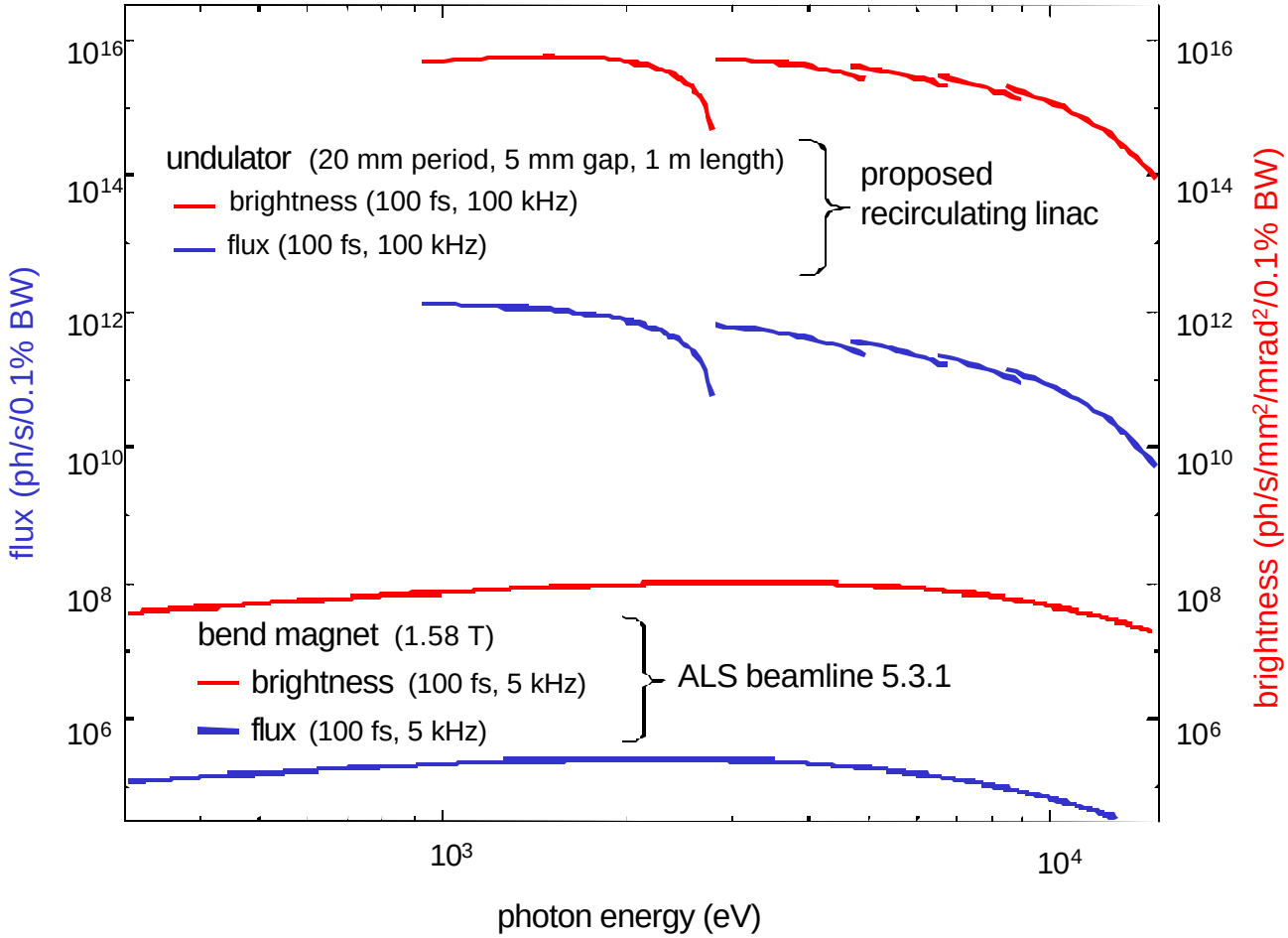

Average femtosecond flux and brightness compared with that of the existing bend-magnet fs beamline.

Details of a start-up and operation

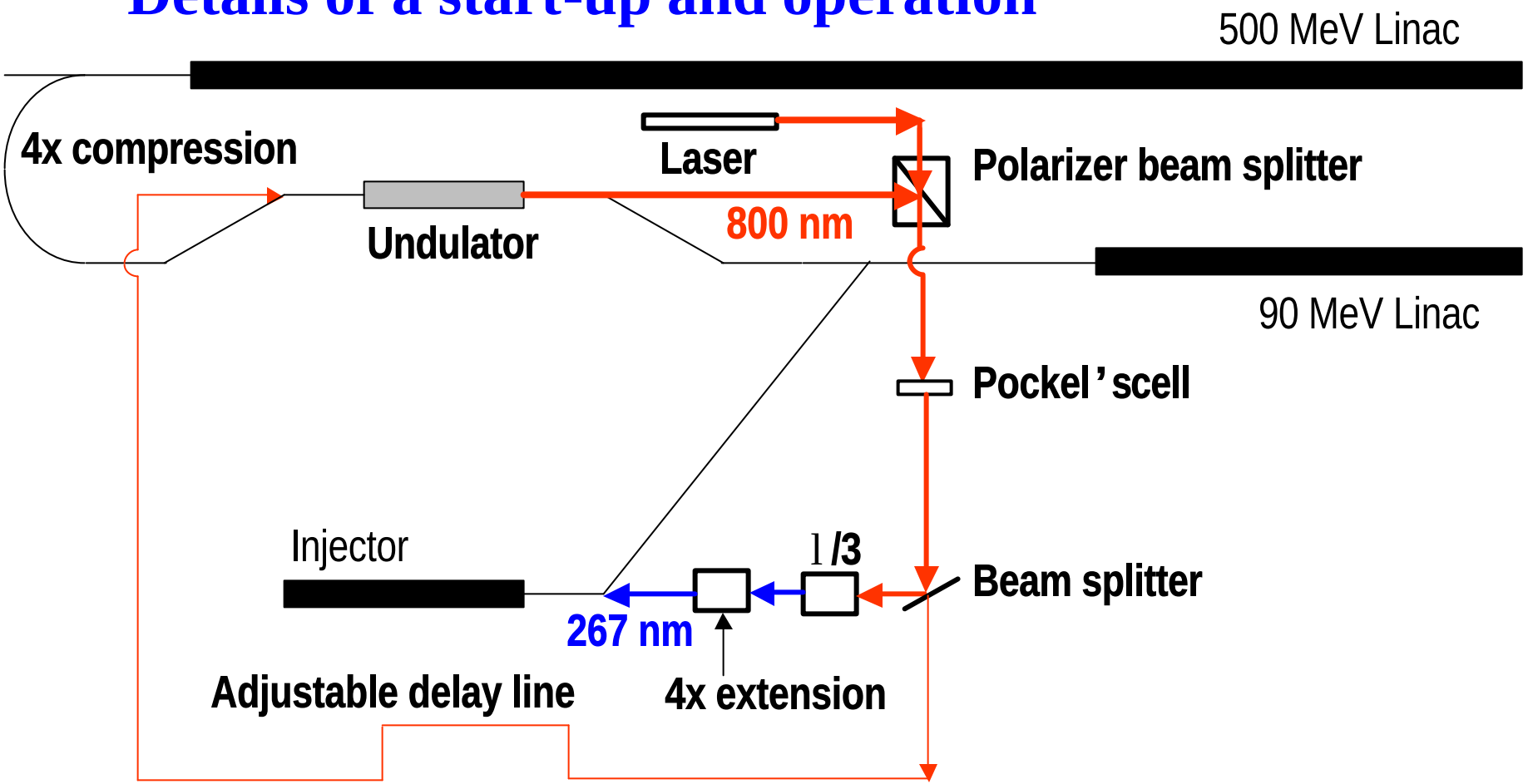

In the regenerative mode (continuous operation):

1 mJ/pulse, 20 MHz rep. rate from FEL amplifier at 800 nm

At a start-up (~ 1 sec):

~100 pulses, 1 mJ/pulse from Ti:sapphire laser at 800 nm

FEL operation

Undulator: length = 2m, period =2 cm, K=2

Peak current = 400 A

Light in = 12.5 μJ

Light out = 2500 μJ

A_w versus Z

19:00:10
2001 01 18
FEMTO
SPARC 10

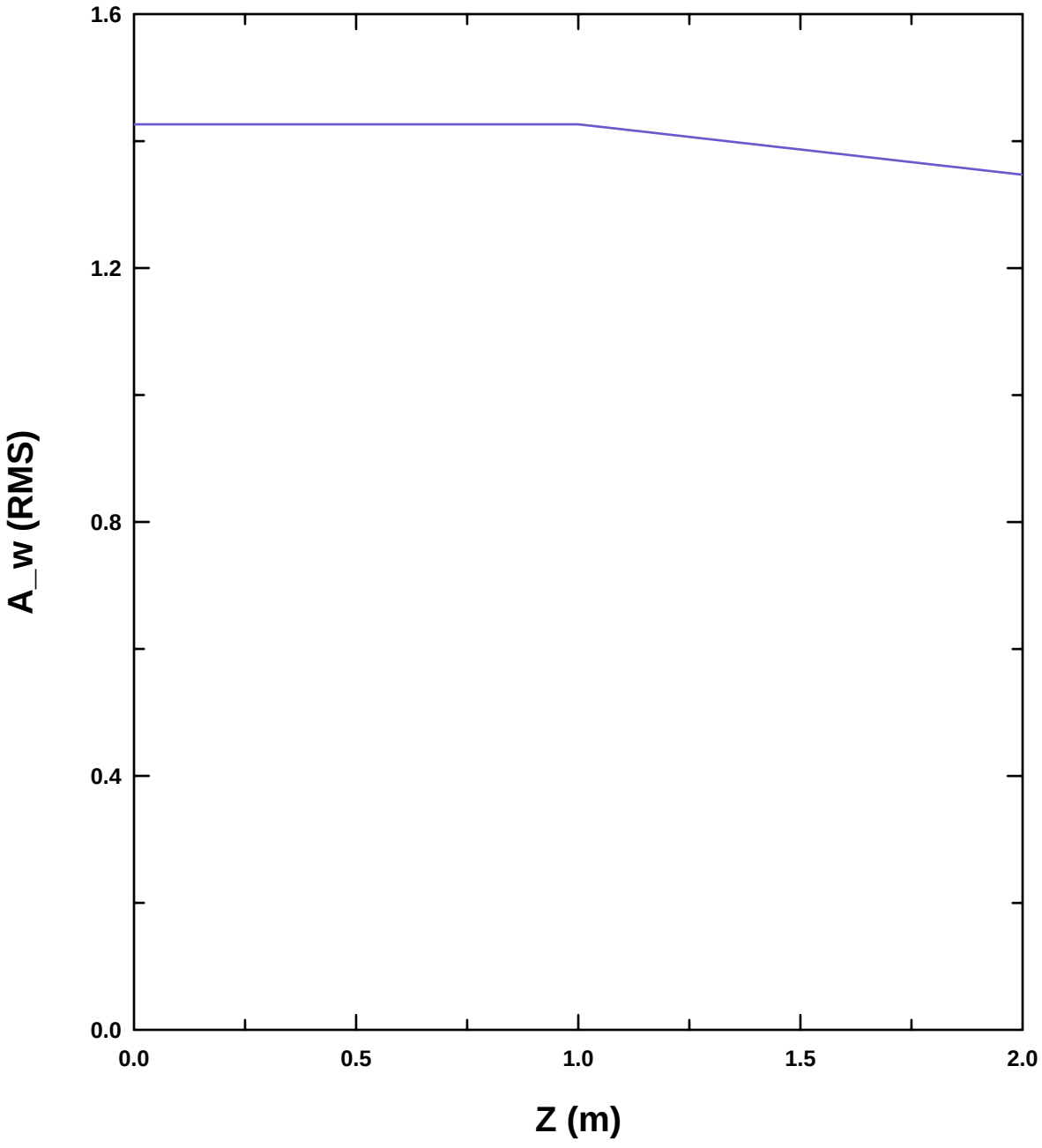

Avg. Field Power vs. Z

19:00:10
2001 01 18
FEMTO
SPARC 10

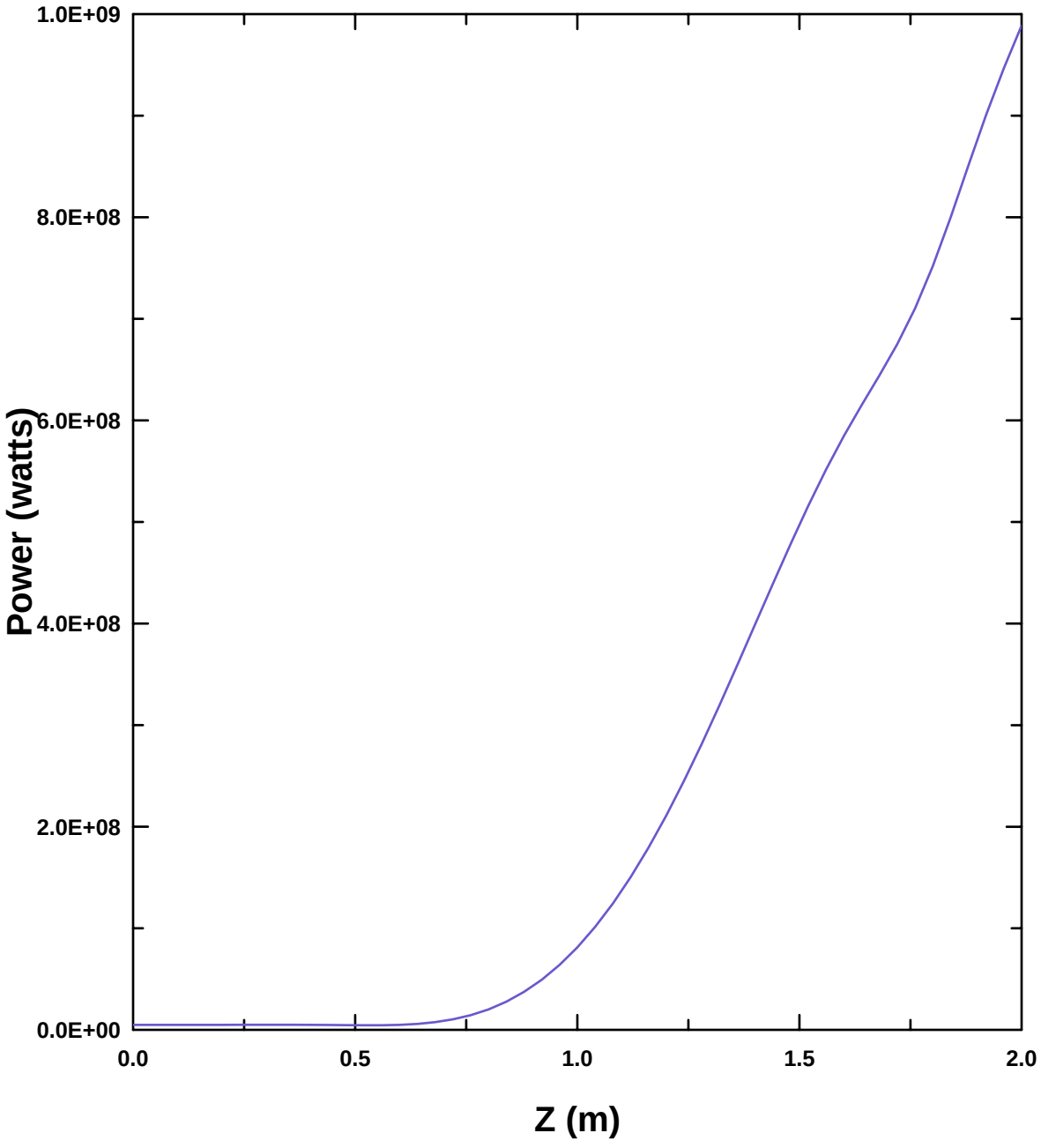

Phase Space at Z = 0.52 M

19:00:10
2001 01 18
FEMTO
SPARC 10

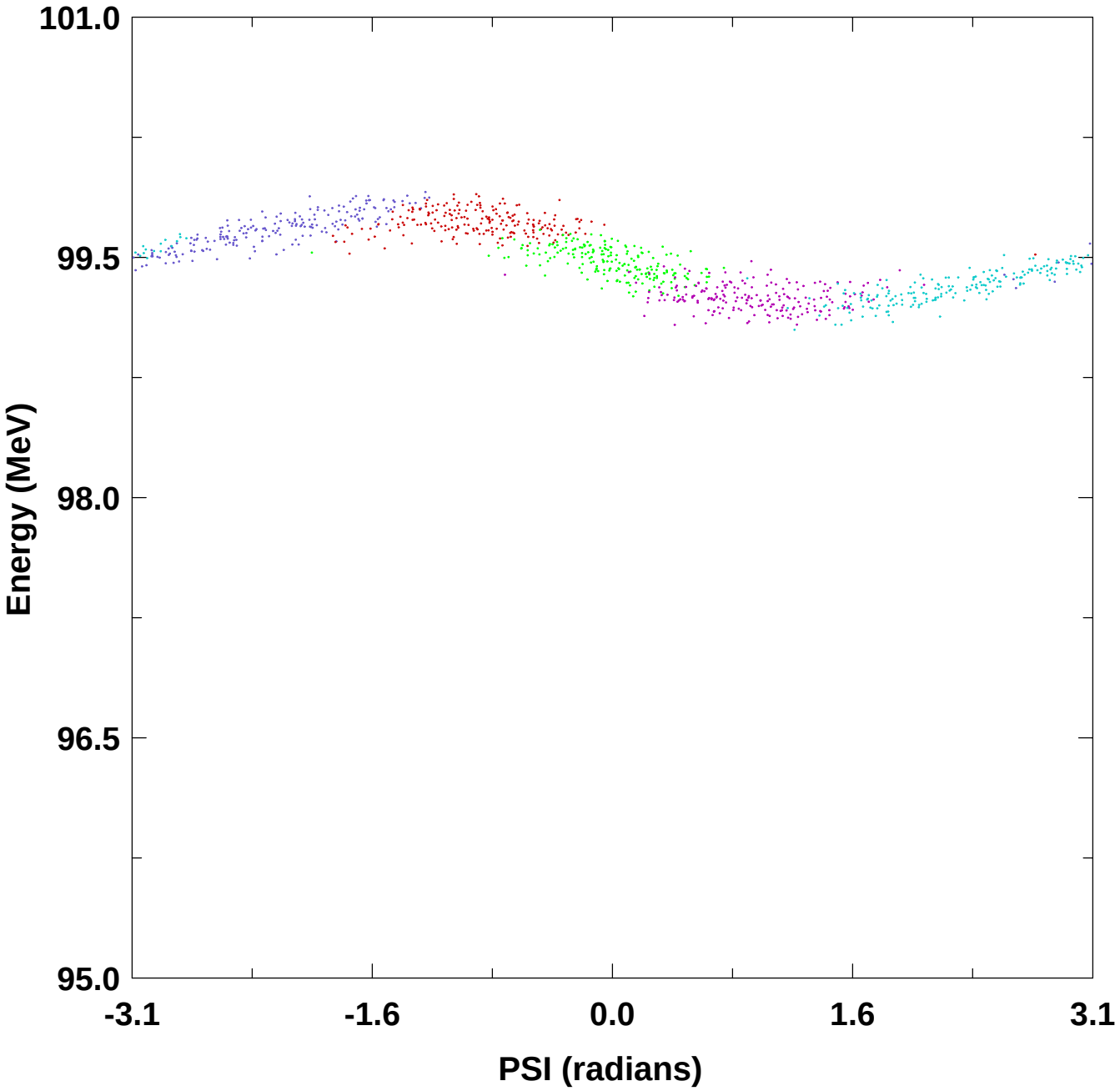

Phase Space at Z = 1.00 M

19:00:10
2001 01 18
FEMTO
SPARC 10

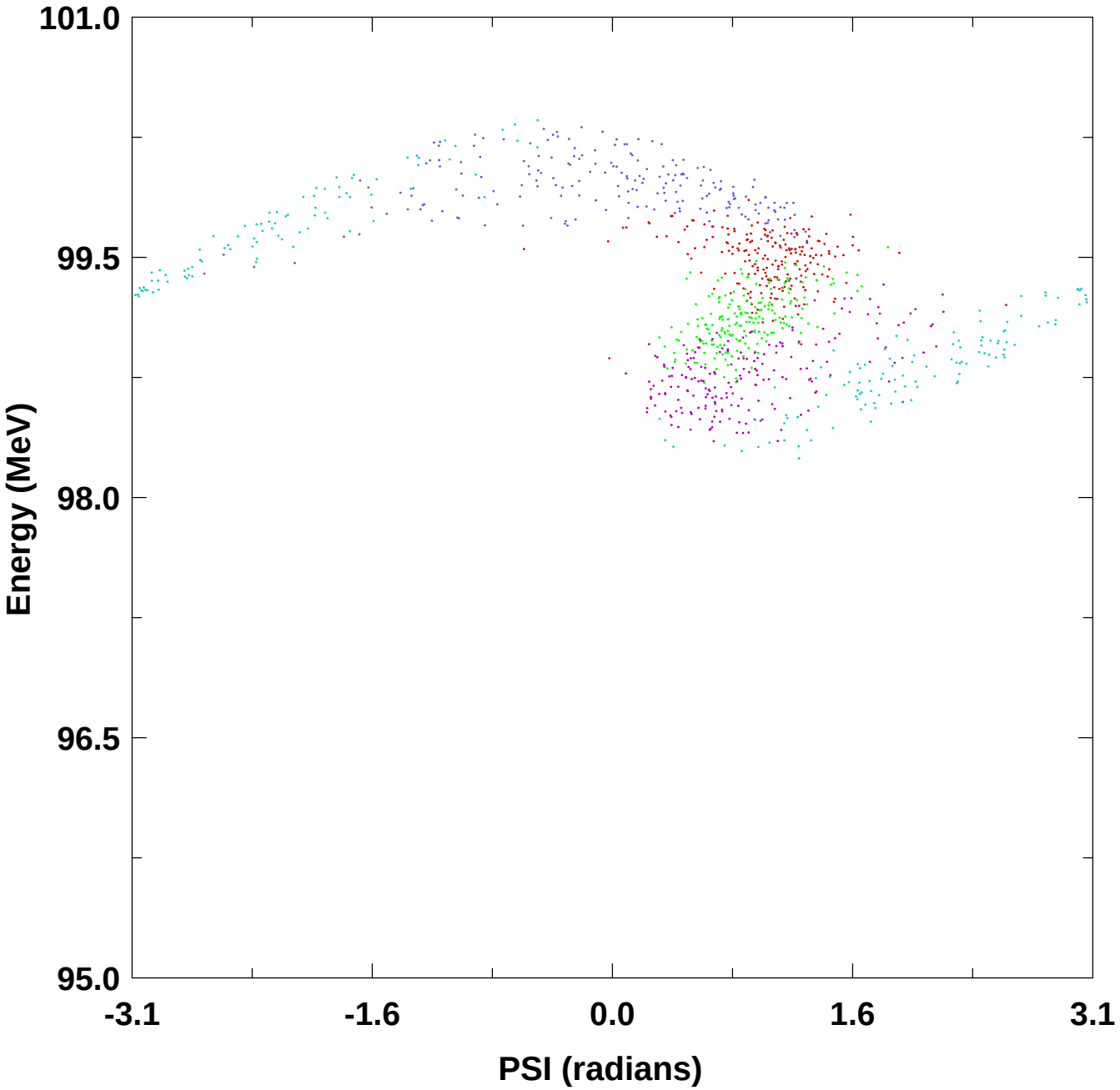

Phase Space at Z = 1.52 M

19:00:10
2001 01 18
FEMTO
SPARC 10

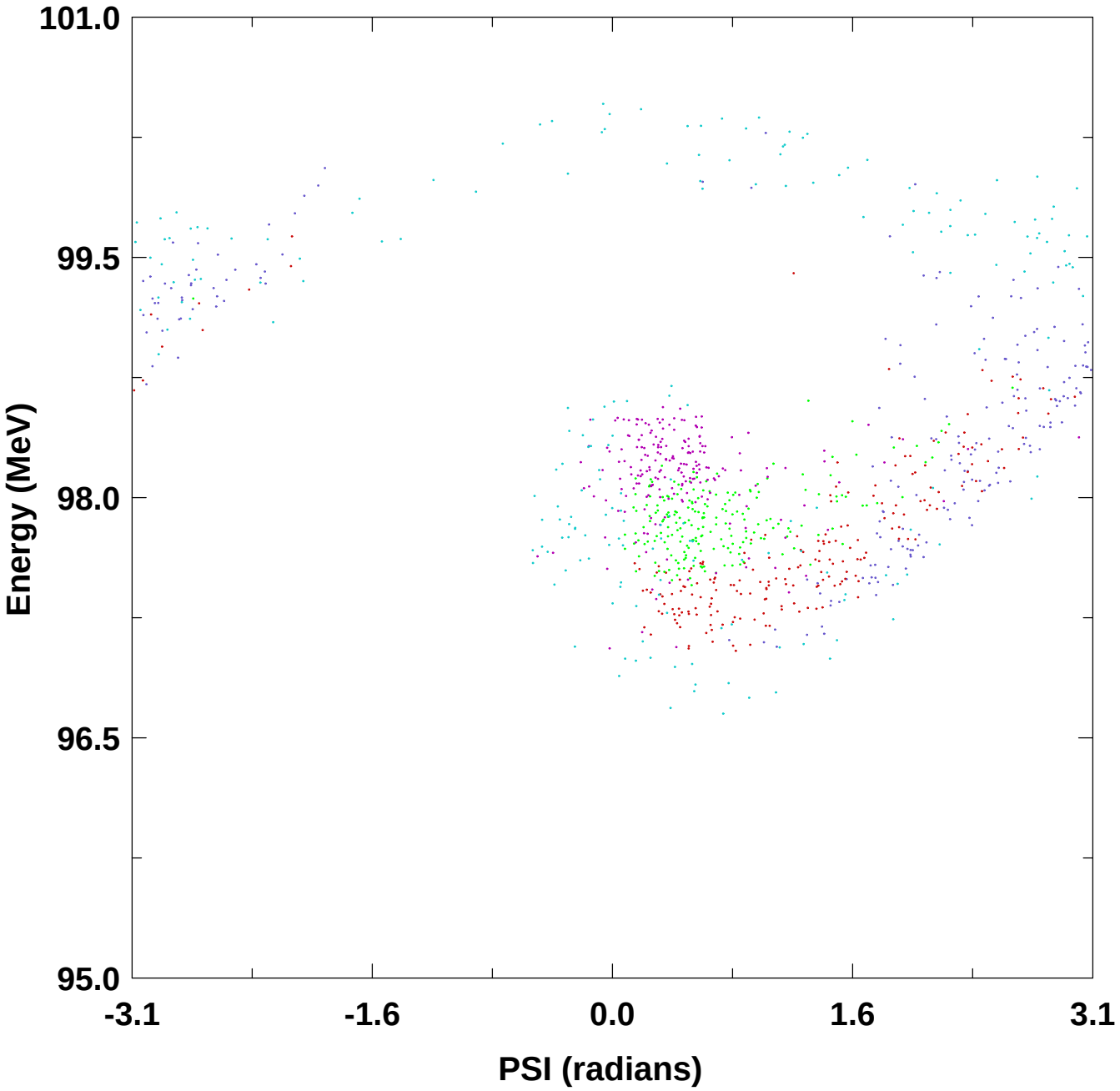

Phase Space at Z = 2.00 M

19:00:10
2001 01 18
FEMTO
SPARC 10

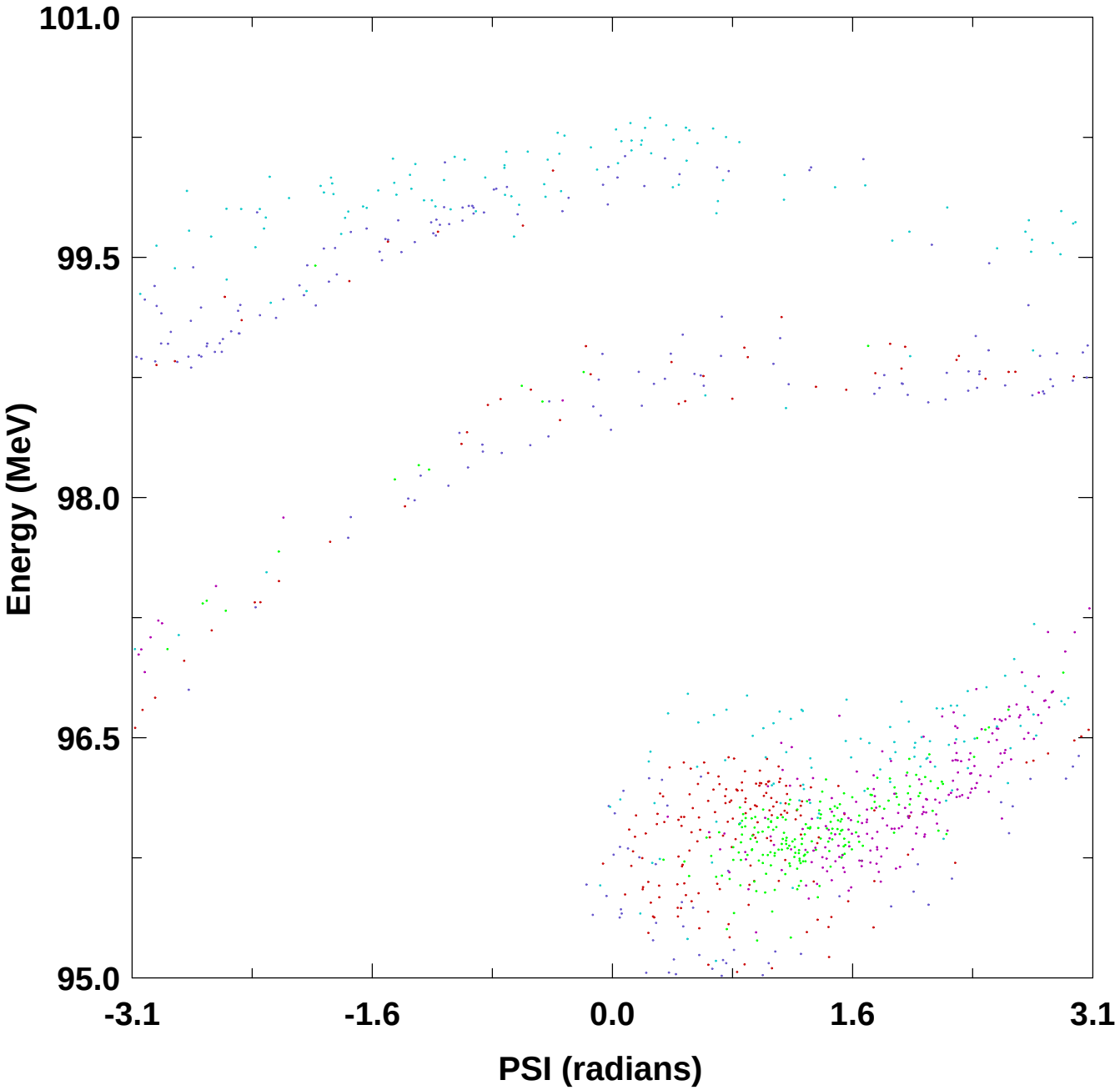

Femtosecond and Picosecond Lasers for Accelerator Applications

Katsuyuki Kobayashi
Sumitomo Heavy Industries (USA), Inc.
c/o Aculight Corporation
11805 North Creek Parkway S. Bothell, WA 98011
E-mail: kobayashi@aculight.com

A part of this work is performed under the management of the Femtosecond Technology Research Association , supported by New Energy and Industrial Technology Development Organization.

Contents

Feasibility study of PERL photoinjector laser

- Multi-laser combination

Accelerator relating laser technologies of out research work

- Timing stabilization of the amplified pulses
- Synchronization of two mode-locked oscillators

PERL photoinjector laser

Requirements for the Laser

Wavelength	**~260 nm**
Pulsewidth	**10 ps**
Rep. Rate	**1.3 GHz**
Ave. Power	**80 W**

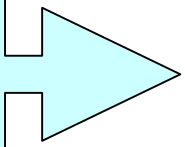

Impossible to achieve with a single laser

130 MHz, 8 W ? Yes !!

Build 10 lasers and combine into one system.

How ?

Plan 1: Pile up on the surface of the cathode

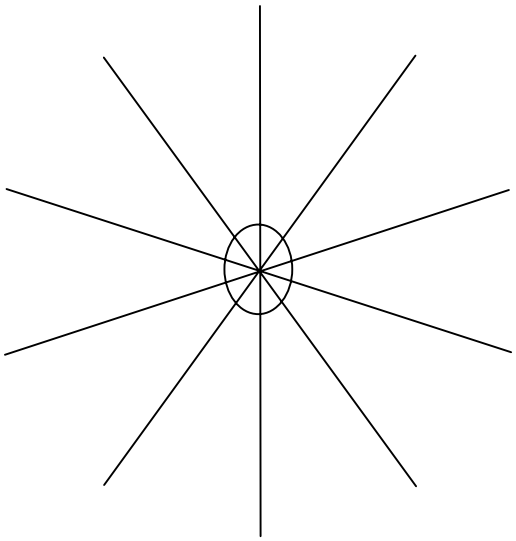

Front view

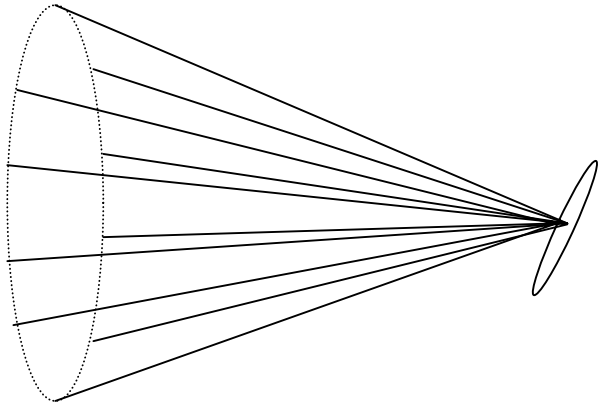

Side view

Advantage

- Simple configuration

Disadvantage

- Requires 10 view ports
- Different incident angles
- Different polarization

Plan 2: Pile up on the surface of the cathode

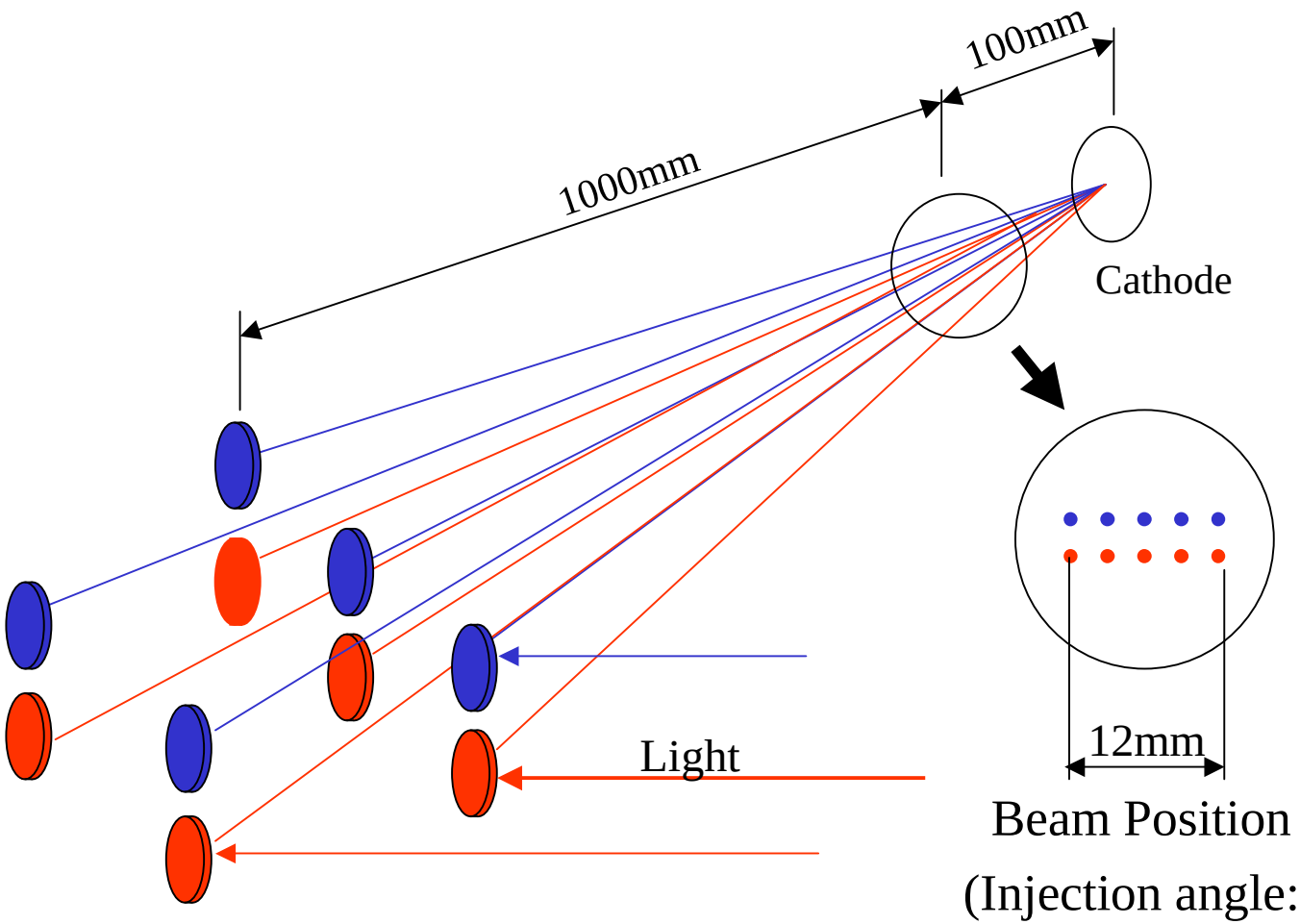

Advantage

One view port

Simple configuration

Disadvantage

Different incident angles

Beam Position at Flange

(Injection angle:68±4 deg.)

Plan 3: Overlap with a grating (wavelength multiplexing)

Advantage

All beams exactly overlap

Disadvantage

Pointing stability
Wavelength stability
Wide spectrum
Longer pulsewidth
Inefficiency at grating

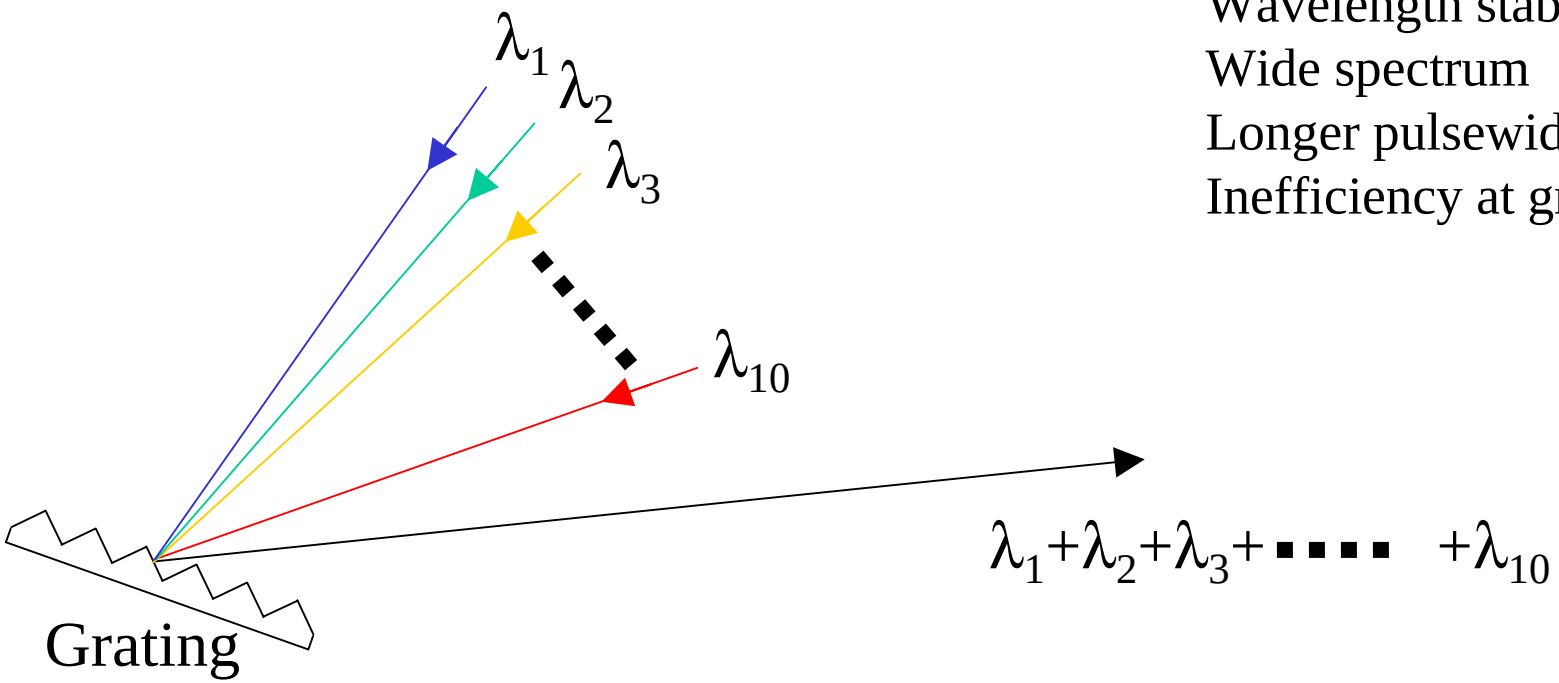

Option: overlapping 2 beams into 1

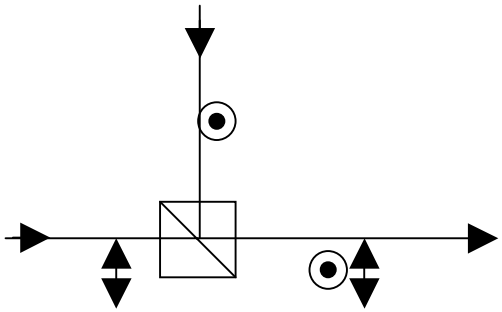

•Two beams are overlapped in a polarized beam splitter.
•Resulting 5 beams incident on the cathode either from 5 directions (plan 1,2) or 1 direction (plan 3).

Single Pulse jitter measurement

Statistical method cannot be adopted to low-repetition amplified pulses

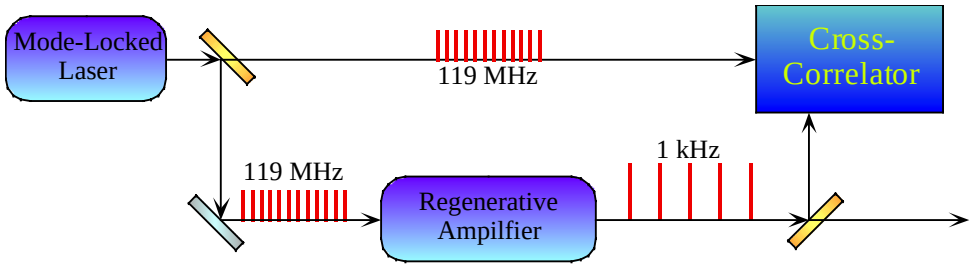

Single shot measurement
Stable oscillator as a reference

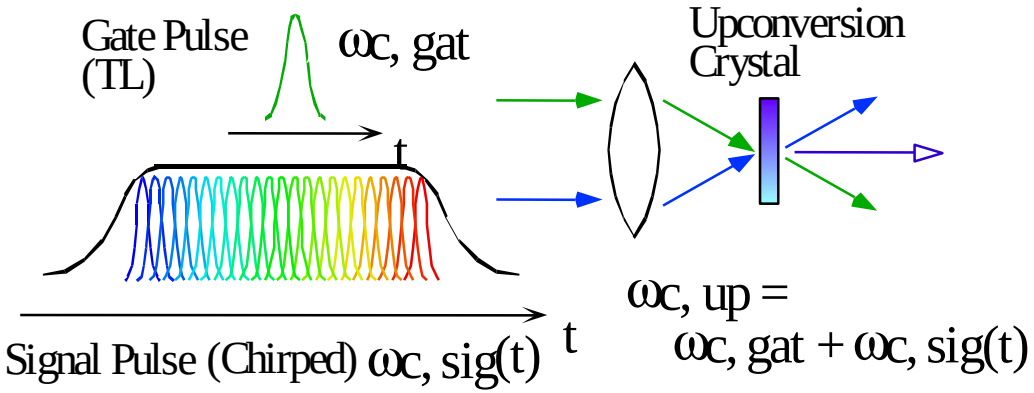

Intentionally stretched pulse

Measurement of timing fluctuation of the amplified pulses

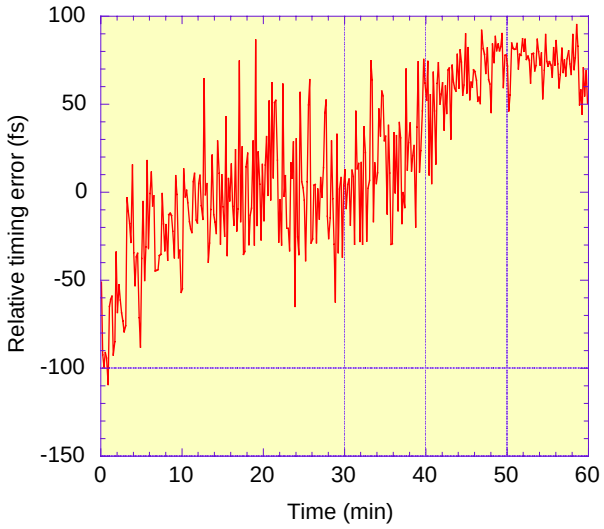

(a) Long term drift

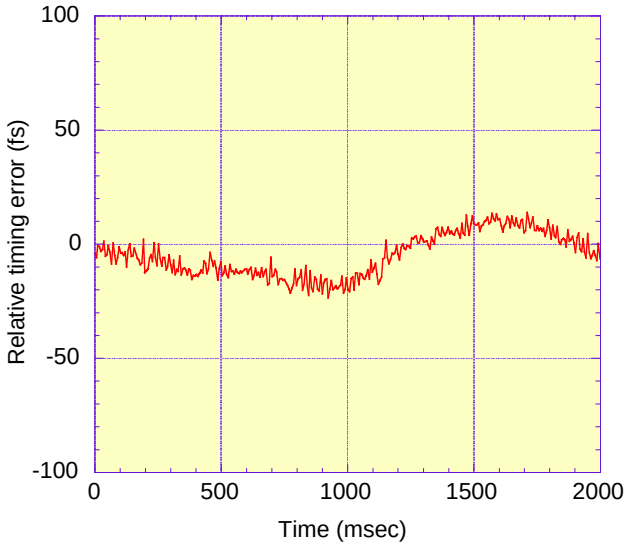

(b) Short term fluctuation

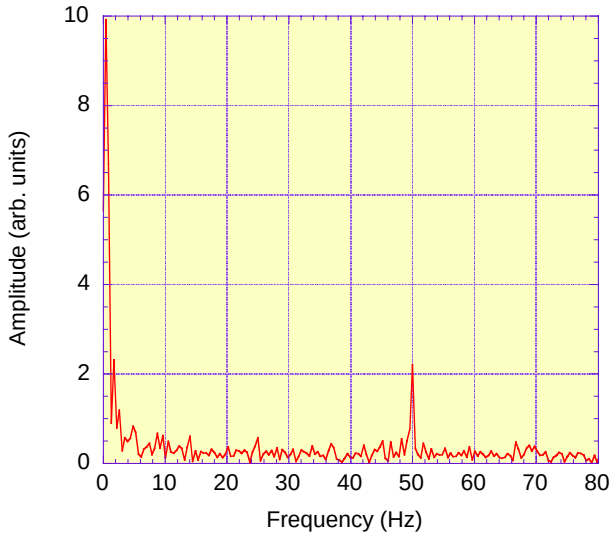

(c) Fourier transform of (b)

Long term (one hour) drift was less than 200 fs.
Short term (several seconds) fluctuation was about 10 fs.

Reduction of timing fluctuation of the amplified pulses

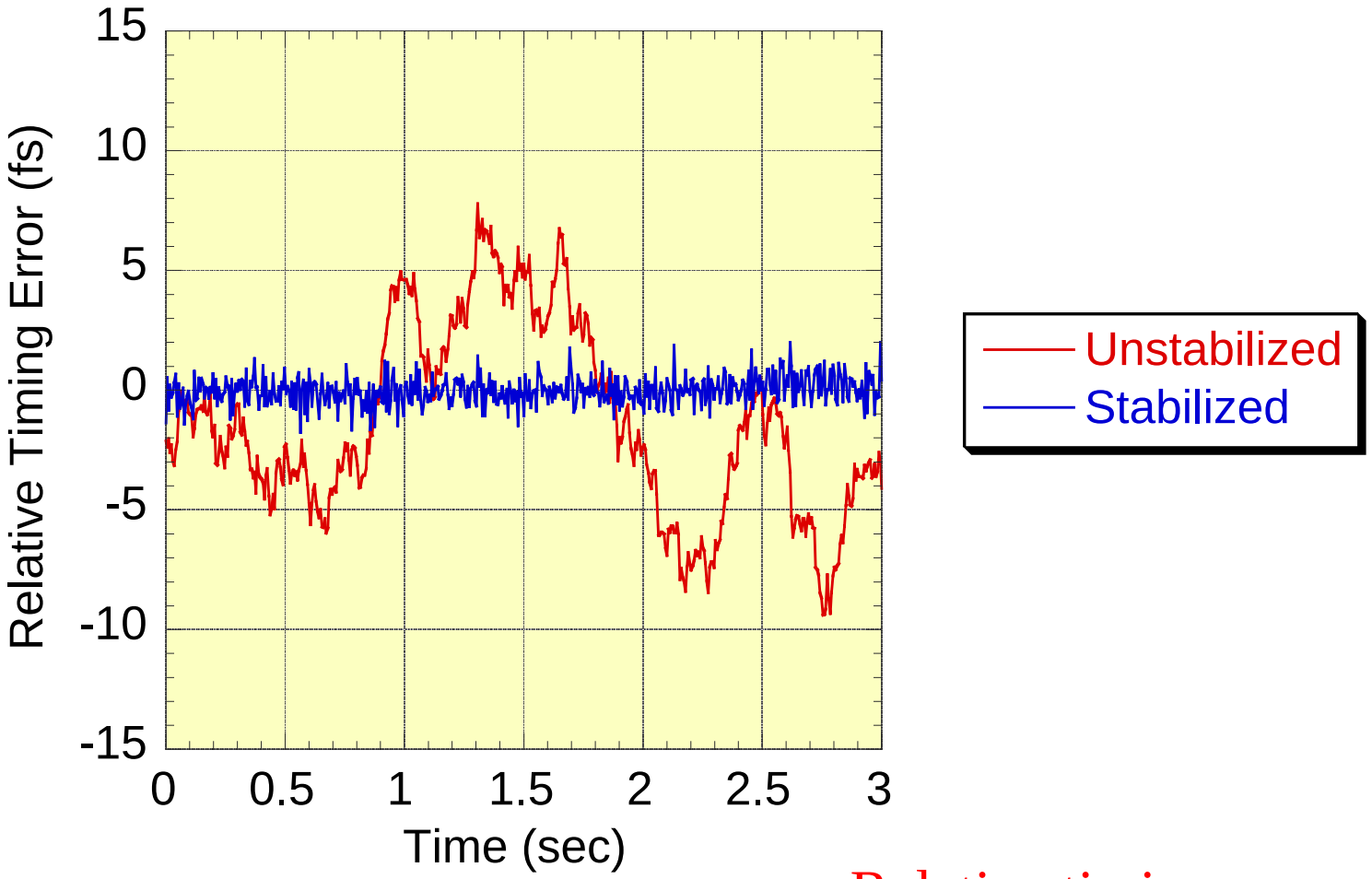

Relative timing error ~0.7 fs (rms)

Synchronization of two mode-locked oscillators

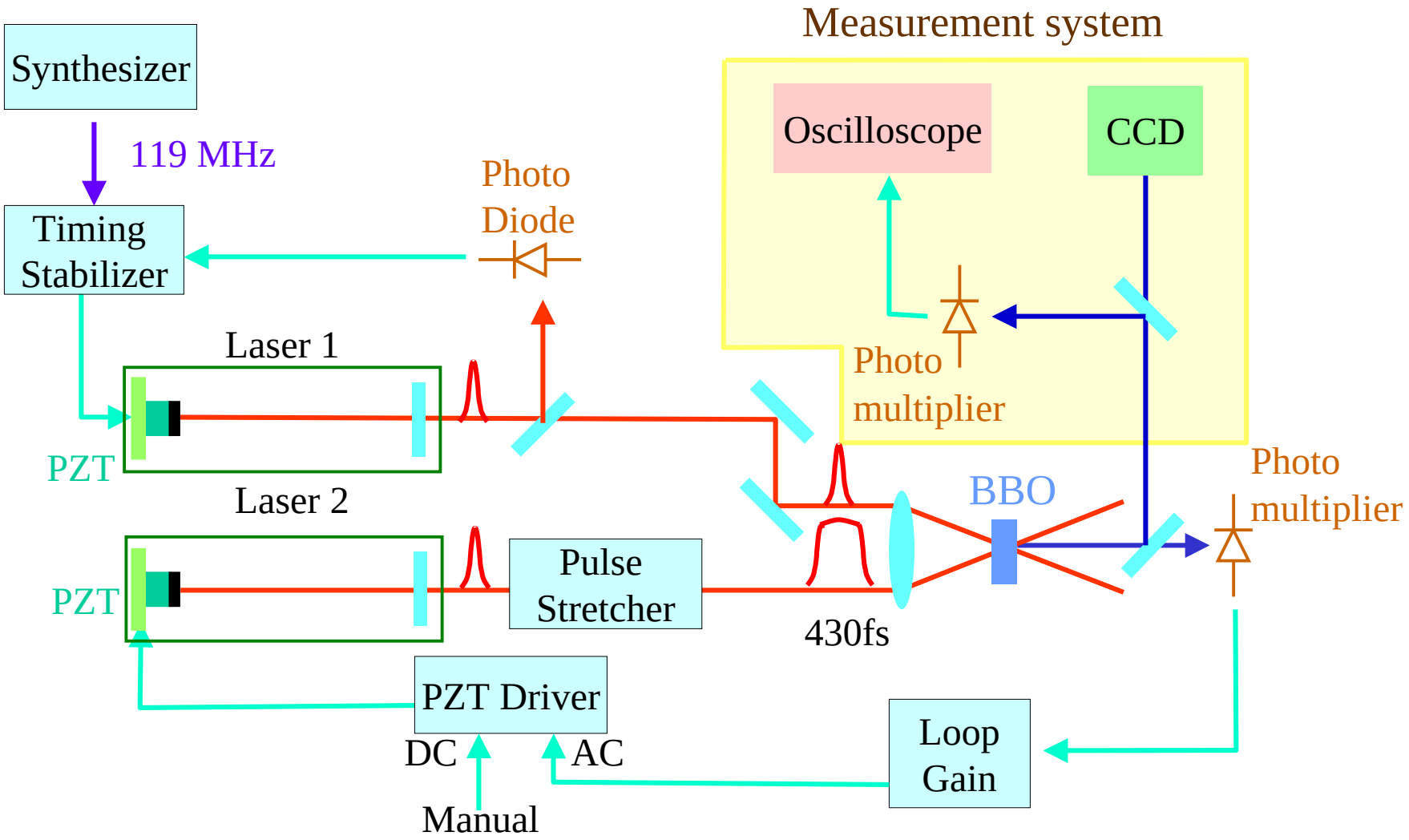

While phase-lock loop is not operating

- The pulse bunches repeated at the beat frequency.
- Each pulse bunch consists of pulses which had the repetition frequency of 119MHz.

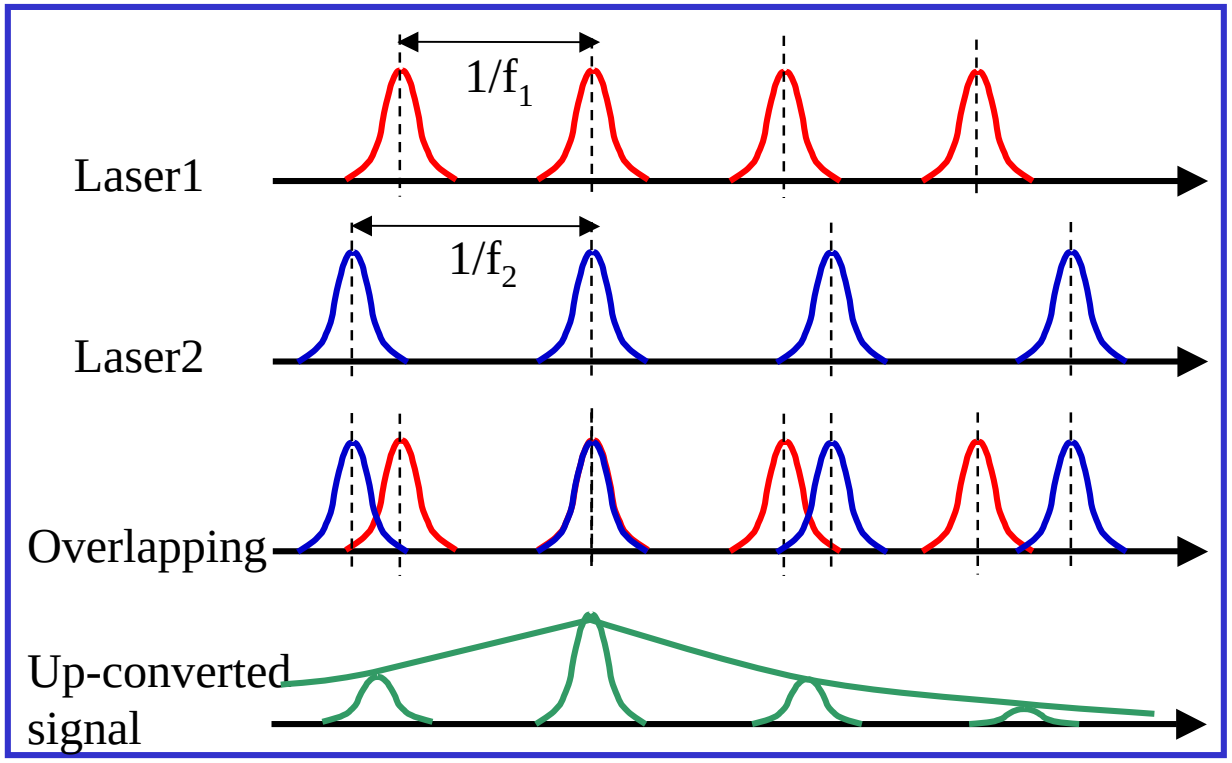

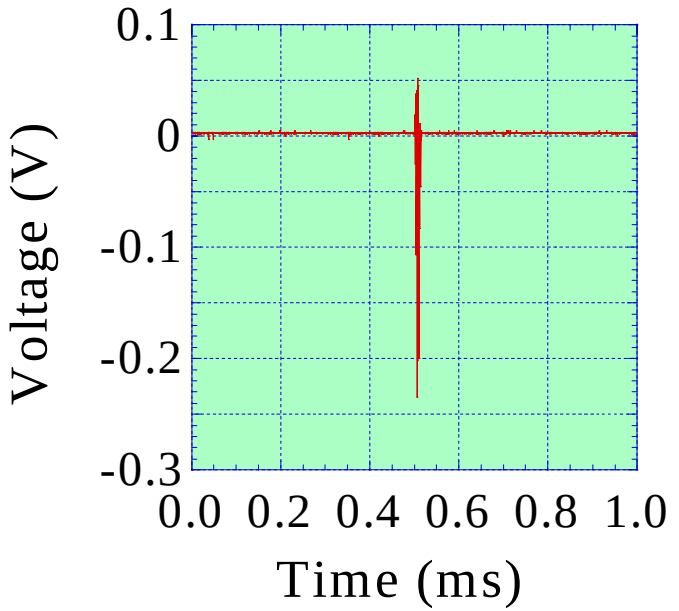

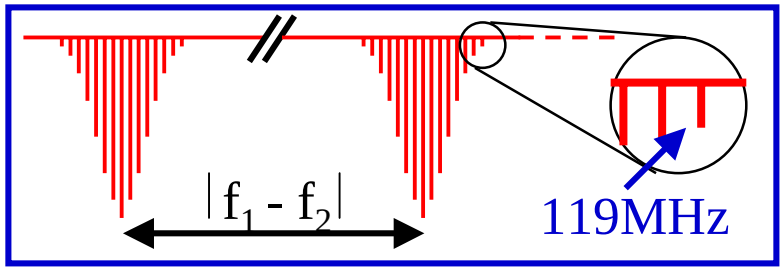

Phase lock loop is in operation

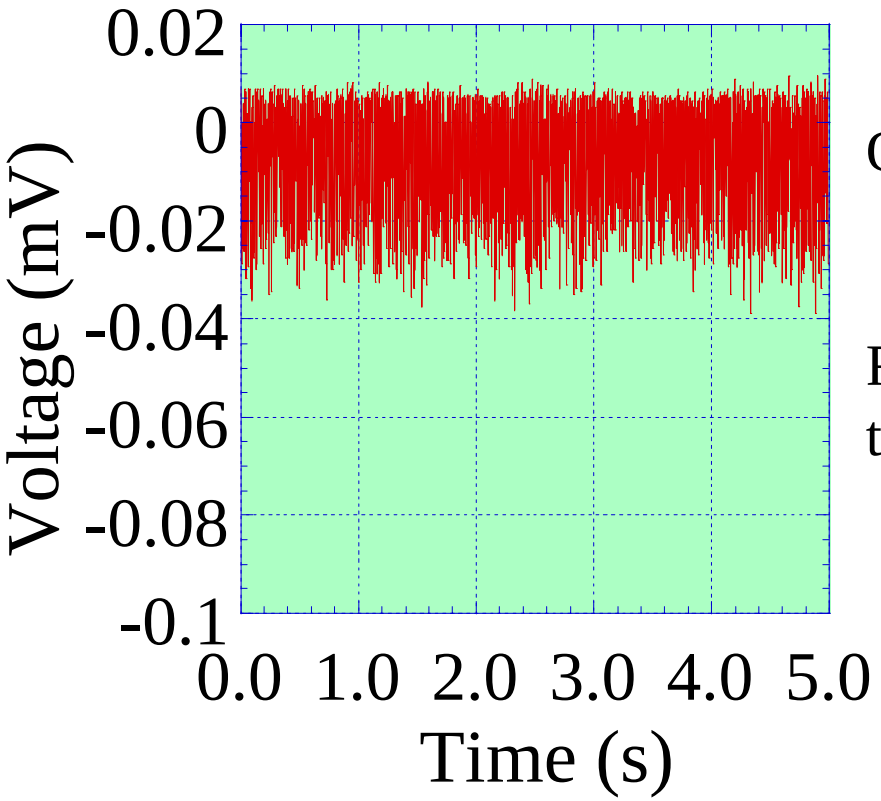

Overlapping time of two pulses is ~30 minutes

Relative timing jitter was suppressed to less than the pulse width of the longer one (430 fs)

Application sample: CO_2 laser seeder

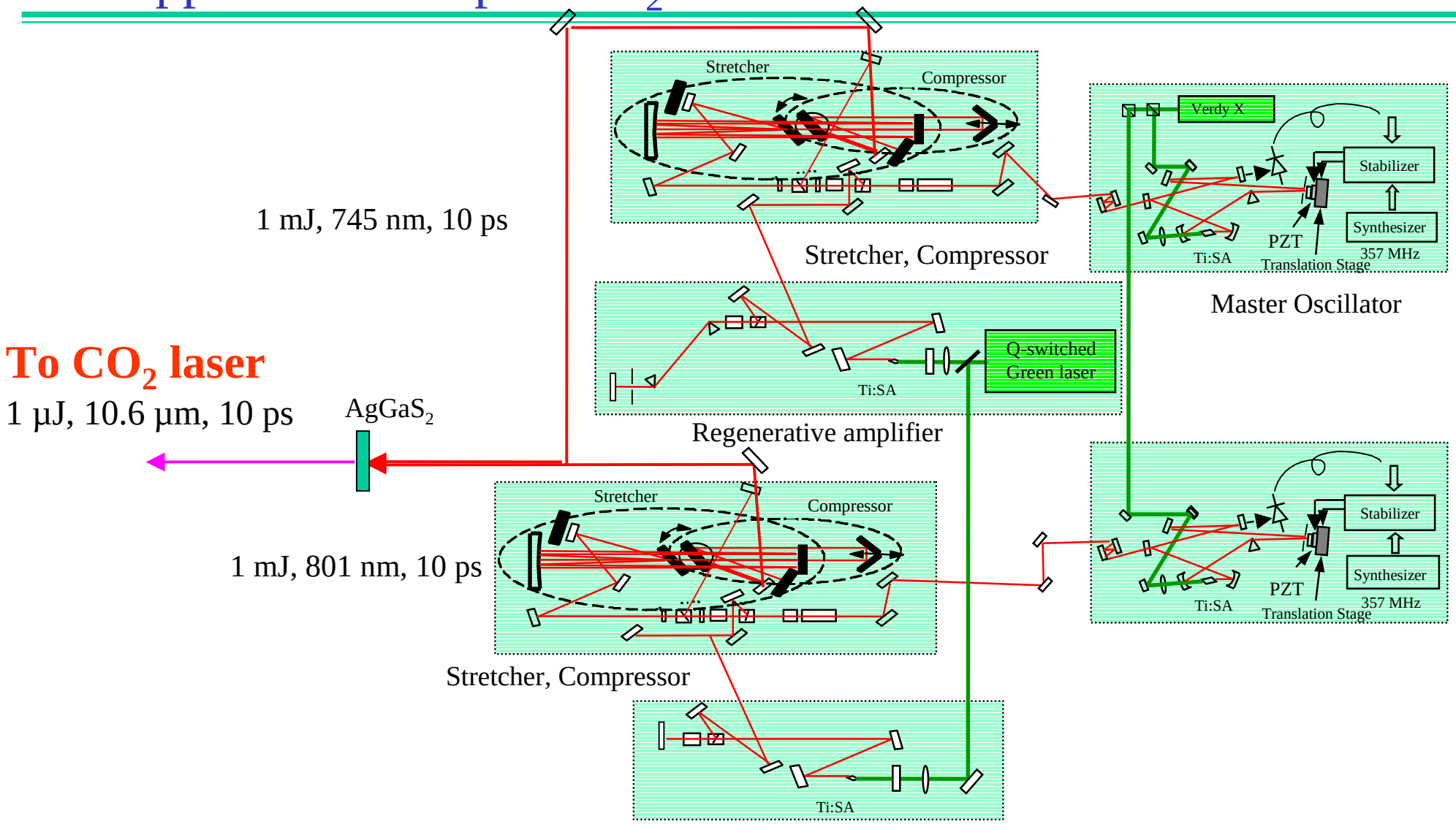

Summery

Feasibility study of PERL photoinjector laser

- Proposed to combine 10 lasers into one system
- Discussed on 3 plans to combine

Accelerator relating laser technologies of out research work

- Stabilized the amplified pulse < 1fs
- Synchronized two mode-locked oscillators

Katsuyuki Kobayashi: kobayashi@aculight.com

Preliminary Beam Parameters of PERL Injector with DC Gun

F.Zhou, I.Ben-Zvi, T.Shaftan, X.Wang

Brookhaven Accelerator Test Facility

Brookhaven National Laboratory

Upton, NY 11973, USA

January 22, 2001

PERL Photoinjector workshop

Outline

- Beam Required at the exit of PERL Injector
- Schematic Layout of PERL Injector with DC Gun
- Preliminary Simulation Results
- Summary and Outlook

Beam Requirements at the Injector Exit

- Beam Current 200 mA,i.e, 0.15 nC/bunch for L-band linac
- Energy about 25 MeV and RMS Energy Spread 25 keV
- RMS Bunch Length:3 ps or 0.9 mm
- Transverse Emittance: 1 mm.mrad @ 0.15 nC

Schematic Layout of the Injector

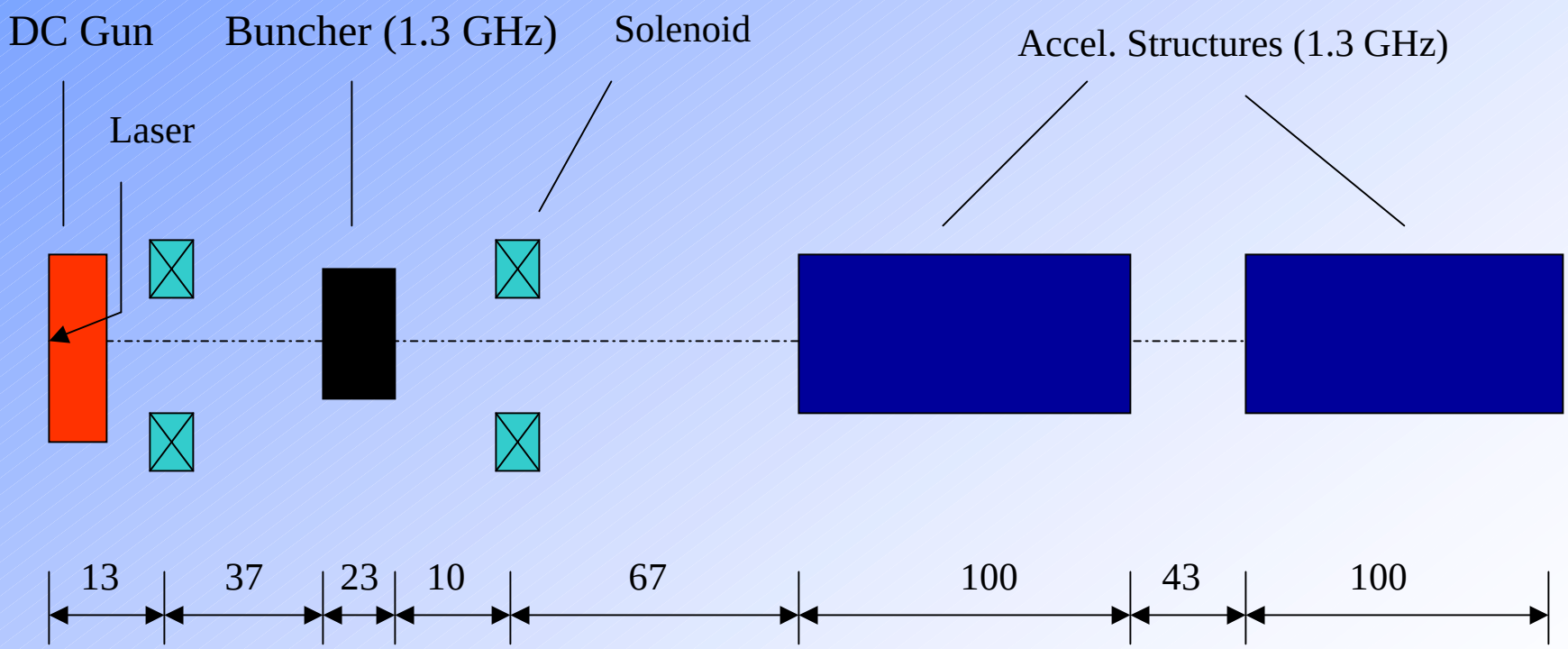

Beam Simulations

- Beam simulations starts from the cathode to the injector exit
- A package of widely used computer codes:
  POISSON (gun and solenoids),
  SUPERFISH (Buncher and accelerating structures)
  and beam dynamics simulation code:
  ASTRA (**A S**pace Charge **T**racking **A**lgoritum), which is newly developed by K.Floettmann from DESY.
- DC gun
  Schematic geometry (5 cm from the cathode to anode)
  and its electric field (500 kV)

DC Gun

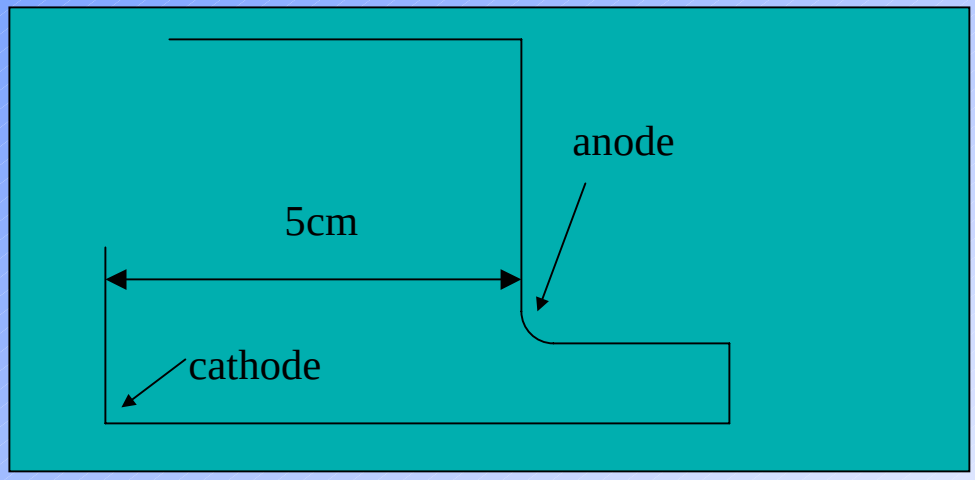
anode
5cm
cathode

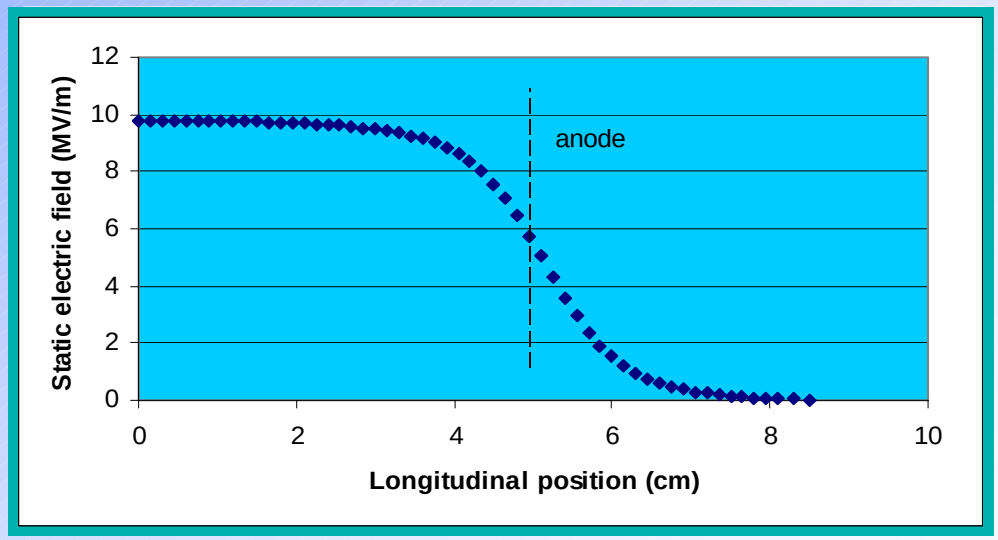
Static electric field (MV/m)
12
10
8
6
4
2
0
anode
0
2
4
6
8
10
Longitudinal position (cm)

Solenoid Fields

- 1st solenoid for the emittance compensation is located at 13 cm from the cathode (just after the gun). Maximum Bz is 520 Gauss.

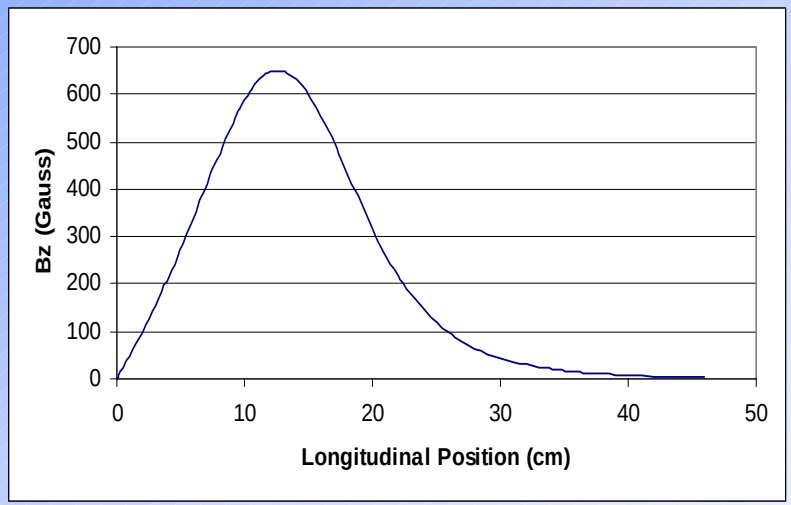

- 2nd solenoid (maximum Bz: 550 Gauss) is located after buncher, which has two functions:

  * further emittance compensation, since the energy is still lower, 2.0 MeV

  * optics matching to the accelerating structures

Buncher

- Buncher is two-cell standing wave structures (1.3 GHz, 7.5 MV/m), which has two functions:

  * bunching the bunch from RMS length 10 ps to 3.0 ps (3mm to 0.9 mm)

  * accelerating the bunch in order to reduce the space charge effect. The RF phase is 30 degrees off-crest and its net energy gain from the buncher is about 1.4 MeV.

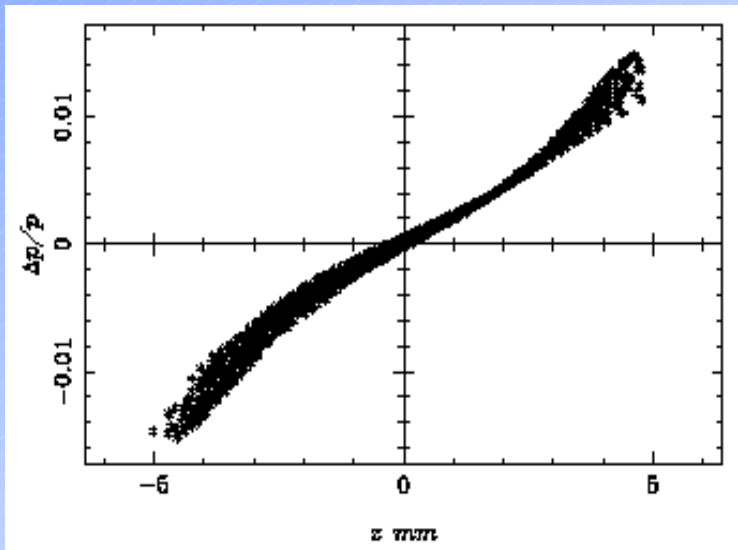

before the buncher

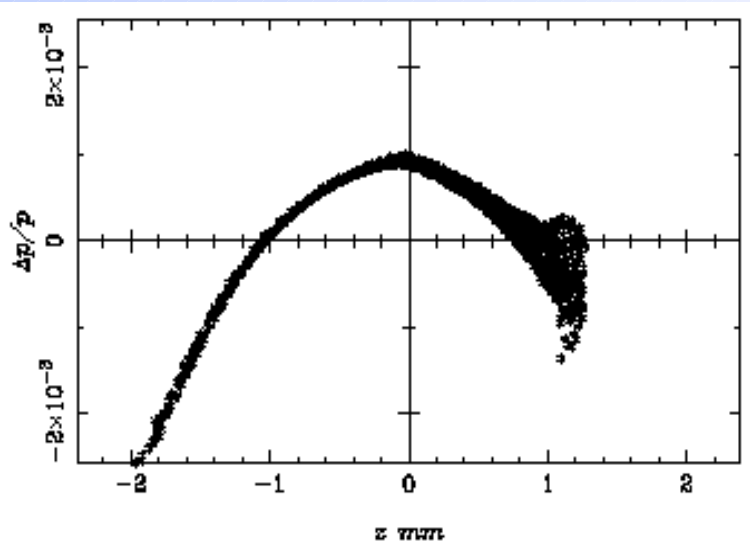

after the buncher

Buncher

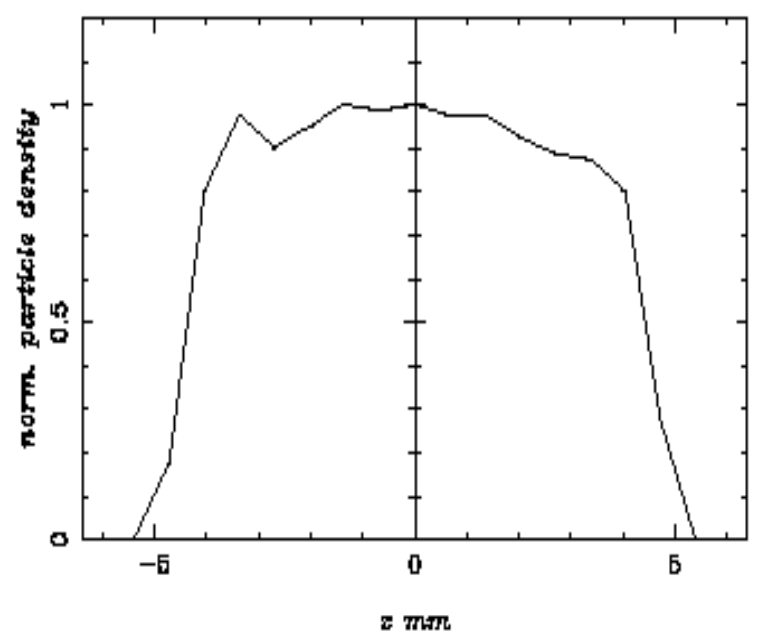

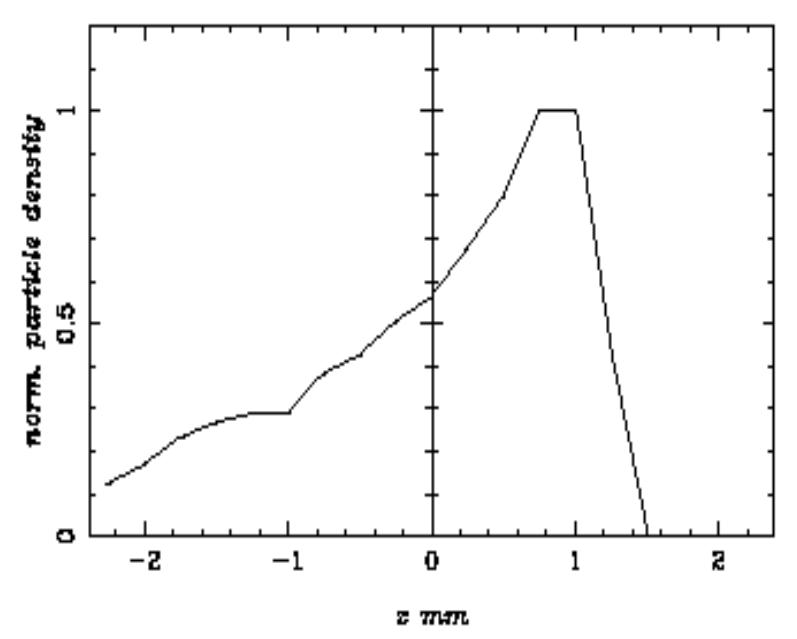

before the buncher

after the buncher

Accelerating Structures

- Using the 2nd solenoid to match the beam optics to two accelerating structures. One structure (1.3 GHz) is 9-cell with 1 m, gradient is 10 MV/m. After the acceleration, the beam divergence is reduced greatly and the emittance is slightly decreased and then keeps to be constant.
- The RMS bunch length is slightly modified through two structures and then kept to 3.0 ps (0.9 mm).
- The energy spread after two structures are 25 keV at the energy of 25 MeV.

Accelerating Structures-Trans. Space

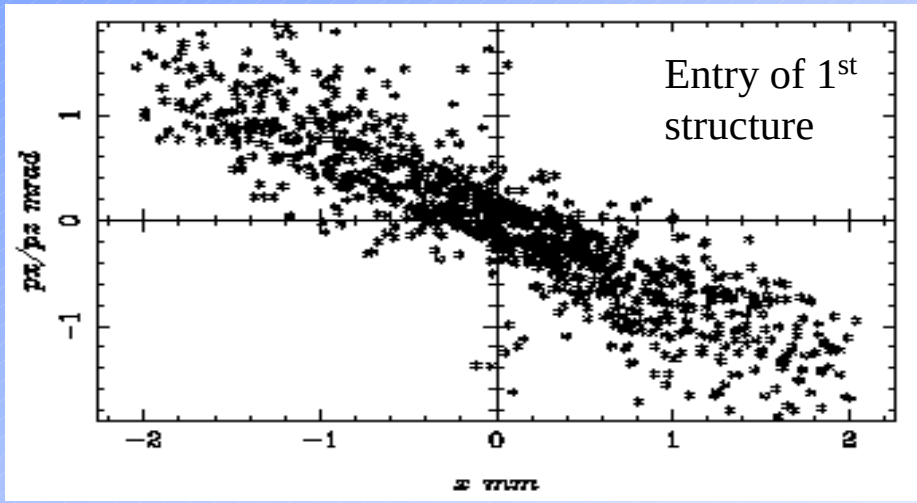

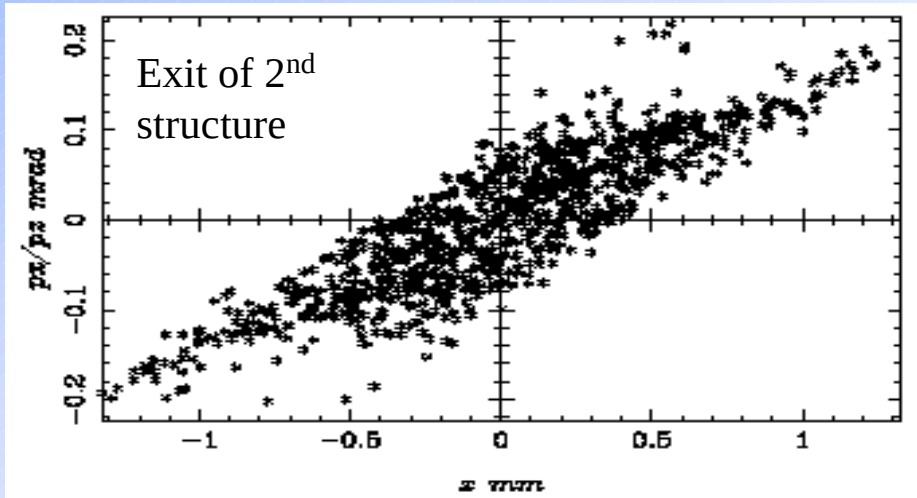

Accelerating structures-bunch length

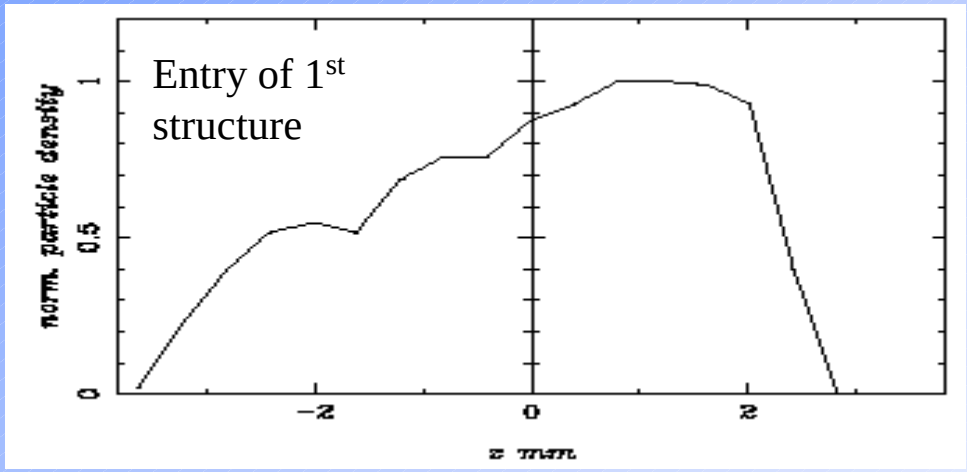

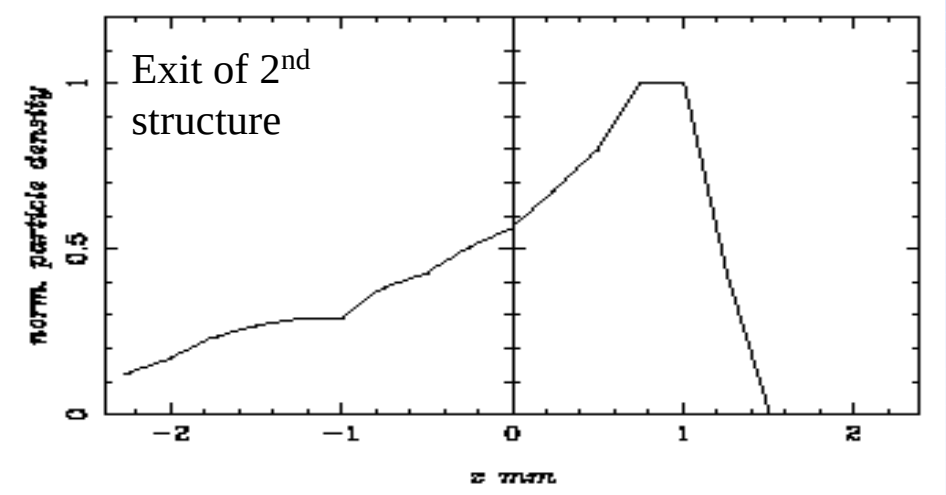

Accelerating structures-Energy spread

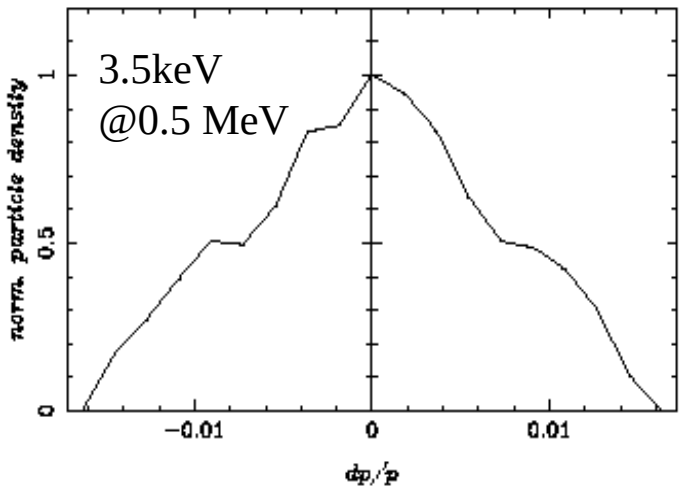

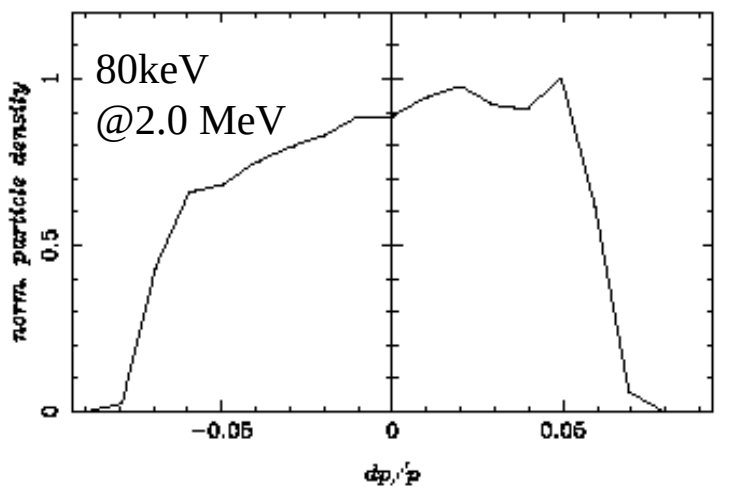

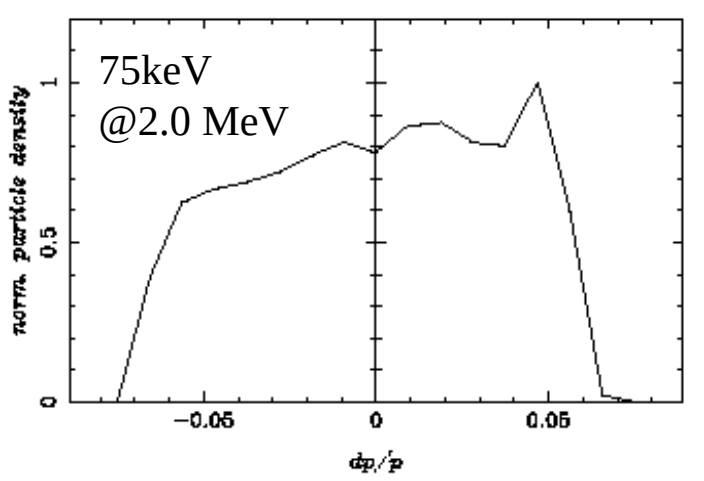

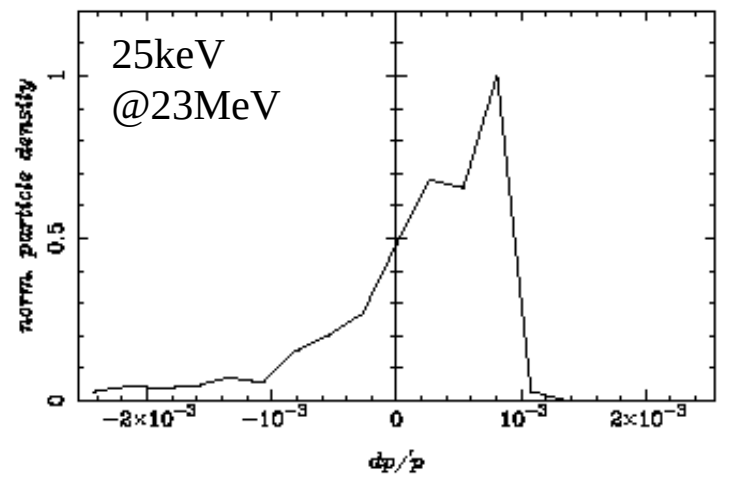

Simulation results

- Simulation starts from cathode. The initial distribution at the cathode :

  Longitudinal: Plateau distribution, 25 ps top, 2 ps for rise and fall time, respectively.

  Transverse: Uniform, RMS 1mm

  Particles: 1000

  bunch charge: 0.15 nC

- Both longitudinal and transverse emittance,beam size, bunch length, energy spread vs longitudinal position

Simulation Results: Laser Longi. Distributions on the cathode

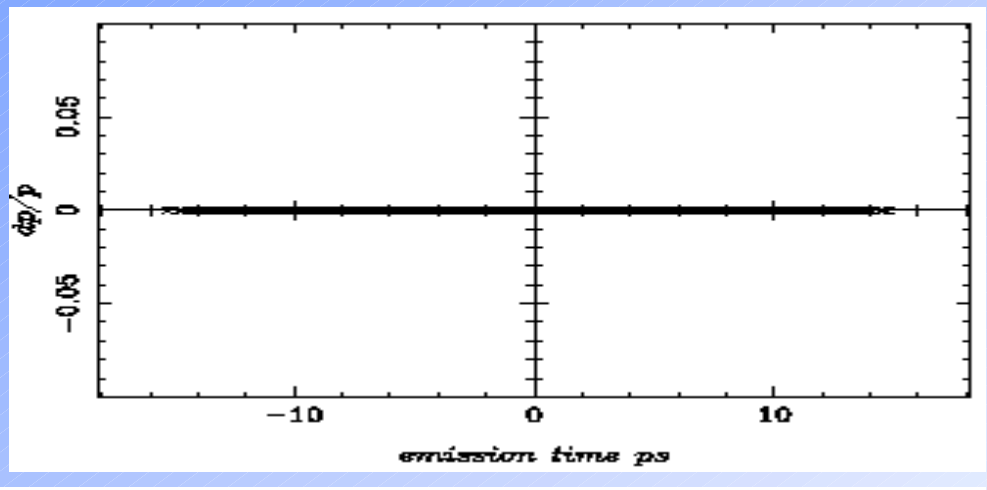

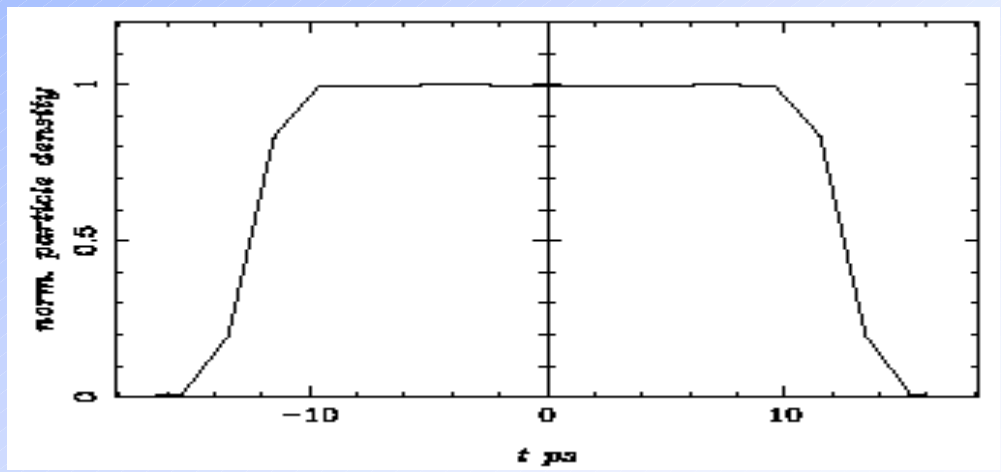

Simulation Results: Laser Trans. Distributions on the cathode

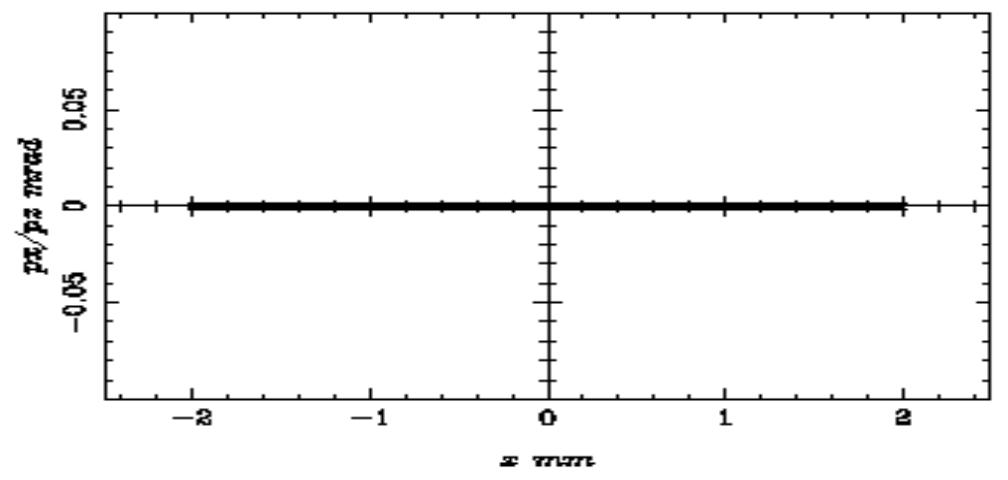

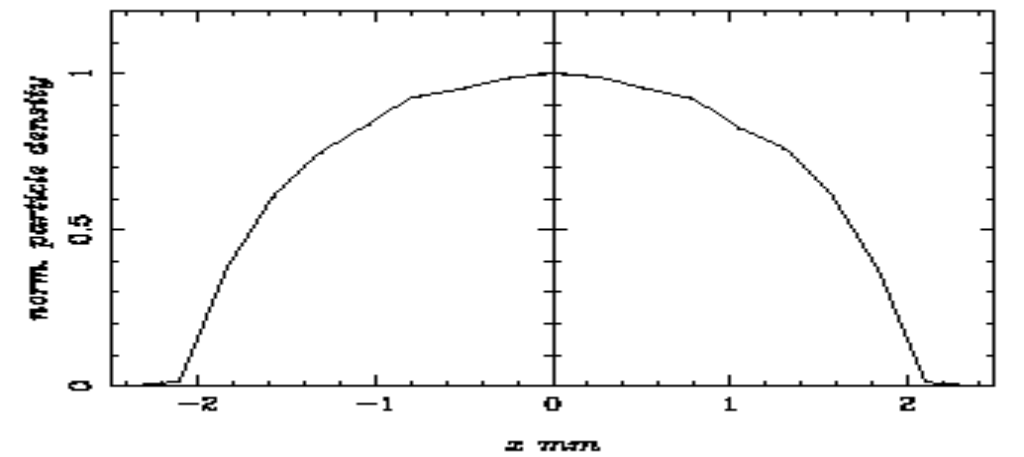

Simulation Results: Transverse Emittance and Beam size

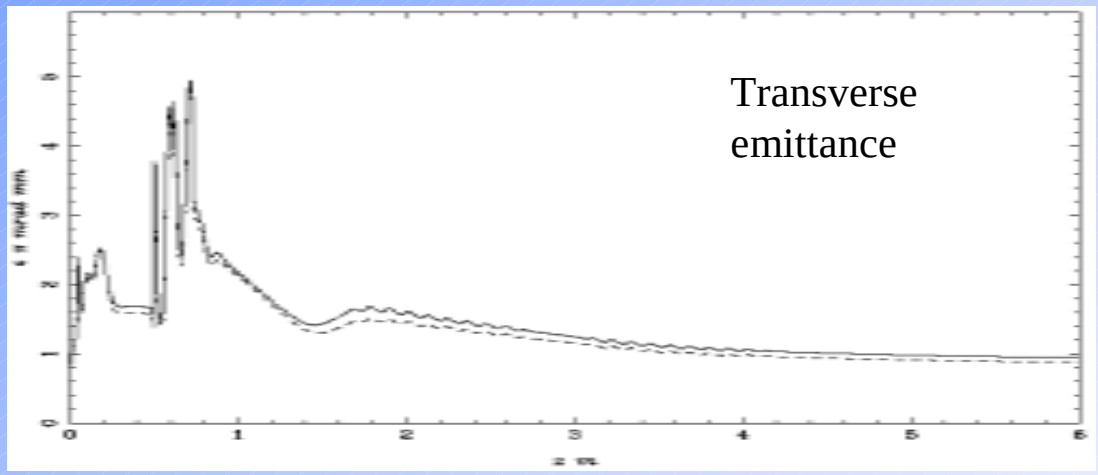

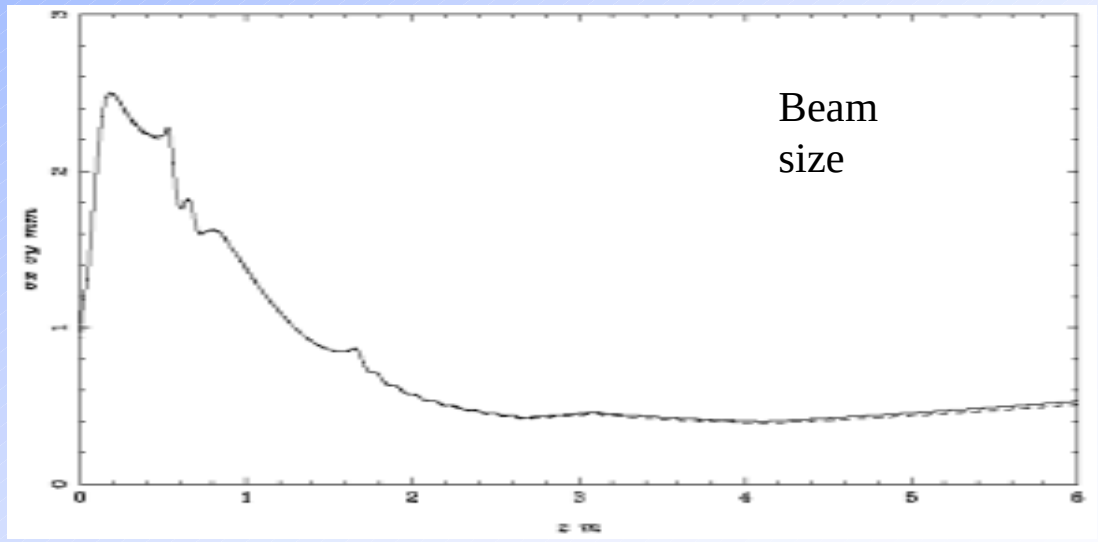

Simulation Results:Beam Divergence

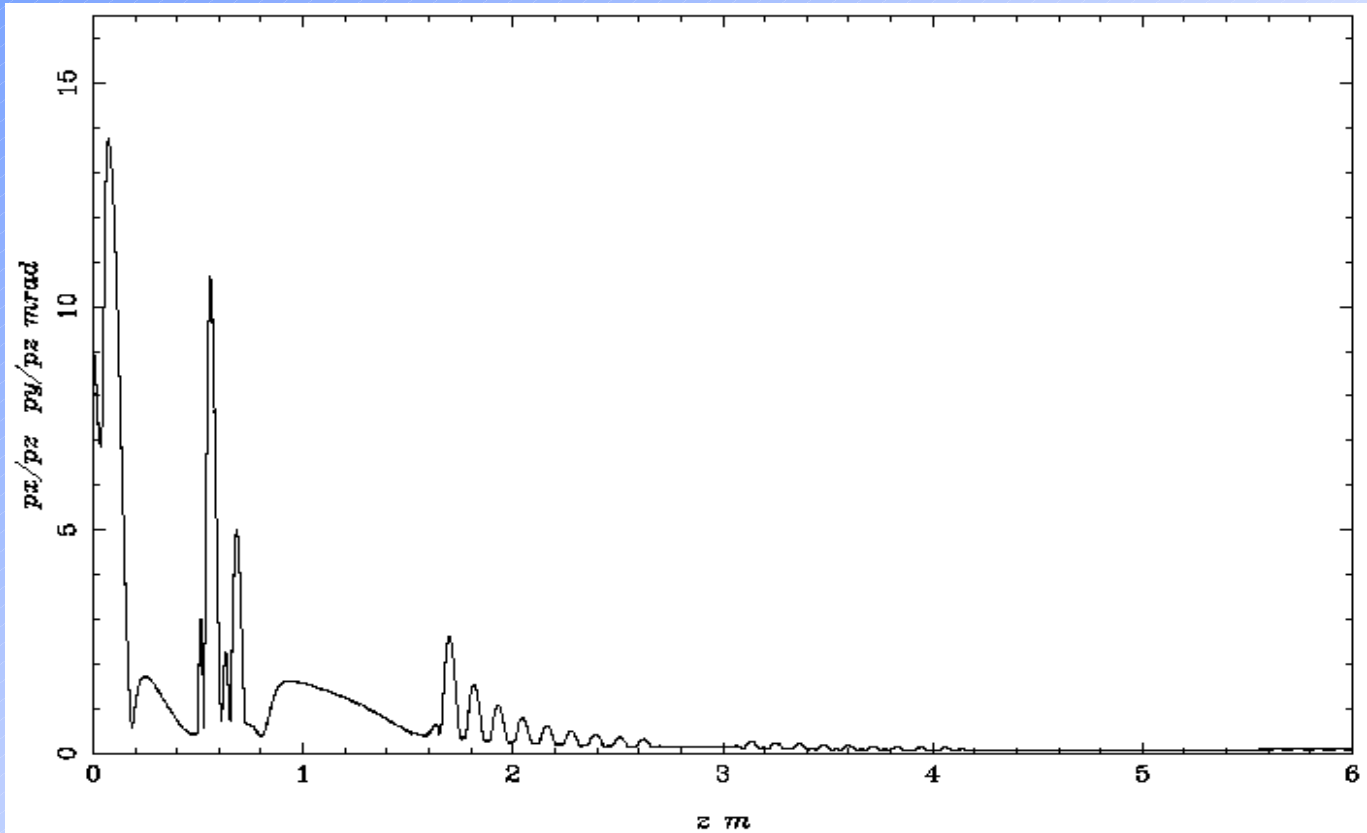

Simuation Results:Longitudinal Emittance and Bunch length

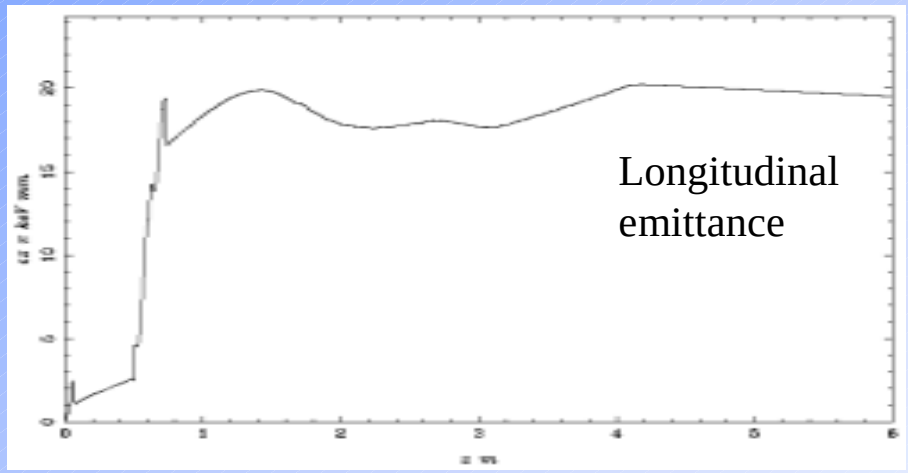

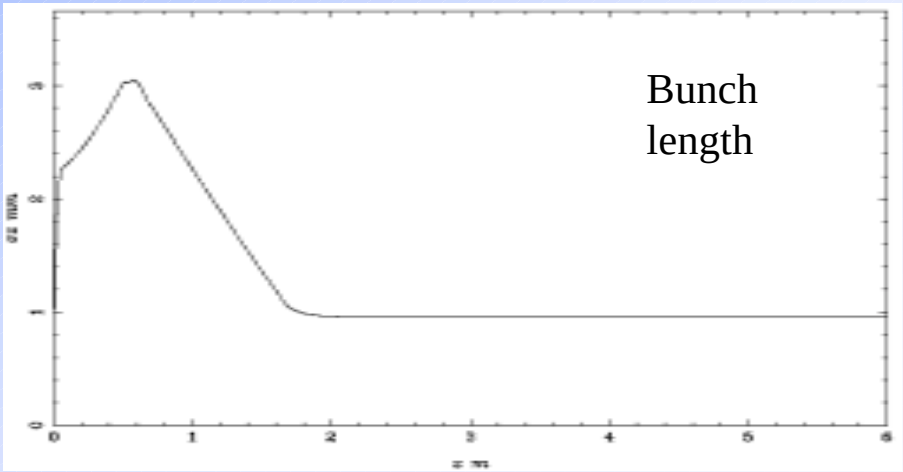

Simulation Results:Energy and Energy Spread

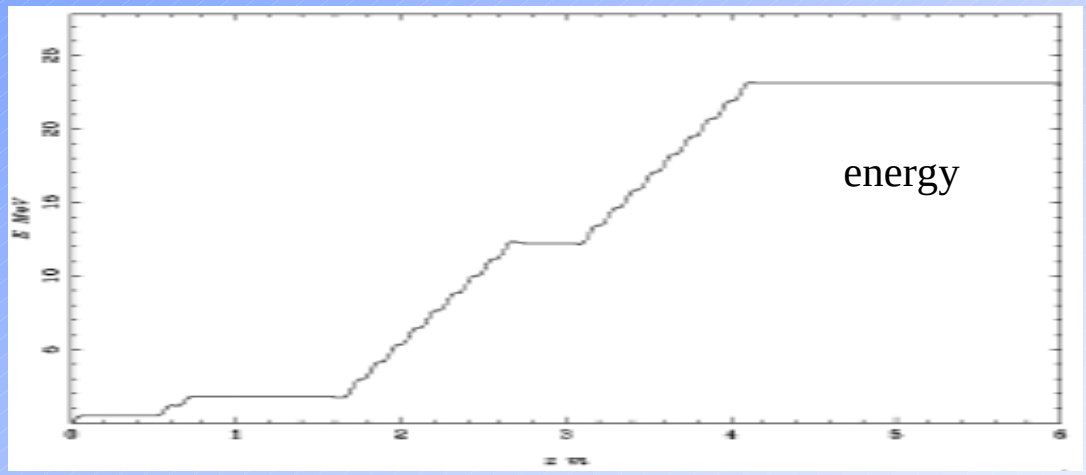

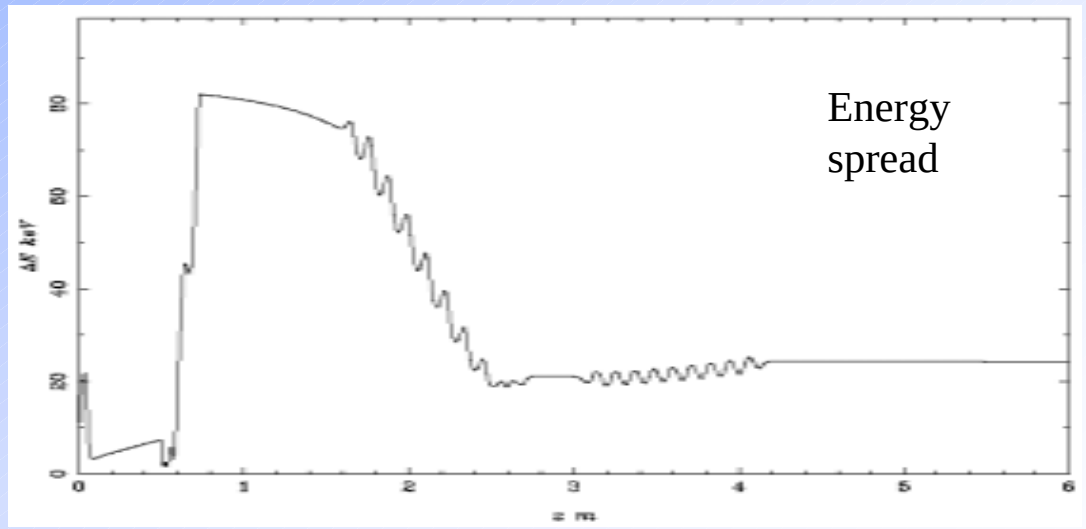

Summary and Outlook

	simulation	required
Energy (MeV)	23	25
RMS energy spread (keV)	27	25
RMS bunch length (ps)	3	3
Bunch charge (nC)	0.15	0.15
Longitudinal emittance (mm.keV)	20	-
Transverse emittance (mm.mrad)	1.0	1.0

The preliminary simulation results for DC gun are encouraging.
And the future work is to optimize the transverse emittance, including:
* two solenoids optimization for both the location and strength,
and buncher optimization for the location and strength, etc.
* loosening the initial laser pulse length on the cathode
* your constructive suggestion…..

Possible use of PEP-II cavity technology for a photocathode RF gun

R. Rimmer

LBNL

Intro. to PEP-II cavity
- design goals
- specifications
- fabrication

A photocathode injector study
- IFRA study
- RF gun cavity
- injector cost estimates
- frequency scaling

A 714 MHz cavity for NLC damping rings
- simplified design
- improved fabrication methods
- costs

A 1.5 GHz cavity for ALS
- simple third harmonic cavity

Intro. to PEP-II cavity

476 MHz, single cell with HOM damping
High gap voltage and heavy beam loading
High HOM load power
High reliability
Thermal stresses high around ports

design: 1 MV, 150 kW, 3A beam, 3.5 MΩ
operation: 850 kV, 95 kW, 2.2A, 3.8 MΩ
highest HOMs ~1.8 kΩ, 144 kΩ/m

Fabrication in-house + industry

Cost <$150k in quantity of 26

PEP-II *B*-Factory

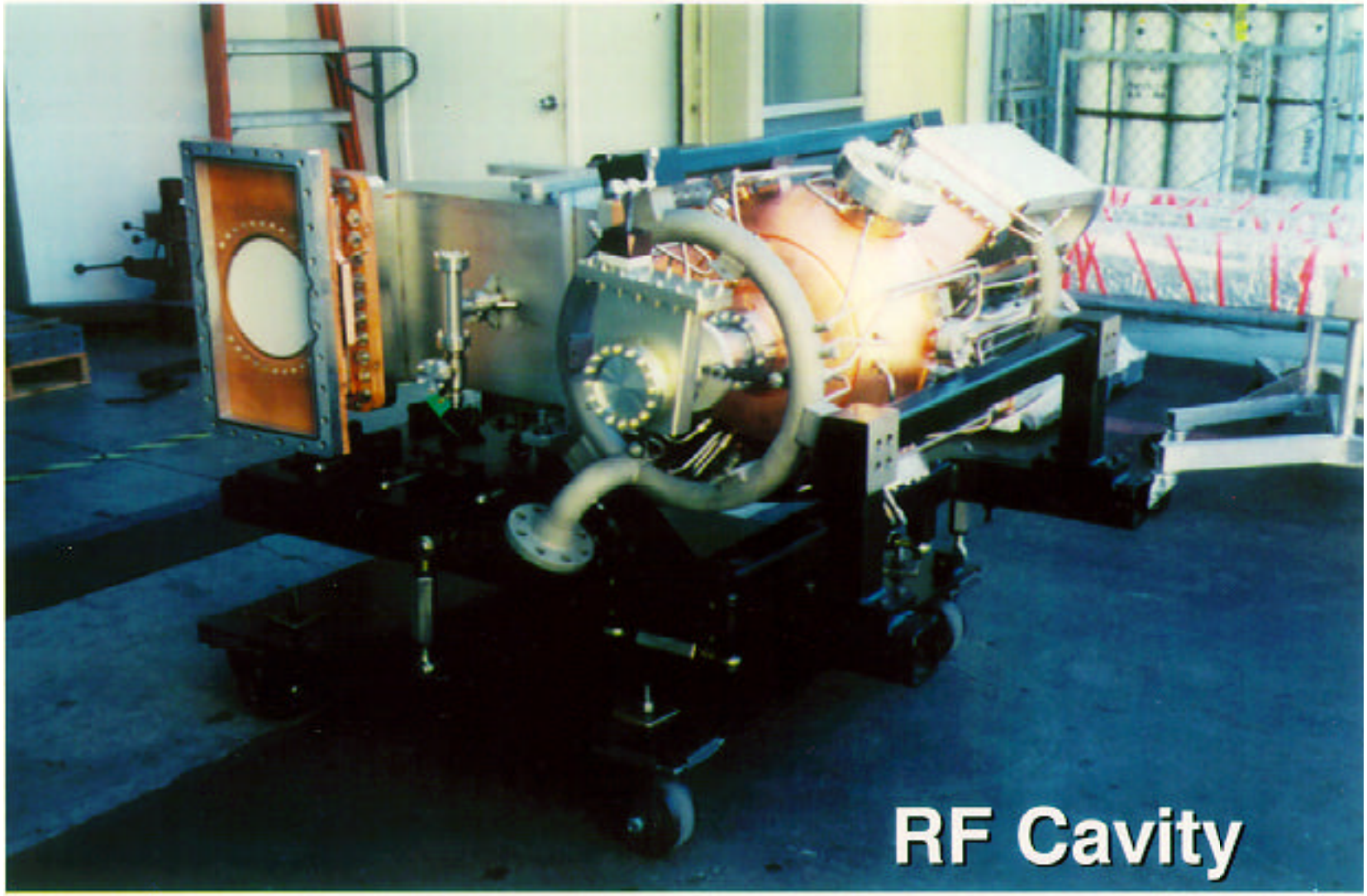

PEP-II *B*-Factory

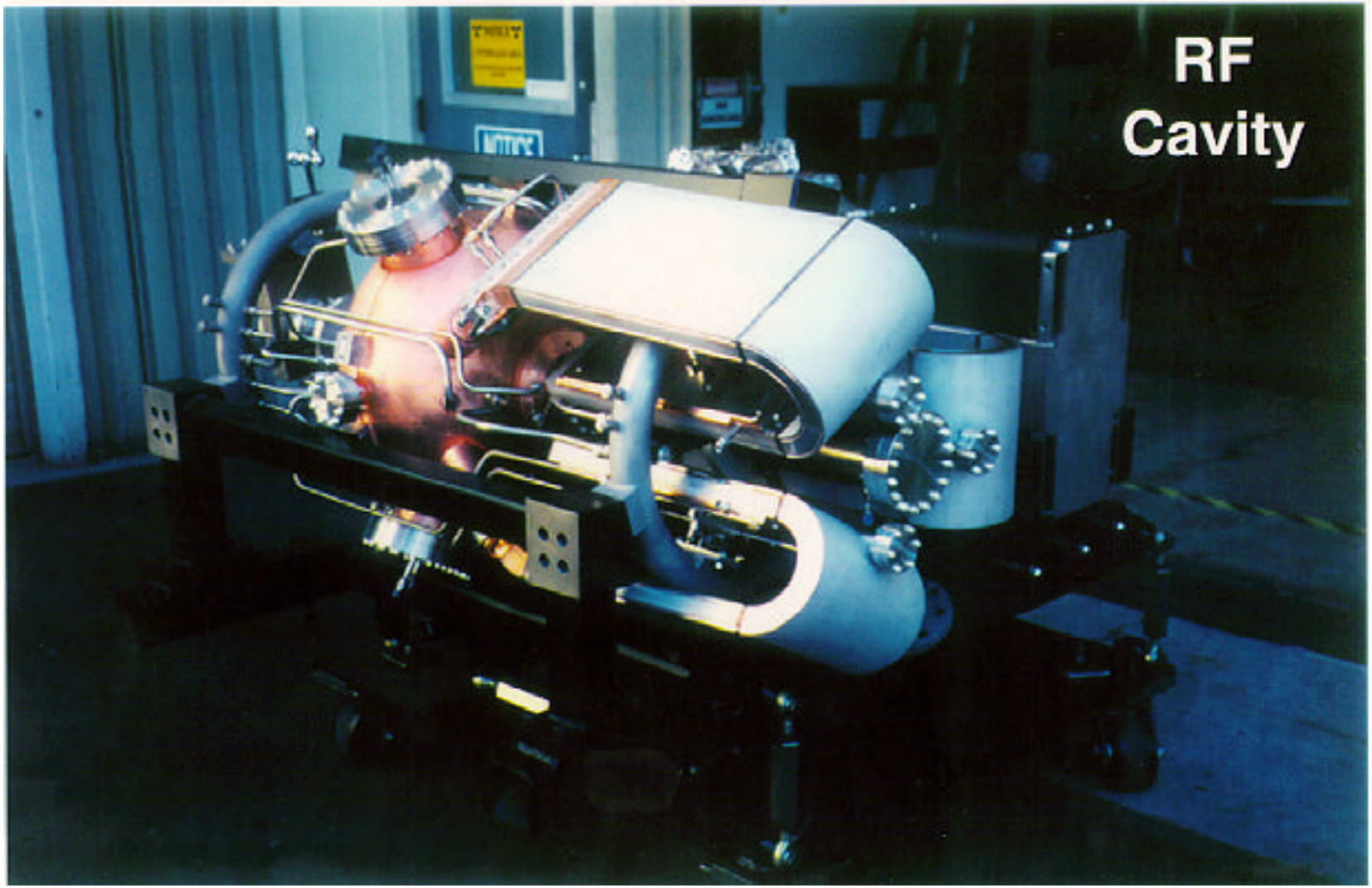

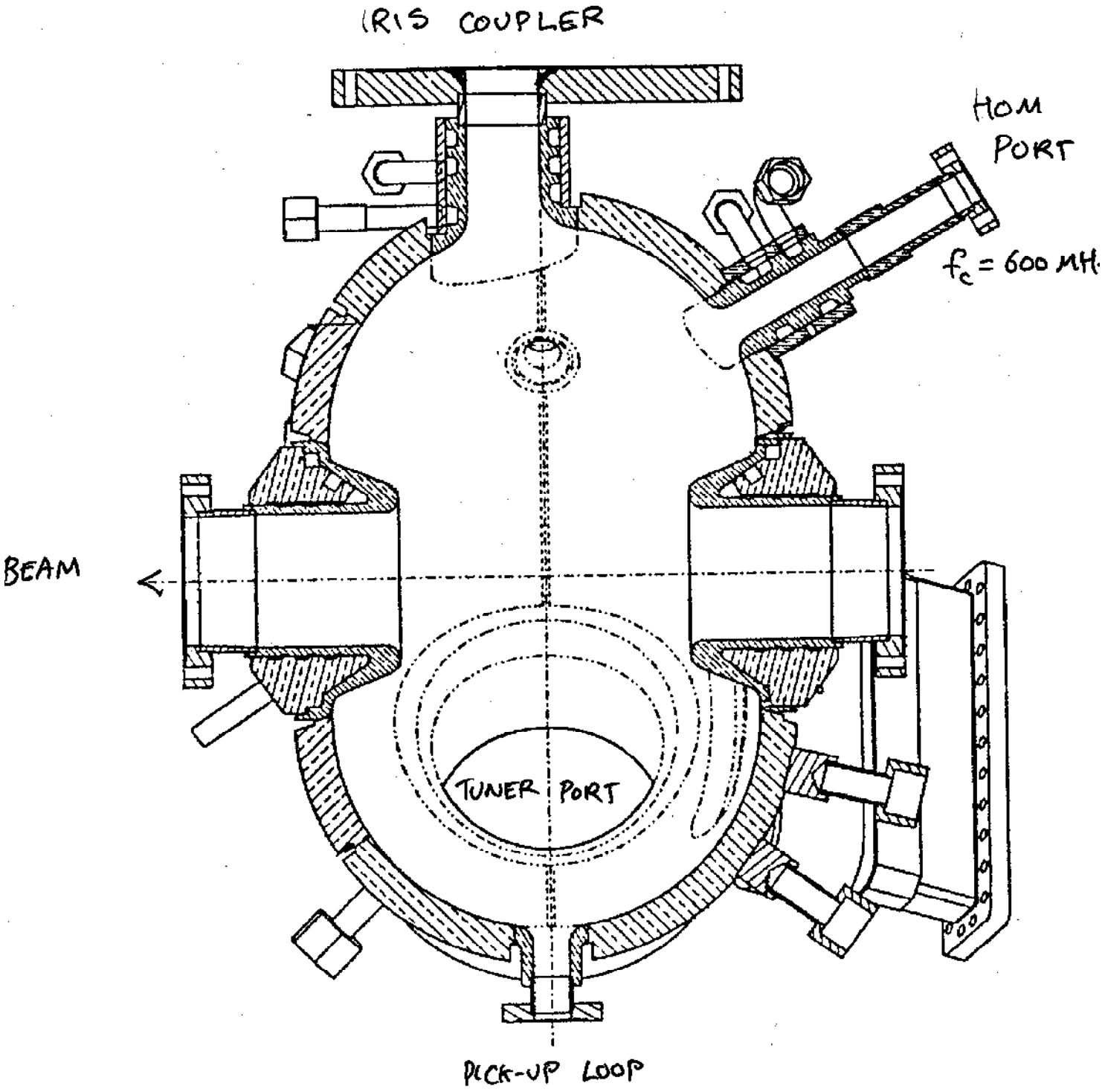

PEP-II RF CAVITY f_0 = 476 MHz

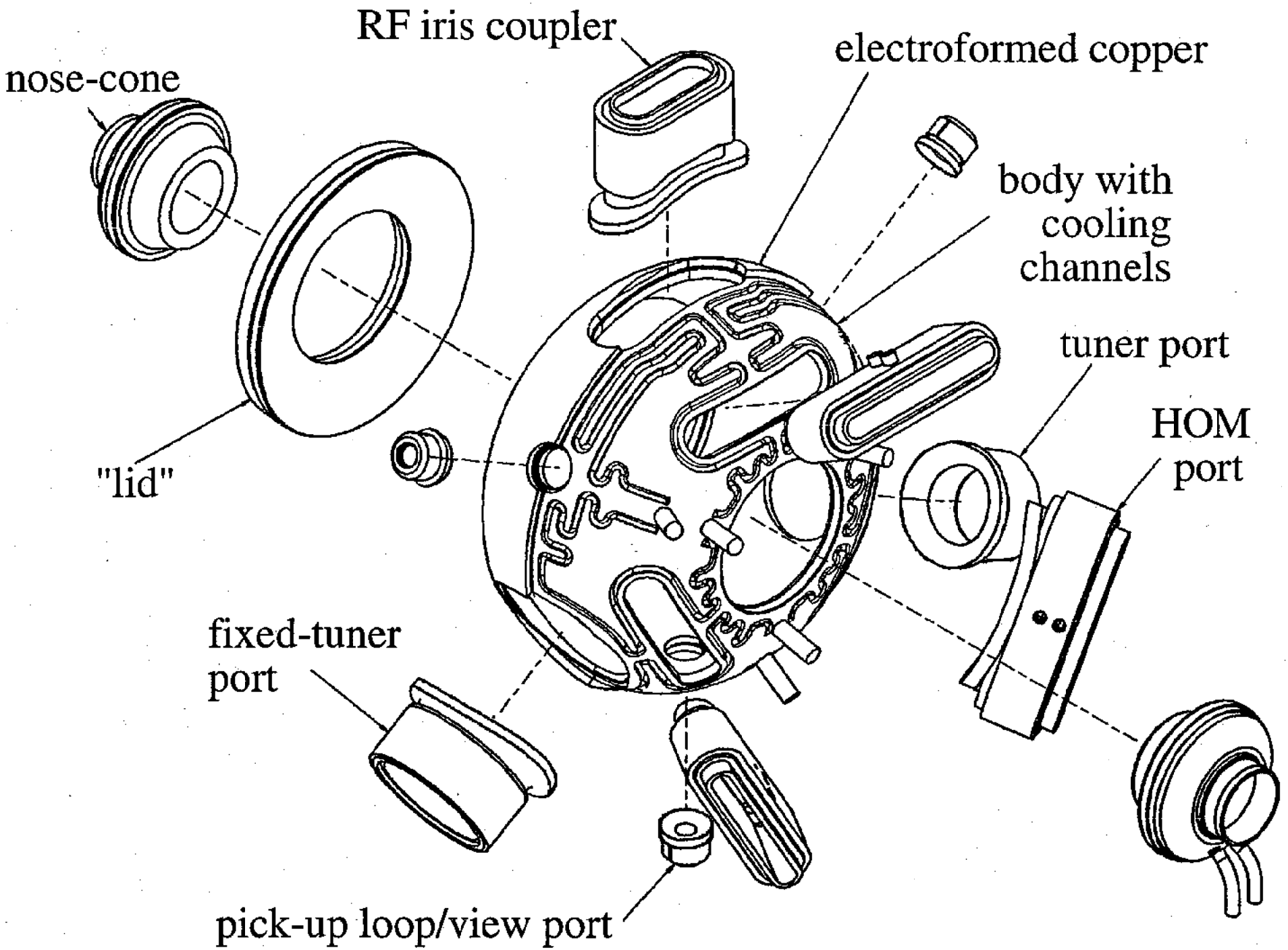
RF iris coupler
electroformed copper
nose-cone
body with
cooling
channels
tuner port
HOM
port
"lid"
fixed-tuner
port
pick-up loop/view port

PEP-II RF Cavity produced by Lawrence Livermore National Laboratory

RF cavity blanks are cold formed from 1" thick flat plate material.

Machined bowls are electron beam welded to form a cavity, then the water channels are cut into the outer contour.

Wax is placed into the water channels prior to plating 3/8" thickness of OFE copper. Note future port location.

Penetrations for various ports are cut through the electroplated cavity body. Note the blue wax in 4 holes.

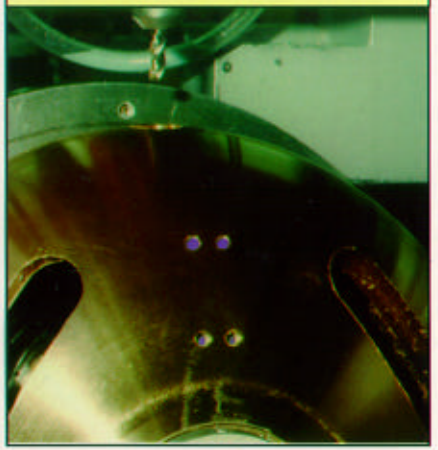

Full penetration EB vacuum welds attach tuner, Iris and HOM ports.

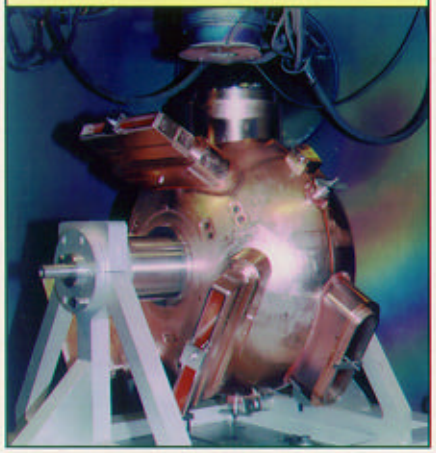

The RF surface is finish turned to a 16 Ra finish using LLNL's Diamond Turning Machine #3.

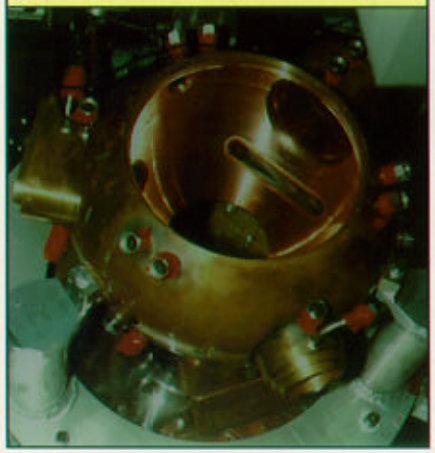

The beams noses are EB welded into the cavity following a precise tuning process.

The final product is cleaned for UHV and ready for shipment.

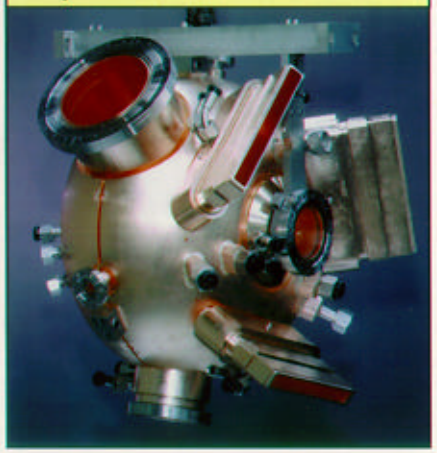

37937-mf-u-001

Lessons learned from PEP-II cavity fabrication

End product works very well

Fabrication processes worked well

- cold-forming of bowls
- vacuum/H_2 brazing
- multi-axis machining
- e-beam welding
- electro-forming

thermal stress problem dominated by current concentration around HOM ports

cost & complexity

- complex cooling channel geometry
- large number of ports, many different types
- most needing multi-axis machining
- tight tolerances for brazed-on water jackets
- rectangular knife-edge flanges

A photocathode injector study

IFRA study for power beaming
- based on "off the shelf" technology

CW RF gun cavity
- shape optimized for low beta, max. Rs
- gradient, emittance limited by P_{wall}
- fabrication would be based on PEP-II

injector cost estimates
- based on PEP-II costs, $-mid-1990's

frequency scaling

Ignition Feedback Regenerative Amplifier

- 200 kW at 0.84 μm
- 200 A peak current
- 0.15 A average current
- 10 mm mrad normalized emittance

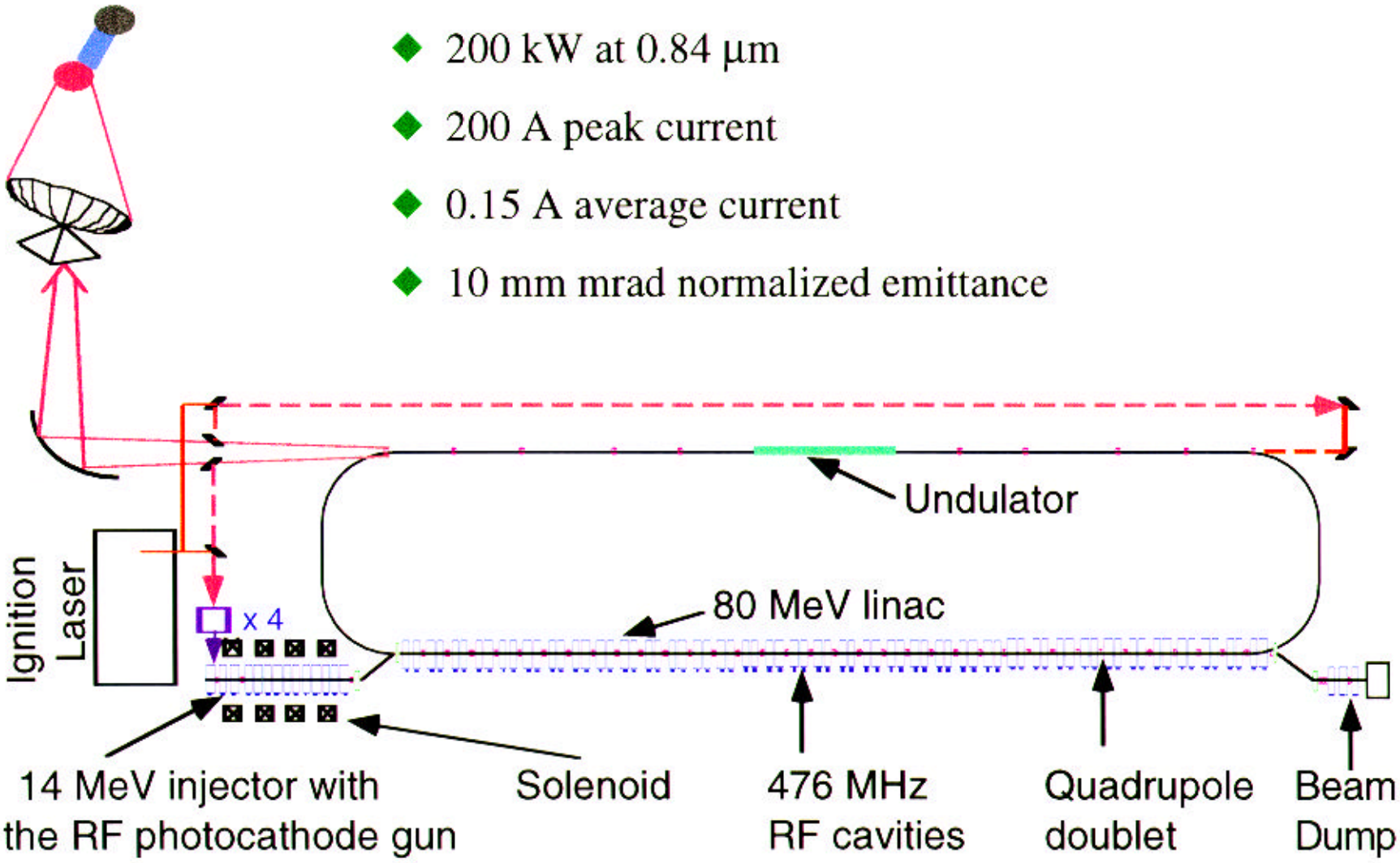

$R = 2.17\ M\Omega$ (no transit-time correction)
$R/Q = 95.7\ \Omega$
$Q = 22687$
$E_{z0} \simeq 18.3\ MV/m$ @ 100 kW.

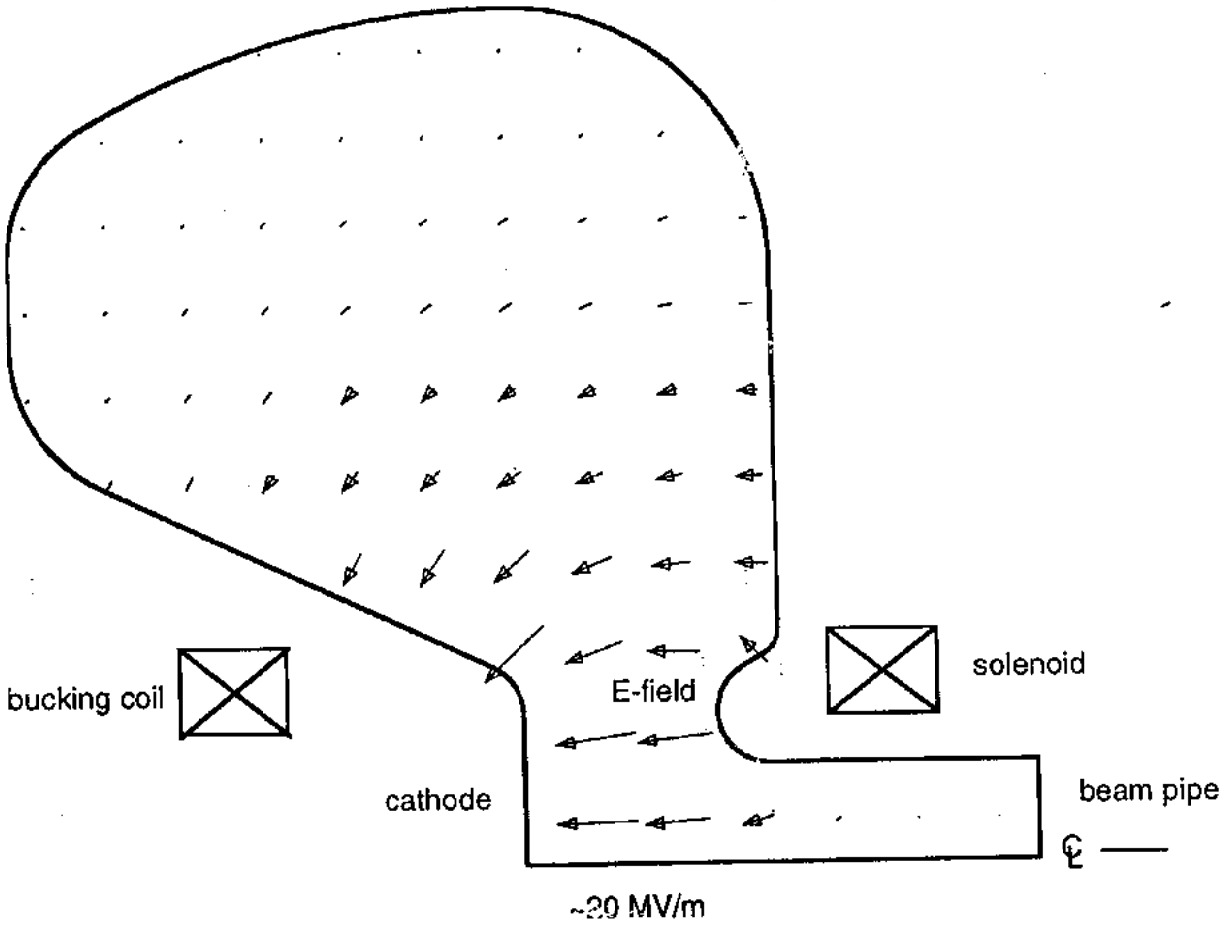

Possible photocathode cavity geometry

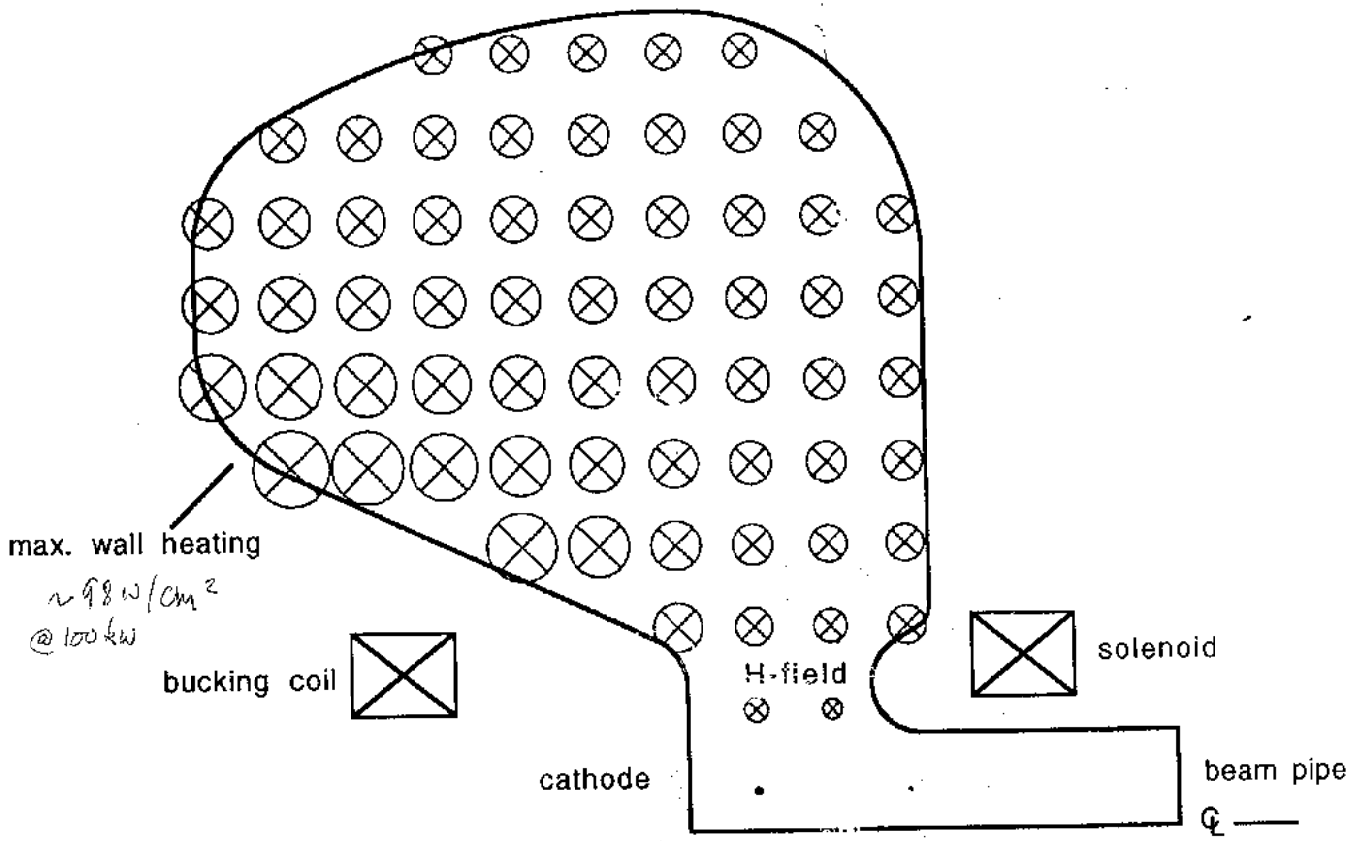

Possible photocathode cavity geometry

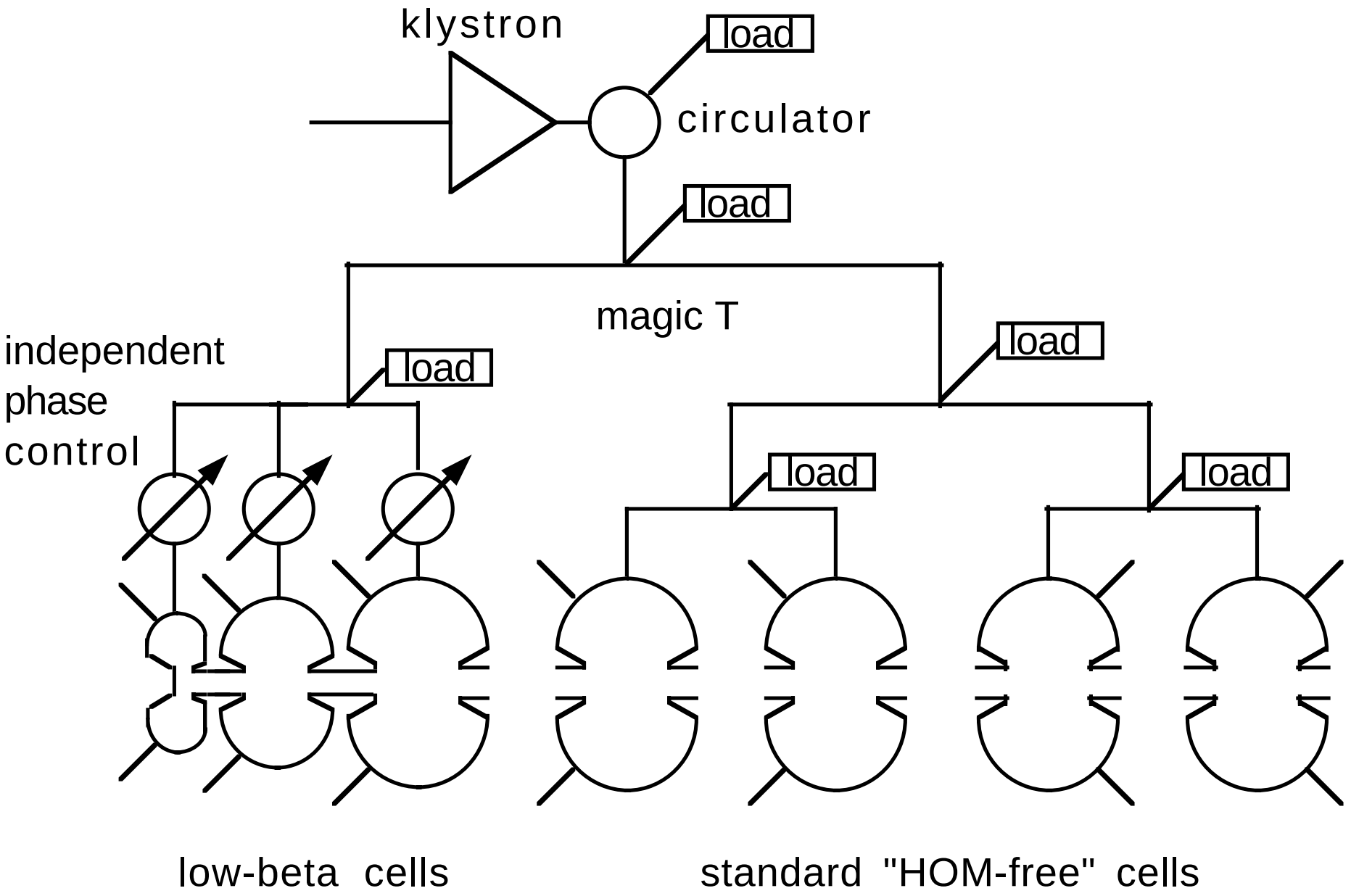
klystron
load
circulator
load
magic T
independent
phase
control
load
load
load
load
low-beta cells
standard "HOM-free" cells

PB RF Stn cost

Item	cost per item	HER		LER		PB	
	k$	# required	k$	# required	k$	# required	k$
Klystron (Phillips, 1.2 MW)	335	1	335	1	335	1	335
Cavity (1 MV max)	150	4	600	2	300	8	1200
HOM loads (3 per cavity)	17	12	204	6	102	24	408
Coupler box (1 per cavity)	19	4	76	2	38	8	152
500 kW Window (1 per cavity)	21	4	84	2	42	8	168
Fixed tuner (1 per cavity)	2	4	8	2	4	8	16
Variable tuner (1 per cavity)	20	4	80	2	40	8	160
Raft (1 per cavity)	12	4	48	2	24	8	96
Circulator (AFT)	155	1	155	1	155	1	155
Waveguide network	68	1	68	1	68	2	136
Low-level RF	85	1	85	1	85	2	170
HV power supply	375	1	375	1	375	1	375
Cooling system	40	1	40	1	40	1	40
Cables	35	1	35	1	35	1	35
Misc., installation etc.	60	1	60	1	60	1	60
total station cost (k$):			2253		1703		3506
total station voltage (kV):			3200		1700		6800
beam power available (kW):			800		990		360
voltage cost performance ($/V):			0.70		1.00		0.52
power cost performance ($/W):			2.82		1.72		9.74

PB RF Stn cost

Item	cost per item	4x5cell		2x5cell	
	k$	# required	k$	# required	k$
Klystron (Phillips, 1.2 MW)	335	1	335	1	335
Cavity (1 MV max)	500	4	2000 ($500k ea)	2	1000 ($500k ea)
HOM loads (3 per cavity)	17	24	408	12	204
Coupler box (1 per cavity)	19	4	76	2	38
500 kW Window (1 per cavity)	21	4	84	2	42
Fixed tuner (1 per cavity)	2	20	40	10	20
Variable tuner (1 per cavity)	20	20	400	10	200
Raft (1 per cavity)	12	4	48	2	24
Circulator (AFT)	155	1	155	1	155
Waveguide network	68	1	68	1	68
Low-level RF	85	1	85	1	85
HV power supply	375	1	375	1	375
Cooling system	40	1	40	1	40
Cables	35	1	35	1	35
Misc., installation etc.	60	1	60	1	60
total station cost (k$):			4209		2681
total station voltage (kV):			12650		8500
beam power available (kW):			300 ?		150 ?
voltage cost performance ($/V):			0.33		0.32
power cost performance ($/W):			14.03		17.87

R.R. 8/98

Gun / injector options

A: Photocathode gun plus 2.5 PEP-II based accelerating modules (length ~ 21 m, cost ~ 10.5 M)

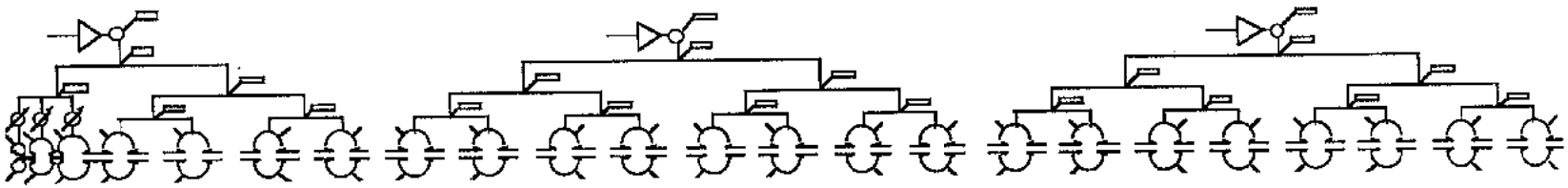

Veff (MV)	0.4/0.4/0.5	4 x 0.75	8 x 0.6	8 x 0.6	
total (MV)	1.4	3.0	4.8	4.8	14 MV
Pcell (kW)	100/36/36	4 x 80	8 x 51	8 x 51	
total (kW)	172	320	408	408	1308 kW
Pb (kW)	60/75/75	4 x 112.5	8 x 90	8 x 90	
total (kW)	210	450	720	720	
	382	770	1128	1128	
Pkly (kW)	1152		1128	1128	3408 kW

B: Photocathode gun plus five five-cell cavities (length ~ 12 m, cost ~ $8.8 M)

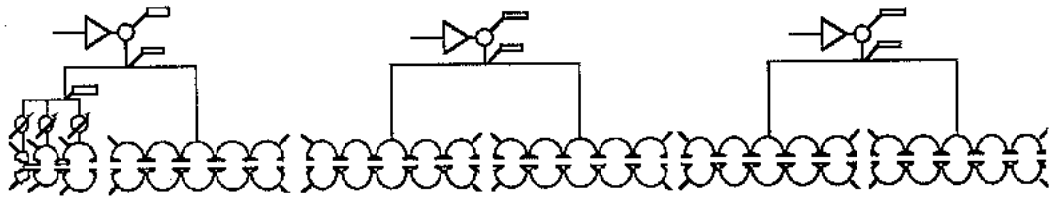

Veff (MV)	0.4/0.4/0.5	5 x 0.6	10 x 0.48	10 x 0.48	
total (MV)	1.4	3.0	4.8	4.8	14 MV
Pcell (kW)	100/36/36	5 x 45	10 x 28.8	10 x 28.8	
total (kW)	172	225	288	288	973 kW
Pb (kW)	60/75/75	5 x 90	10 x 72	10 x 72	
total (kW)	210	450	720	720	
	382	675	1008	1008	
Pkly (kW)		1057	1008	1008	3073 kW

R.R. 8/98

IFRA accelerator options (14 - 80 MV)

A: Module based on eight PEP-II cavities

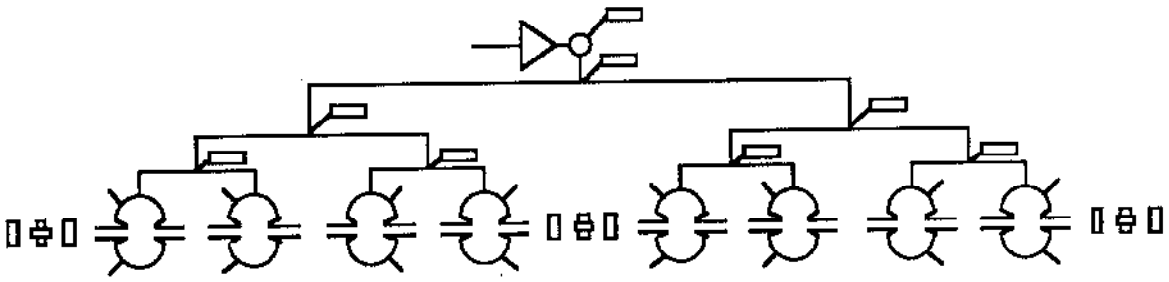

Rs = 8 x 3.5 MΩ (70% of MAFIA Q) = 28 MΩ
V = 8 x 0.85 MV (length ~ 6.927 m) = 6.8 MV (~ 1 MV/m)
P = 8 x 103 kW = 824 kW
cost = $3.5M ea., 80 MV requires 12 stations + 1 spare
total cost = $45.5M, length = 90 m, operating power= 9.9 MW + injector - $56M

B: Module based on four five-cell cavities

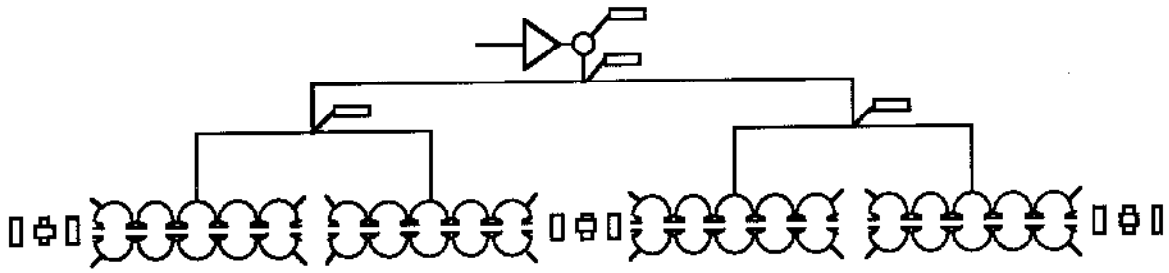

Rs = 20 x 4 MΩ (80% of MAFIA Q) = 80 MΩ
V = 20 x 0.6 MV (length ~ 8.6 m) = 12 MV (~ 1.5 MV/m)
P = 20 x 45 kW = 900 kW
cost = $4.2M ea., 80 MV requires 7 stations + 1 spare
total cost = $33.6M, length = 69 m, operating power = 6.3 MW

C: Module based on two high-power five-cell cavities

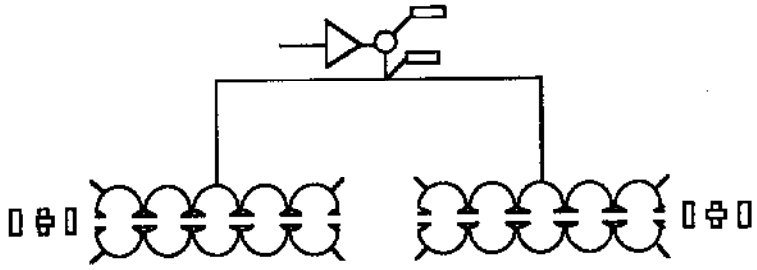

Rs = 10 x 3.5 MΩ (70% of MAFIA Q) = 35 MΩ
V = 10 x 0.85 MV (length ~ 4.281 m) = 8.5 MV (~2 MV/m)
P = 1= x 103 kW = 1030 kW
cost = $2.7M ea., 80 MV requires 10 stations + 1 spare
total cost = $29.7M, length = 47 m, operating power = 10.3 MW + injector = $8.5M

Scaling

for a set shape R/Q is a constant. Scaling the size to different frequencies for a given voltage the parameters vary as follows:

Quality factor Q, and shunt impedance $R_s \alpha 1/\mathrm{sqrt}(f)$

power α sqrt(f)

surface area $\alpha 1/f^2$

wall-power density $\alpha f^{2.5}$

Electric field strength increase α f

Kilpatrick criterion increases with frequency

Cavity with 500 kV at 714 MHz similar to PEP-II at 800 kV

$$f = 1.64\, E_k e^{(-8.5/E_k)}$$

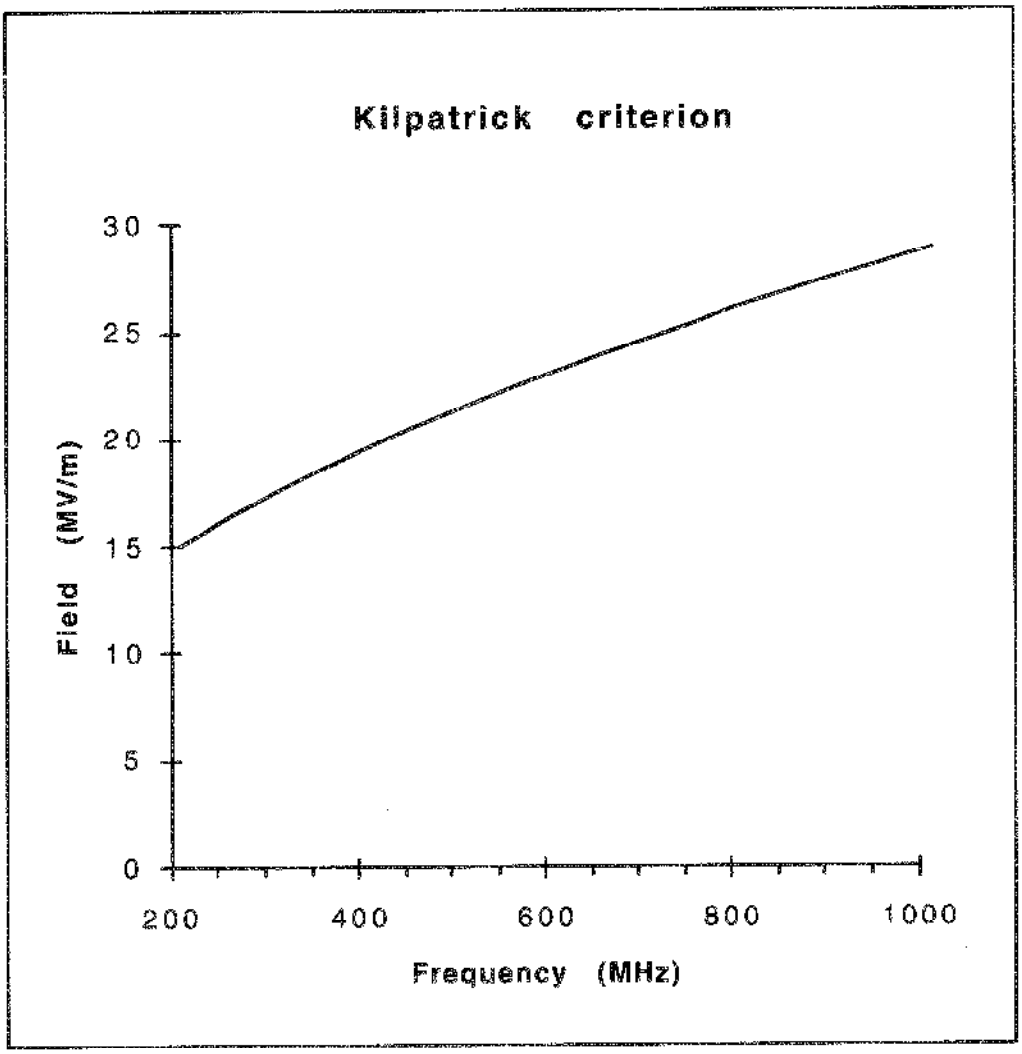

A 714 MHz cavity for NLC damping rings

simplified design
- rounded body, "dumbbell" HOM ports

improved fabrication methods
- fewer, simpler parts and operations

costs
- $100-150k ea. depending on labor rates
- ($200k+13,600 hours for 10 cavities)

Cheaper in China!

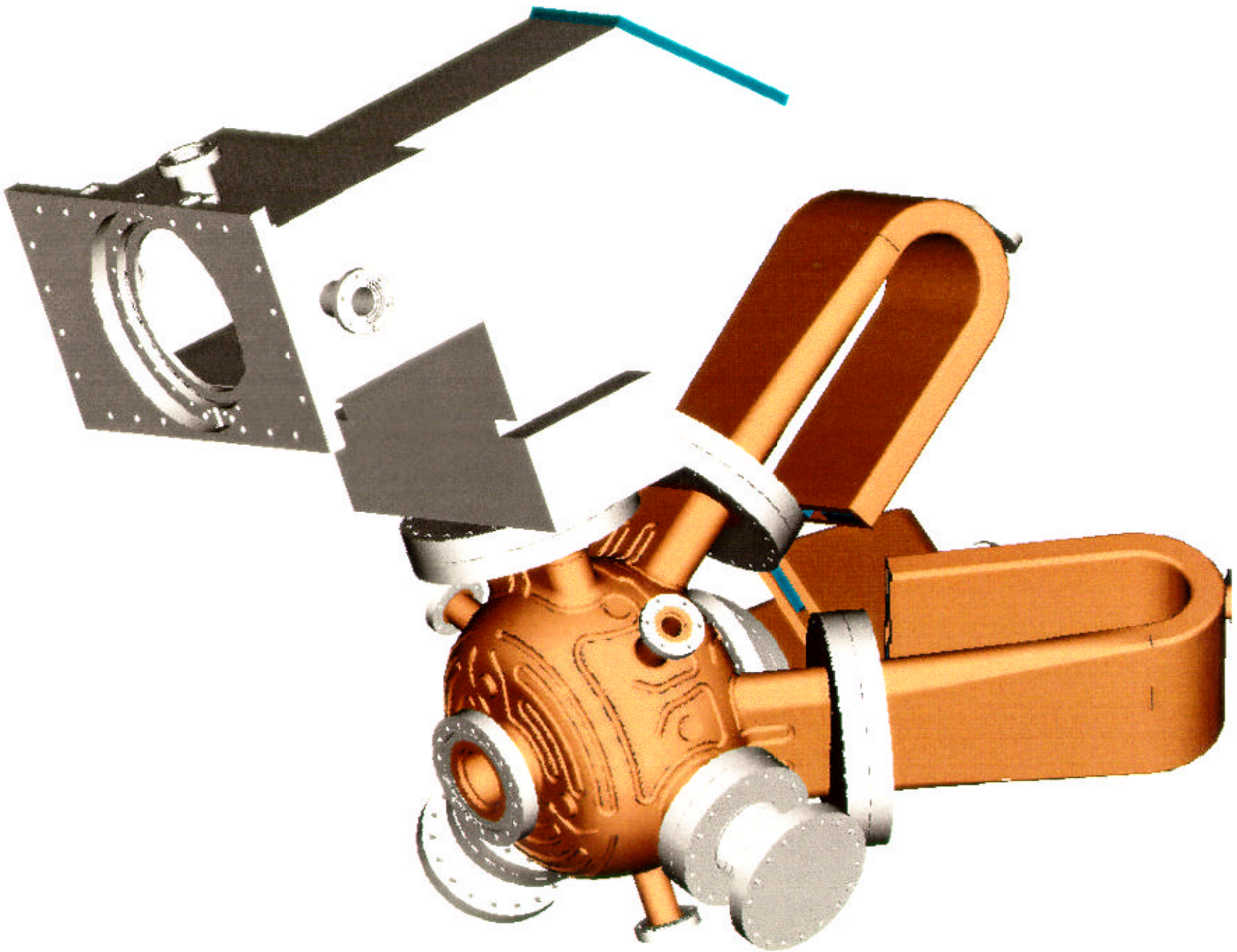

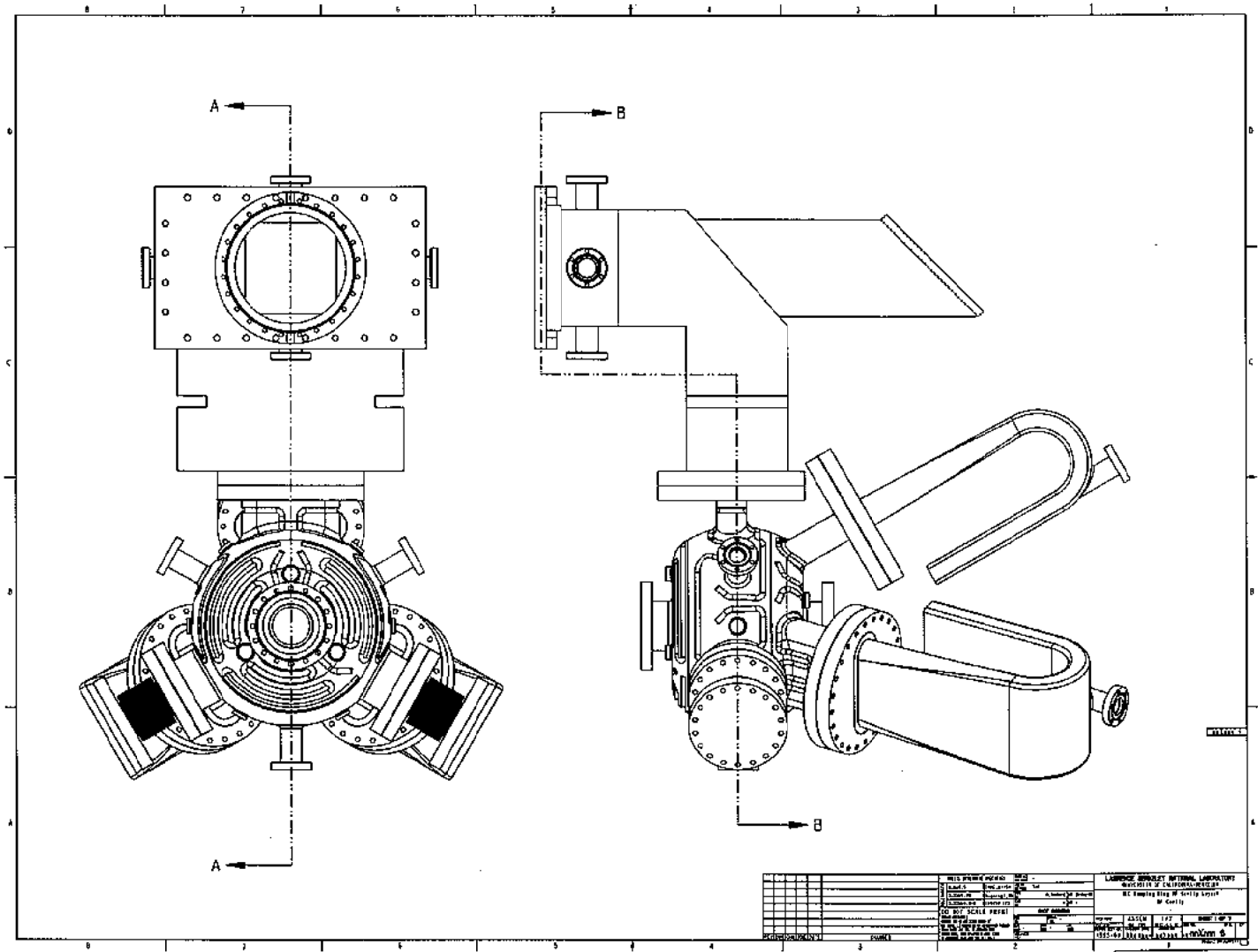

nnXnnn 6

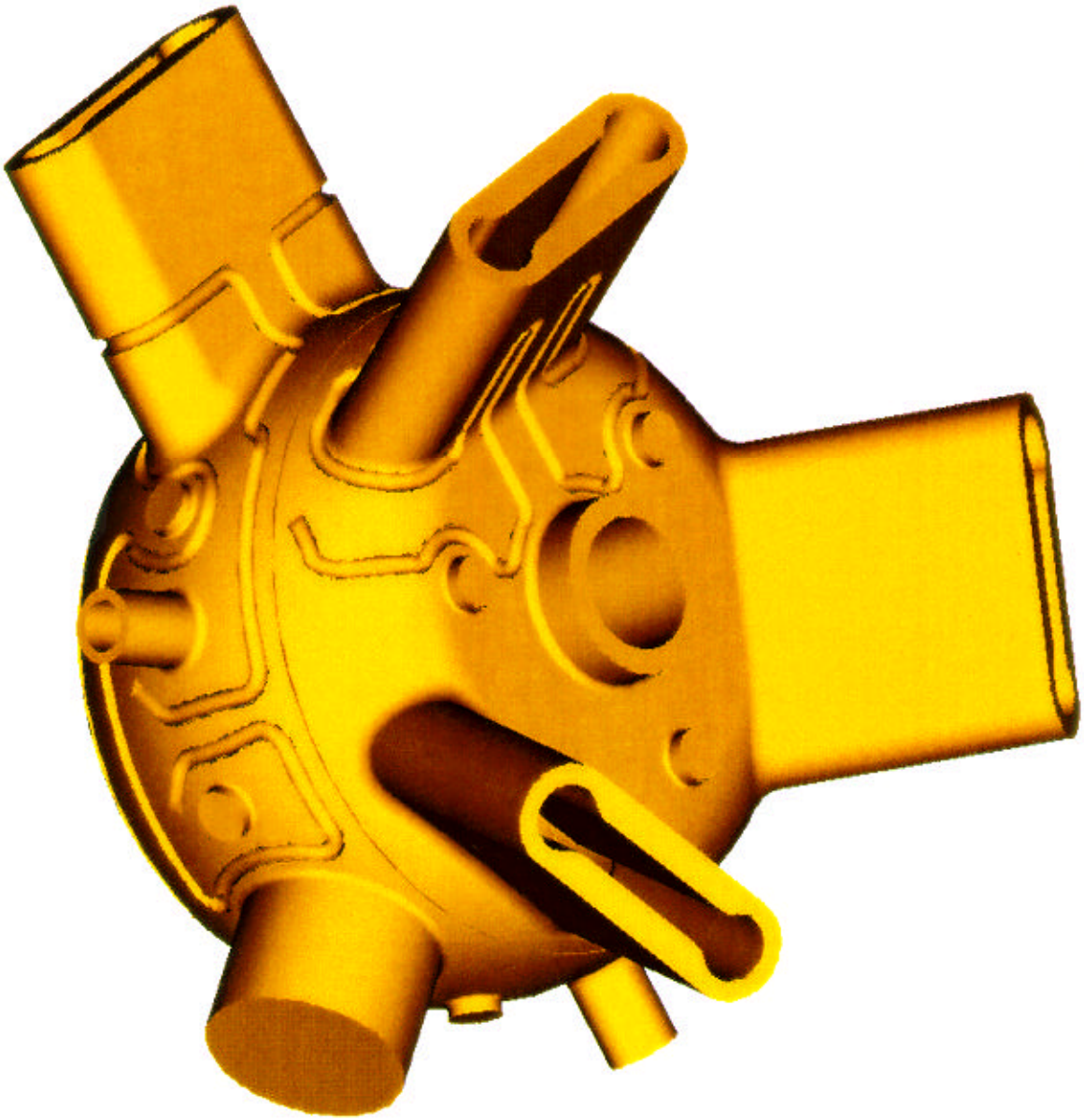

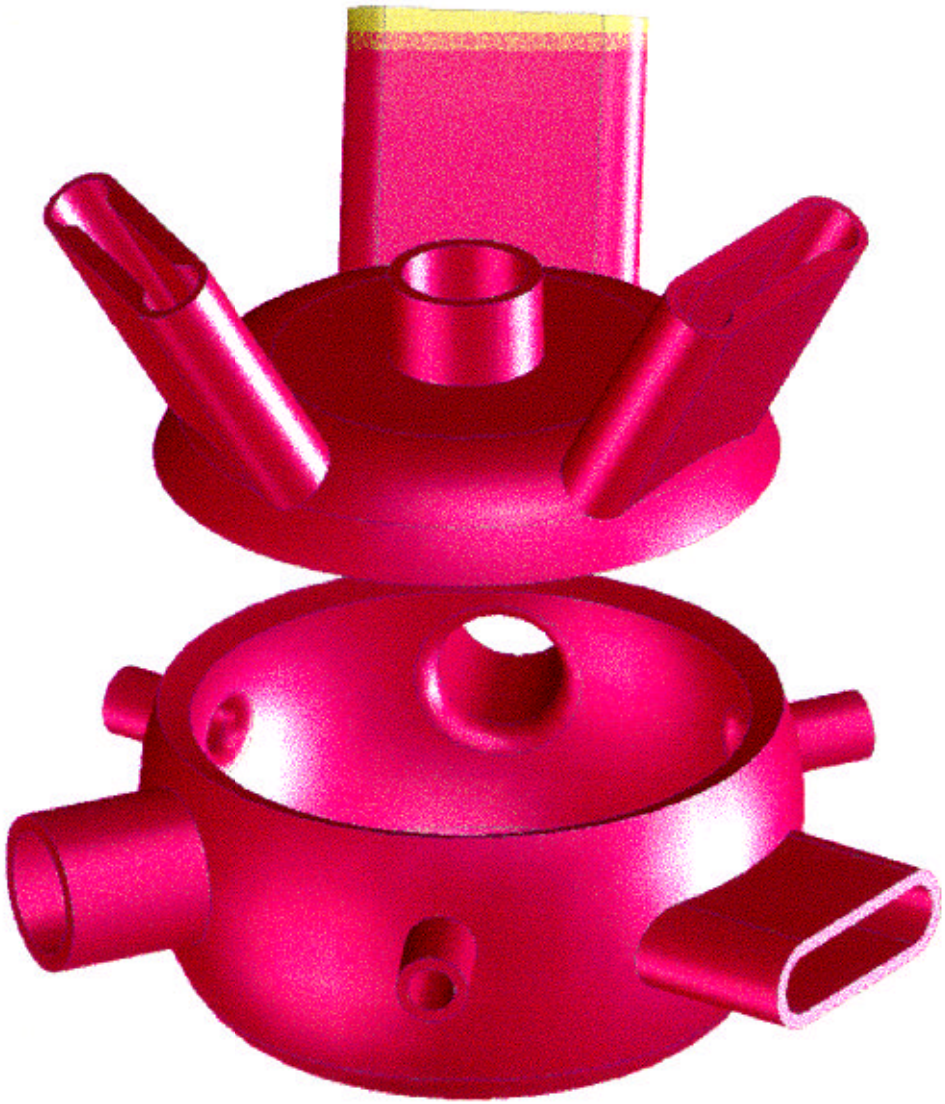

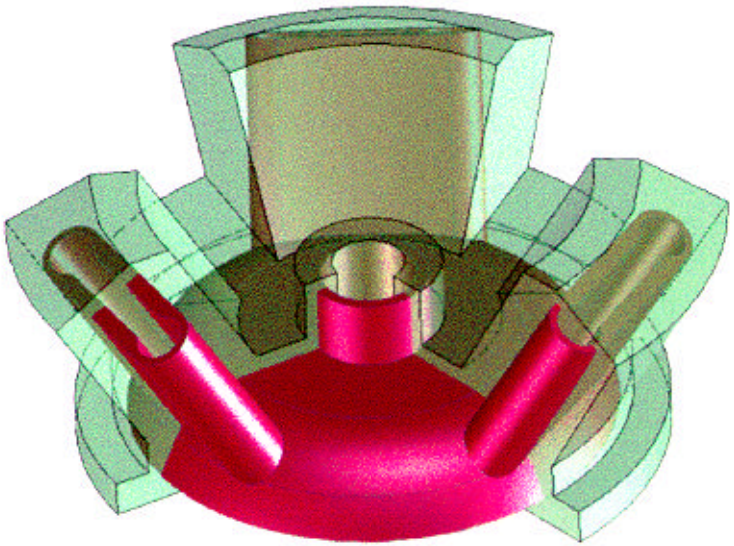

Figure 46. "Lid" forging.

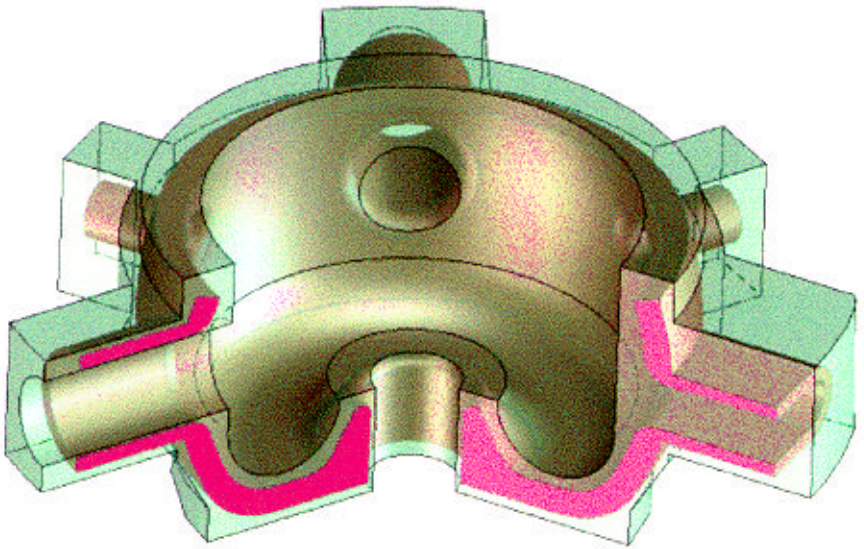

Figure 47. "Body" forging.

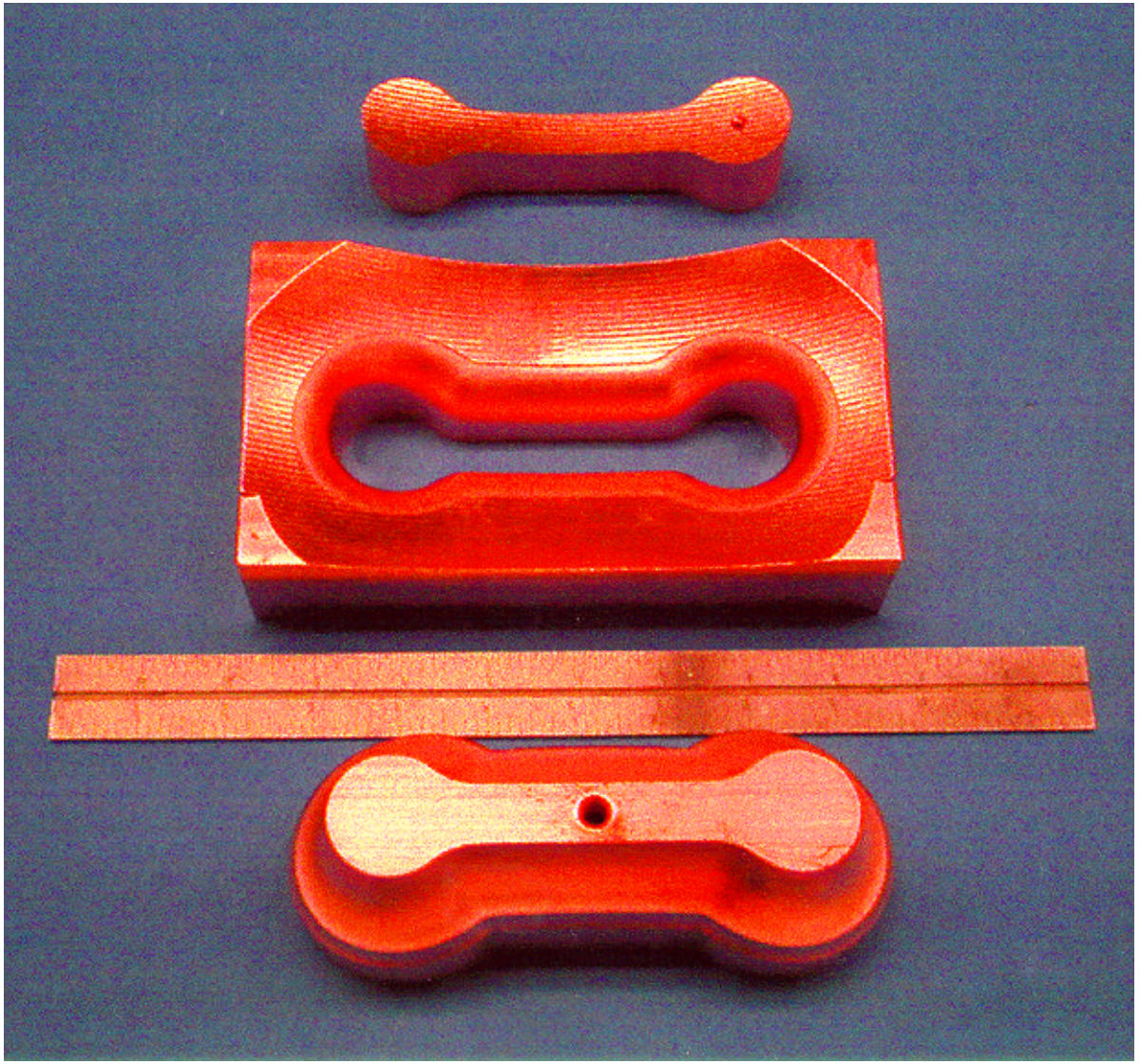

A 1.5 GHz cavity for ALS

6 simple third harmonic cavities

5 kW CW, 125 kV (conservative)

no HOM ports

PEP-II type body channels

made from OFE Cu plate stock

e-beam welded and plated

made in house and quickly so $$$! (~100k ea.)

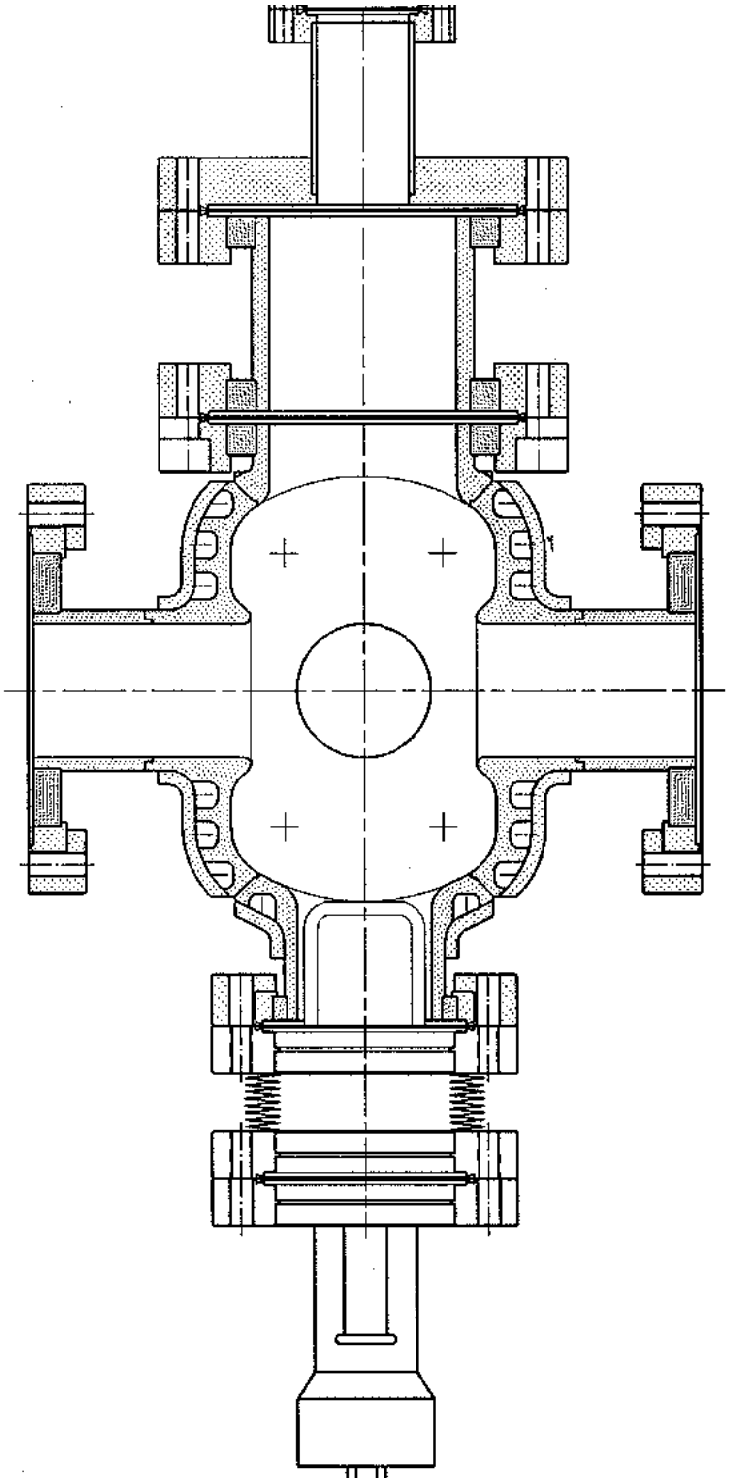

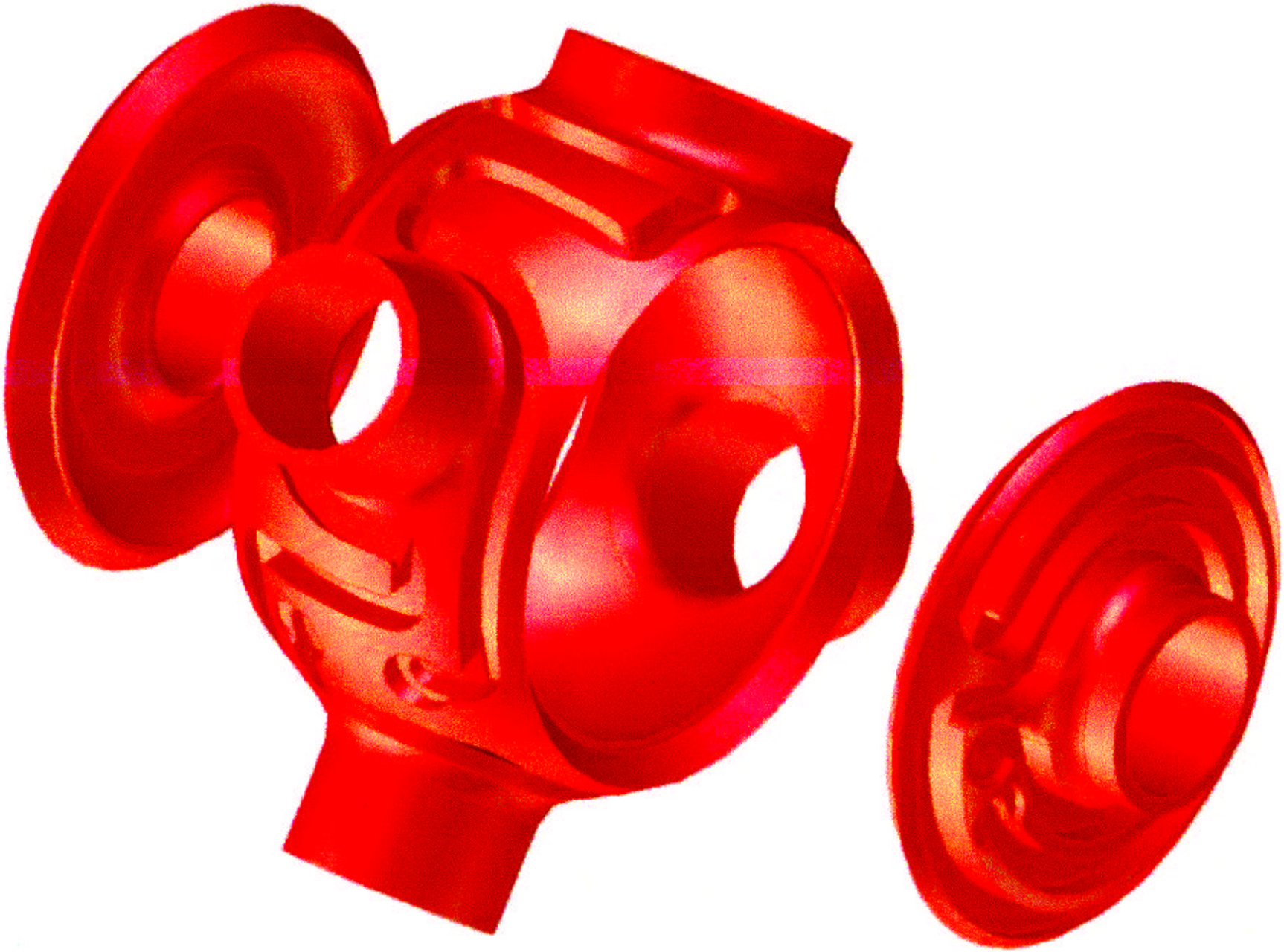

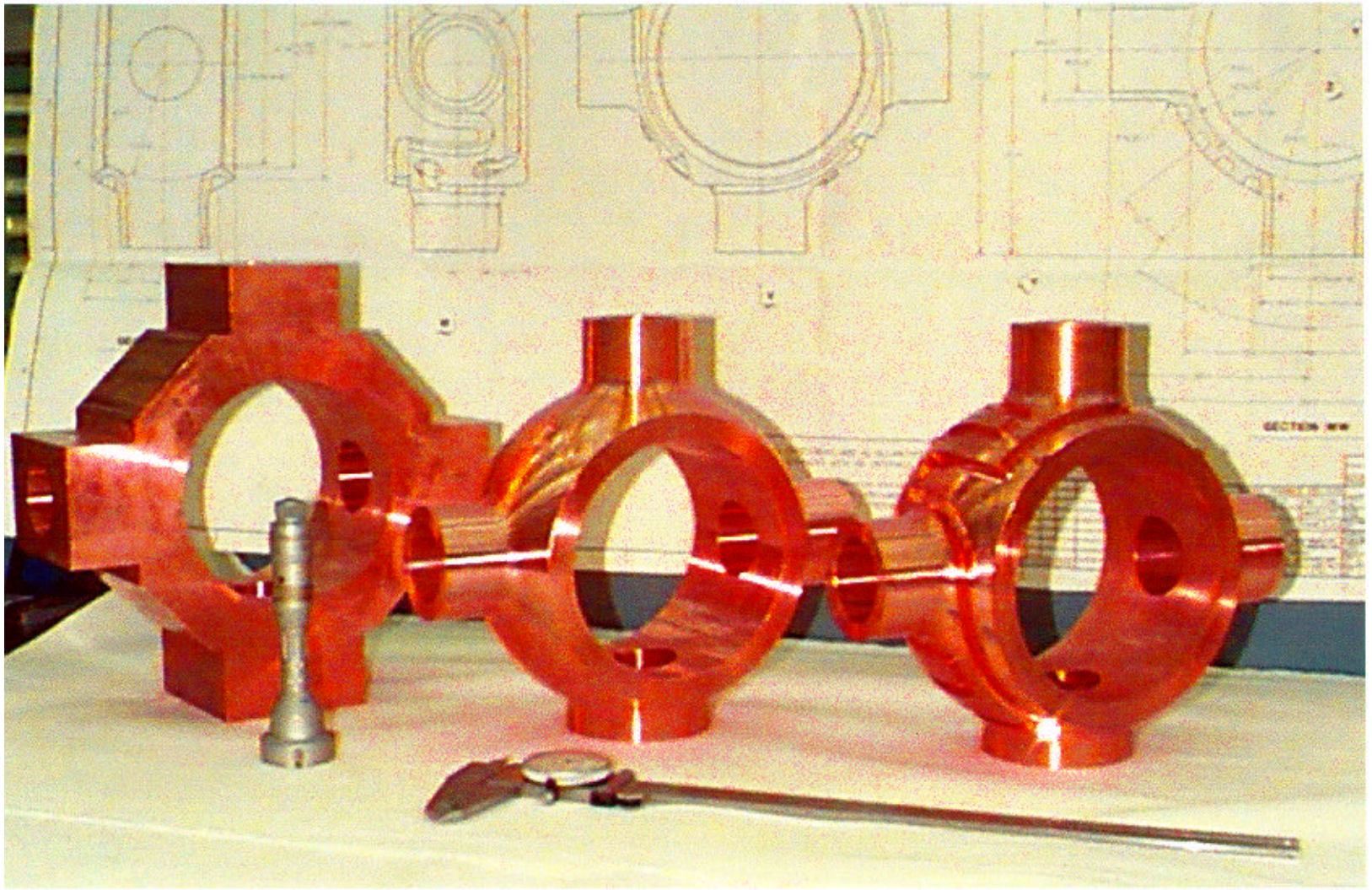

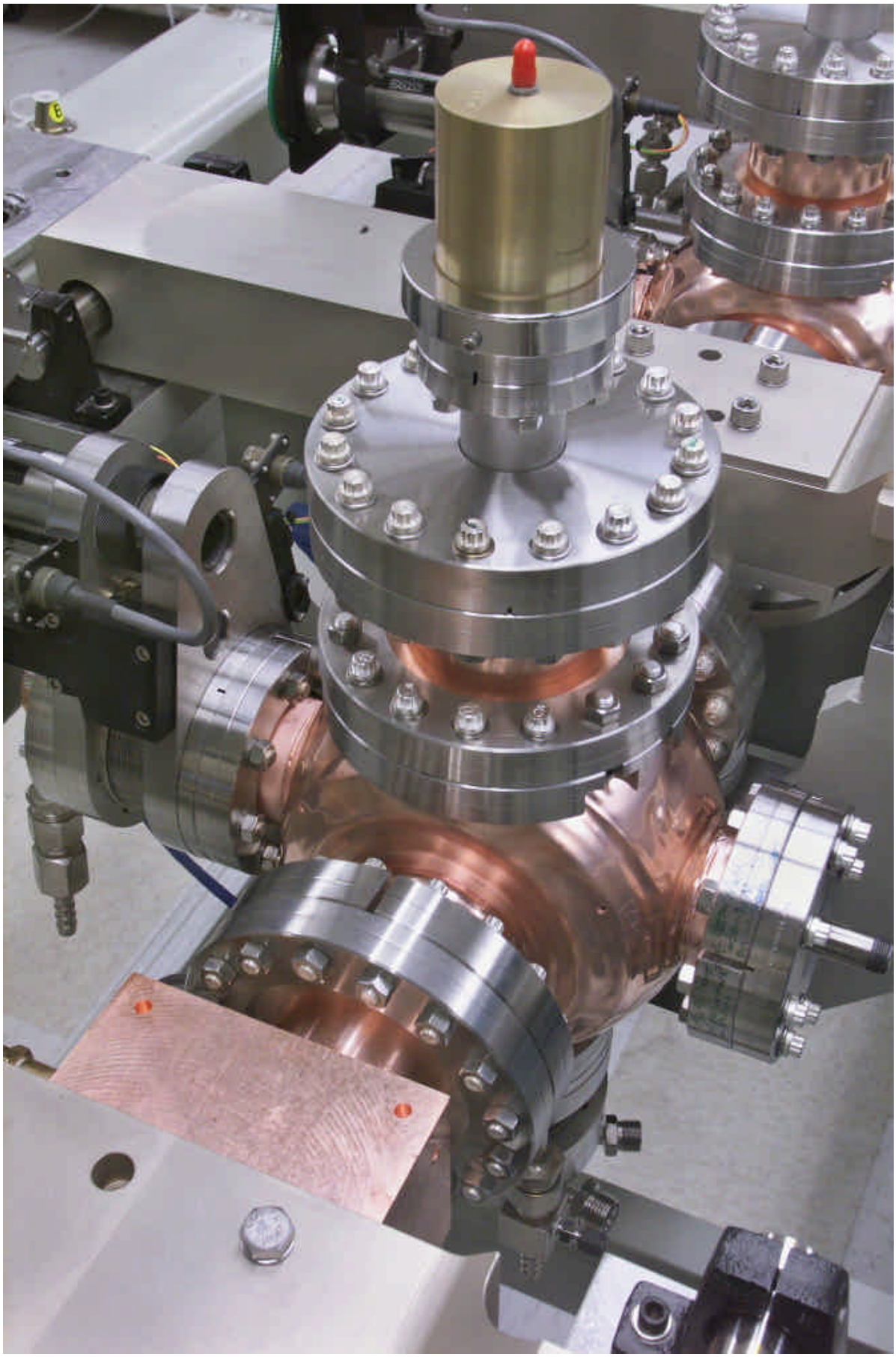

A 433 MHz Cavity Based Photocathode RF Gun Injector For PERL

David H. Dowell
Boeing Physical Sciences Research Center
Seattle, WA

PhotoInjector Talk Outline

I. PhotoInjector Design Philosophy.

II. Non-Linearities in Bunch Compression

III. Bunch Compression Using a RF Linearizer

IV. Experimental Results
CSR and Space Charge Effects

VI. Strawman Design for PERL

VII. Conclusions

Photoinjector Design Philosophy

Use a CW low frequency photocathode gun to generate high charge (1-5 nC) and long (50 ps) micropulses.

Advantages:

Capable of CW operation
High charge
Long micropulses

→ **Excellent Beam Quality at High Beam Current**

Disadvantage:

Cathode field limited to 25-30 MV/m

Accelerate in Low frequency RF cavities.

Advantages:

Minimizes wakefields
CW operation

Disadvantage:

Accelerating gradient limited to 5 MV/m

Linearize and compress to high peak current at 20 MeV.

Advantages:

Linearizing improves compression
Reduces space charge emittance growth

Disadvantage:

Emittance growth due to coherence synchrotron radiation

Layout of the 433 MHz PhotoInjector

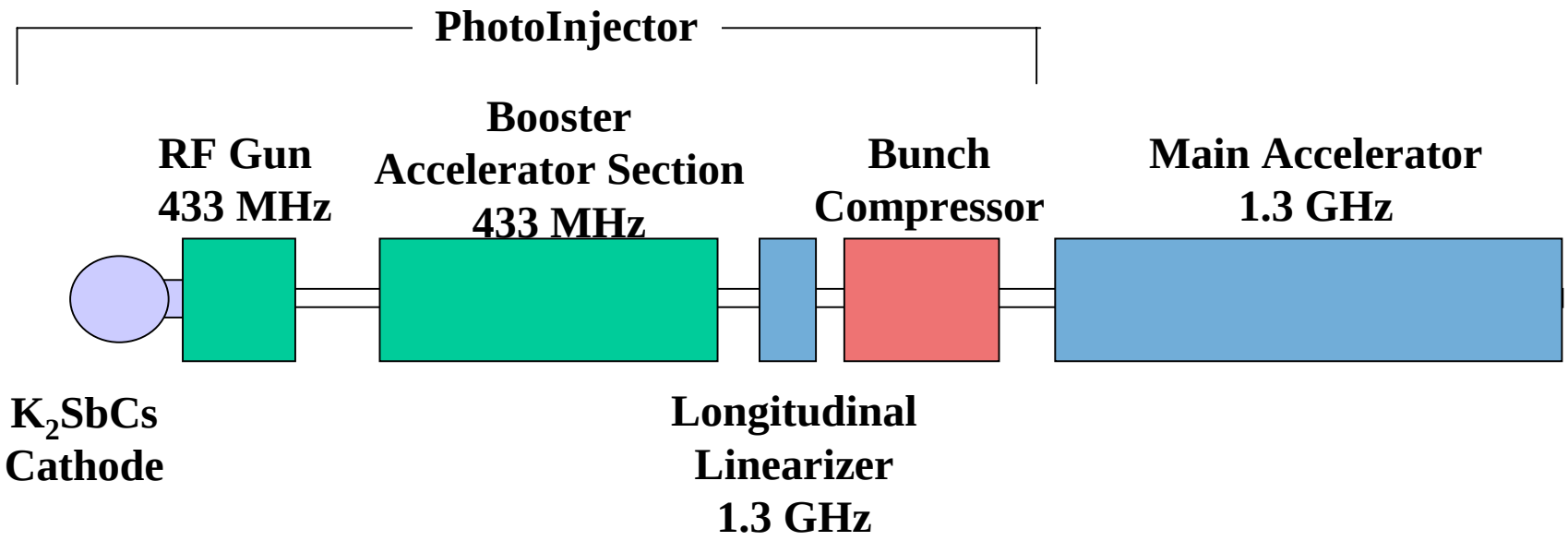

Non-Linearities in Bunch Compression

Long microbunches are distorted in longitudinal phase space due to wakefields and RF curvature.

433 MHz cavities introduce minimal wakes, but still cause significant curvature.

Introduce a RF section at third harmonic (1300 MHz) to cancel curvature of 433 MHz booster.

Magnetic Pulse Compression Using a Third Harmonic RF Linearizer
D.H. Dowell, T.D. Hayward and A.M. Vetter,
Proceedings of the 1995 PAC, pp.992-994.

Bunch Compression Using a RF Linearizer

Transform initial longitudinal paraxial coordinates, ΔE and Δt, through the booster:

$$\Delta E_1 = E_{433}\left[\cos(\omega_{433}\Delta t_0 + \phi_{433}) - \cos(\phi_{433})\right] + \Delta E_0$$
$$\Delta t_1 = \Delta t_0$$

Perform similar transformation through third harmonic section:

$$\Delta E_2 = E_{1300}\left[\cos(\omega_{1300}\Delta t_1 + \phi_{1300}) - \cos(\phi_{1300})\right] + \Delta E_1$$
$$\Delta E_2 = E_{1300}\left[\cos(3\omega_{433}\Delta t_0 + \phi_{1300}) - \cos(\phi_{1300})\right] + E_{433}\left[\cos(\omega_{433}\Delta t_0 + \phi_{433}) - \cos(\phi_{433})\right] + \Delta E_0$$
$$\Delta t_2 = \Delta t_1 = \Delta t_0$$

The third harmonic RF cancels the 433 MHz curvature when second derivative wrt Δt_2 is zero:

$$\left.\frac{d^2\Delta E_2}{d\Delta t_2^2}\right|_{\Delta t_2 = 0} = 0 \longrightarrow E_{1300}\cos(\phi_{1300}) = -\frac{E_{433}\cos(\phi_{433})}{9}$$

Generally, ϕ_{433}=0, and ϕ_{1300} is chosen to generate energy slew:

$$\Delta E_3 = \Delta E_2$$
$$\Delta t_3 = R_{56}\Delta E_2 + \Delta t_2$$

$\longrightarrow$ For E_{433}=20 MeV, R_{56}=50 ps/MeV:
E_{1300}=3.2 MeV, ϕ_{1300}=50^0

The 20 MeV RF Photoinjector

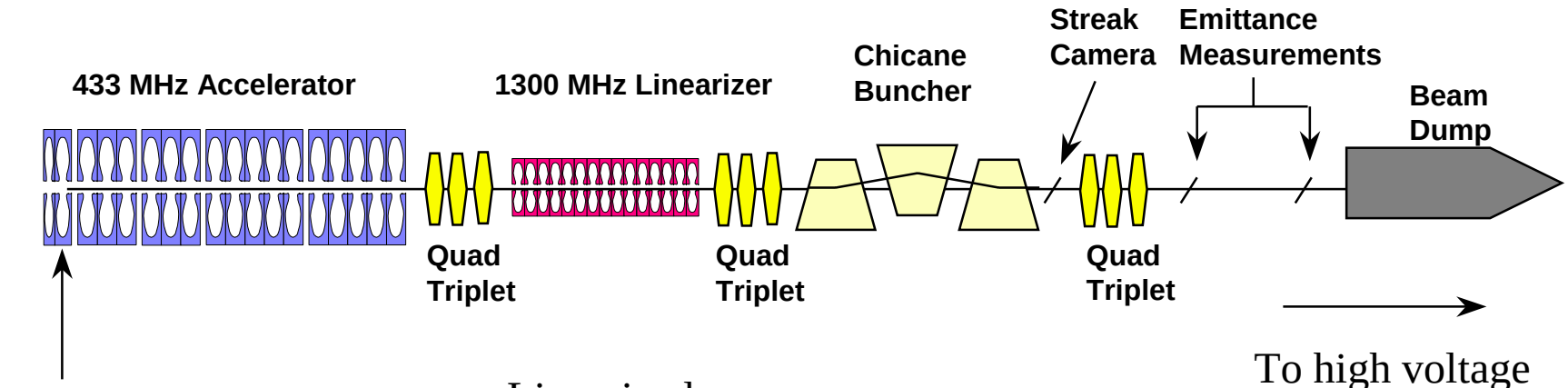

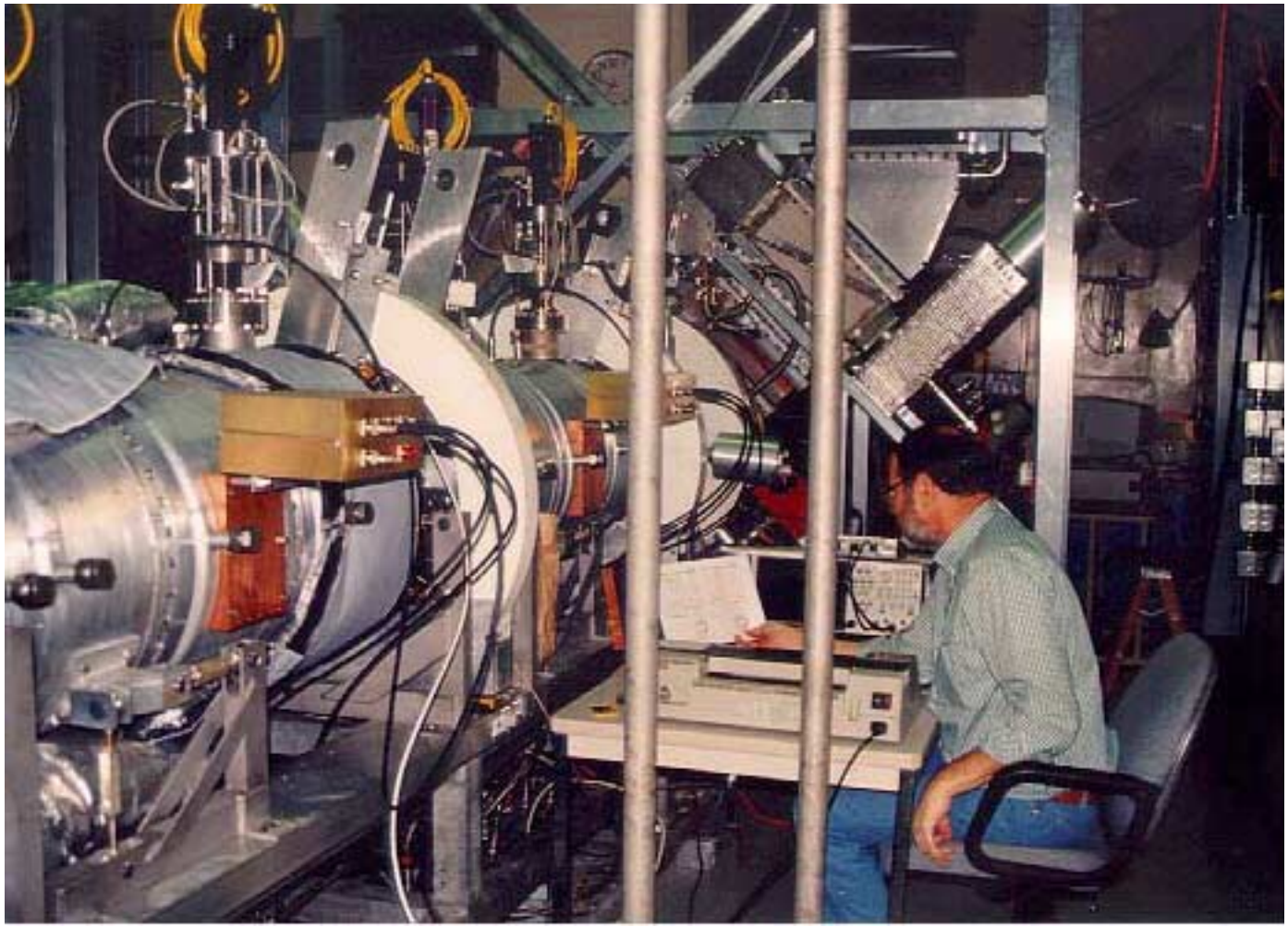

Cooling and RF Feed for 433 MHz 5-Cell Section

3-Cell and 5-Cell APLE Cavity Booster

3-Cell Accelerator Cavity **5-Cell Accelerator Cavities**

RF Characteristics of 433 MHz Booster Cavities

RF characteristics of APLE 5-cell cavity # 2 Derived from measurements

Parameter		Value	
frequency	f	433.33	MHz
shunt impedance	$R=V^2/P_c$	41.5	MΩ
coupling coefficient	β	2.56	

Operating parameters of APLE 5-cell cavity # 2 Optimized for PERL conditions.

Parameter		Value	
nominal accelerating voltage	V	3.5	MV
wall loss power	P_c	295	kW
beam power @ I_{avg}=200 mA	P_b	700	kW
forward power required	P_k	1015	kW
reflected power	P_r	20	kW

Tables provided by A.M. Vetter.

5-Cell APLE Cavity Power Allocation
Peak Energy Gain = 3.5 MV

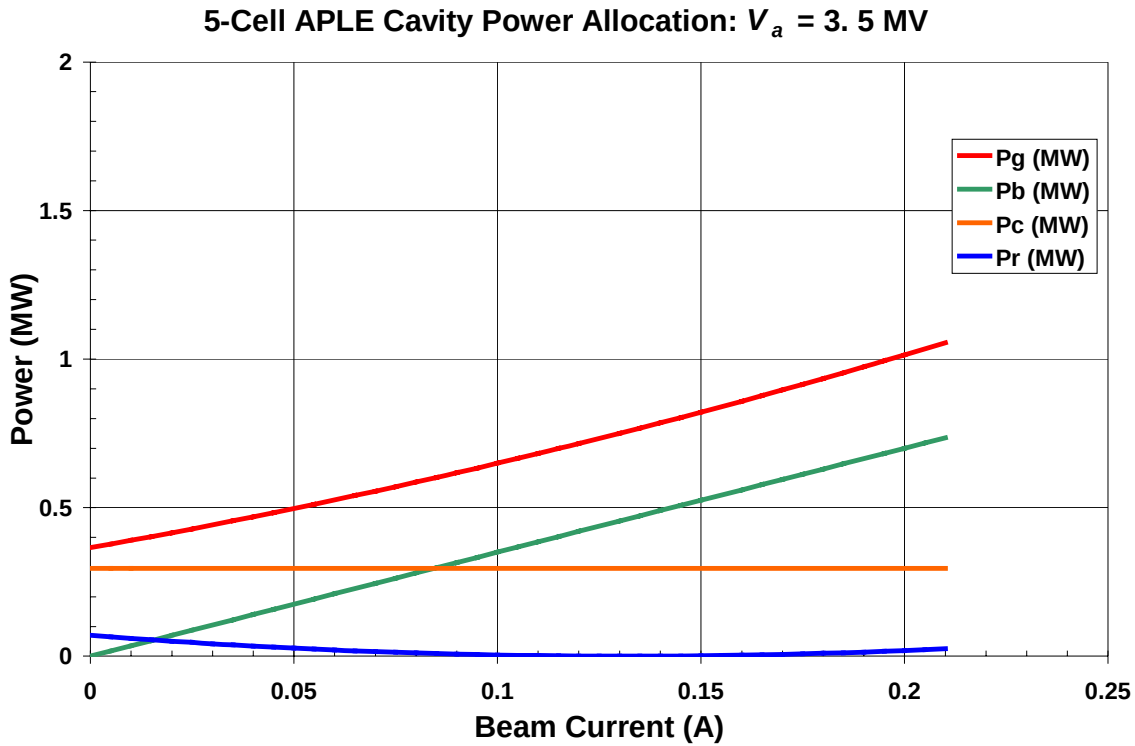

Generator, beam, cavity loss, and reflected power as functions of beam current for 5-cell APLE cavity operation at 3.5 MV. Optimized for PERL operation.

Figure courtesy of A.M. Vetter.

1300 MHz Linearizer and Three-Dipole Chicane Compressor

1300 MHz (third harmonic) energy spectrum programming for bunch compression

Three dipole magnetic buncher and diagnostics

Boeing Chicane Buncher

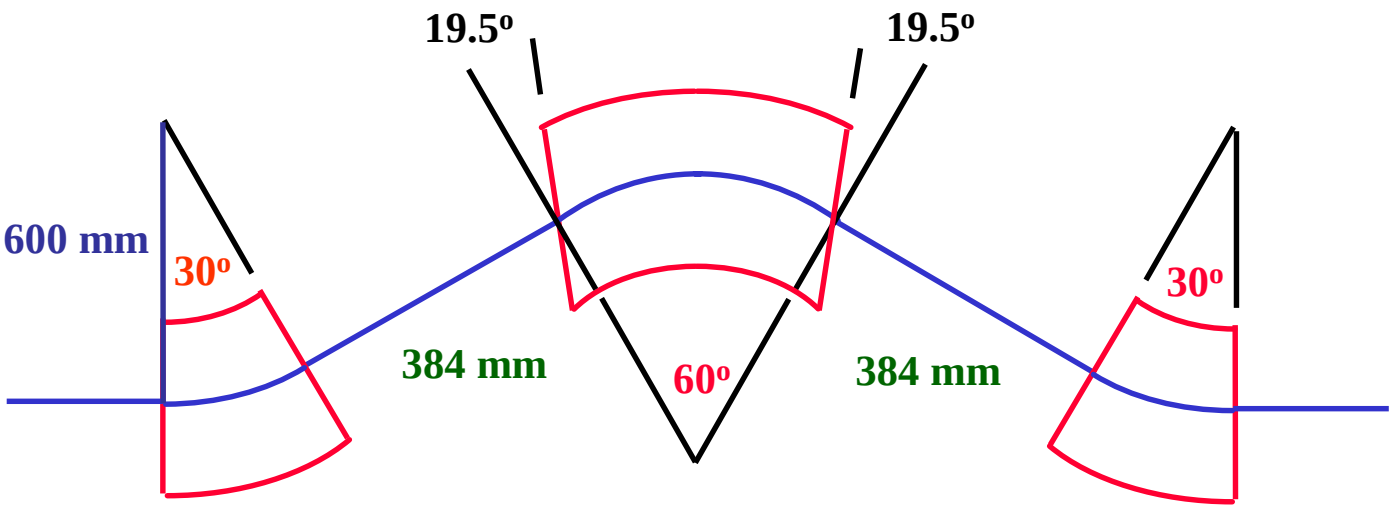

Achromatic chicane composed of three n=1/2 dipoles.

Pulse compression occurs at two linearizer phases, but the pulse is linearized only at the decelerating phase and at 1/9 the 433 MHz RF field.

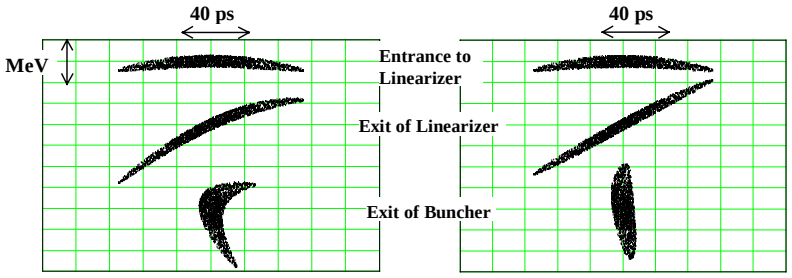

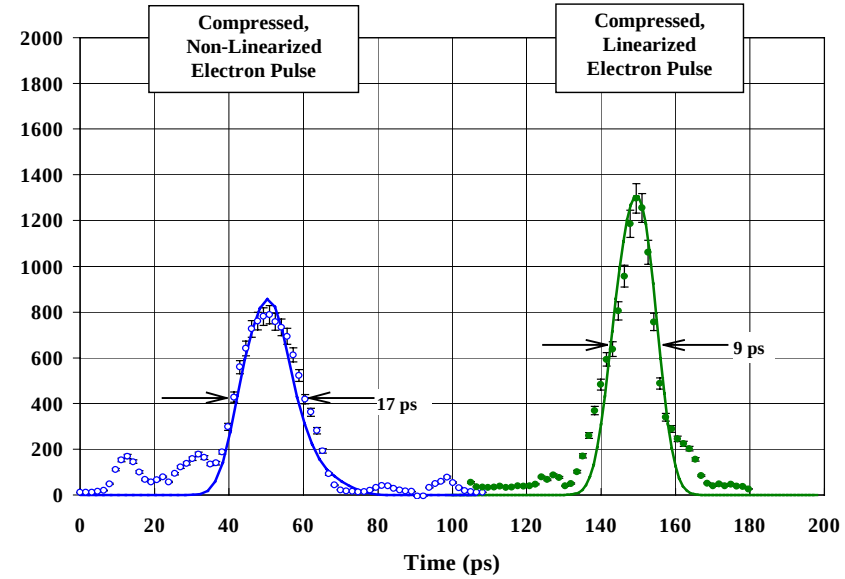

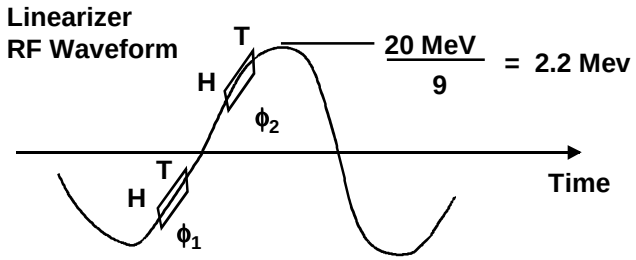

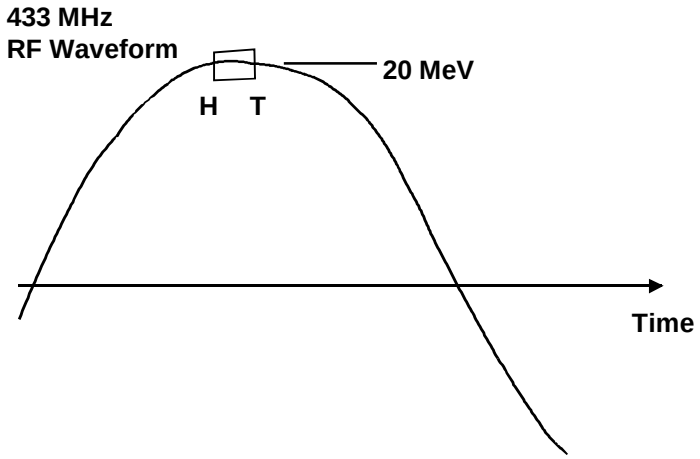

Bend Plane Emittance Growth During Pulse Compression

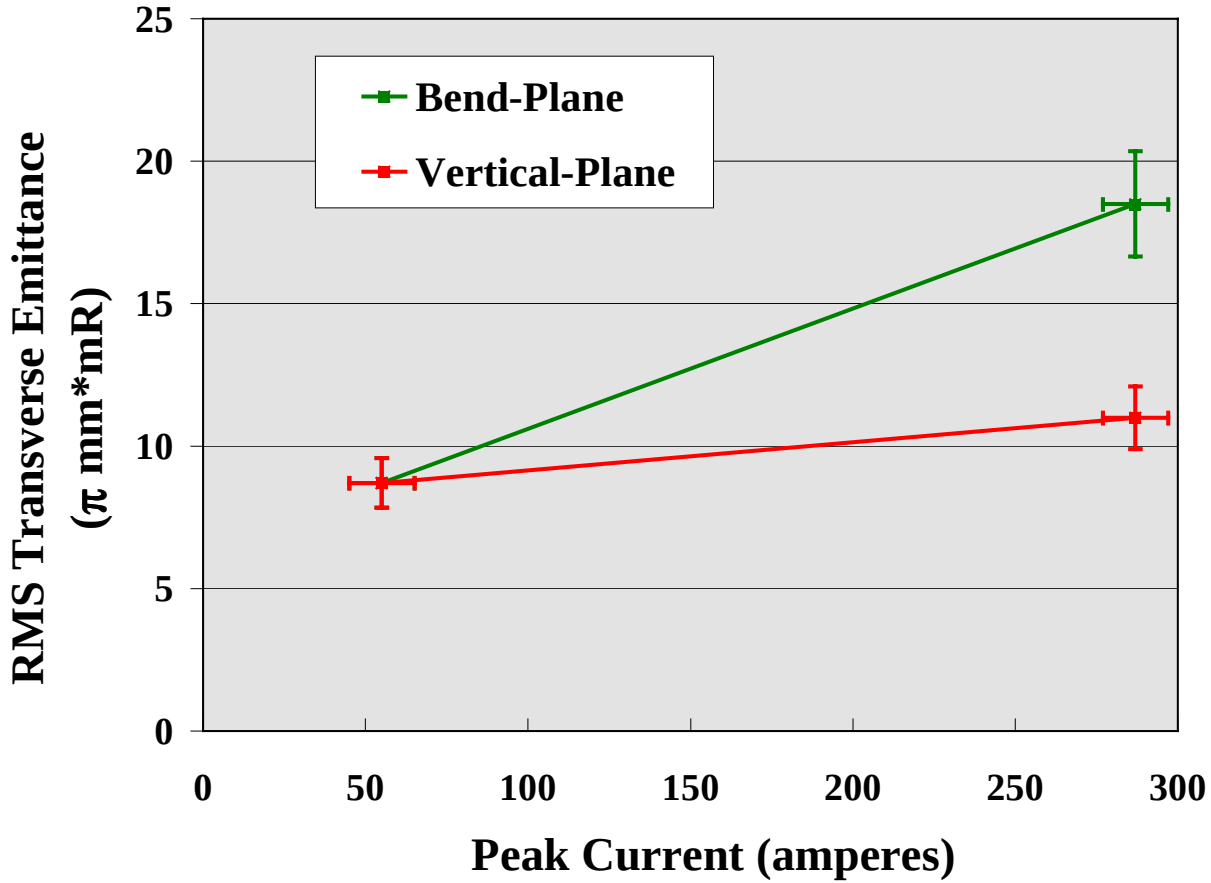

Coherent Synchrotron Radiation Induced Emittance Growth

Electron Microbunch Traveling in an Arc

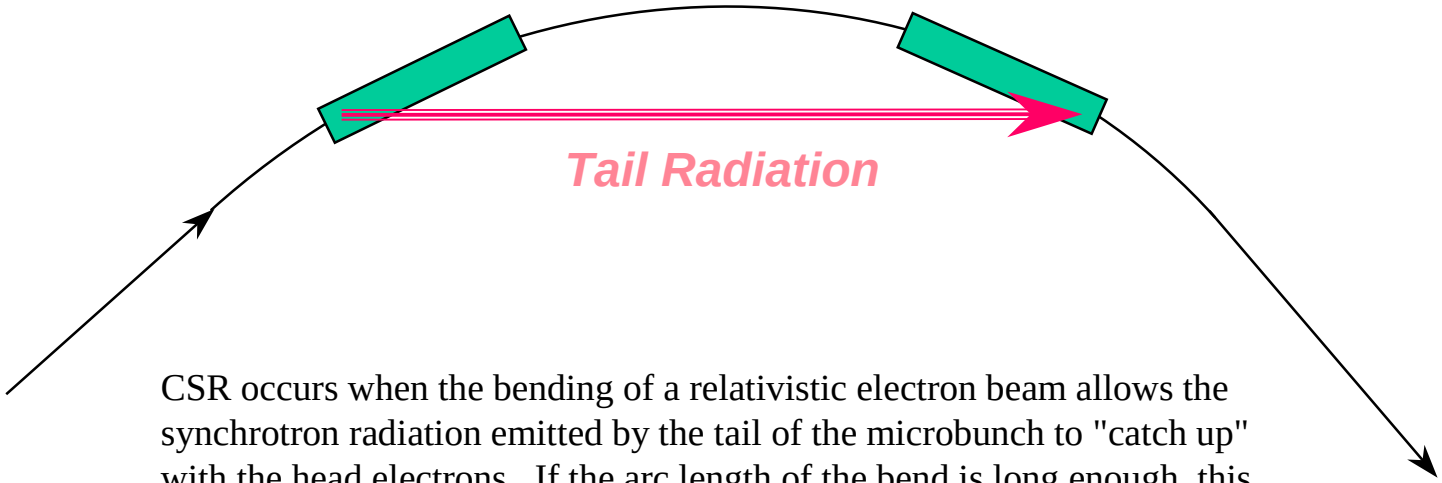

CSR occurs when the bending of a relativistic electron beam allows the synchrotron radiation emitted by the tail of the microbunch to "catch up" with the head electrons. If the arc length of the bend is long enough, this radiation sweeps along the entire length of the microbunch and transfers energy from the tail to the head. Therefore CSR tends to increase the energy of the head while lowering that of the tail.

Ref: Y.S. Derbenev et al., DESY TESLA-FEL Technical Note 95-05(1995)

Transient CSR Radiation at the Magnetic Field Boundary

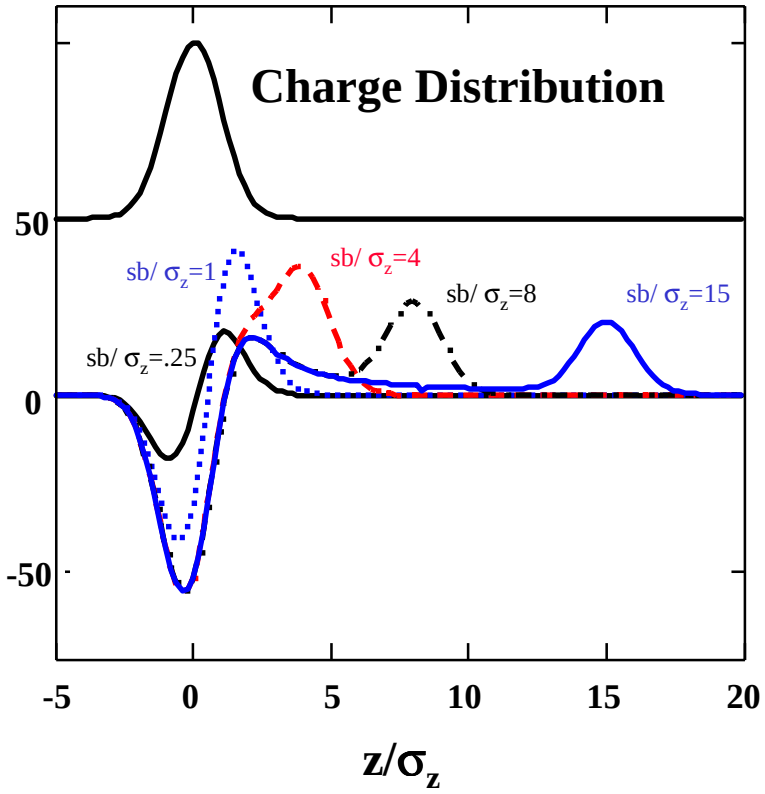

$$\lambda(s) = \frac{1}{\sqrt{2\pi}\,\sigma_z} e^{-s^2/2\sigma_z^2}$$

$$F_1(sb, x) = \int_{x-sb}^{x} \frac{dx'}{(x-x')^{1/3}} \frac{\partial \lambda(x')}{\partial x'}$$

Ref: D.H. Dowell and P.G. O'Shea, "Coherent Synchrotron Radiation Induced Emittance Growth in a Chicane Buncher", contribution to PAC'97.

Coherent Synchrotron Radiation Induces Correlated Emittance Growth

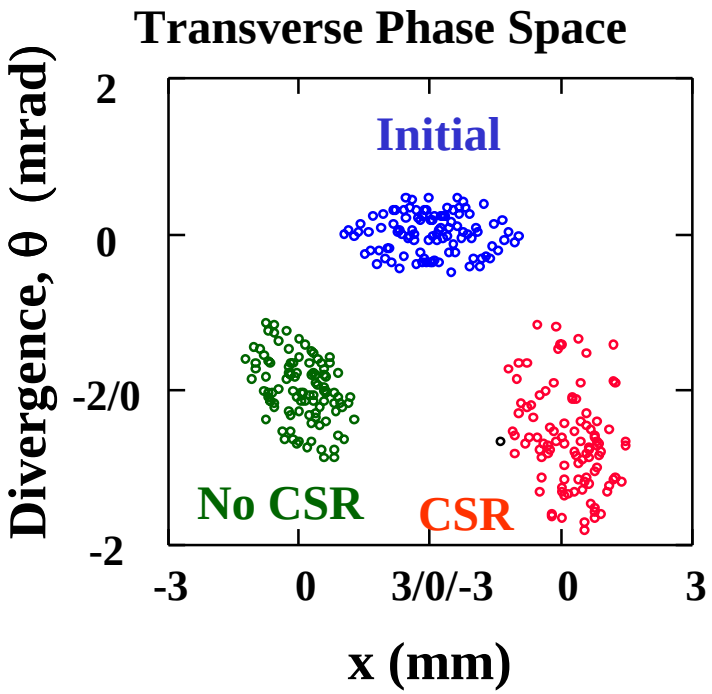

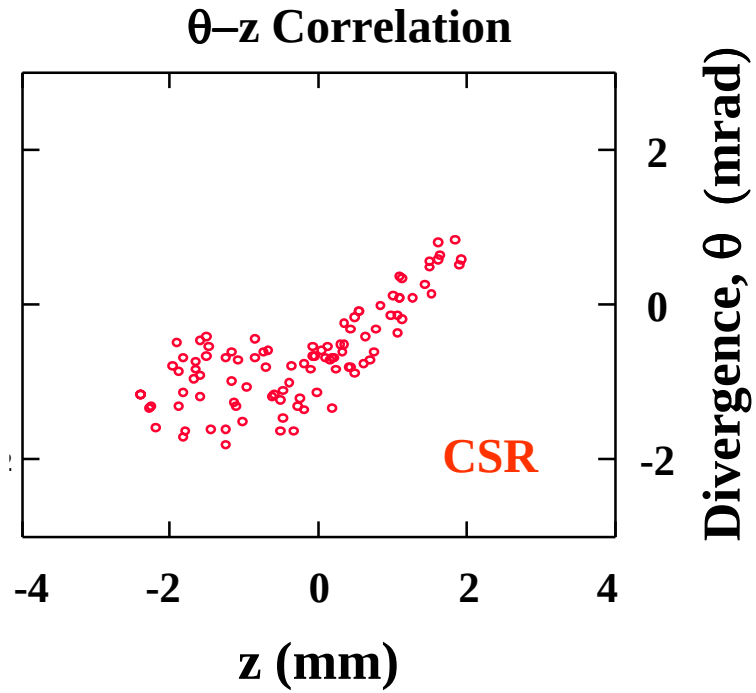

The initial and final transverse phase space distributions, with and without CSR, when the microbunch is compressed. The distributions are offset for display only.

The correlation of divergence with longitudinal position at the exit of the chicane due to CSR.

Comparison of Experiment with PARMELA and CSR Emittance Calculations.

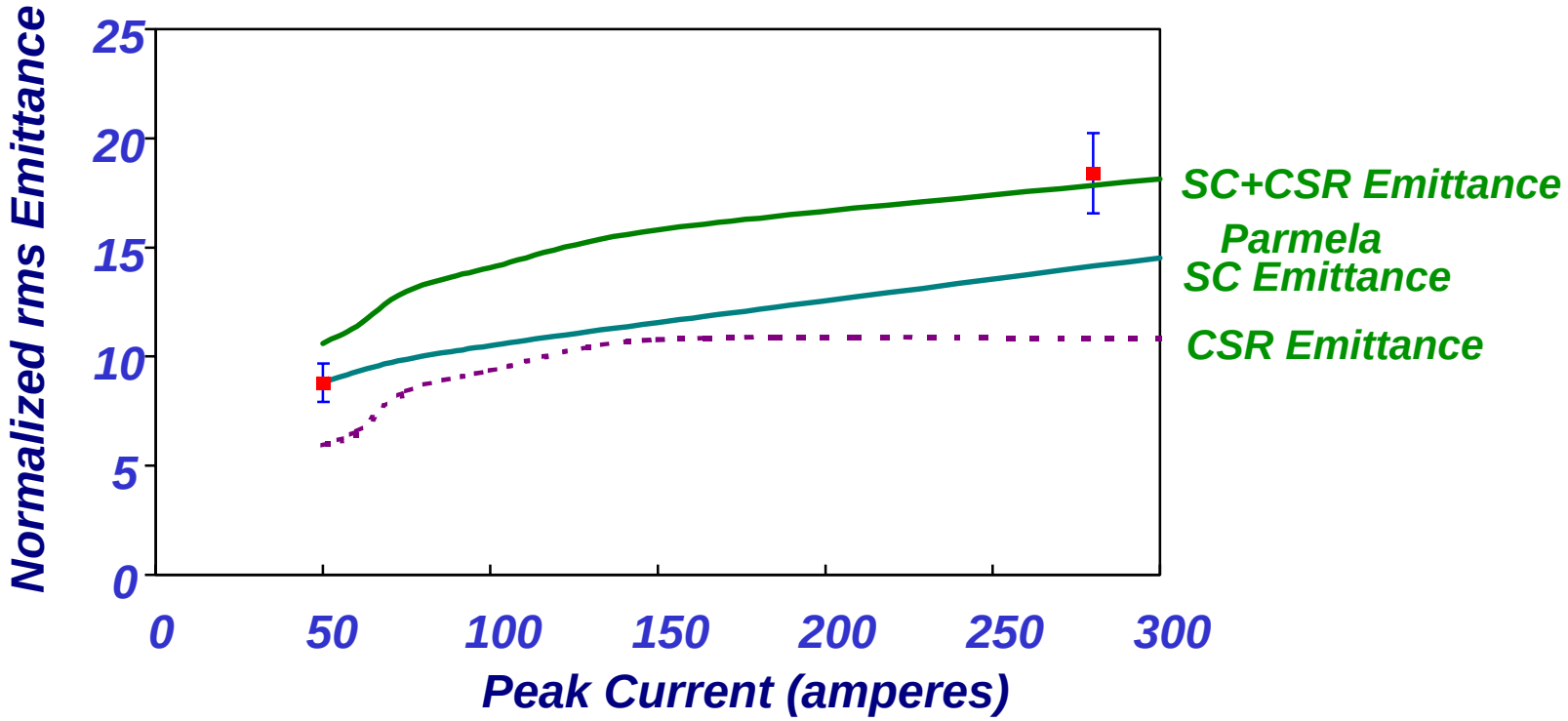

New CSR Experiments:
LEUTL
SDL

Experimental Configuration for Measuring CSR Correlations

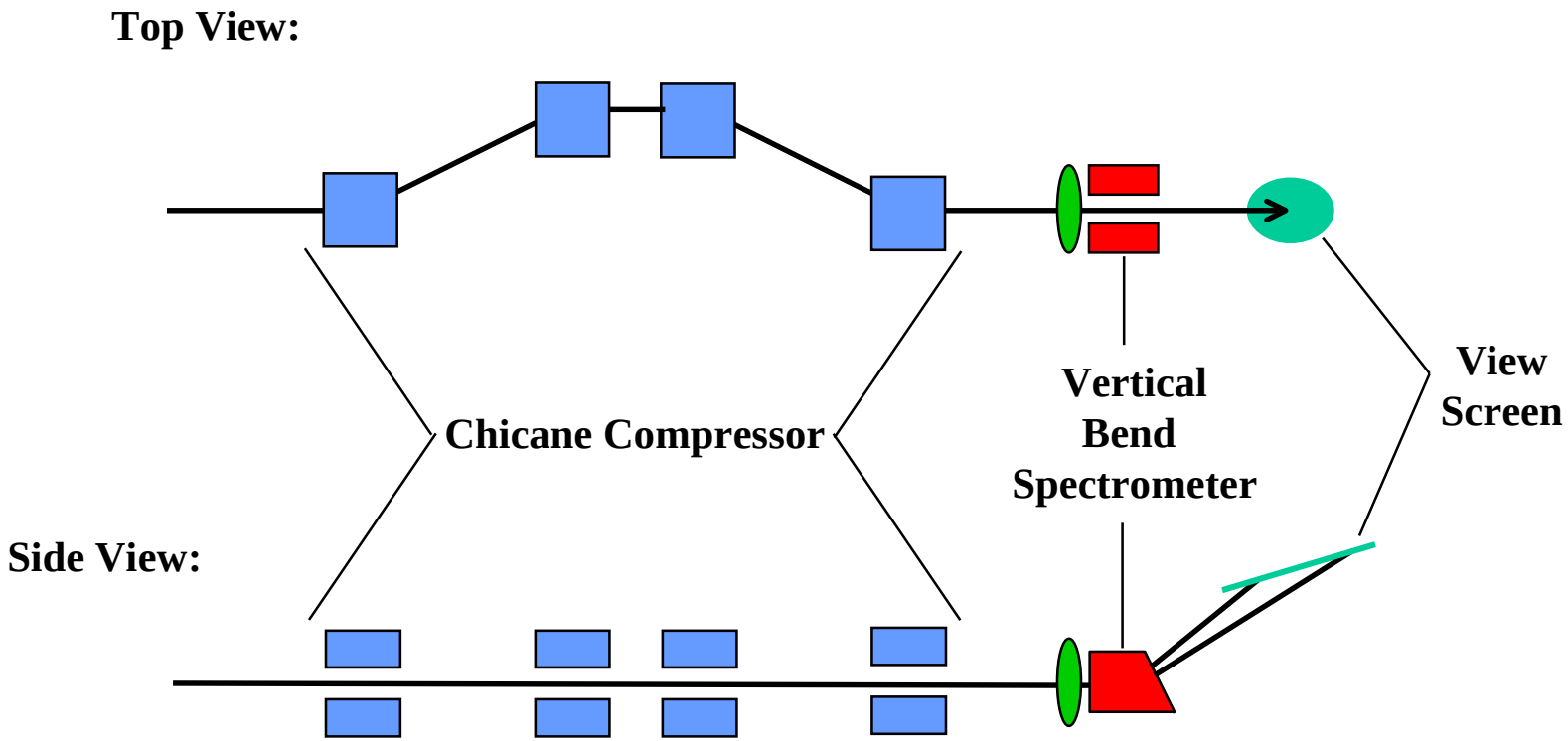

PARMELA Generated Initial Distribution for SDL at Spectrometer Focal Plane

Initial emittance: 2.2 π, Final emittance: 6.0 π

Compression to 1000 amperes

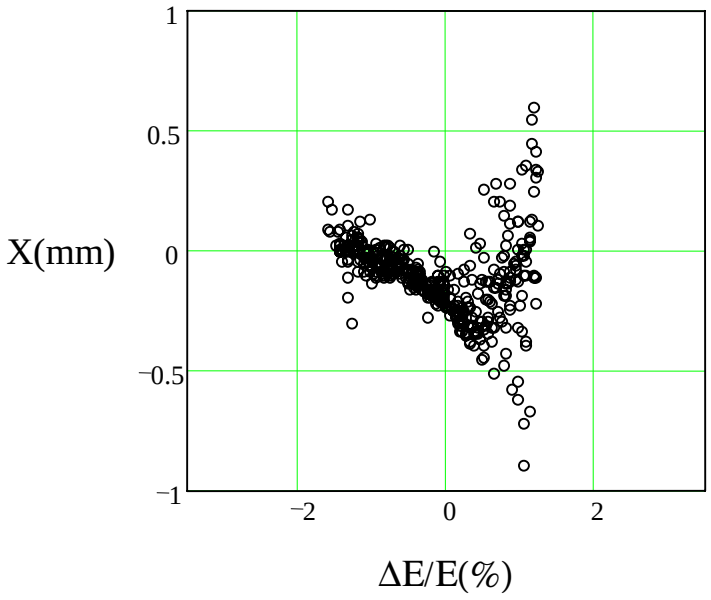

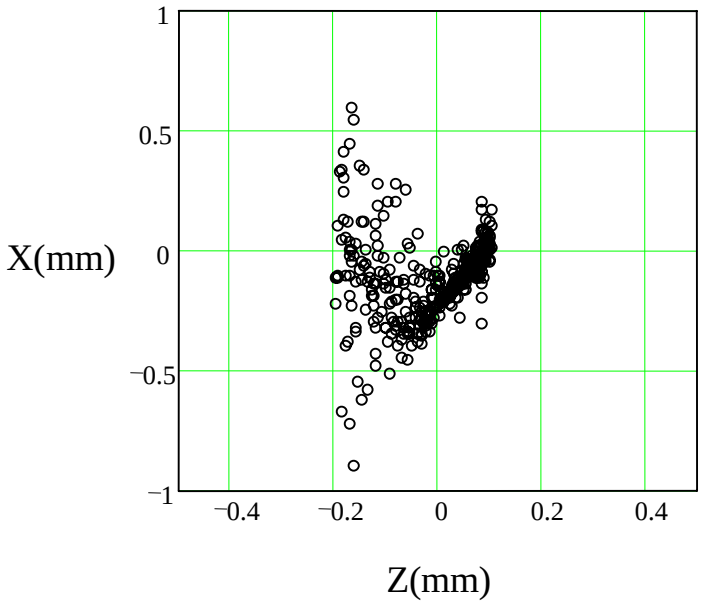

Focal Length = 500 mm

Compressor and CRS Diagnostic at LEUTL (APS-ANL)

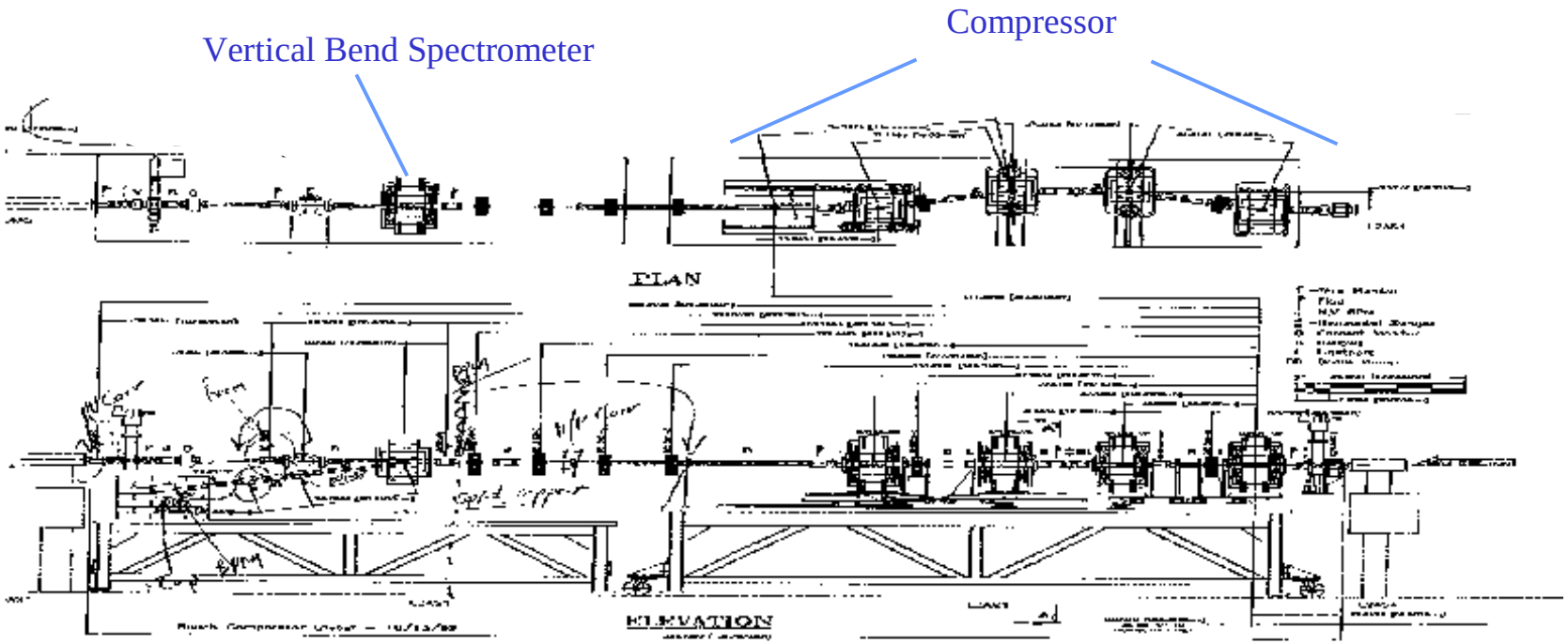

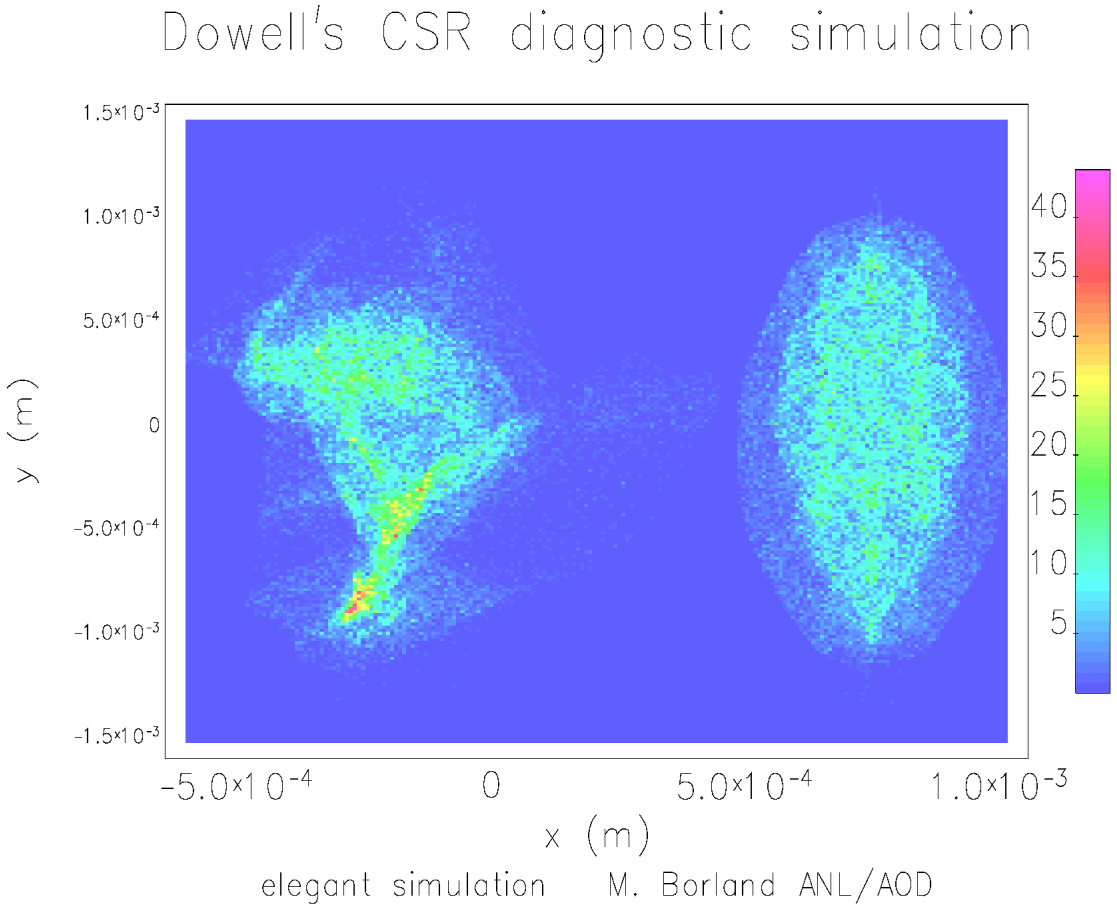
Dowell's CSR diagnostic simulation
1.5x10-3
1.0x10-3
5.0x10-4
0
-5.0x10-4
-1.0x10-3
-1.5x10-3
y (m)
40
35
30
25
20
15
10
5
-5.0x10-4
0
5.0x10-4
1.0x10-3
x (m)
elegant simulation M. Borland ANL/AOD

Strawman Design for PERL:

Compression

Re-circulation

Compression With PERL Parameters, Linearized Phase Space

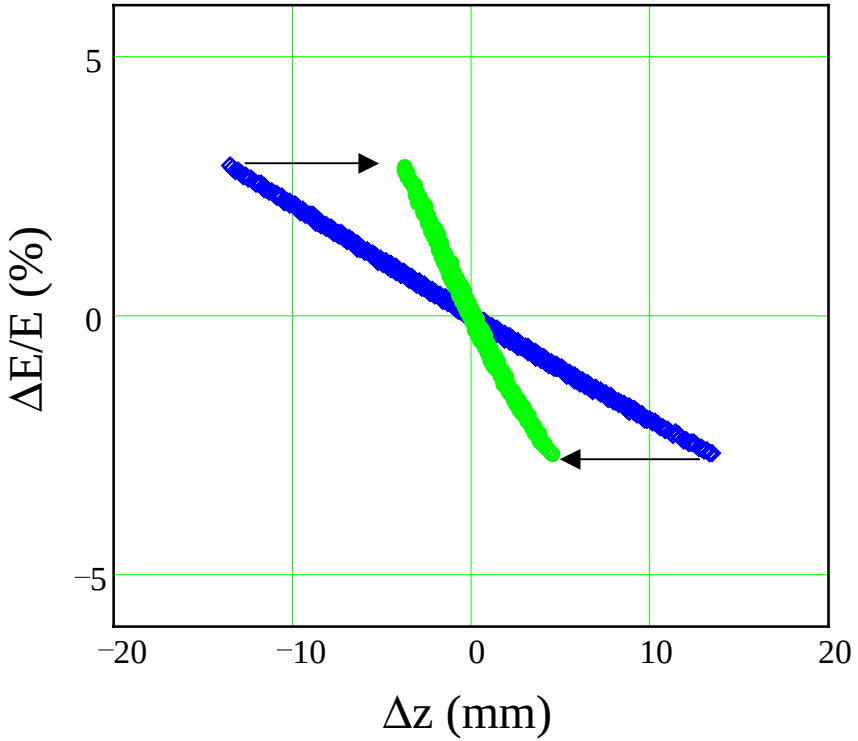

Microbunch Shape

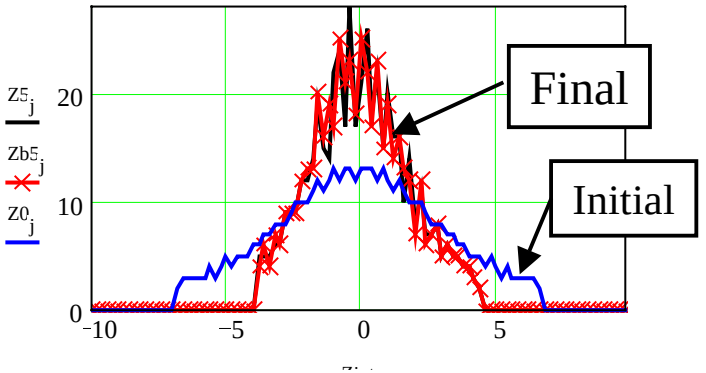

Δz (mm)

Energy Spectra

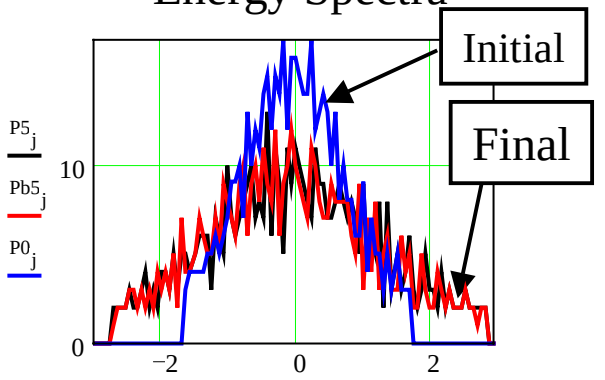

ΔE/E (%)

Boeing Style Compressor
10 MeV Compression
Bunch Length: 49=>15 ps
Emittance (CSR only): 1=>1.3 microns
Peak Current: 10=>34 amps

Compression With PERL Parameters, Non-Linearized Phase Space

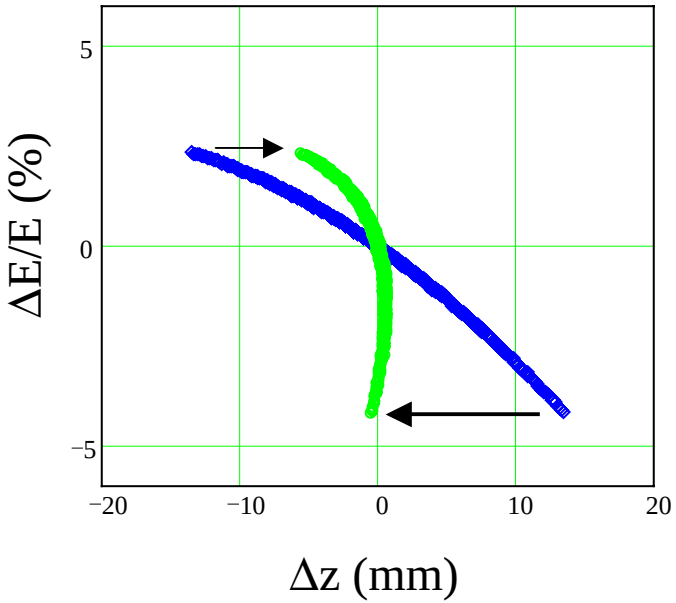

Microbunch Shape

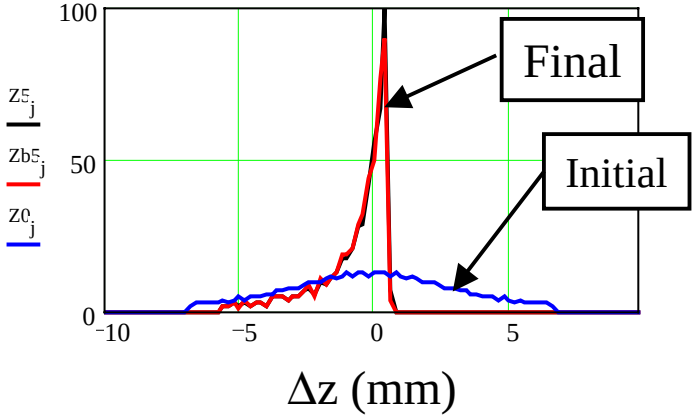

Energy Spectra

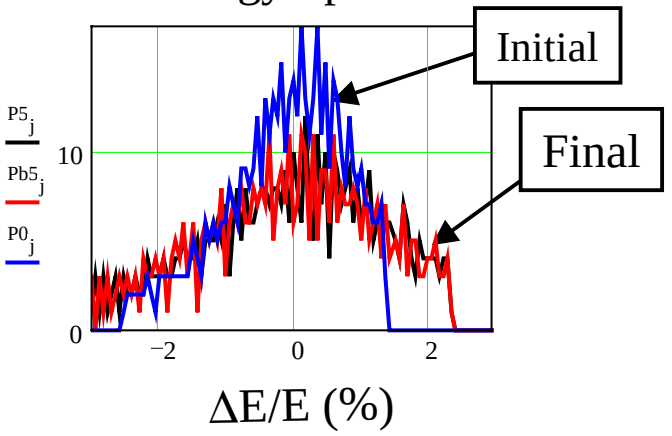

Boeing Style Compressor
10 MeV Compression
Bunch Length: 47=>10 ps
Emittance (CSR only): 1=>1.05 microns (?)
Peak Current: 10=>48 amps

Possible PERL Configuration

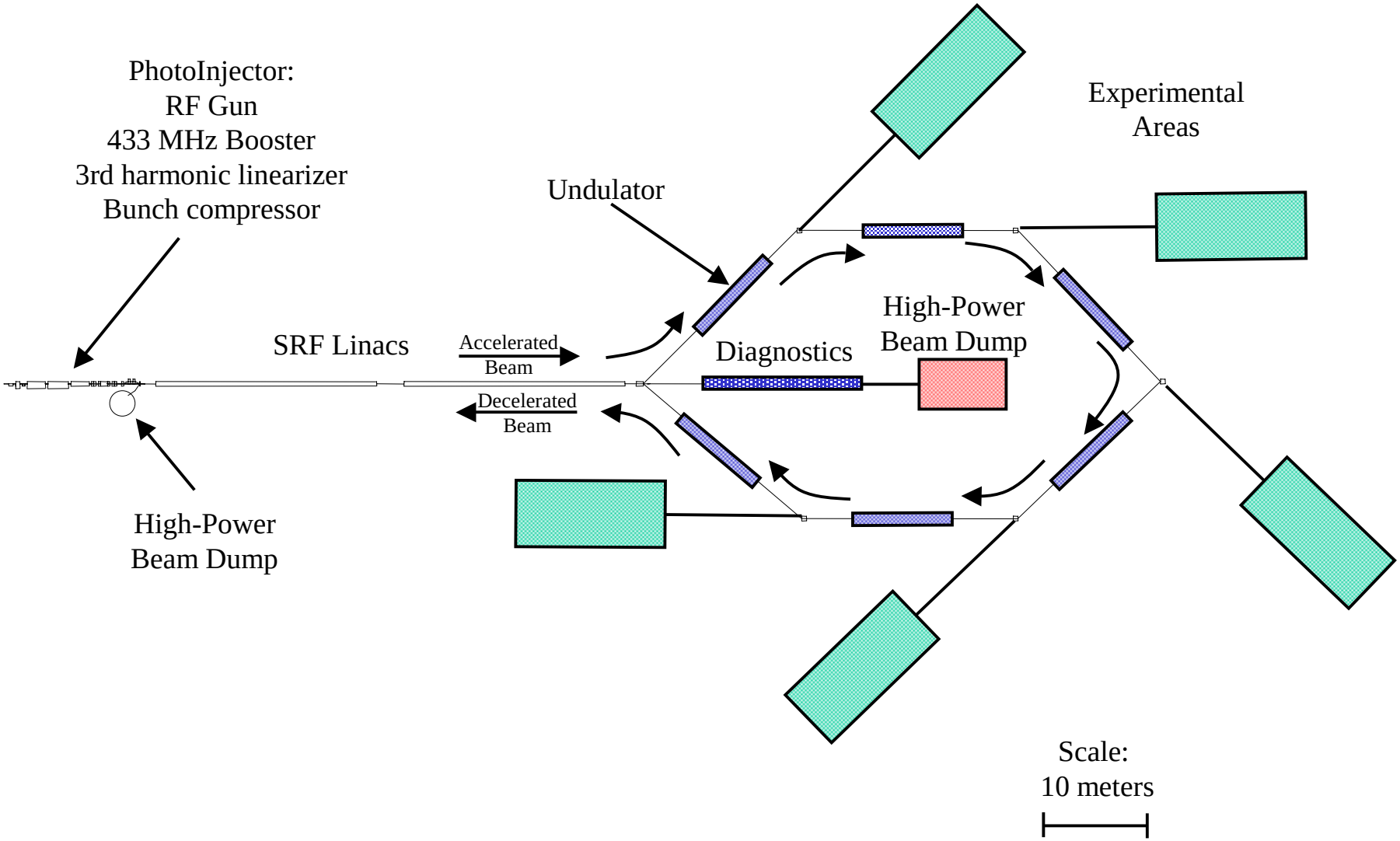

Summary and Conclusions

433 MHz-Based PhotoInjector Configuration:
Gun, Booster, Linearizer, Compressor

Non-linearity Due to RF Waveform
Requires Third-Harmonic Linearizer

433 MHz APLE Cavities Satisfy PERL Requirements

Short 1300 MHz SRF Section Needed for Linearizer

Preliminary CSR Calculations Show Some Emittance Growth
Full Start-to-End SC+Wakes Calculation Still Needed

Counter-Propagating Beams in E-Recovery Proposed

Results of the Fermilab High-Brightness RF Photo-injector

Jean-Paul Carneiro (Fermilab and Université d'Orsay),
For the A0 Group (N. Barov, D. Carrigan, M. Champion, D. Edwards, H. Edwards, M. Fitch, J. Fuesrt, W. Hartung, A. Melissinos and J. Santucci)

Presented at the Workshop on Photo-injector for Energy Recovery Linac, BNL, 01-22-01.

BEAM PARAMETERS

- Total Energy ≈ 17 MeV (typical run)
- Gun peak accelerating field = 35 to 40 MV/m (4.5 to 5 MeV)
- Superconducting on axis cavity accelerating field = 12 MV/m
- Energy spread @ 1 nC = 0.25%

- Bunches per macropulse = 800 (design), 10-100 (typical run)
- Bunch spacing = 1 μs
- Repetition Rate = 1-10 Hz (design), 1 Hz (typical run)

- Bunch charge = 1 to 8 nC
- Bunch length @ 8 nC uncompressed ≈ 10 ps sigma (measured)
- Bunch length @ 8 nC compressed ≈ 2 ps sigma (measured)
- Peak current @ 8 nC for a compressed beam ≈ 1.6 kA (measured)

- Beam radius at cathode = 1.5 mm @ 1nC, 3 mm @ 8nC
- Transverse rms emittance, normalized @ 1nC ≈ 3-4 mm-mrad (measured, uncompressed)
- Transverse rms emittance, normalized @ 8nC ≈ 13 mm-mrad (measured, uncompressed)

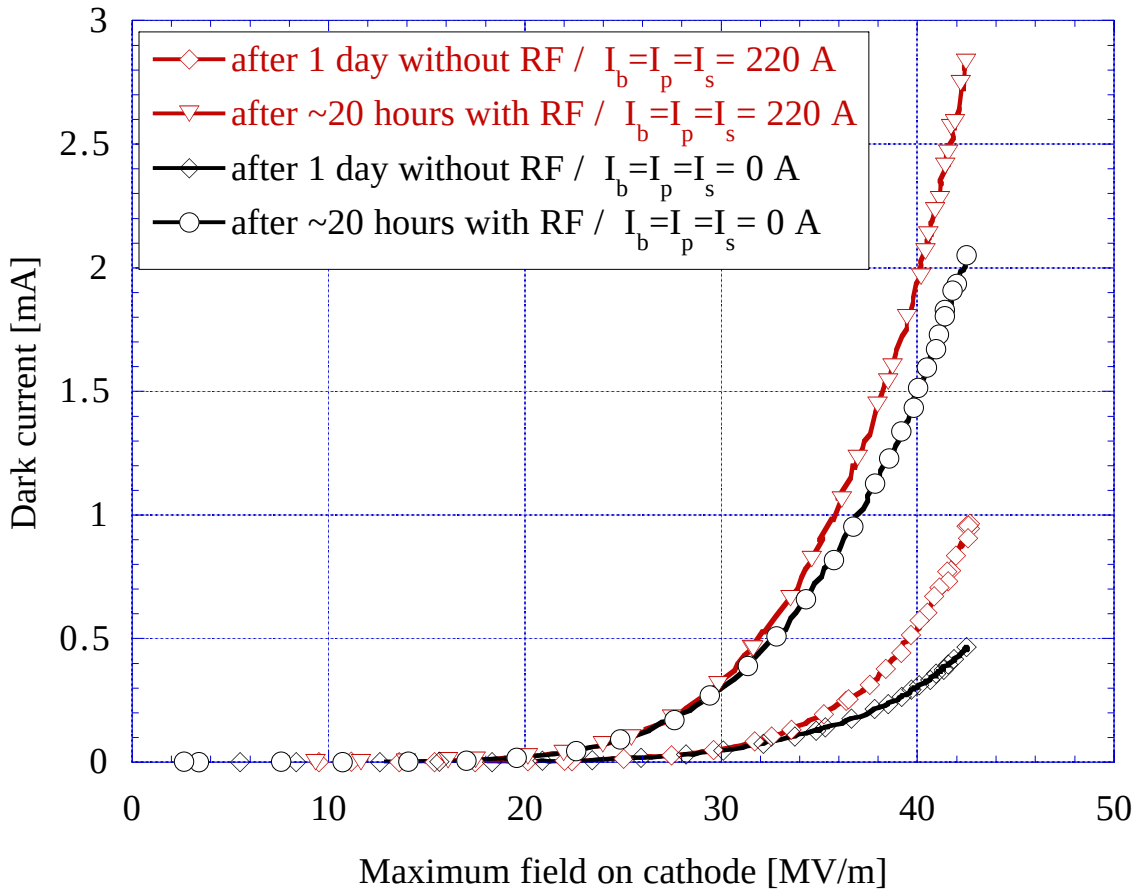
after 1 day without RF / I_b=I_p=I_s= 220 A
after ~20 hours with RF / I_b=I_p=I_s= 220 A
after 1 day without RF / I_b=I_p=I_s= 0 A
after ~20 hours with RF / I_b=I_p=I_s= 0 A
Dark current [mA]
Maximum field on cathode [MV/m]
0
0.5
1
1.5
2
2.5
3
0
10
20
30
40
50

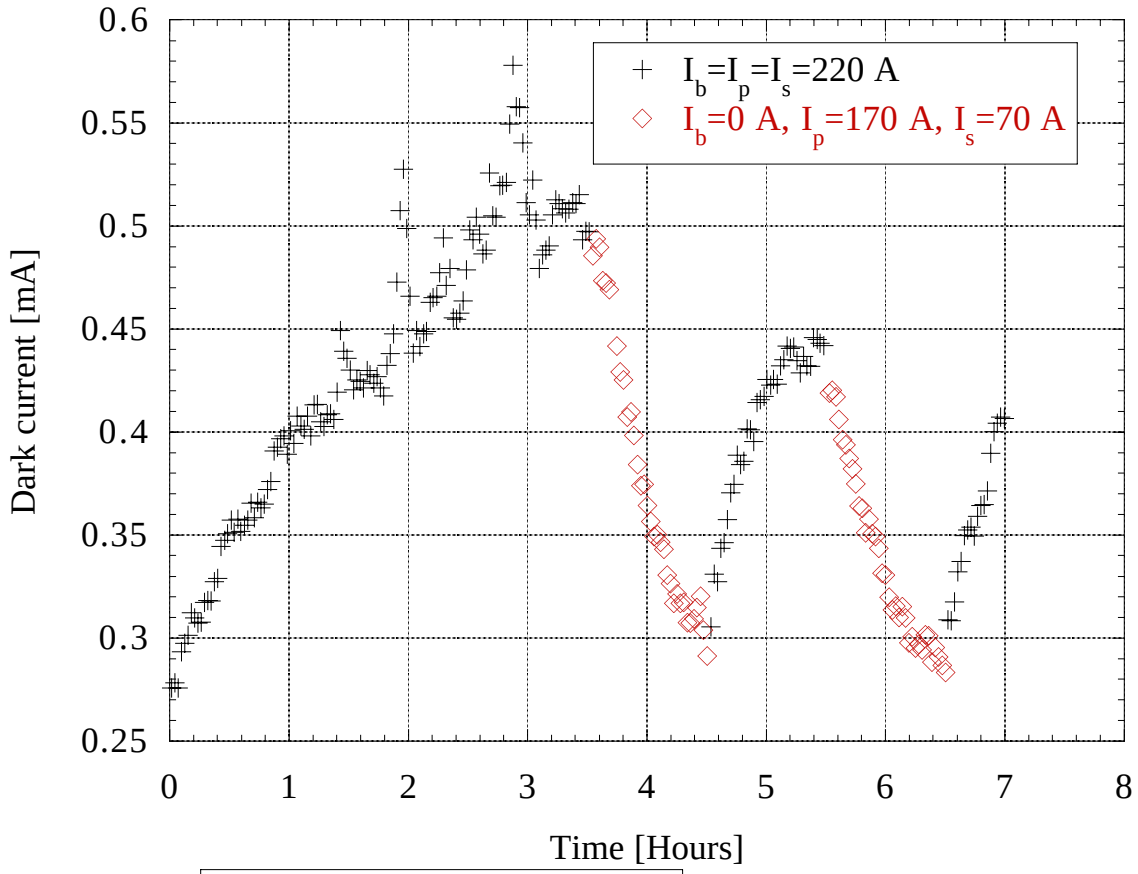
Dark current [mA]
Time [Hours]
I_b=I_p=I_s=220 A
I_b=0 A, I_p=170 A, I_s=70 A
0.6
0.55
0.5
0.45
0.4
0.35
0.3
0.25
0
1
2
3
4
5
6
7
8

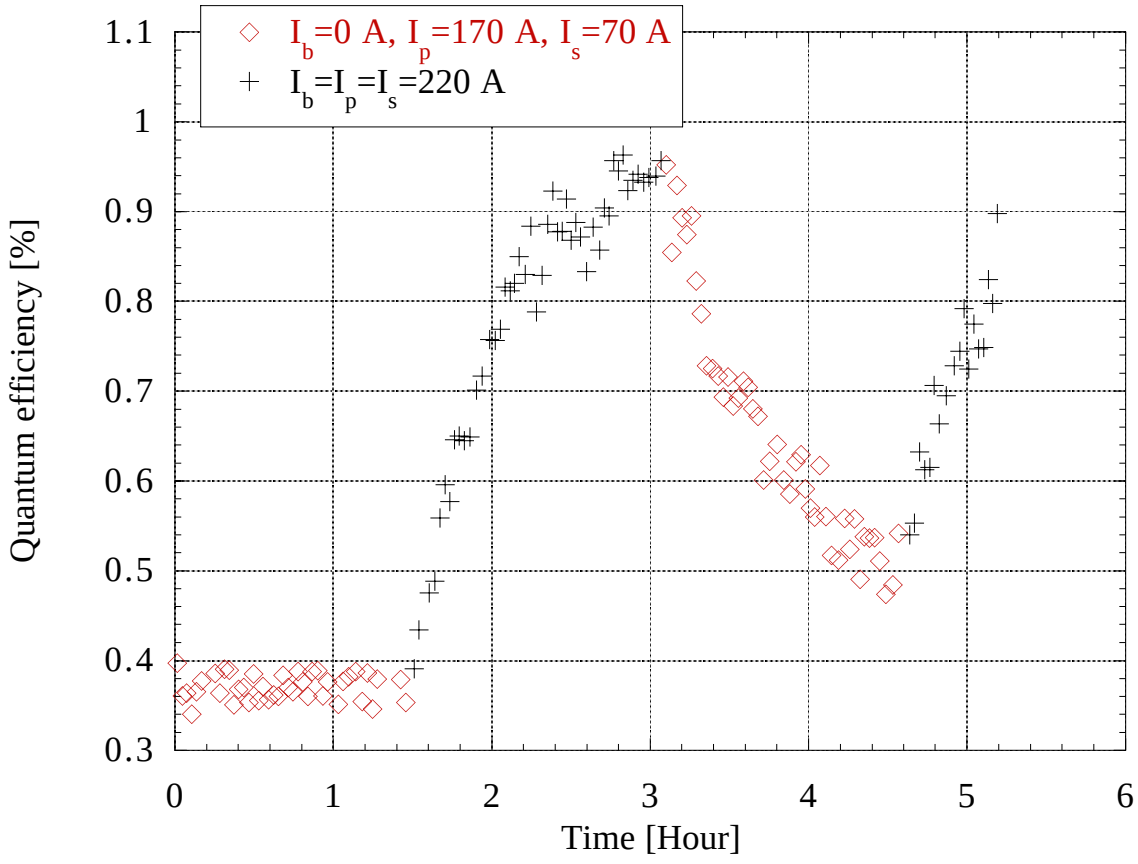
Quantum efficiency [%]
Time [Hour]
I_b=0 A, I_p=170 A, I_s=70 A
I_b=I_p=I_s=220 A
1.1
1
0.9
0.8
0.7
0.6
0.5
0.4
0.3
0
1
2
3
4
5
6

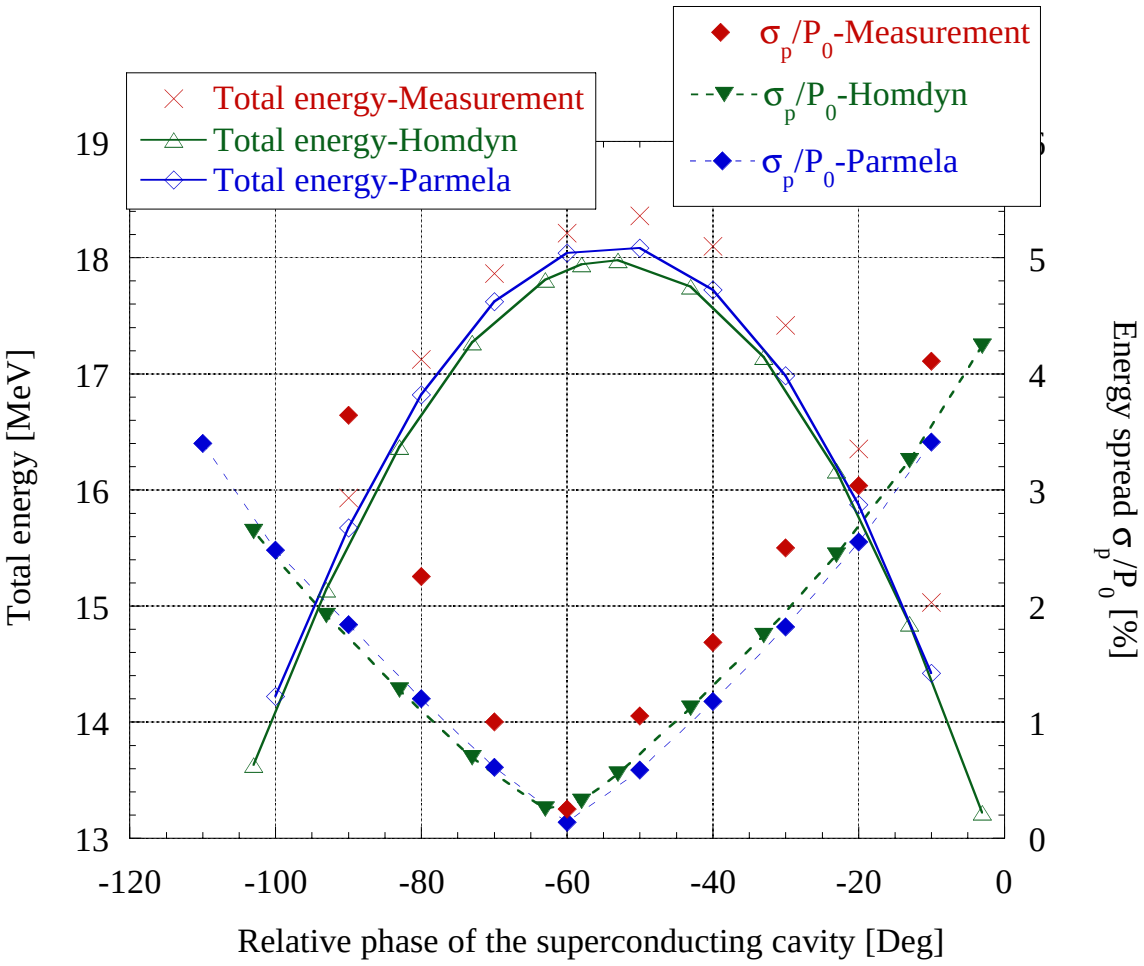
Total energy-Measurement
Total energy-Homdyn
Total energy-Parmela
σp/P0-Measurement
σp/P0-Homdyn
σp/P0-Parmela
Total energy [MeV]
Energy spread σp/P0 [%]
Relative phase of the superconducting cavity [Deg]
19
18
17
16
15
14
13
5
4
3
2
1
0
-120
-100
-80
-60
-40
-20
0

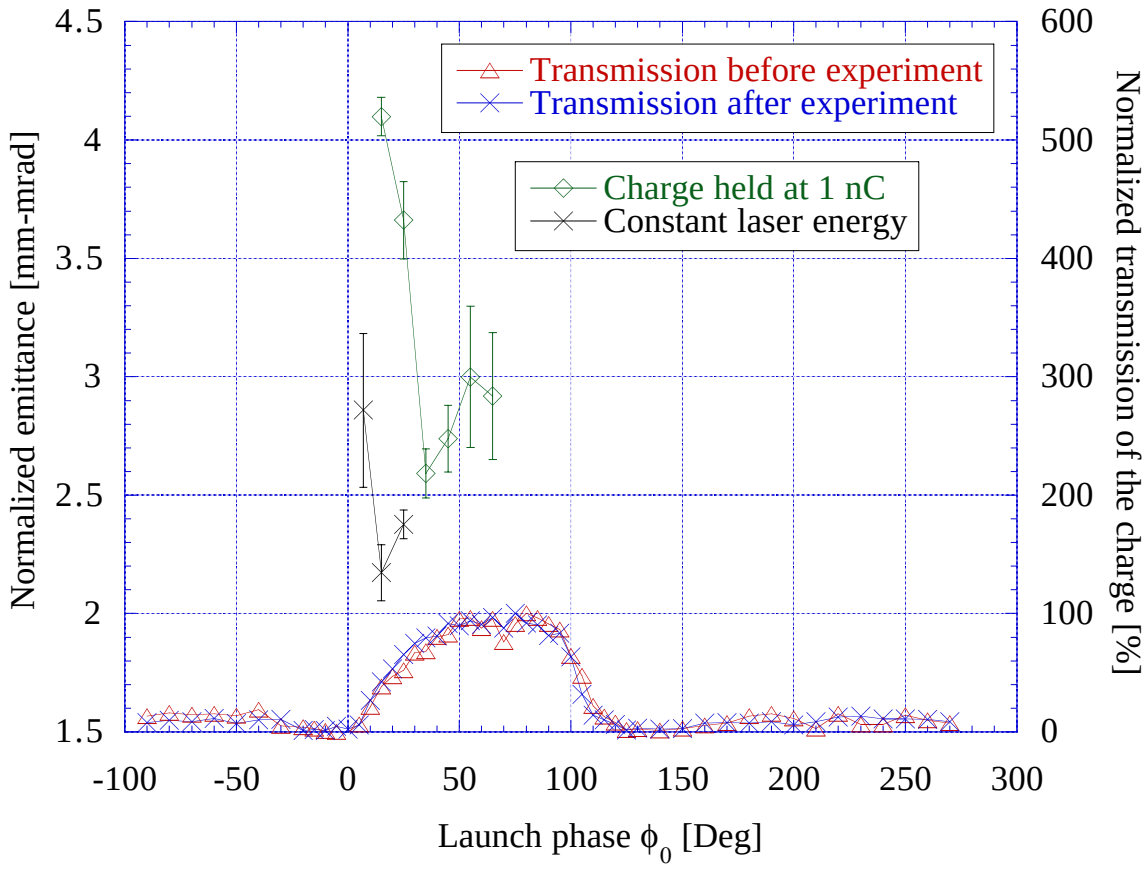
Transmission before experiment
Transmission after experiment
Charge held at 1 nC
Constant laser energy
Normalized emittance [mm-mrad]
Normalized transmission of the charge [%]
Launch phase ϕ0 [Deg]
4.5
4
3.5
3
2.5
2
1.5
600
500
400
300
200
100
0
-100
-50
0
50
100
150
200
250
300

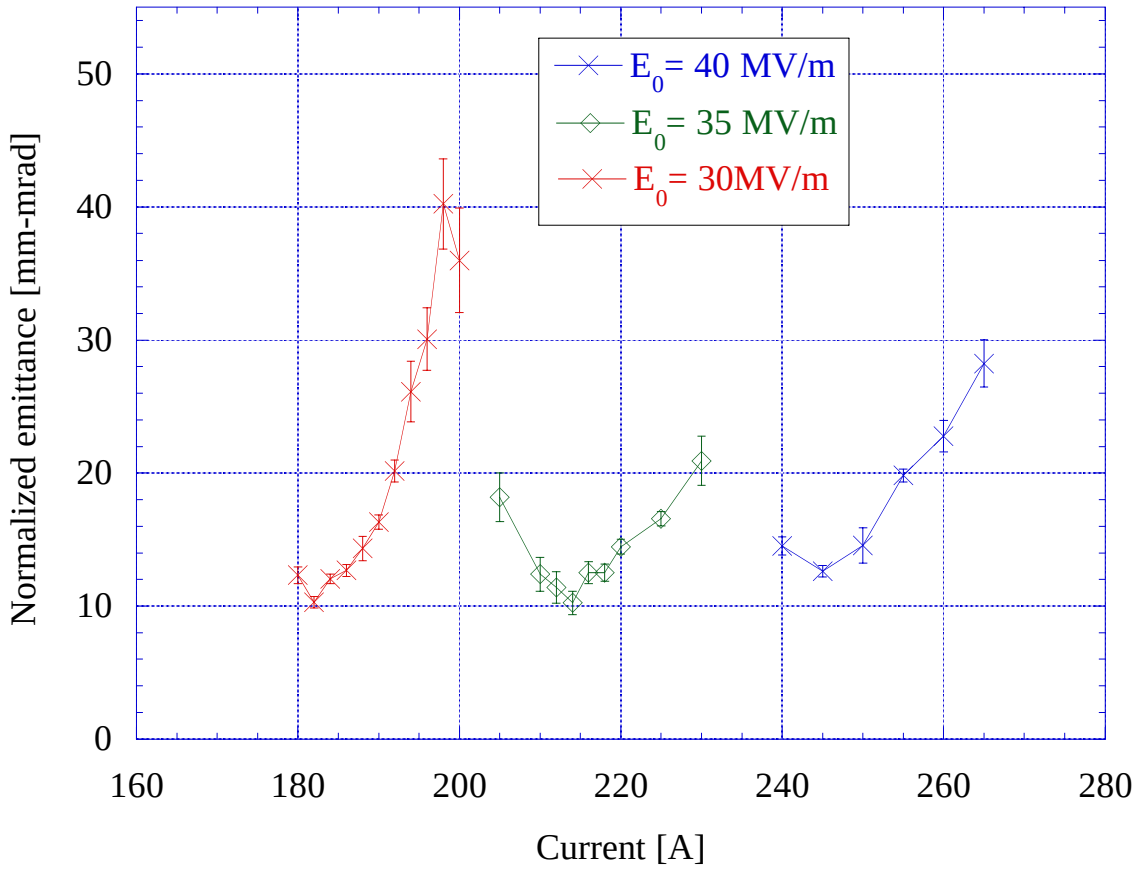
E0= 40 MV/m
E0= 35 MV/m
E0= 30MV/m
Normalized emittance [mm-mrad]
Current [A]
0
10
20
30
40
50
160
180
200
220
240
260
280

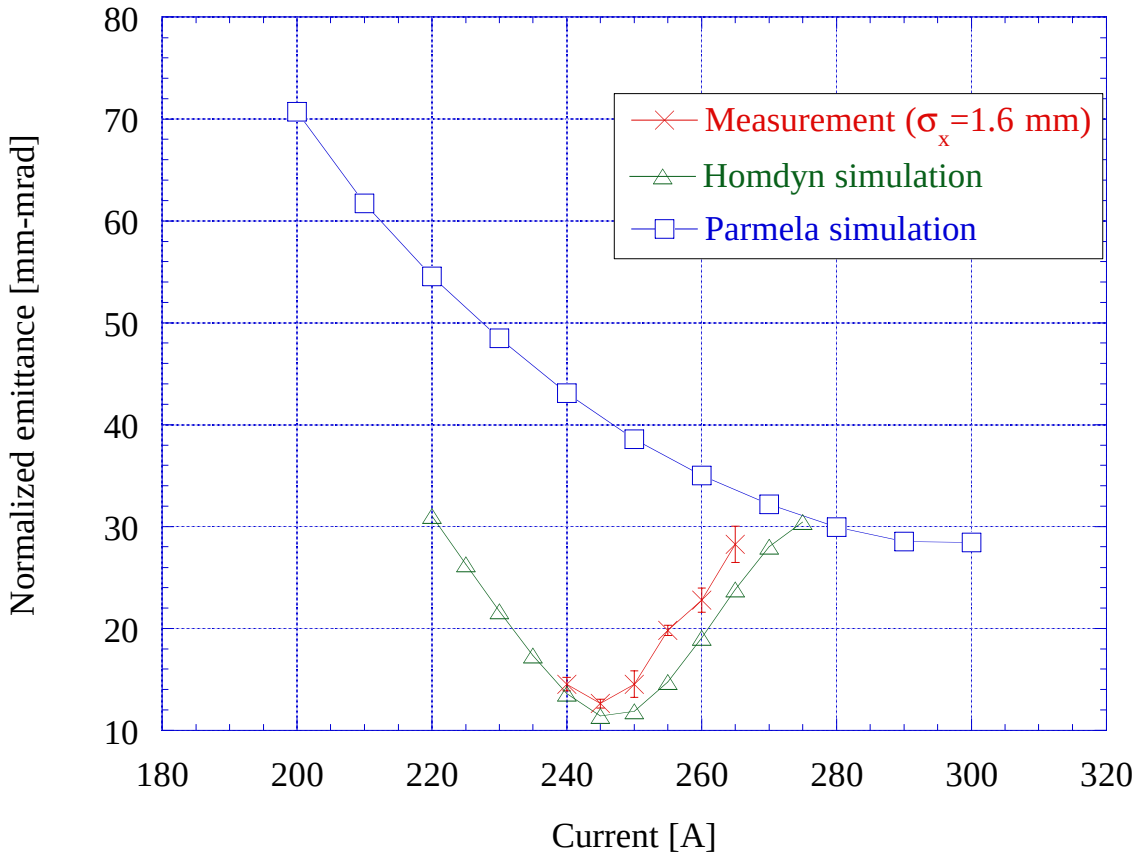
Measurement (σx=1.6 mm)
Homdyn simulation
Parmela simulation
Normalized emittance [mm-mrad]
Current [A]
10
20
30
40
50
60
70
80
180
200
220
240
260
280
300
320

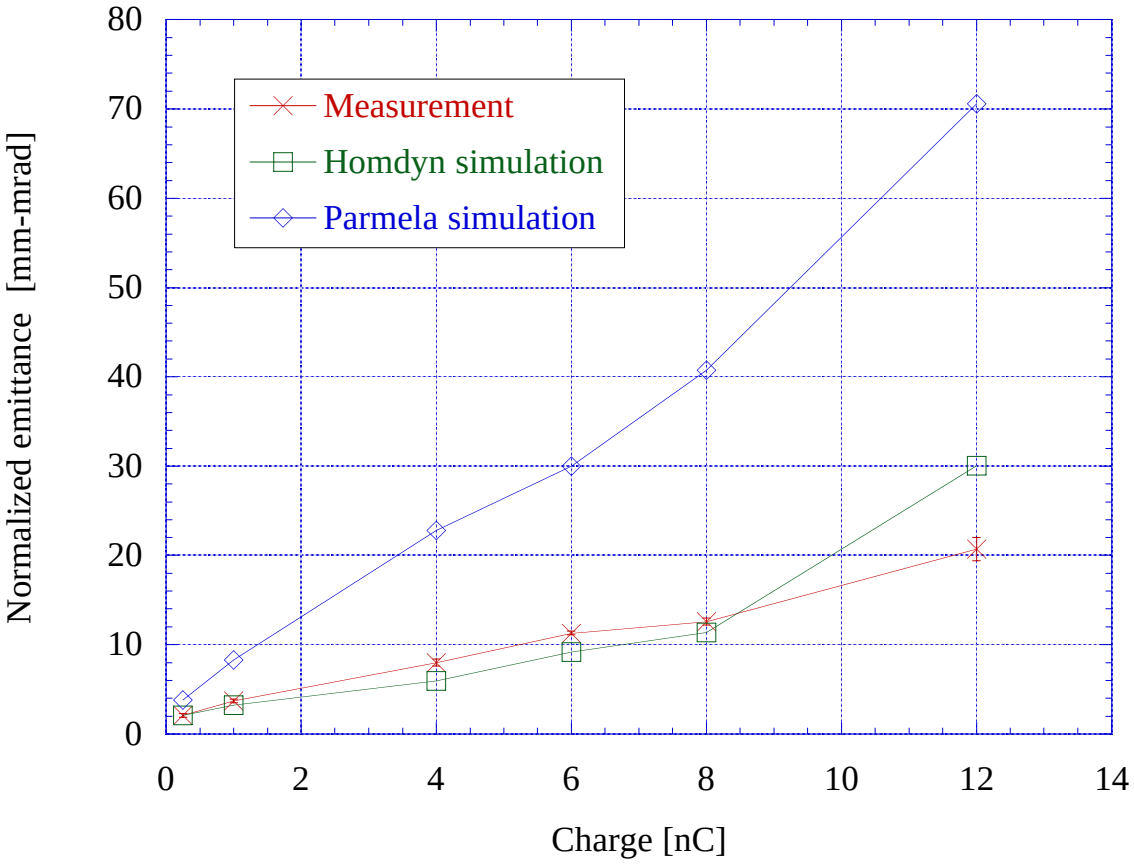
Measurement
Homdyn simulation
Parmela simulation
Normalized emittance [mm-mrad]
Charge [nC]
0
10
20
30
40
50
60
70
80
0
2
4
6
8
10
12
14

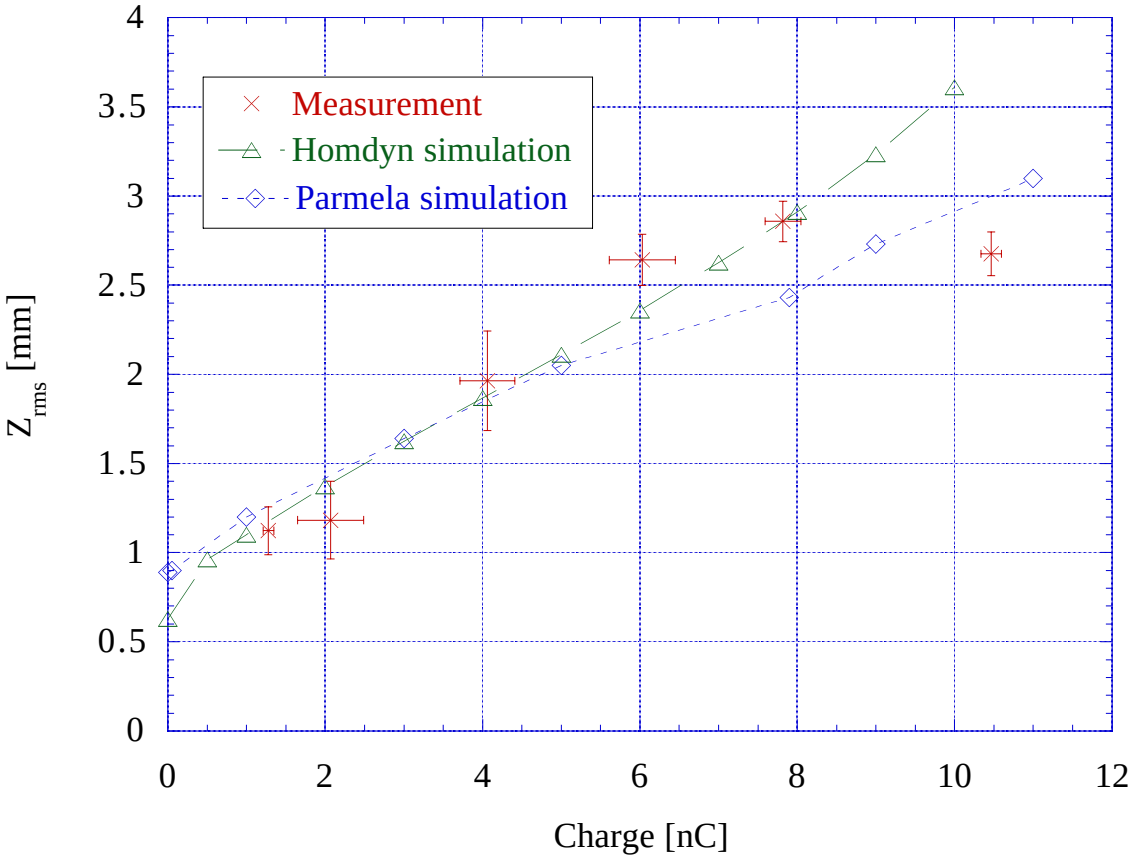
Measurement
Homdyn simulation
Parmela simulation
Z_{rms} [mm]
Charge [nC]
0
0.5
1
1.5
2
2.5
3
3.5
4
0
2
4
6
8
10
12

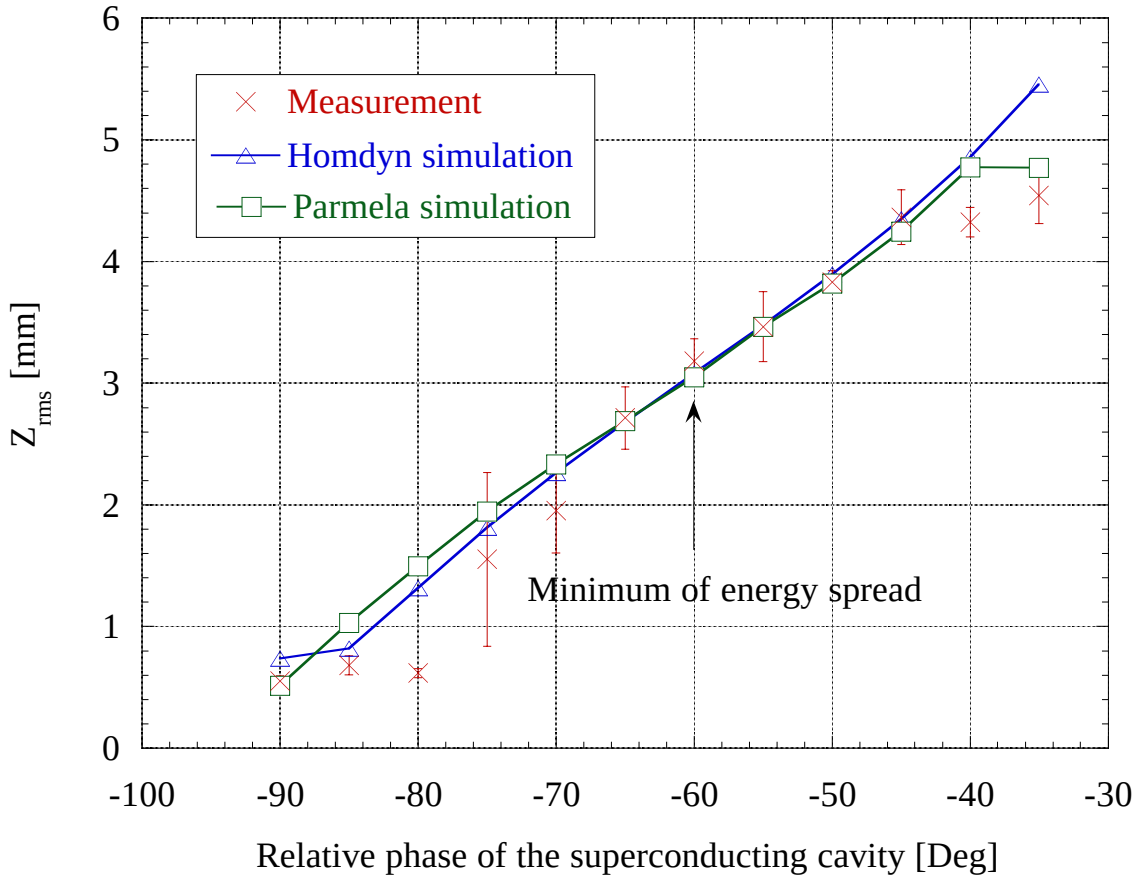
Measurement
Homdyn simulation
Parmela simulation
Minimum of energy spread
Z_{rms} [mm]
Relative phase of the superconducting cavity [Deg]
0
1
2
3
4
5
6
-100
-90
-80
-70
-60
-50
-40
-30

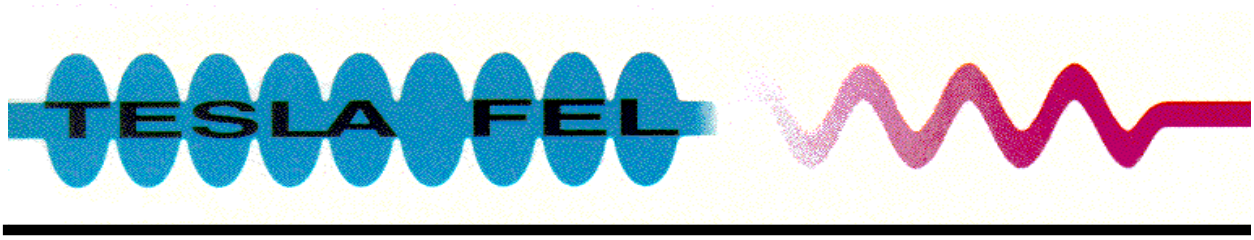

High Brightness Photo-Injectors for the TESLA X-FEL, TTF II User Facility and...

Ph. Piot
injector (beam dynamics) working group:
M. Ferrario (INFN-LNF), K. Flöttmann (DESY), B. Grigoryan (YerPhi), T. Limberg (DESY) and Ph. Piot (DESY)

Abstract

The TESLA linear collider will integrate a X-ray (1 Angstr.) free-electron laser which requires electron bunches with 5000 kA peak current and slice emittance (over the cooperation length) of 1.6 mm-mrd. On an other end the Tesla Test Facility will be upgraded to drive a User Facililty (TTF II) capables of lasing around 6 nm. Both projects require high performance electron sources. We discuss the concept adopted for beam generation up to the emittance-dominated regime along with the first stage compression.

-Contents-

Introduction: some learnings from Tesla Test Facility I

- overview
- injector
- compression

“Ingredients” for a new Injector Design:

- new gun design
- new simulation tools

Proposed TESLA X-FEL Injector [report TESLA-FEL 01-03]:

- overview and requirements for the TESLA X-FEL
- beam dynamics issues

Modification for TTF II User Facility:

- overview and requirement for the TTF User Facility
- practical issue
- discussion of a low charge option

Conclusions and Future Directions

- the Test Facility in DESY-Zeuthen (Berlin)
- ...

TTF phase I - Injector Overview-

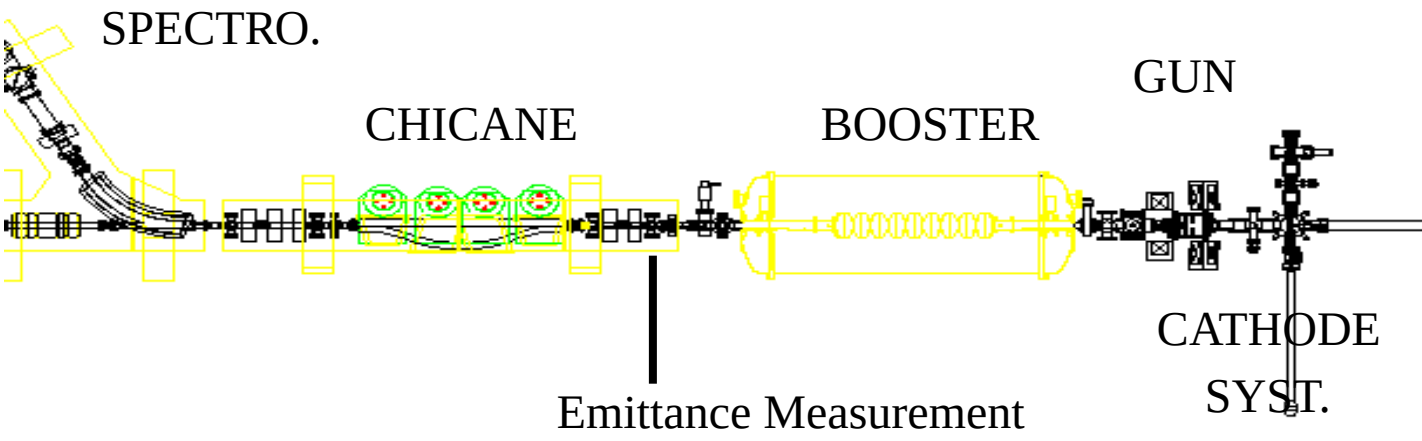

TYPICAL OPERATION: 1 nC (FEL mode), 4 nC (LC mode)

LASER: Gaussian pulse (5 ps rms -> 12 ps)

λ=260 nm

for 1 nC, r=1.5 mm

GUN: 1+1/2 L-Band (f=1.3 GHz) Gun “FERMI GUN”;

peak field=35 MV/m

RF “flat top” up to 800 msec

“two solenoids splitted scheme”

BOOSTER: single 9-cell TESLA cavity

average gradient 11.5 MV/m

phase chosen to compensate correlated energy spread from gun

CHICANE: not commissioned yet!

DIAGNOSTICS: spectrometer line for energy + energy spread

four OTR/ YaG / alumina screens

one multislit device for emittance meas.

several locations where emittance can be measured with the “quad scan” technique

EMITTANCE MEASUREMENTS at 1nC

Most of the measurement performed with the multislit mask, but also with the quadrupole scan technique. Measurements have been compared with simulations with ASTRA.

Sensitivity to gun phase

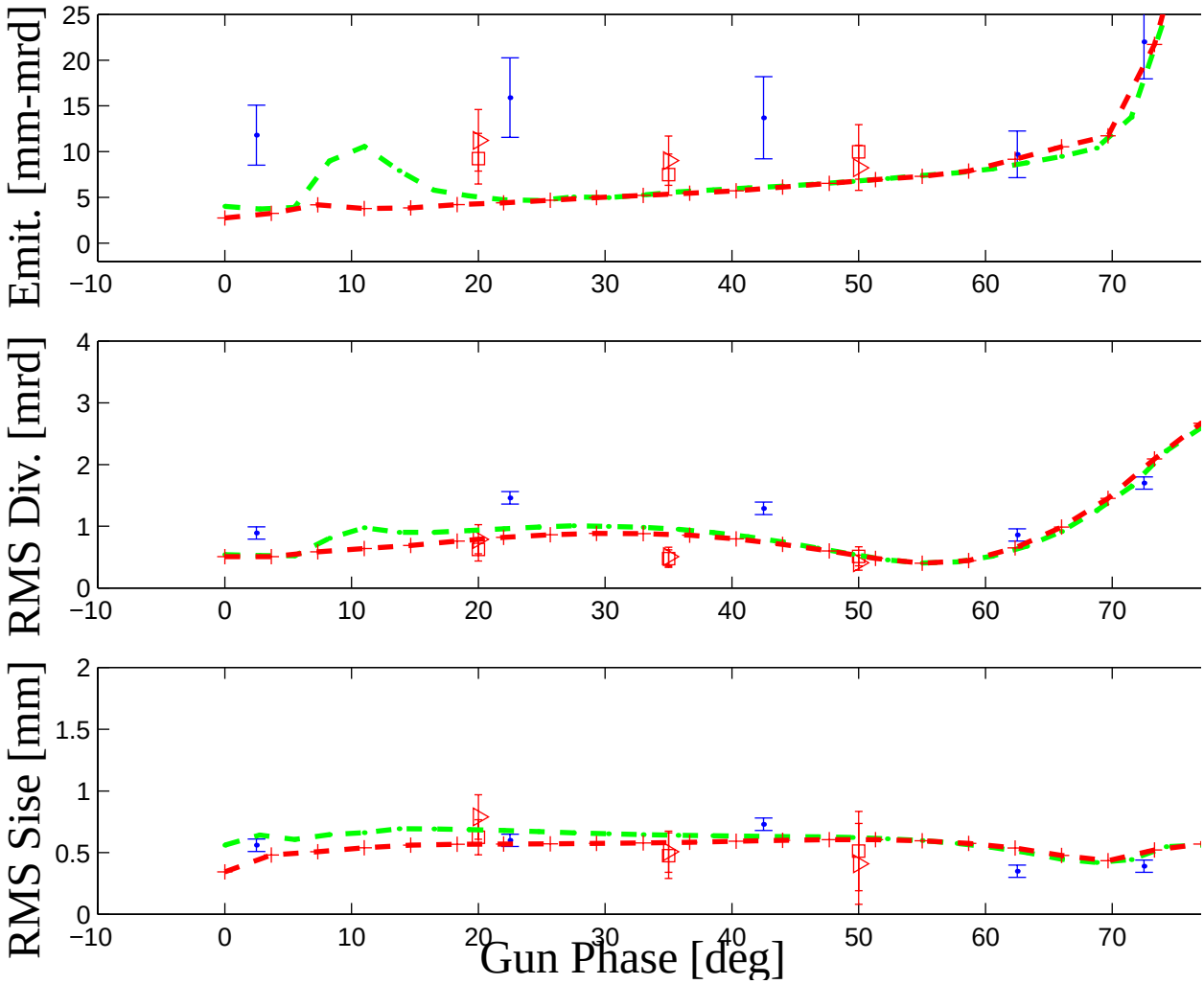

dots: multislits; square/ diamond: quad scan (x/y)
green: simulation with Astra
red: simulation with Astra including Schottky effect

sensitivity versus solenoids settings

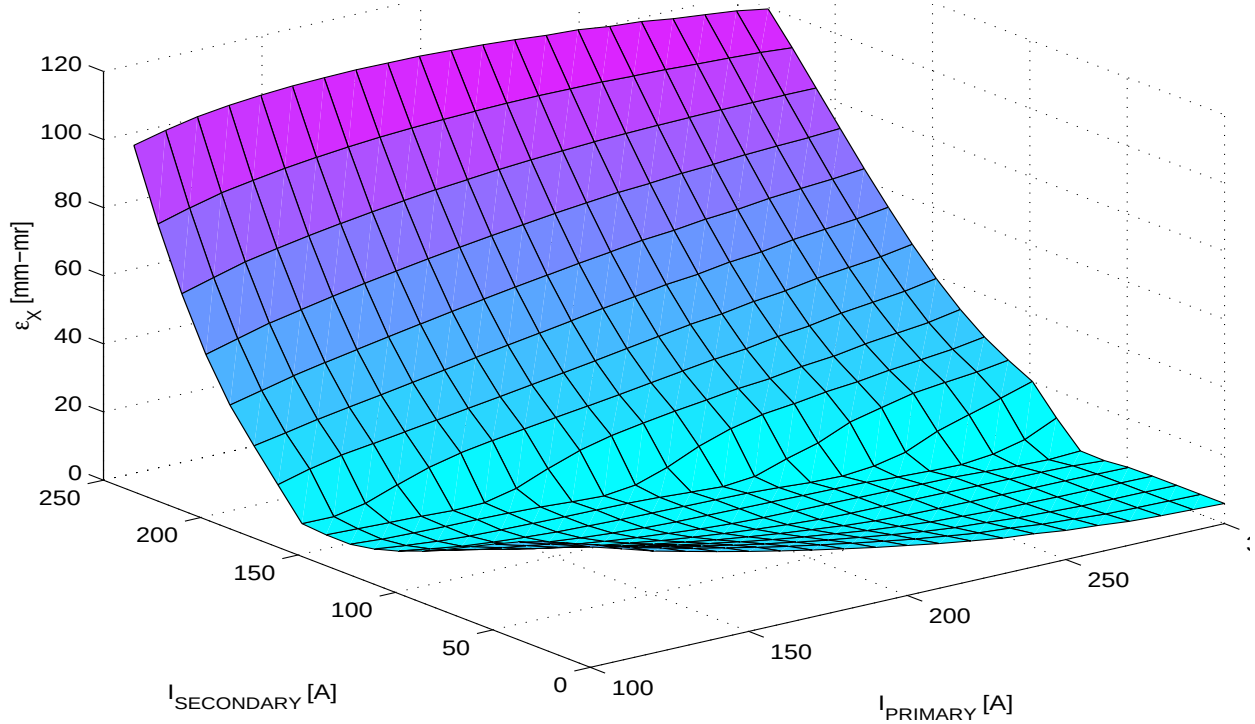

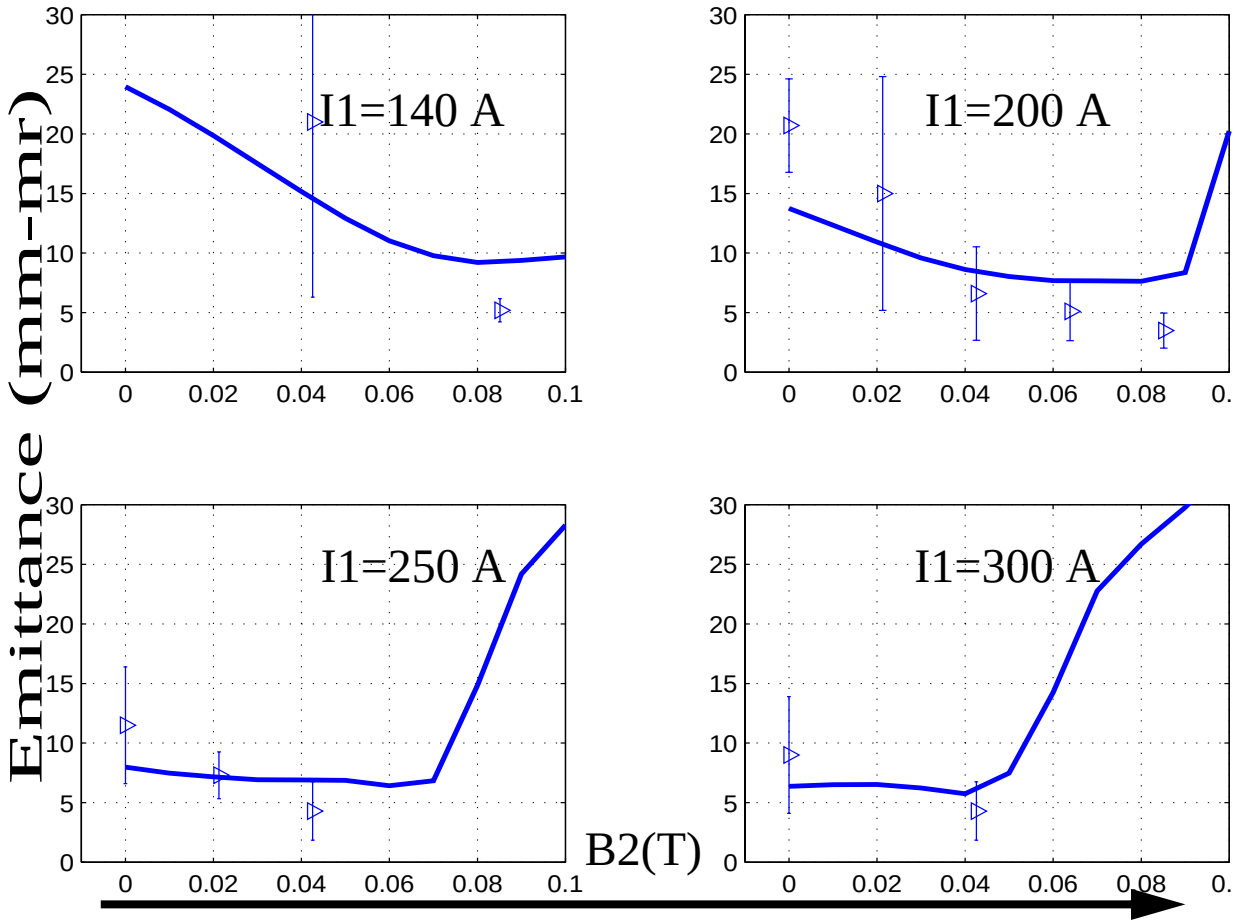

Ph. Piot, Deutsches Elektronen Synchrotron HH / JAN-2001

TTF phase I - Compression Issues-

* bunch compression to 500 microns (RMS) with magn. chicane

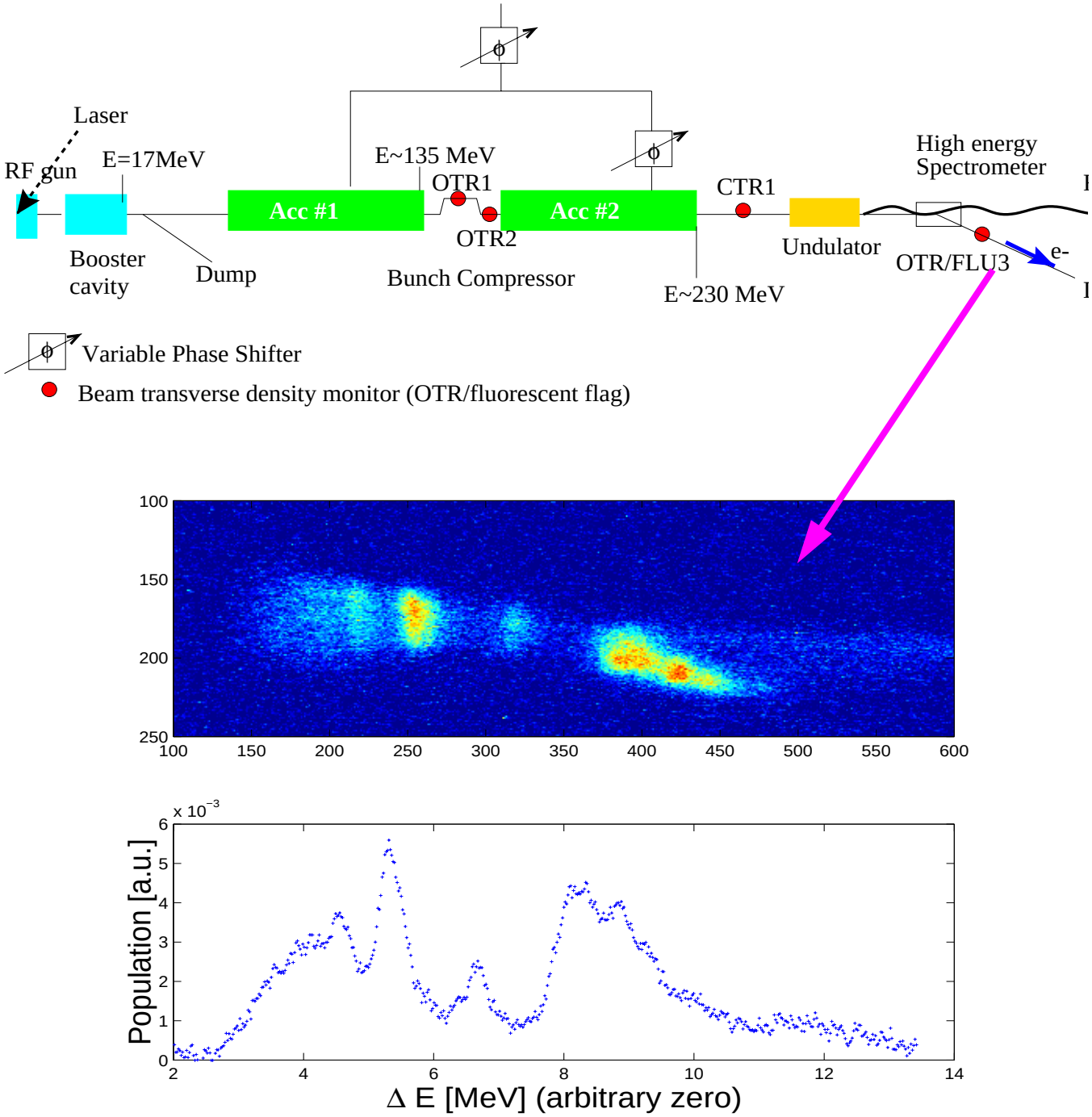

-> anytime the bunch compressor was operated for max. compression we observed a “fragmentation” of the energy profile: wakefield in ACC #1 (NO!), CSR (MAYBE...)

TTF Phase I - Compression issue -

Dependency of the energy profile vs Δϕ of ACC #1

(max comp for ϕ=-8 deg)

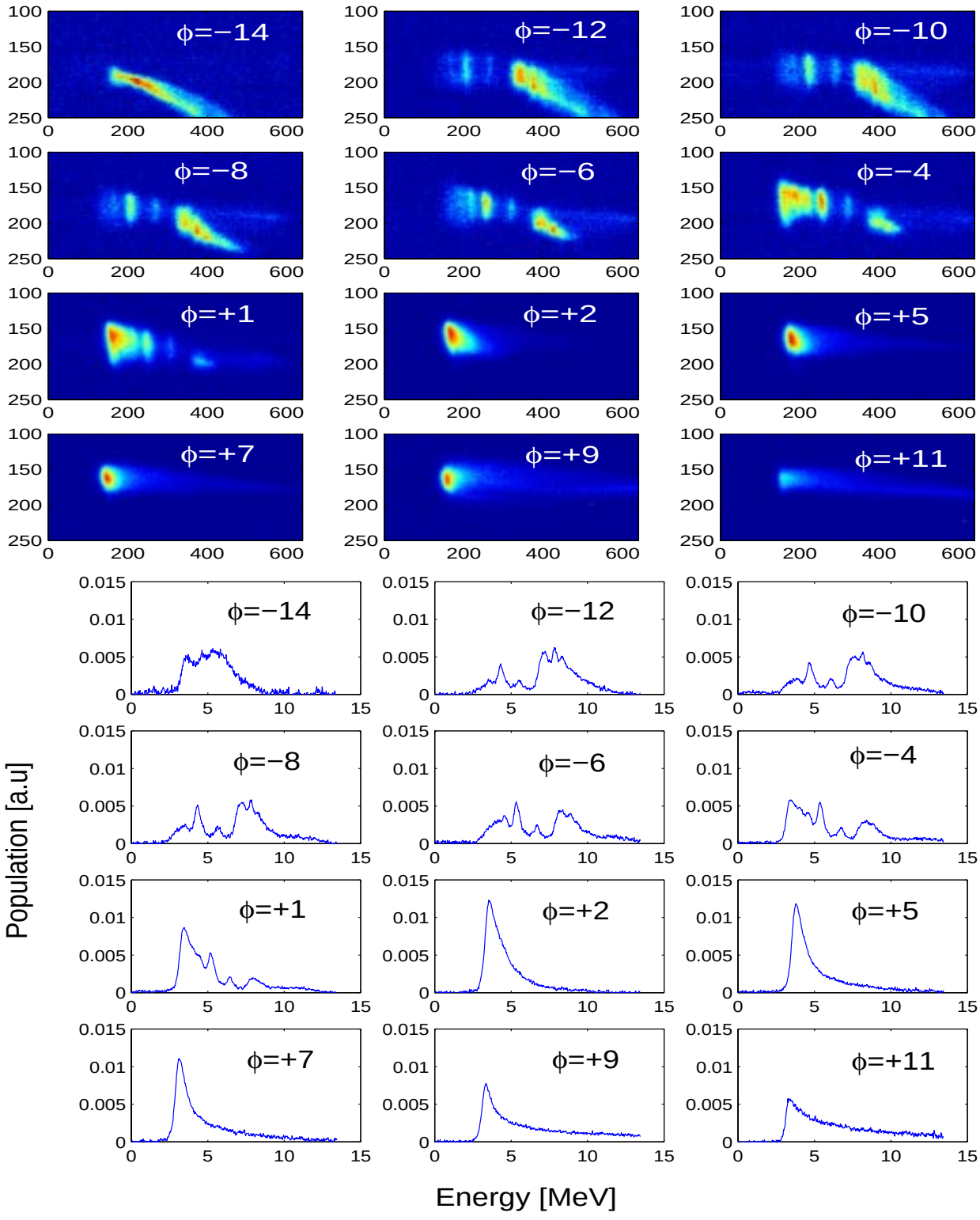

TTF 1 - modeling of the compression -

Magnetic Bunch Compressor

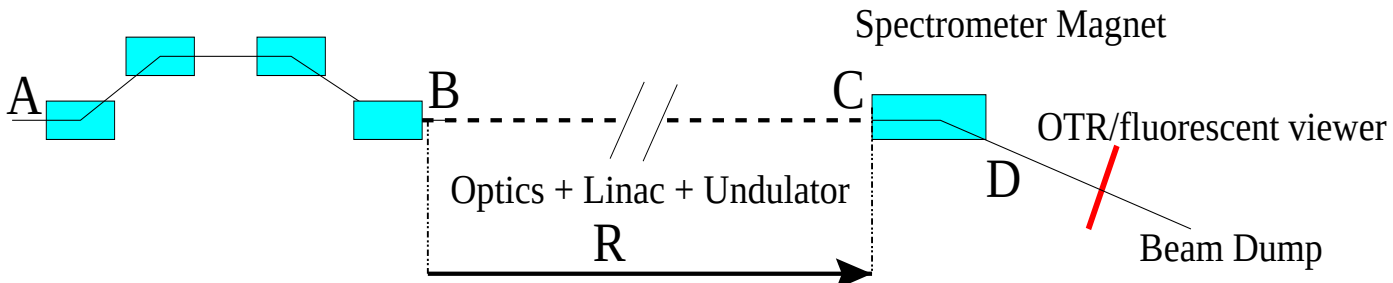

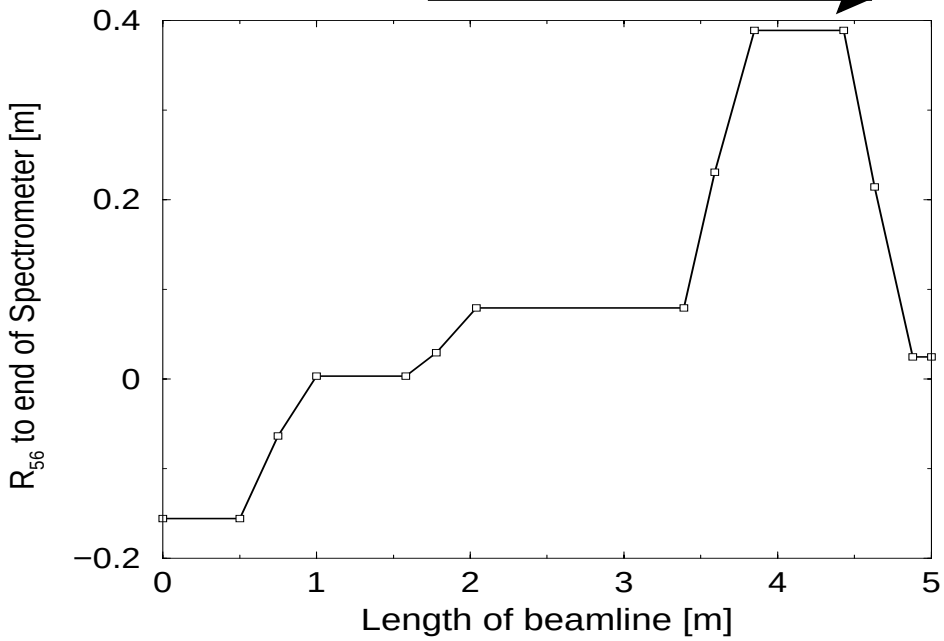

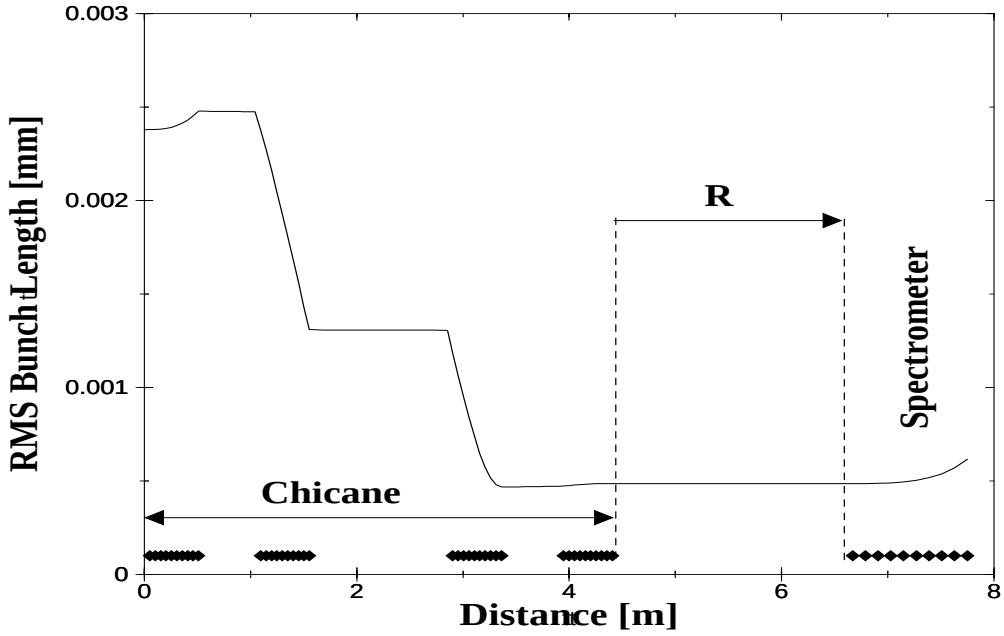

TTF I -compression modeling -

* Initial phase space obtained from ASTRA macroparticle code simulations of the realistic injector.

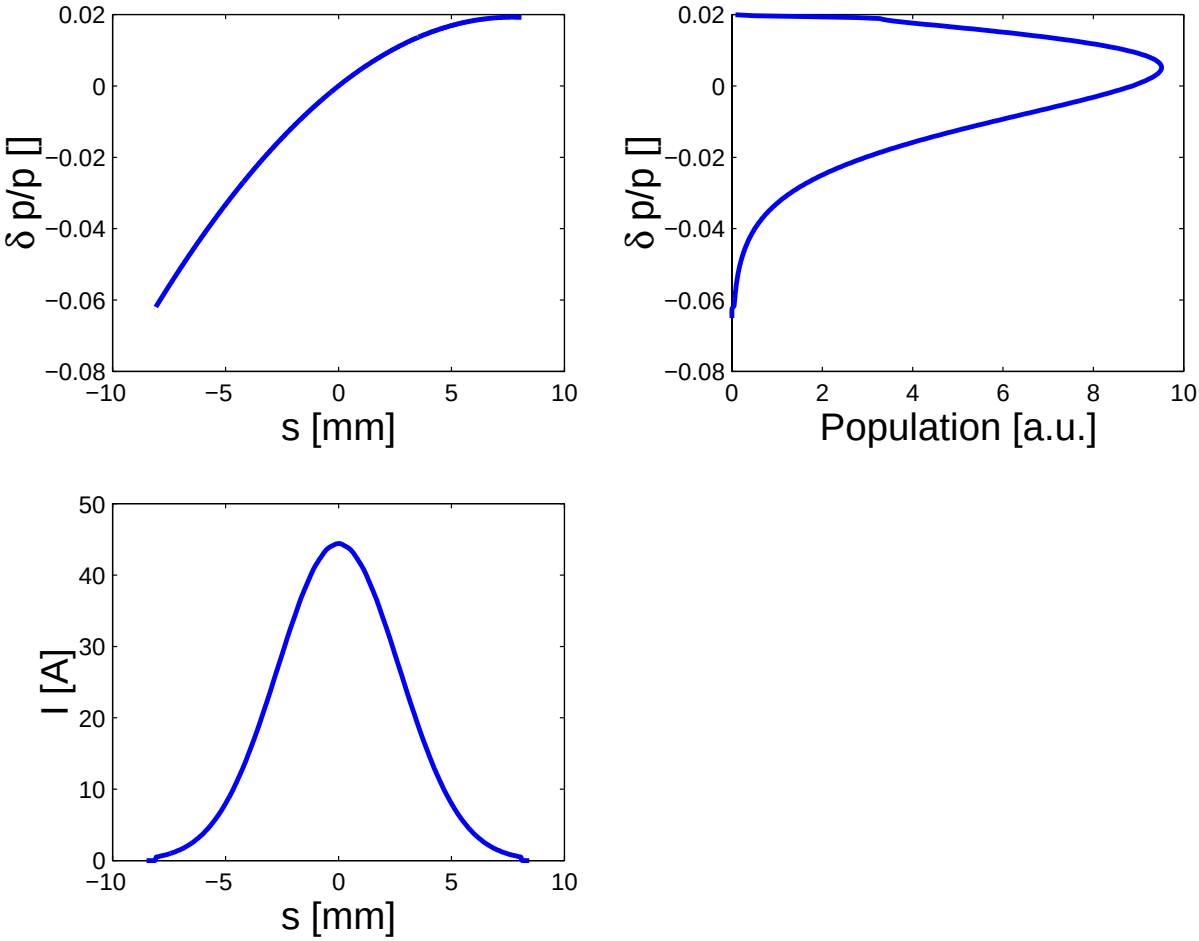

* because of rather long bunch (estimated to 2.5 mm) at the injector front end -> the bunch accumulates curvature during acceleration in accelerator module ACC #1

* this “curvature” can strongly enhanced the CSR wake (see Rui Li’s paper at EPAC 2000 Wien Austria)

Modeling of the compressor [R56=180 mm]

Use of TraFiC4 with 1200 macroparticles, using a self consistent algorithm.

Longitudinal phase space at compressor exit

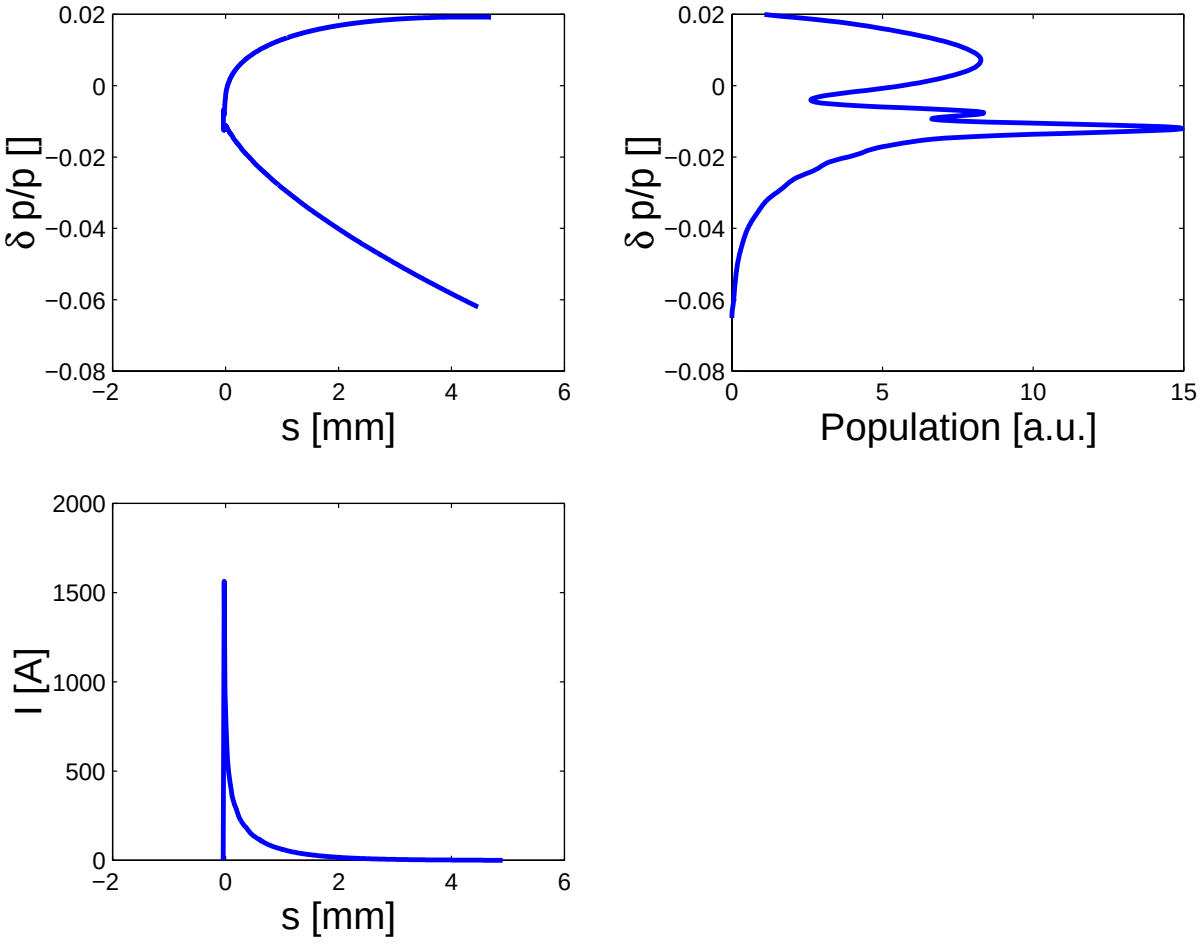

=> energy profile fragments

Longitudinal phase space at spectrometer exit

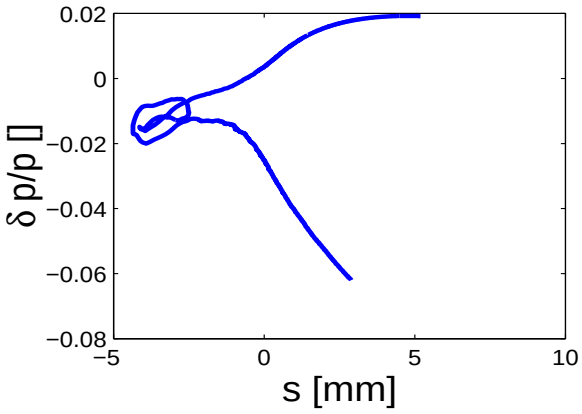

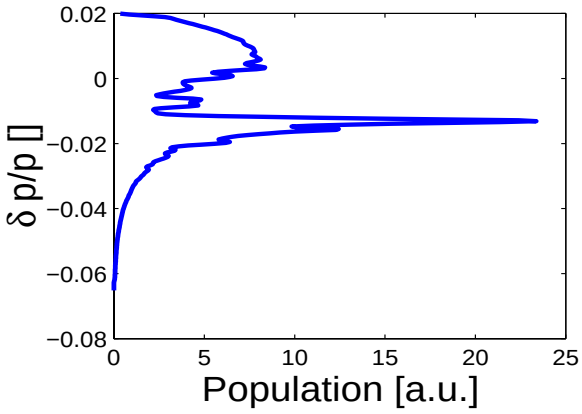

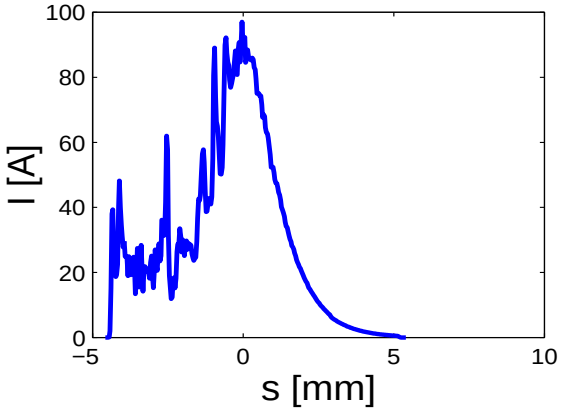

Comparison with the observed energy profile

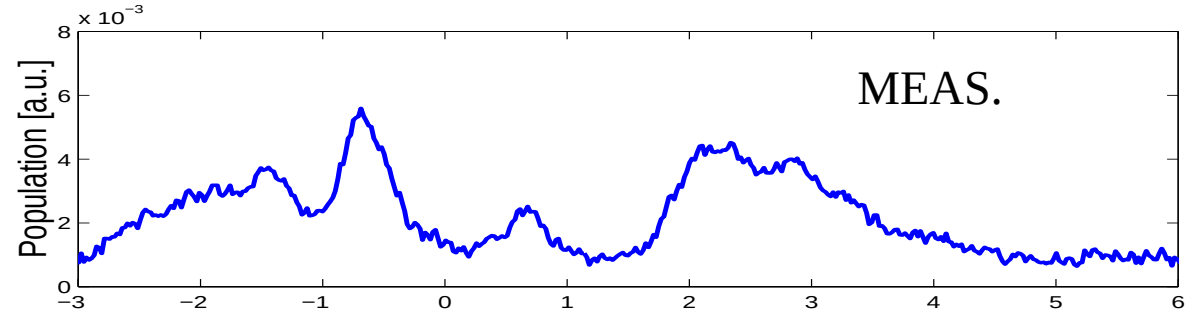

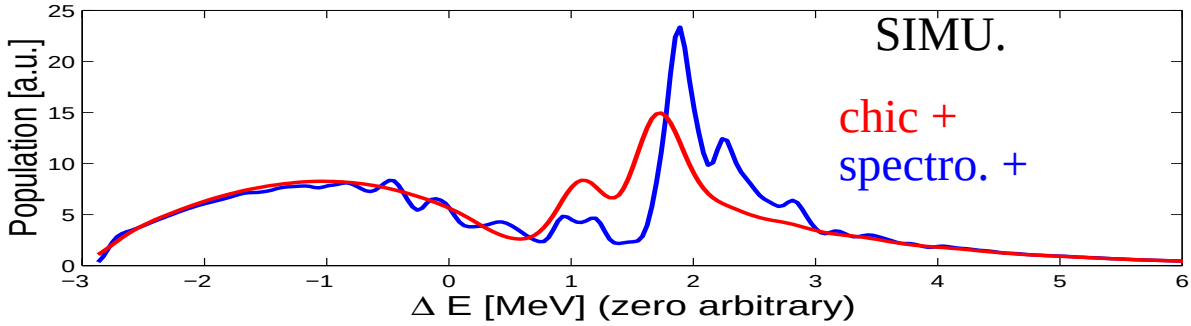

New “Ingredients” for the design of the TESLA XFEL injector

new tools: ASTRA [K. Floettmann], HOMDYN [M. Ferrario]

- ASTRA: a macroparticle code with radial mesh grid, that includes space charge +.
- HOMDYN: a multislice envelope code based on a semi-analytical approach. Slices are uniform cylinder.

HOMDYN very fast --> allows a large scan of the parameters
ASTRA slower but include nonlinear space charge --> used for fine optimization + generation of “realistic distributions” for integrated modeling [e.g. using ELEGFANT, GENESIS]

new gun (fully symmetric)

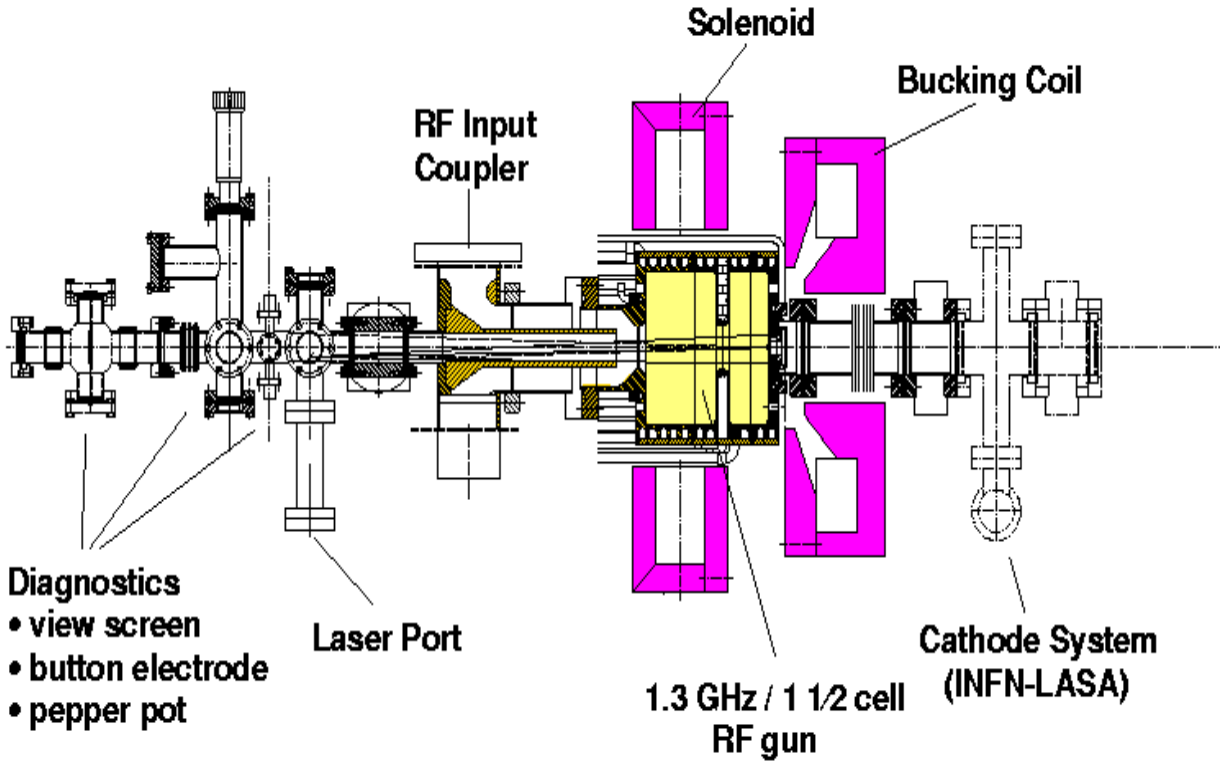

DESIGN PHILOSOPHY:

* Starting point: optimum operation point of LCLS [M. Ferrario]
- confirmed with Astra
- scaled to f=1.3 GHz

* then use the field profiles of the DESY gun + solenoid configuration and optimized. Gun peak field taken: 60 MV/m

OPTIMIZATION OF THE LASER PARAMETERS

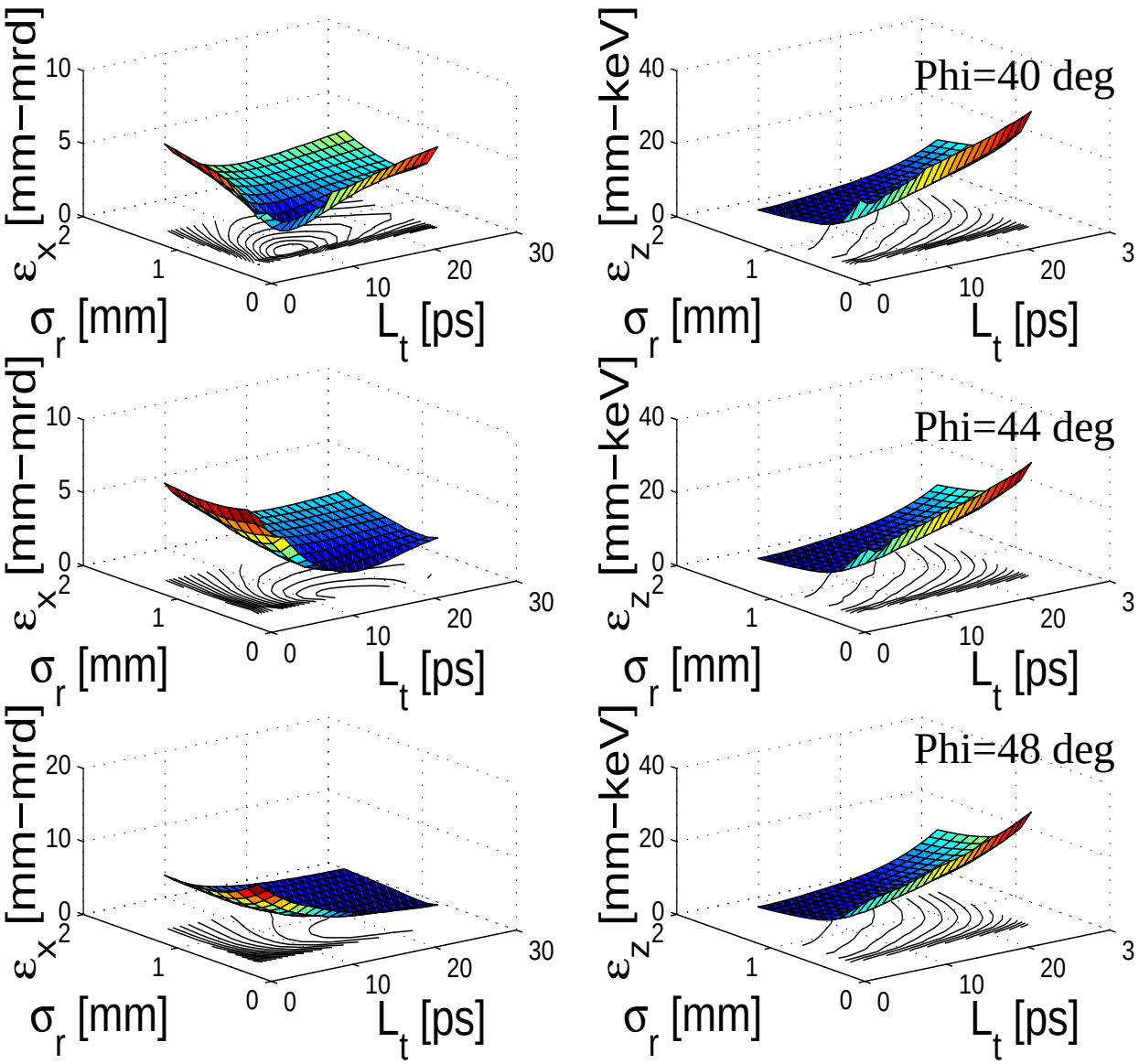

LASER + GUN PARAMETERS

spot size= 1.5 mm radius (unif.) pulse length=20 ps,
launch phi=44 deg, Gun peak field=60 MV/m

COMPENSATION DRIFT and ACCELERATION

One possible matching is the invariant envelope match, the beamspot, σ_r, at a SW booster entrance should obey:

$$\sigma'_r = 0$$

$$\sigma_r = \frac{2}{\bar{\gamma}'}\sqrt{\frac{I}{3I_A\gamma}}$$

I: peak current, γ: incoming beam energy, I_A Alvfen current, and γ': average accelerating gradient of the booster.

❒ The match is achieved in a way that it corresponds to a point where emittance is naturally decreasing
❒ The effects of the booster is to: (1) shift the minimum emittance to higher energy and (2) provide some emittance damping => solenoid peak field=0.2 T

CHOICE OF BOOSTER:

A TESLA standard cryomodule (i.e. 8 9-cell TESLA cavity).
After optimization: the first 4 cavities are operated at 12 MV/m, and the next 4 to the maximum expected gradient 25 MV/m
❒ reached energy is 142 MeV
❒ Injection of long bunch in the accelerating cavity yields curved longitudinal phase space => set a limit on bunch compression!!!

ACHIEVED PARAMETERS:

transverse emit < 0.5 mm-mrd (without thermal emittance)
longitudinal emit ~350 keV-mm!!!

CORRECTION OF LONGITUDINAL PHASE SPACE

[report TESLA-FEL-01-04]

Most of the longitudinal emittance is coming from curvature (i.e. an electron energy offset is correlated to the longitudinal position): $\delta(s) = \alpha_1 s + \alpha_2 s^2 + O(s^3)$

=> can use some higher RF field harmonic to correct this nonlinear dependence [well known trick in storage ring (flat topping) also applied to linear accelerator at BOEING FEL]

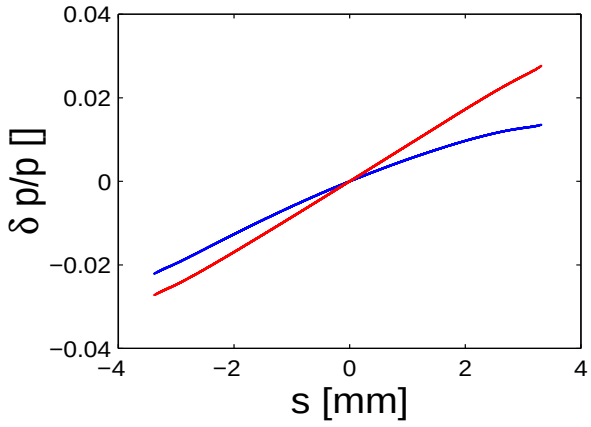

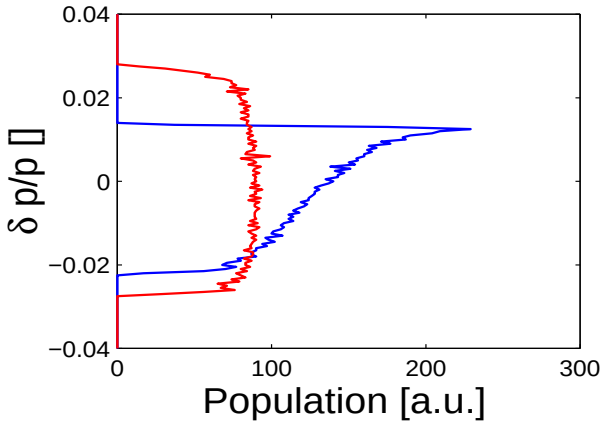

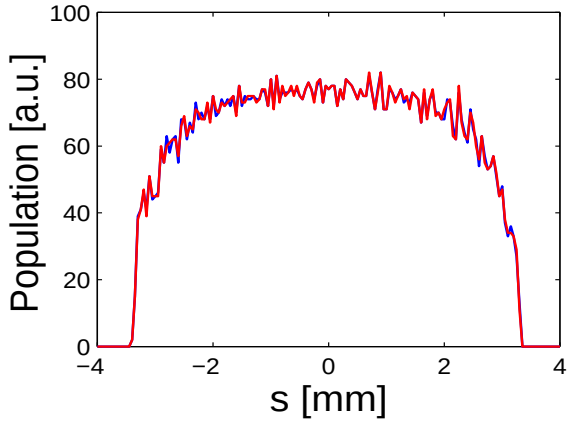

BEAM PARAMETERS ALONG THE BEAMLINE

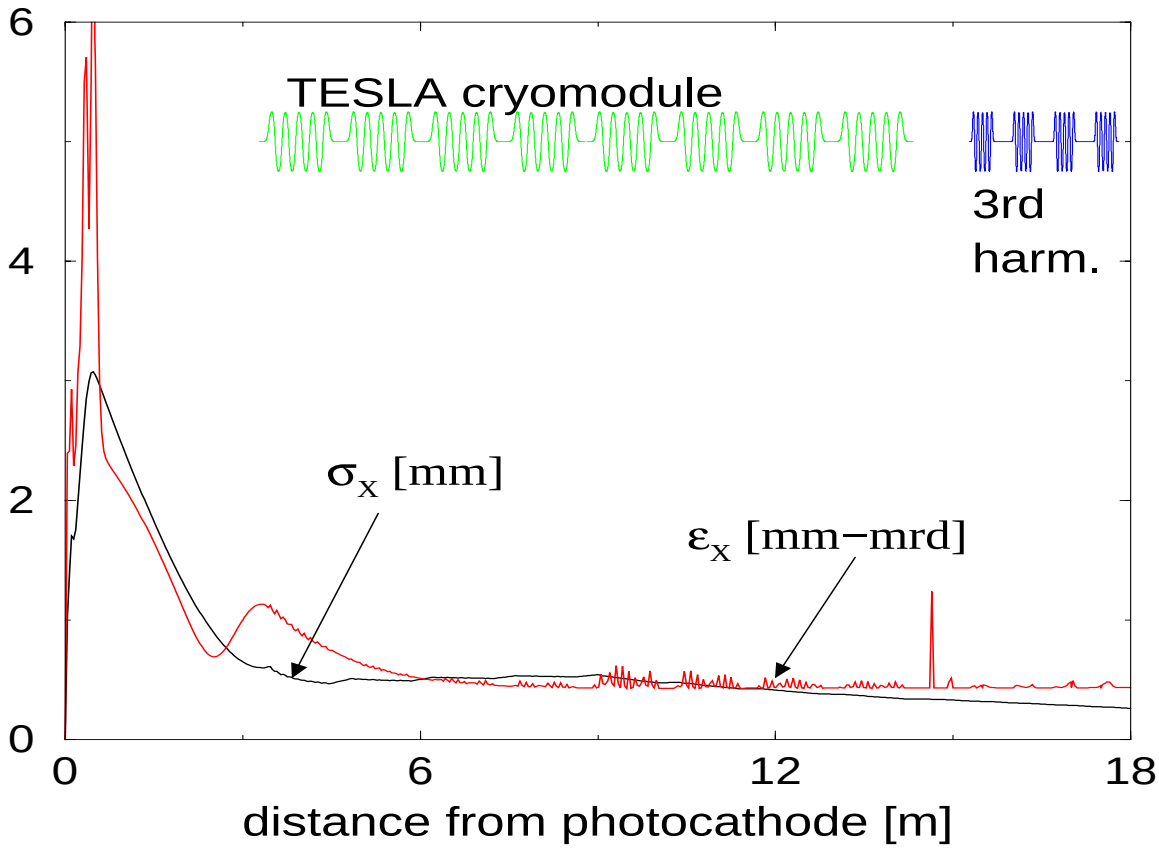

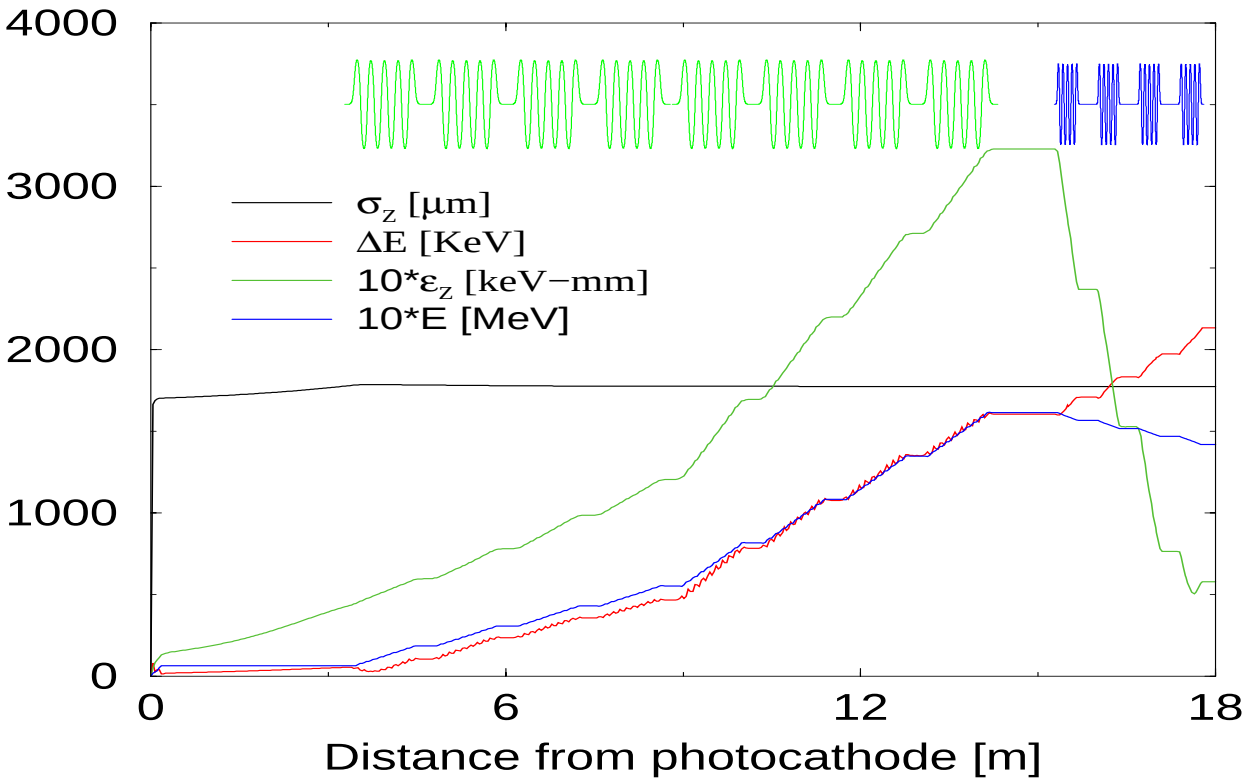

EXAMPLE OF COMPARISON BETWEEN (r,r') space from ASTRA & HOMDYN

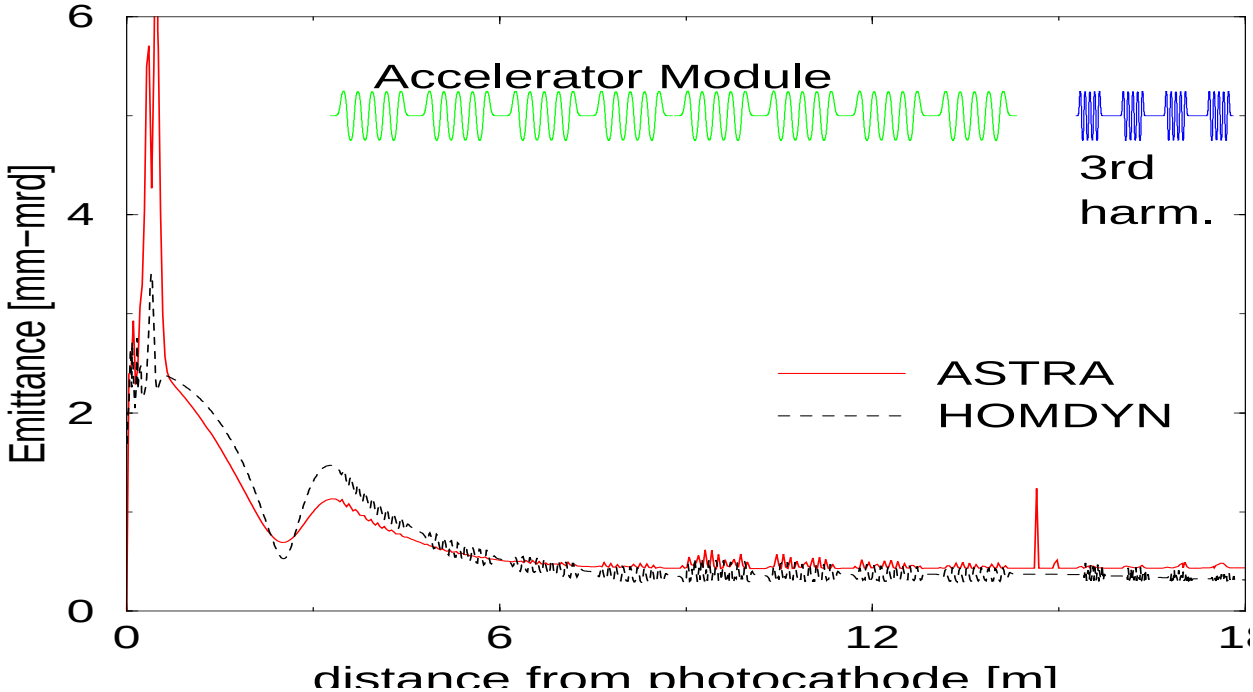

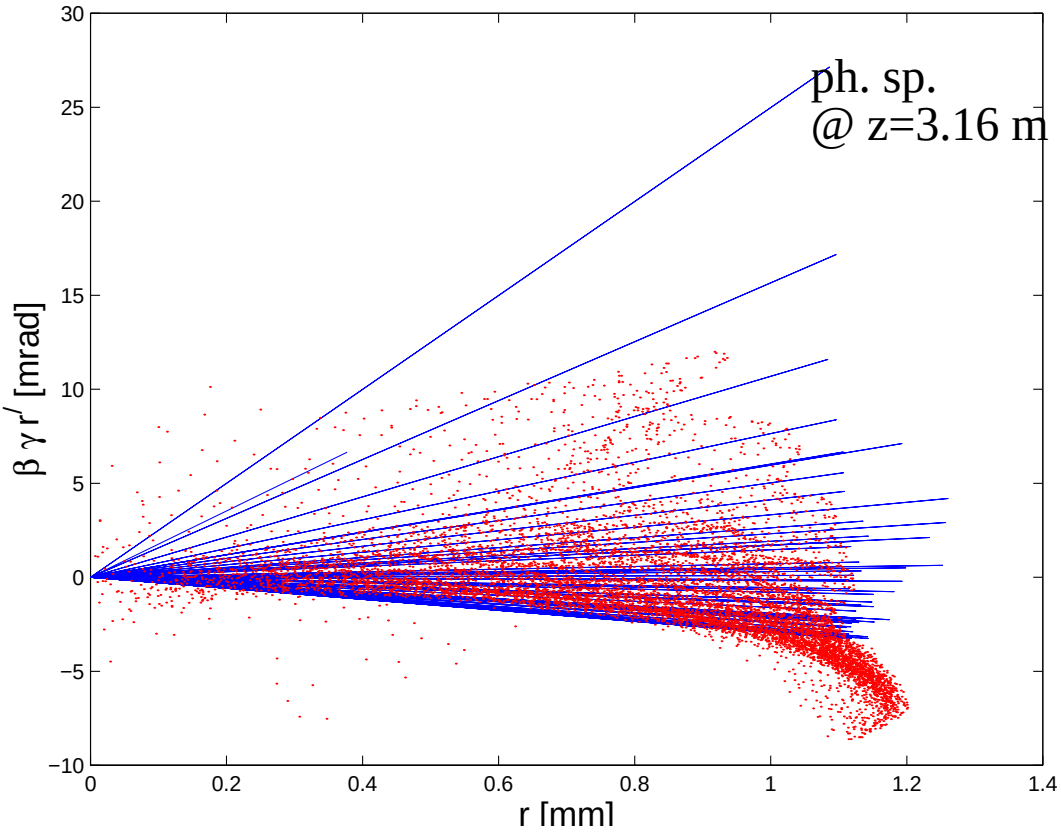

(for the long. phase space the codes show better agreement)

Generation line + compressor + diagnostics section

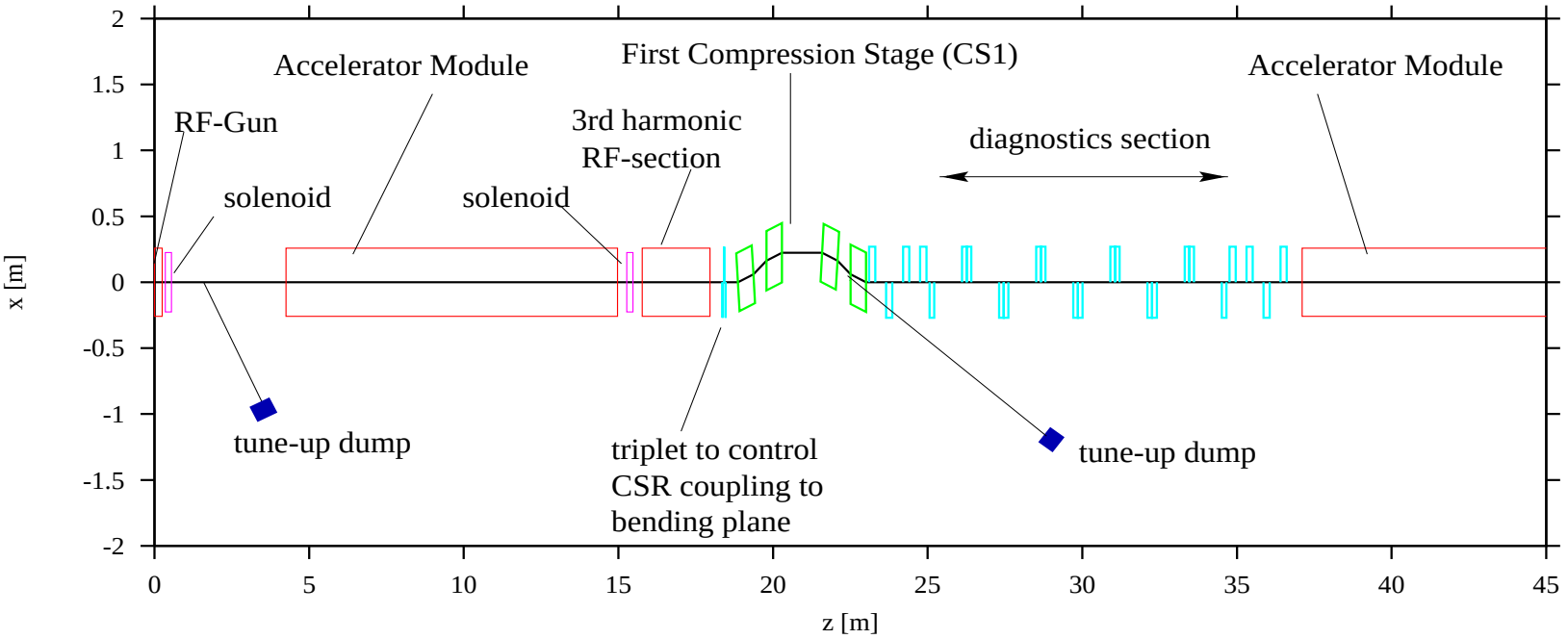

Ph. Piot, Deutsches Elektronen Synchrotron HH / JAN-2001

Parameters obtained downstream of the generation line (z=18 m)

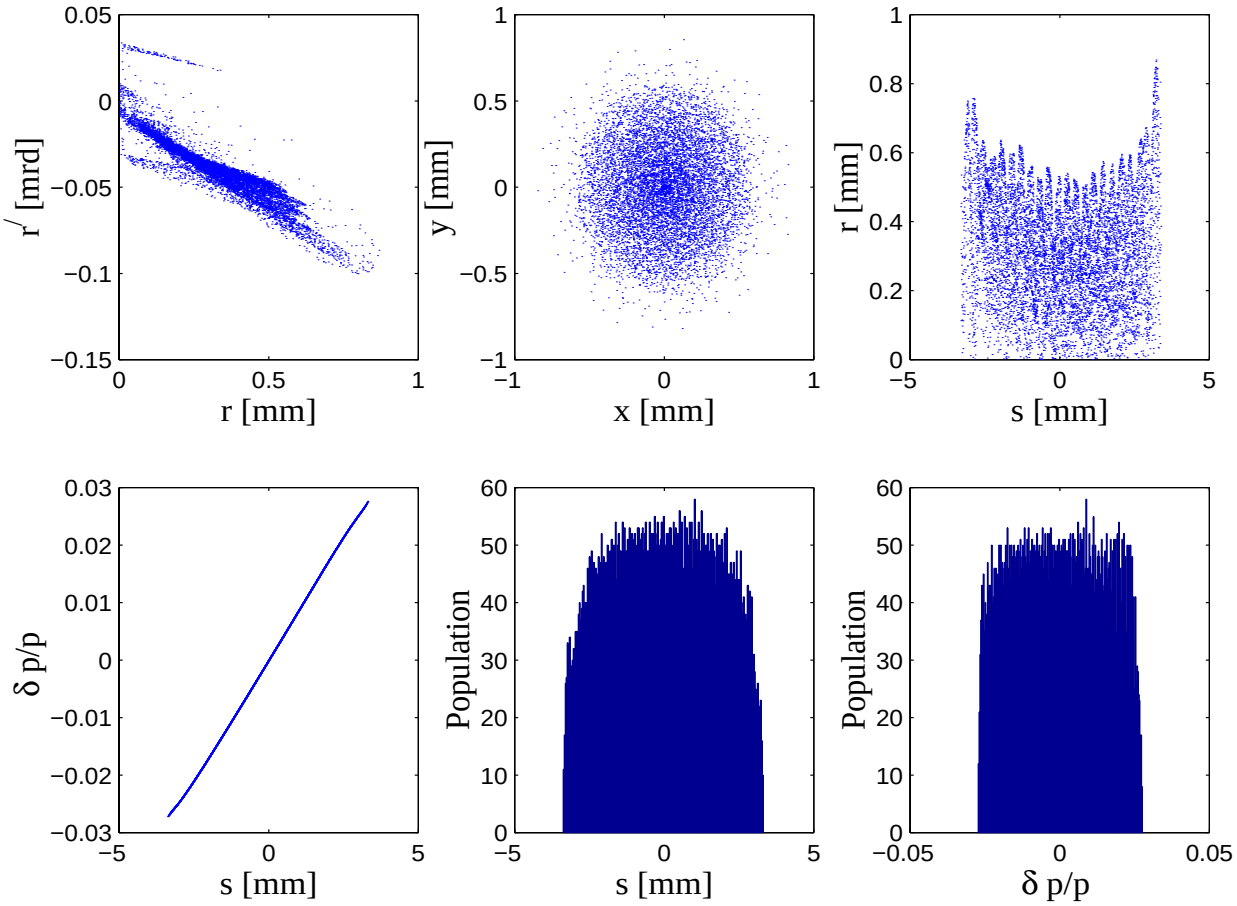

Table 1: beam param @ gener +

parameters	values	units
rms bunch length	1.77	mm
kinetic energy	142.4	MeV
rms energy spread	2132.3	keV
transverse emittance	0.43	mm-mrd
trans. emit. (w. 0.73 th. emit.)	0.90	mm-mrd
longitud. emittance	57.79	keV-mm
betaX/ betaY	43.35/43.74	m
AlphaX/AlphaY	5.15/5.20	---

Simulation of the compressor using TraFiC4 code

* Minimize emittance growth by proper matching
* Many iterative runs --> Optimum requires shielding with 8mm height beam pipe

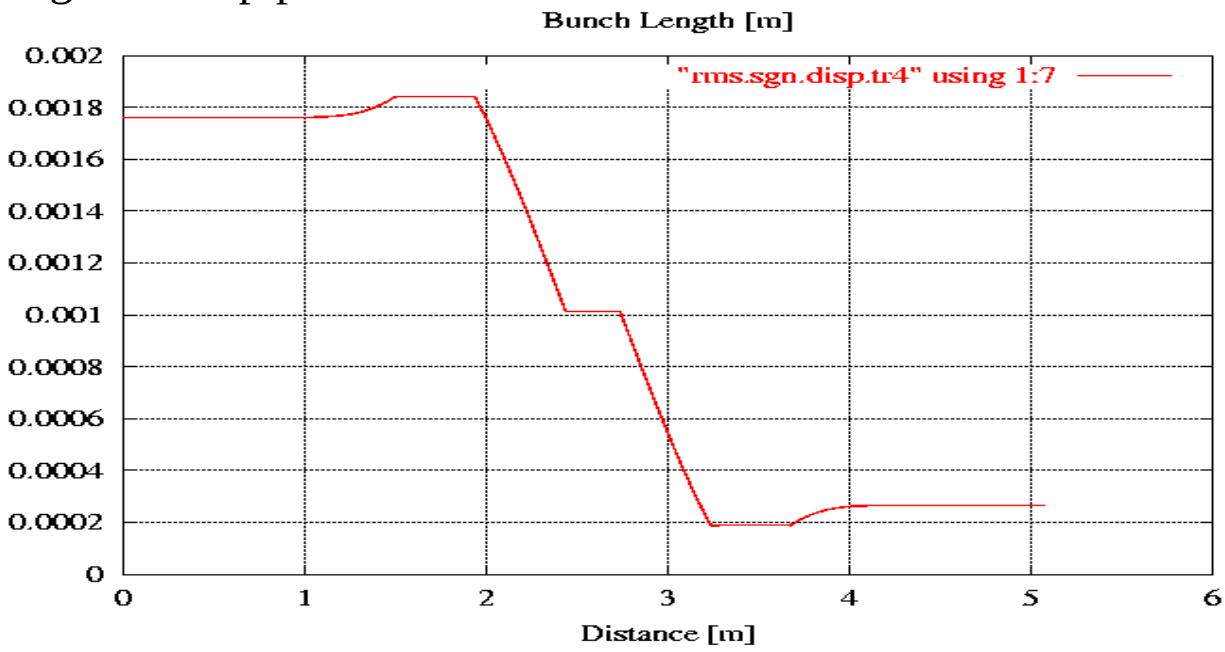

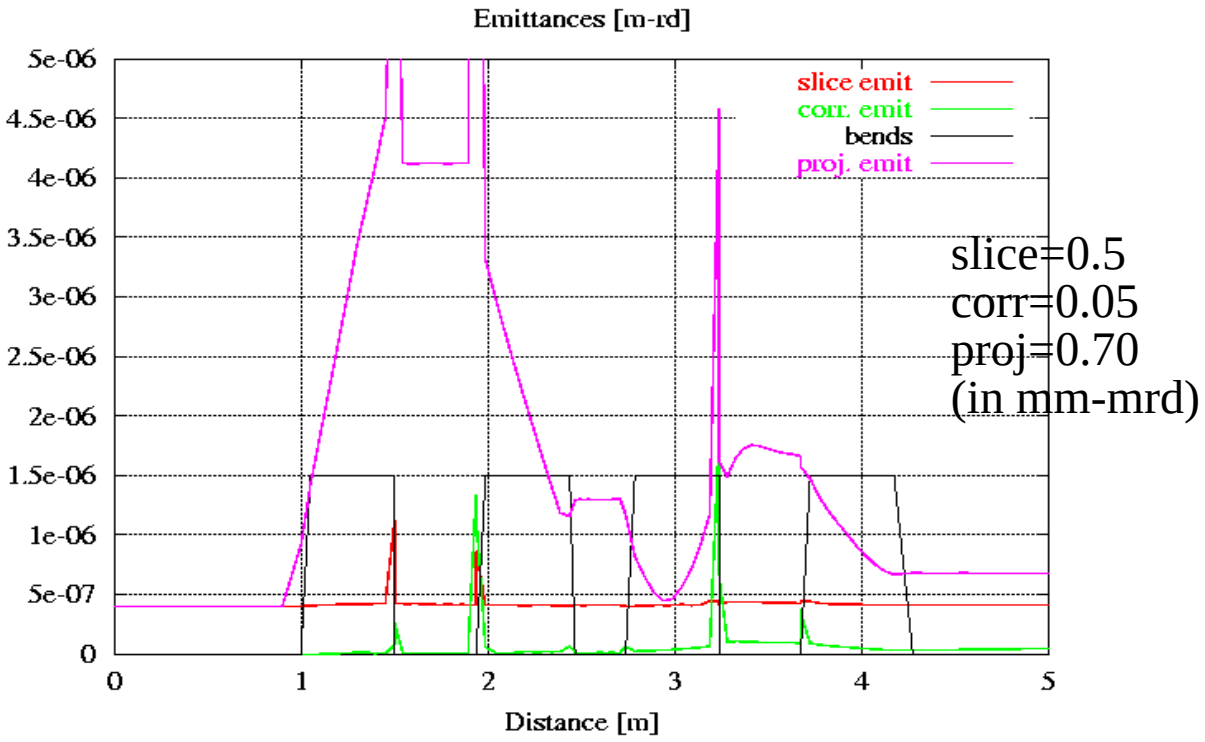

slice=0.5
corr=0.05
proj=0.70
(in mm-mrd)

Effects of beam compression in CS1 on the beam density

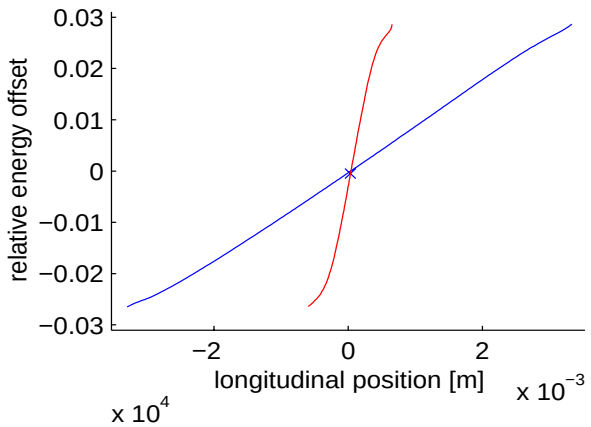

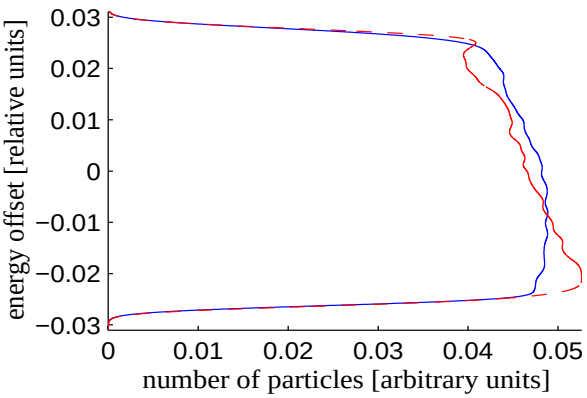

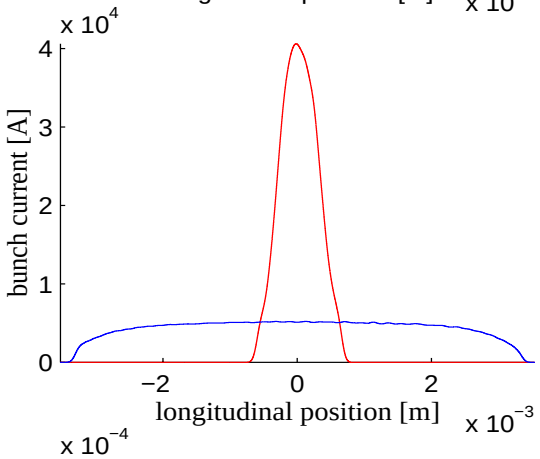

s_{rms} (initial): 1763.440 μ m

s_{rms} (final): 268.926 μ m

δ_{rms}(initial): 1.540 [%]

δ_{rms} (final): 1.555 [%]

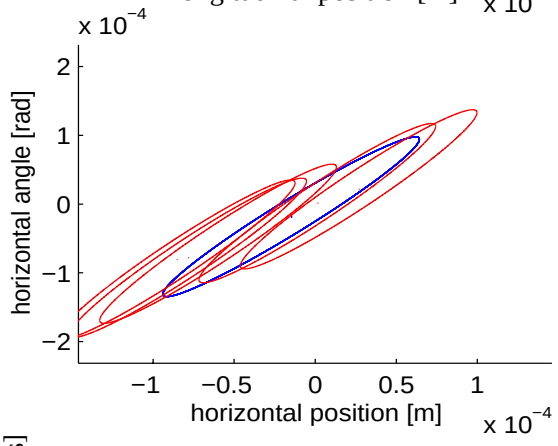

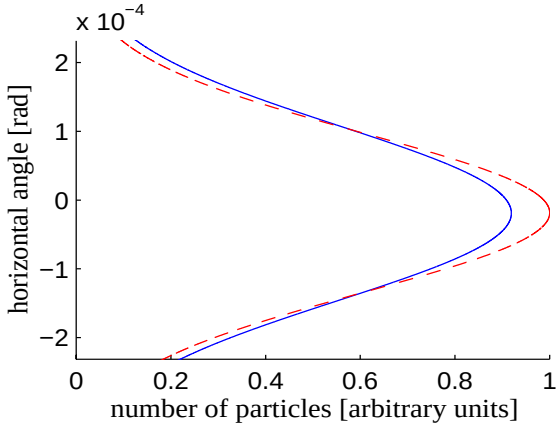

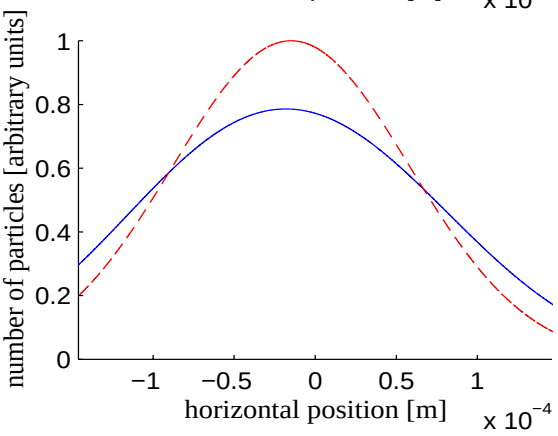

x_{rms} (CSR): 87.978 μ m

x_{rms}: 72.439 μ m

xp_{rms}(CSR): 119.544 μ rad

xp_{rms}: 112.203 μ rad

Ph. Piot, Deutsches Elektronen Synchrotron HH / JAN-2001

TTF User Facility (TTF Phase II): Overview + Requirement
[see report TESLA-FEL 95-

mode of operation: train of 800 bunches @ 1MHz;
train rep. rate: 10 Hz

Table 2: 1 nC beam requirements, λ=6 nm

parameters	values	units
Bunch charge	1	nC
Peak Current	2.5	kA
Trans. Emit.	2.0	mm-mrd
Long. Emit.	30	KeV-mm
dp/p	0.001	--

Table 3: 100 pC beam requirements, λ=6 nm

parameters	values	units
Bunch charge	0.1	nC
Peak Current	600	A
Trans. Emit.	1.0	mm-mrd
Long. Emit.	10	keV-mm
dp/p	0.001	--

First lasing light for users 20 nm ==> requirement are relaxed
e.g. at 1 nC, Transv. emit. 4 mm-mrd

TTF2 - INJ. UPGRADE (*STILL UNDER DISCUSSION*)

A - SHORT TERM (for commissioning + 1st light 20 nm)

current gun: 40 MV/m
laser: five stacked 2 ps (rms) Gaussian pulse
gun moved close to the cryomodule + capture cavity removed

B - LONGER TERM (toward 6 nm light)

symmetric gun: 40 MV/m
realistic laser five stacked 2 ps (rms) Gaussian pulse
==> compare to (A) better emittance

C - LONGER++ TERM (6 nm light)

symmetric gun: 40 MV/m
realistic laser five stacked 2 ps (rms) Gaussian pulse
install 3.9 GHz RF-section
==> 6 nm User Facility with specs.

D - CONTINUOUS UPGRADE

Design is flexible enough to quickly modify the low energy region depending on what we learn from our Gun Test Facility in DESY-Zeuthen [BERLIN].
==> step-by-step the injector will evolve toward the TESLA X-FEL injector

---

BUT (C) relies on the availability of a 3.9 GHz RF-system. An R&D effort just started within the TESLA coll. to scale the 1.3 GHz TESLA cavity to 3.9 GHz.

==> everybody is welcome to join this effort!

TRANS. BEAM PARAMETERS IN TTF2 INJECTOR

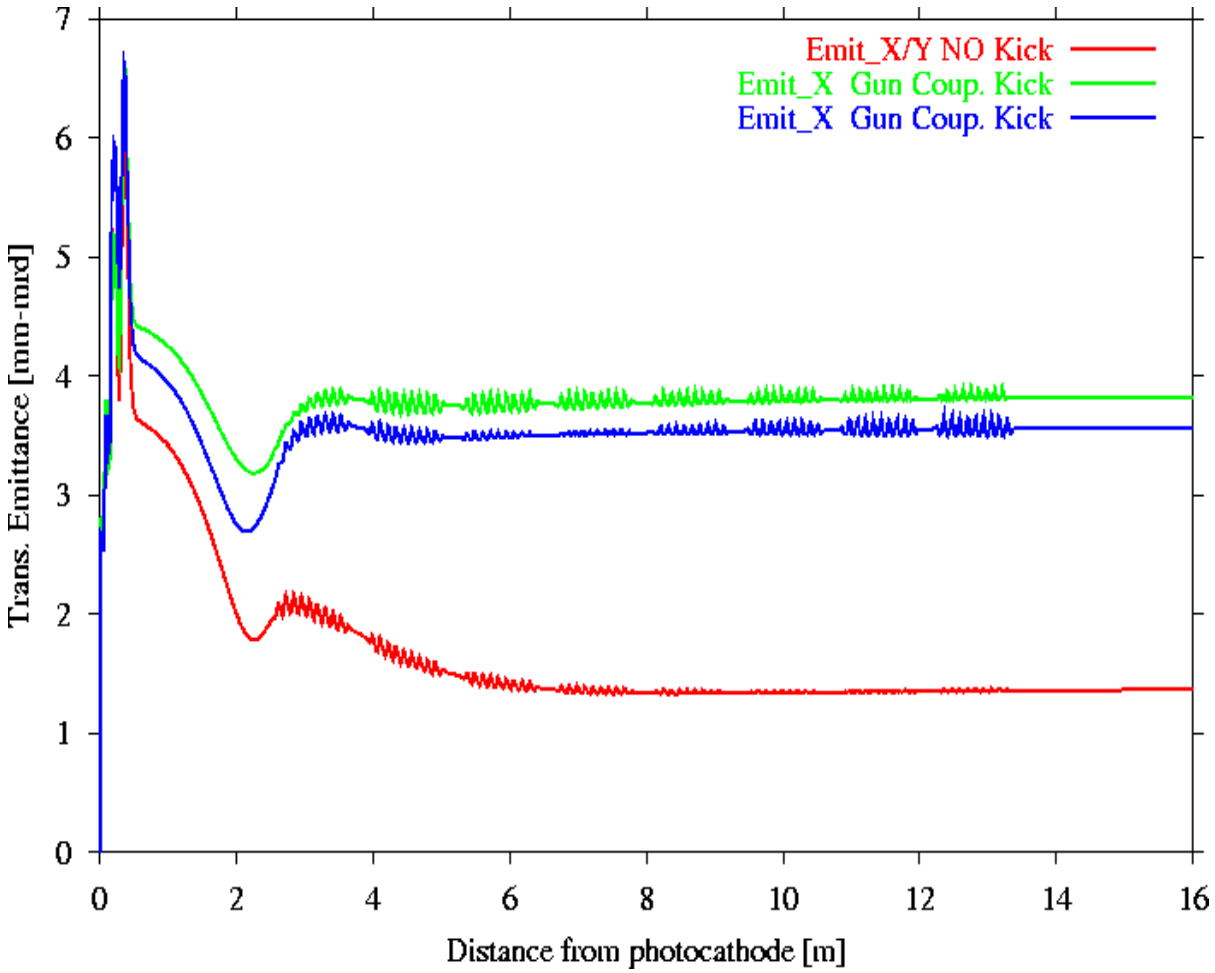

* coupler kick simulated in ASTRA using meas./HFSS simulations from E. Colby (A0, FERMILAB
* long. beam parameters: not a problem to achieve what we want

COMMENTS ON LOW CHARGE OPERATION
(100 pC/BUNCH)

- reduce all the charge dependent effects
- parameter can be achieved

==> BUT **average** power of the FEL decrease....

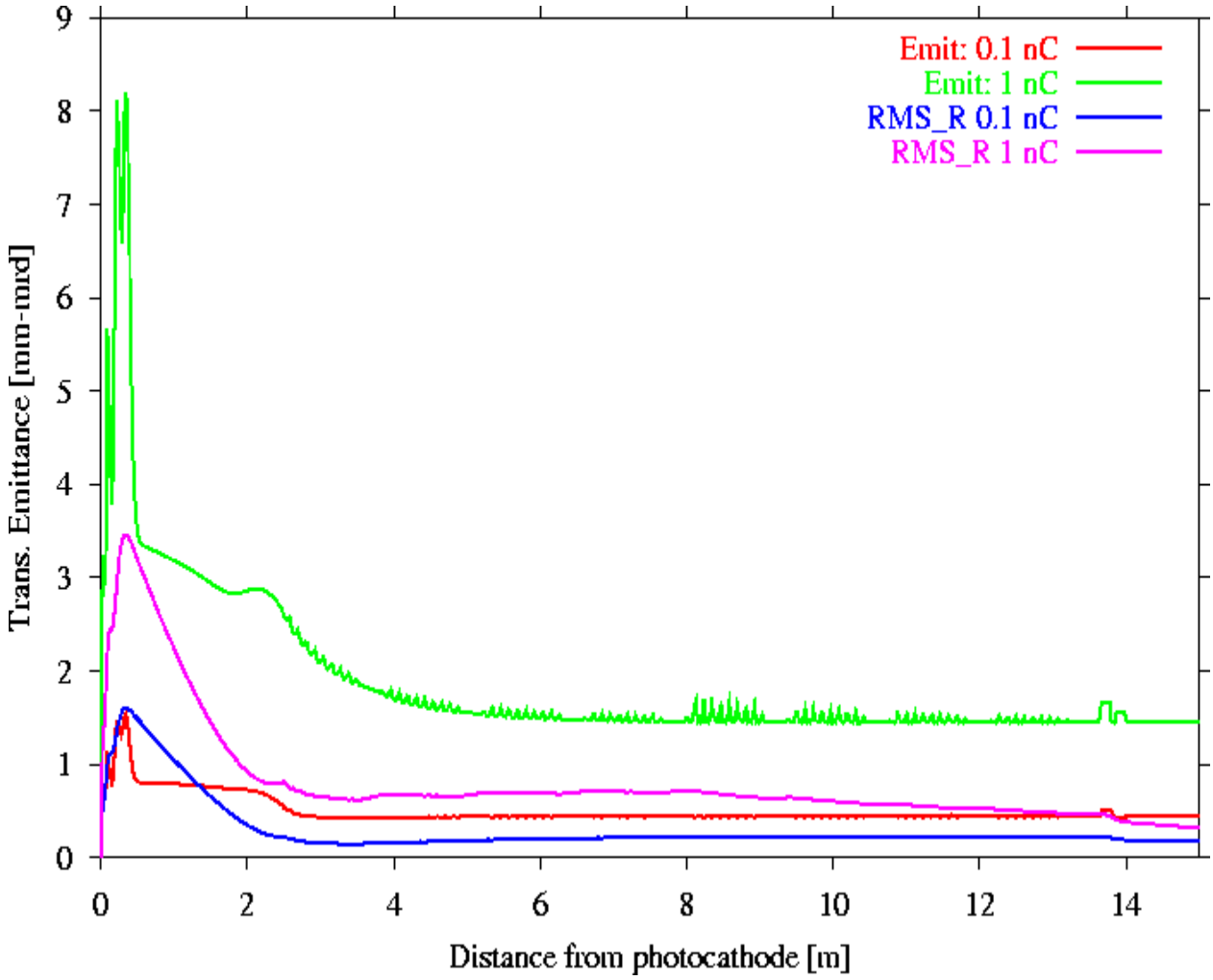

THE PHOTOINJECTOR TEST FACILITY AT DESY ZEUTHEN

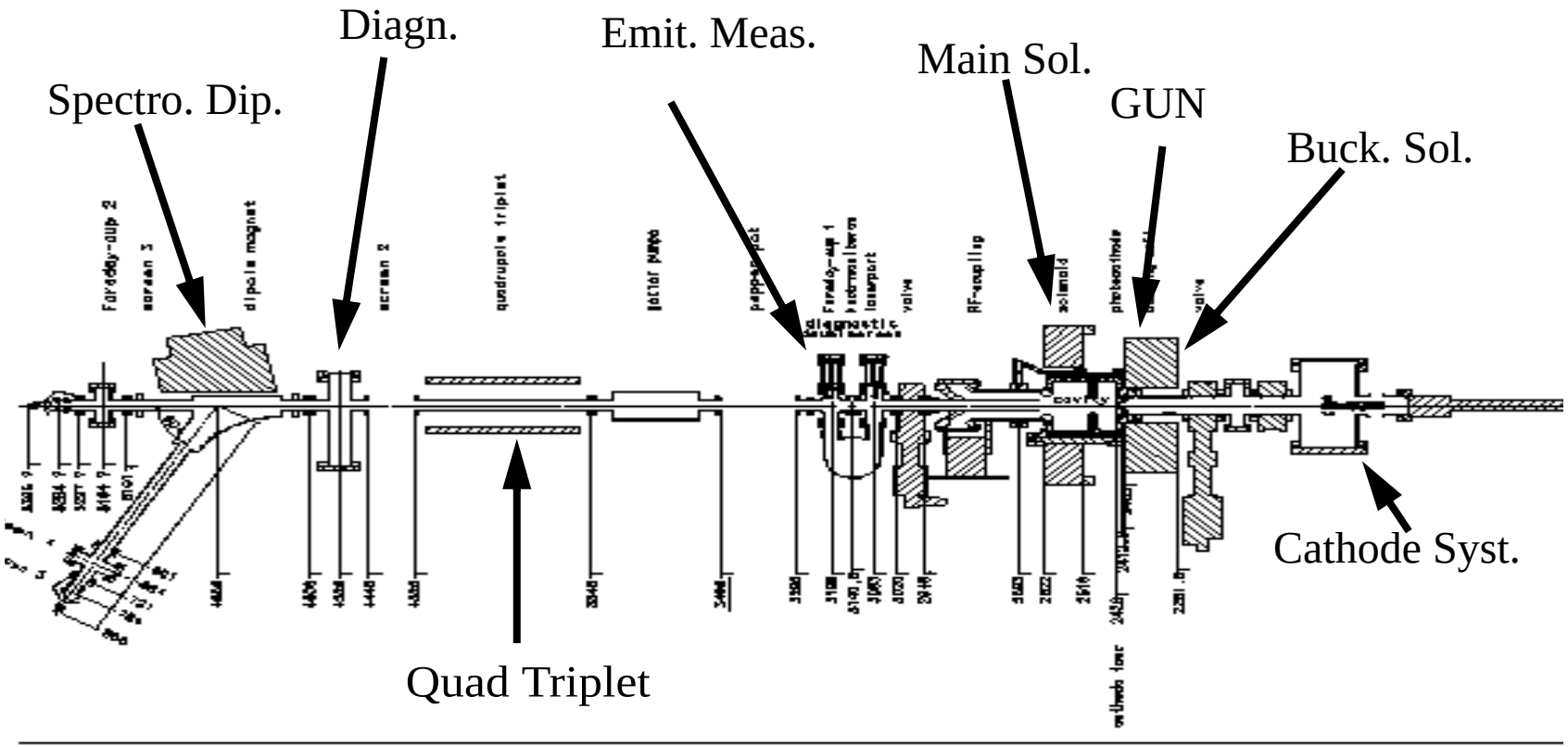

EXPERIMENTAL PROGRAM AT THE PHOTOINJECTOR TEST FACILITY IN ZEUTHEN (NON-EXHAUSTIVE LIST!):

PHASE I: concentrate on generation line (gun +drift)

- test a new laser system from Max Born Institute
- gun characterization (test of new design)
- charge scaling
- benchmark of space charge algorithm
-...

PHASE II: acceleration

- test the new Cut Disk Structure (CDS) [V. Paramonov] design in the context of TESLA positron injector
- demonstrate the emittance damping + matching concept
- generation of flat beam
- und viele mehr!

PHASE III: ???

Ph. Piot, Deutsches Elektronen Synchrotron HH / JAN-2001

CONCLUSION

* Full simulation of injectors systems for TESLA X-FEL, for the TTF II User Facility have been performed. Emittance within specification can be achieved

* In the case of the TESLA X-FEL emittance in the sub-mm-mrd can be achieved downstream of the first stage compression at 142 MeV

* for TESLA X-FEL, full tracking of the generated phase space density using TraFiC4, Elegant thereby including collective effects (CSR, resistive + geometric wake field) results in a transverse emittance of 0.9 mm-mrd (slice) and 2.6 mm-mrd (projected) upstream of the undulator ==> phase space density passed to GENESIS (for simulation of the FEL properties)

* TTF II proposed new injector (by multi-stage upgrade) will be a step toward the TESLA X-FEL injector.

* EXPERIMENTAL SIDE:
--> This summer our Injector Test Facility should produce first e-beam
--> dedicated beam time at Tesla Test Facility:
to perform study of CSR bunch self interaction,
to study the impact of surface roughness on the beam

First order simulations of L-band RF gun for PERL

X.Y. Chang,X. J. Wang and I. Ben-Zvi
Brookhaven Accelerator Test Facility
National Synchrotron Light Source
Brookhaven National Laboratory
Upton, NY 11973, USA

Outline

- Introduction
- First order simulations of L-band RF gun for PERL
- Conclusion and Summary

Introduction

- **Requirements for beam parameters:**

  PERL requires 200 mA, and 0.5 mm-mrad normalized RMS Emittance. 25Mev at linac exit. For 1300Mhz RF gun it needs 150pc per bunch.

- **Why use L-band injector?**

  A. Same as main linac frequency, simplify operation, such as cost, synchronization.

  B. Potential for higher field operation ($\propto\sqrt{f}$) which can reduce space charge effect.

■ Major issues in L-Band RF Gun injector.

A. Field on cathode for a 1.6 cell RF gun:

Field gradient	45 C°	LN_2
50Mv/m	4.5MW	1.1MW
25Mv/m	1.1MW	350KW
15Mv/m	350KW	110KW

A LN_2 cooling method is proposed to improve Q and vacuum, therefore, reduce required power and extend cathode lifetime.

B. Heat dissipation problems:

We can relieve this problem by trying using a bigger size cavity works at higher order mode.

■ Longitudinal phase space ($\propto \varphi^3$):

Our major promise is to make the volume of 6-D phase space minimum at linac exit, Not only the transverse or longitudinal emittance. ($\varepsilon_z \times \varepsilon_x^2$)

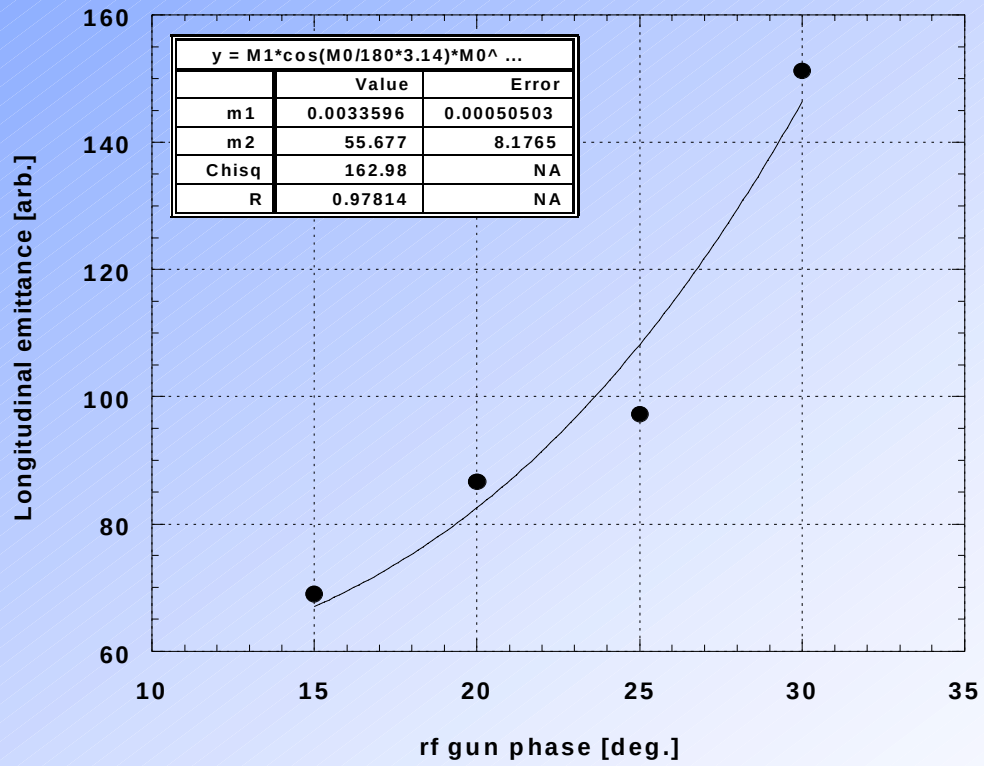

Introduction of ANL gun:

The starting point for our studies is based on ANL gun, which is originally used for high intensity short bunch injector. This saves our time of quickly getting start.

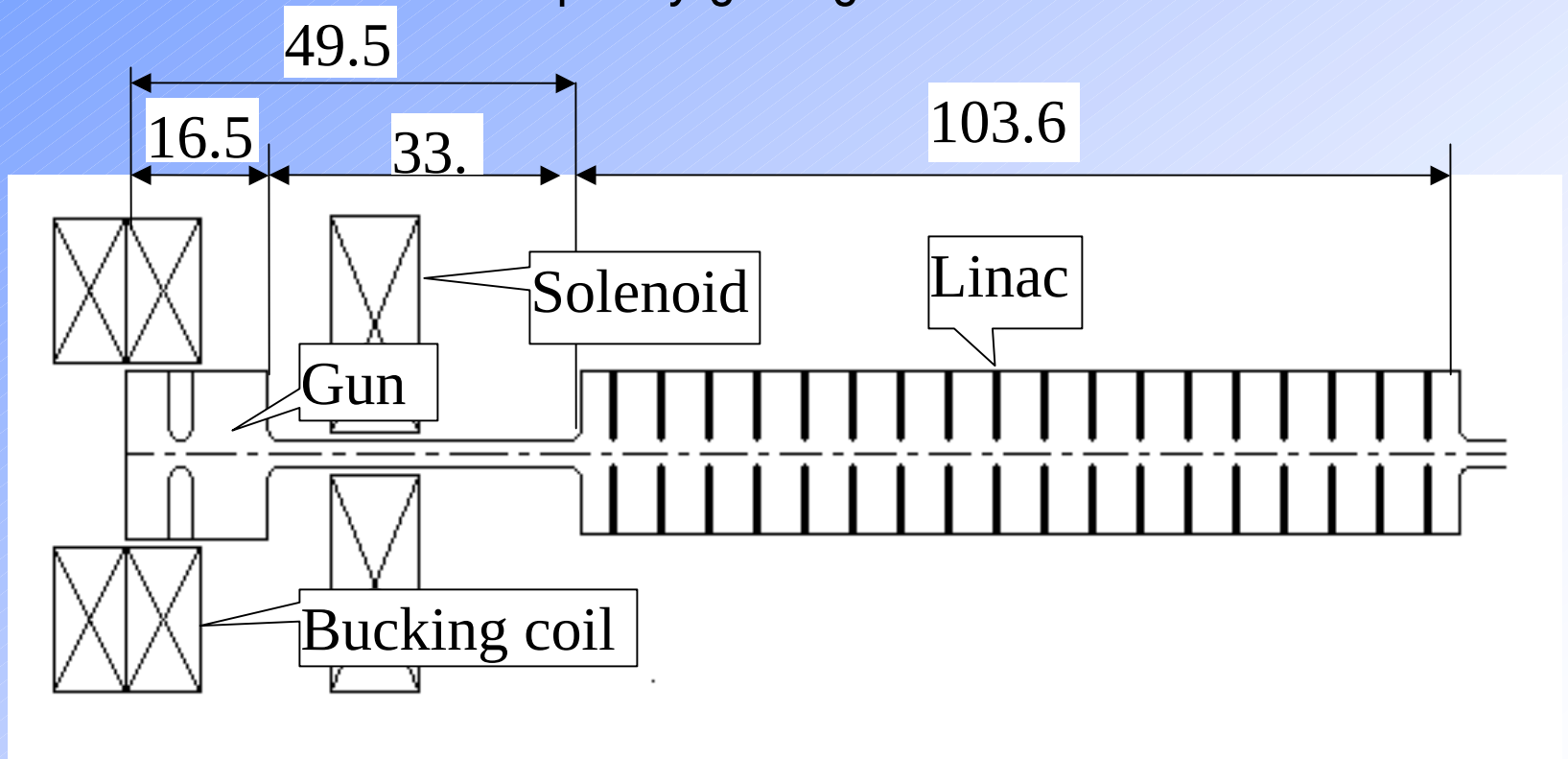

Schematic of L-band RF injector system at ANL(cm)

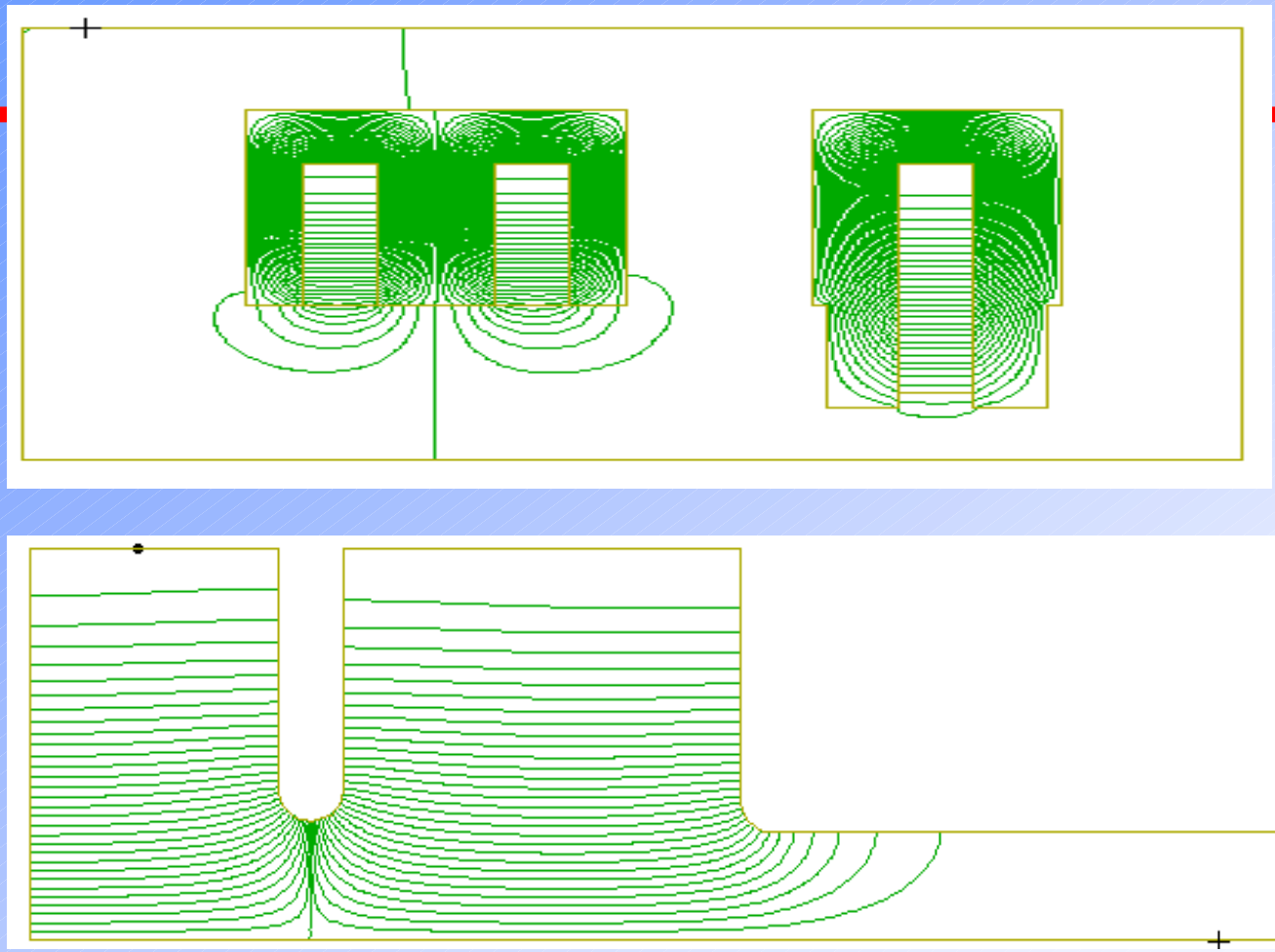

Field distributions of ANL solenoid and 1.5 cell gun

Simulation

- Programs be used:

  POISSON (for solenoids).

  SUPERFISH (Gun, Buncher and accelerating structures)

  PARMELA (for beam dynamics).

- Layout of L-band RF gun injector for PERL

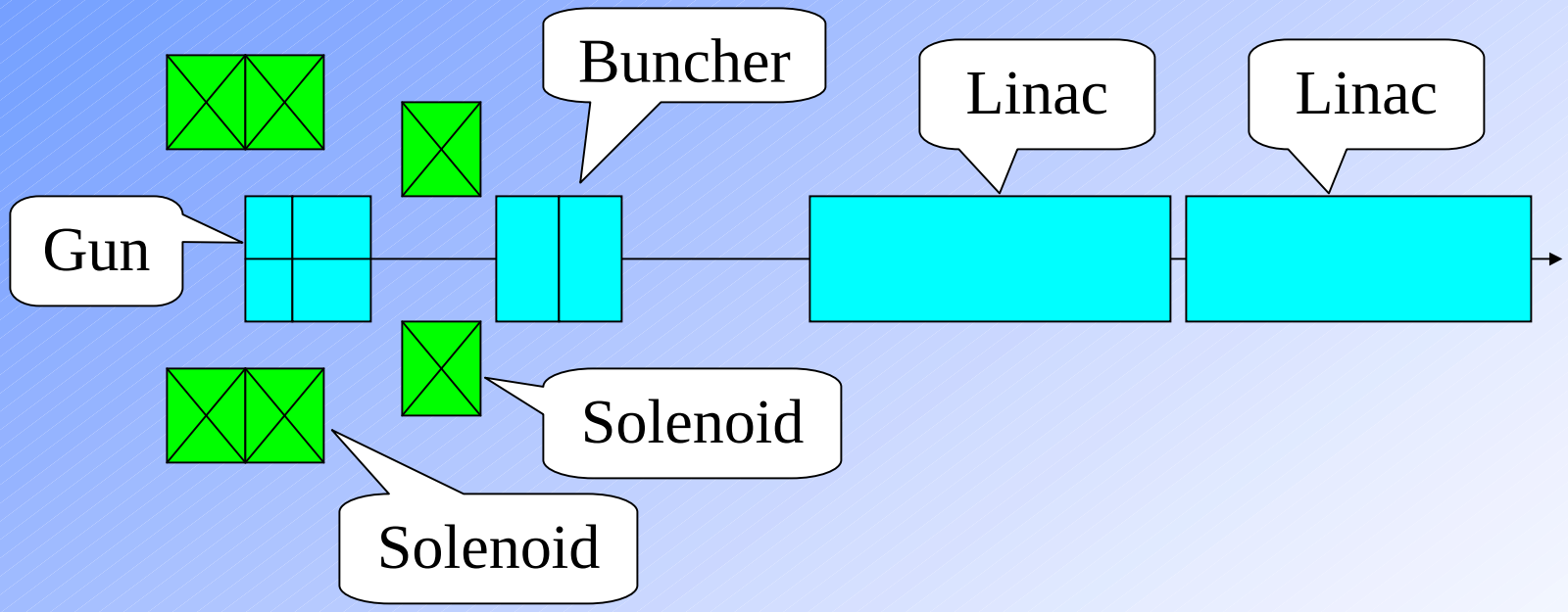

Layout of L-band RF gun injector for PERL

Comparison of 25Mv/m and 15Mv/m fields on cathode.

To minimize the heat problem, we decided to concentrate on 15 MV/m case.

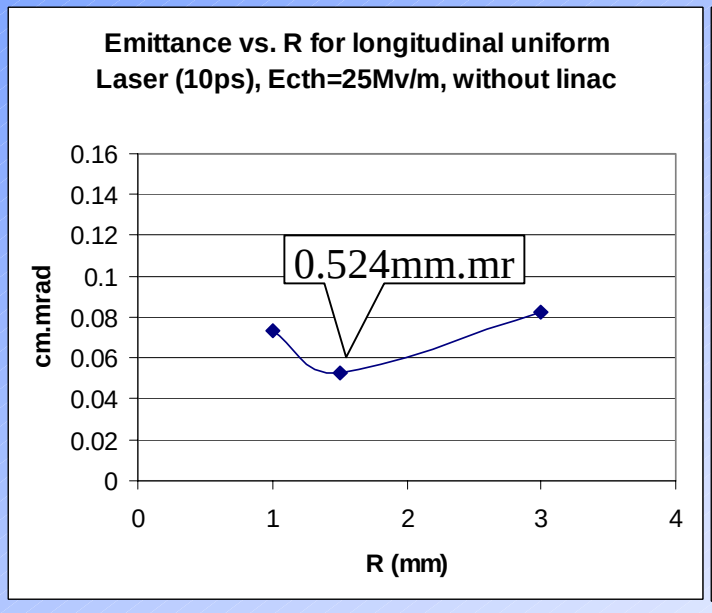

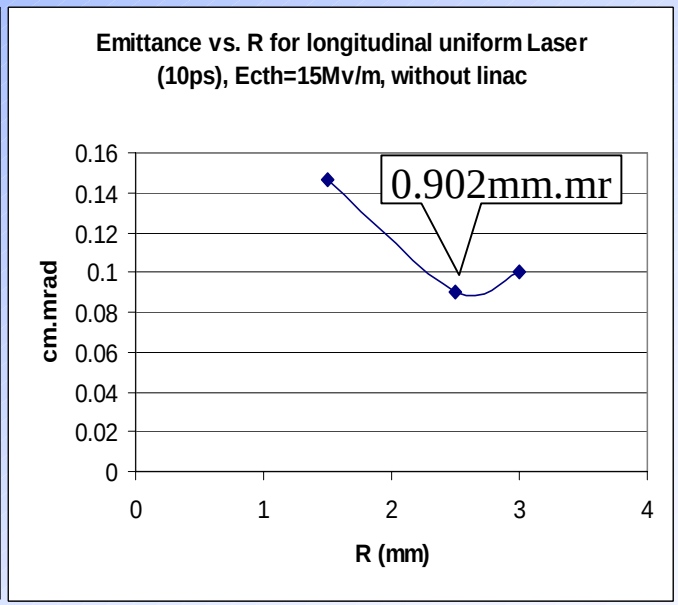

Comparison of 25Mv/m and 15Mv/m fields on cathode

Performance of 15Mv/m field on cathode, no linac. 1.5 gun

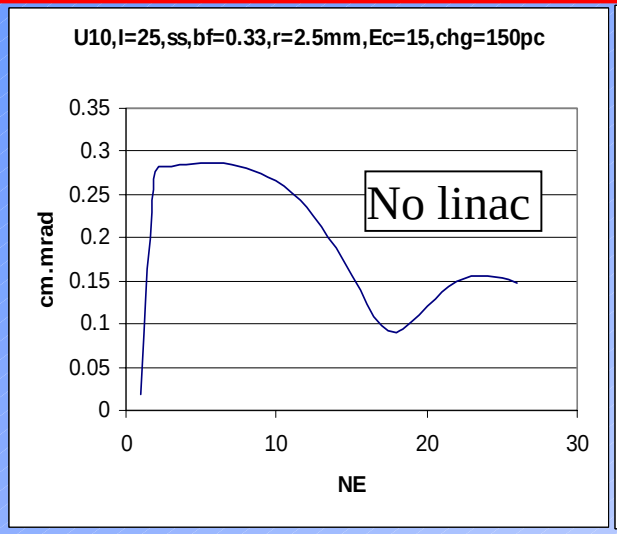

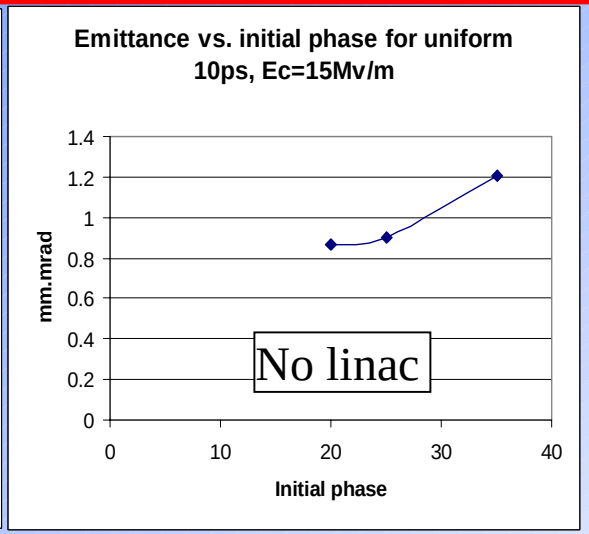

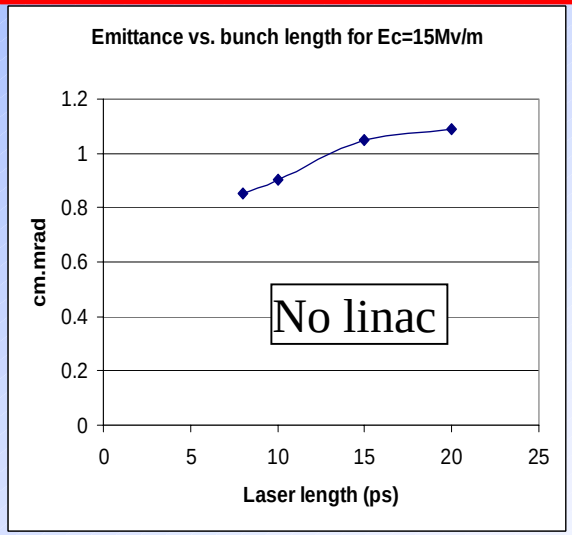

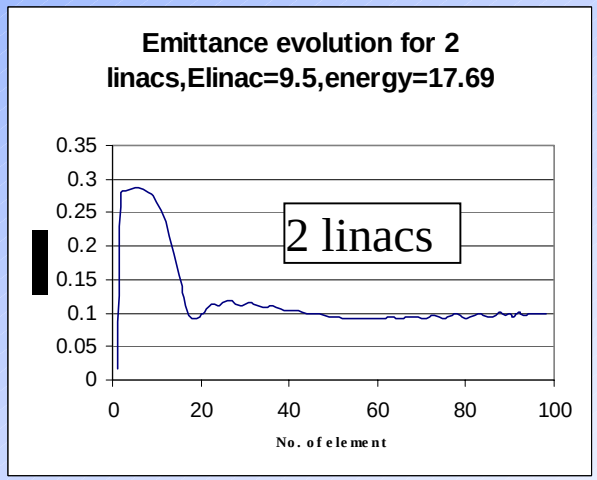

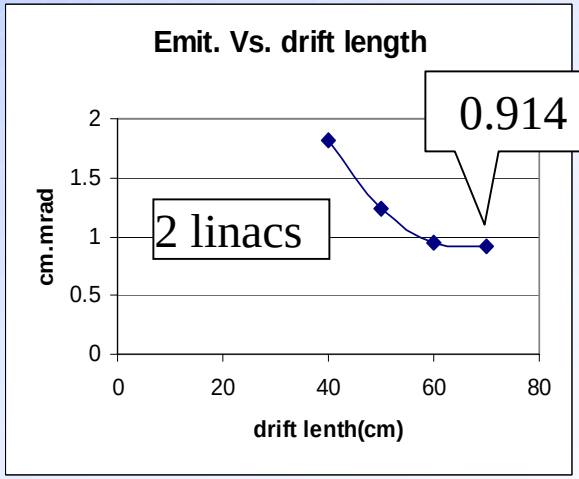

- 2.5 cell gun.

A. Why use 2.5 cell gun ?

For 30 % increase power, to achieve higher energy at gun exit (1.4---2.35 MeV), which leads to significant reduce in space charge effect.

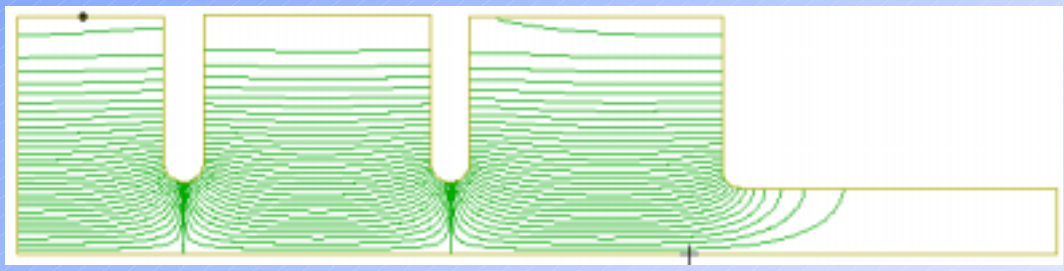

Field distribution for 2.5 cell gun

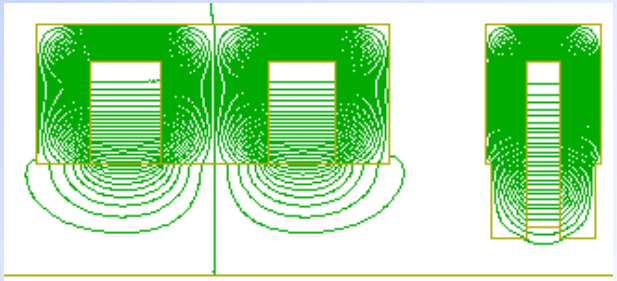

Solenoid for 2.5 gun

Performance of a 2.5 cell gun, no bunching cavity

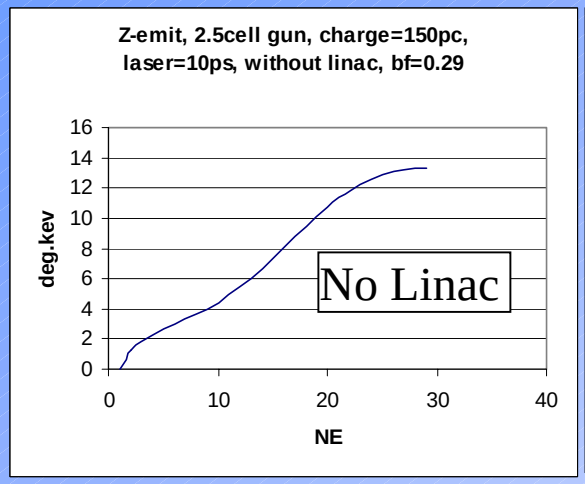

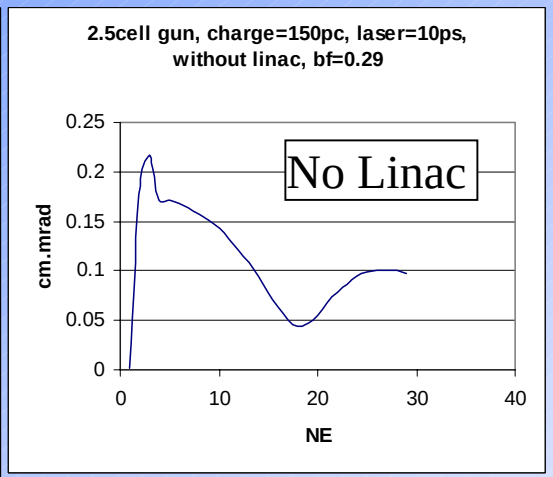

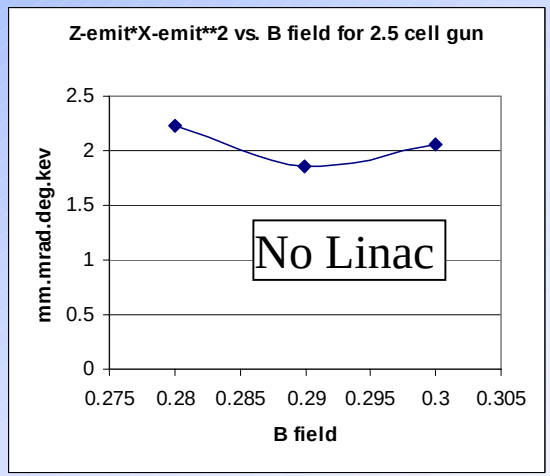

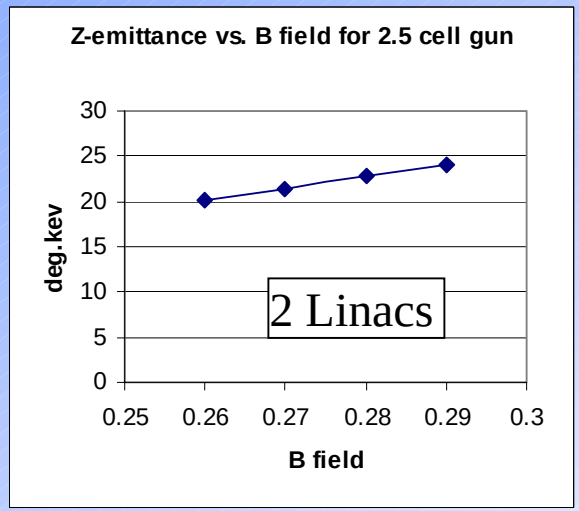

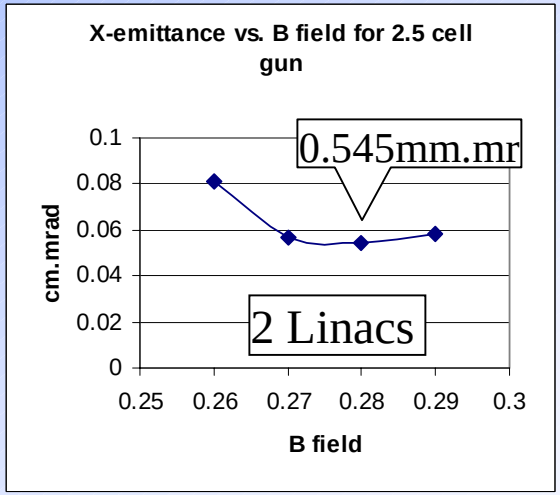

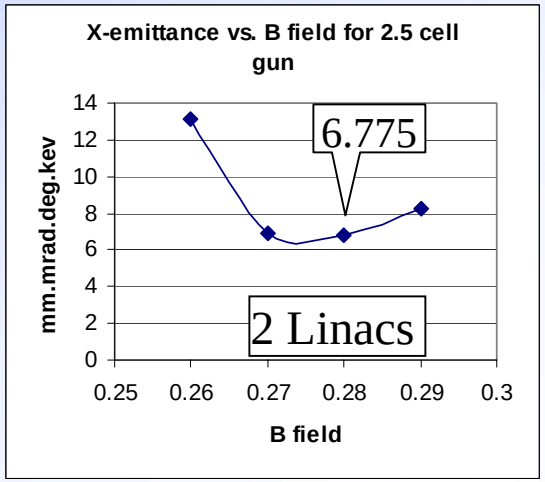

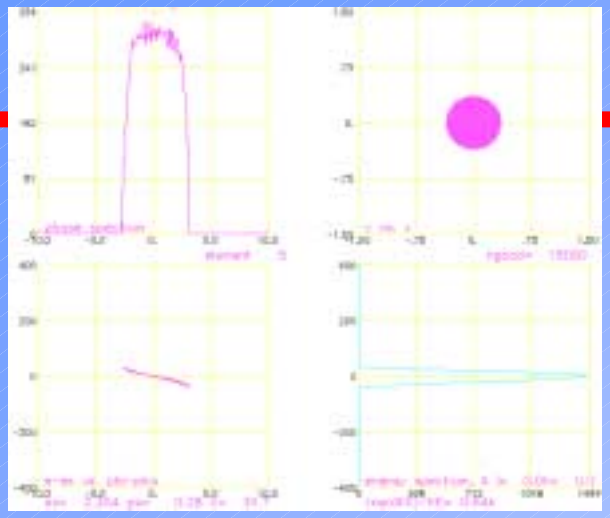

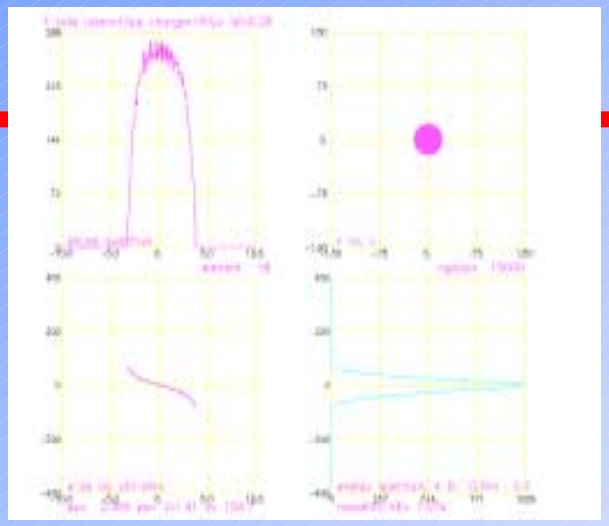

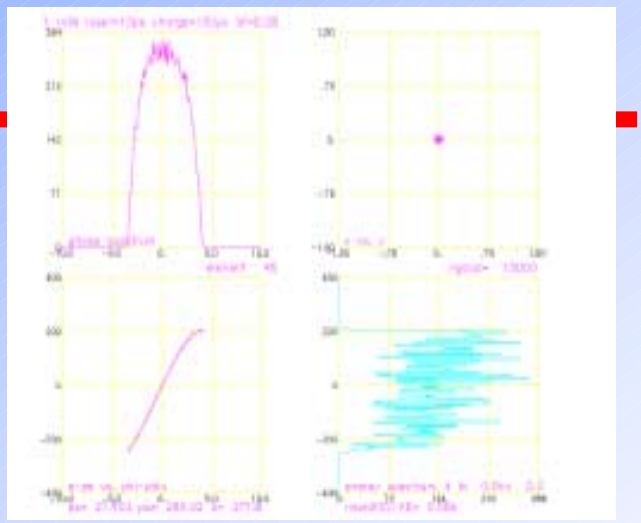

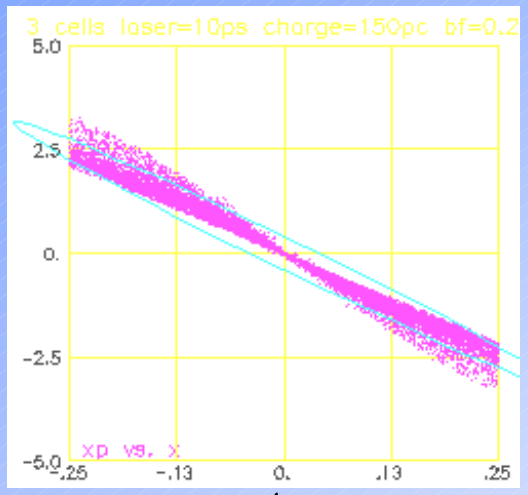

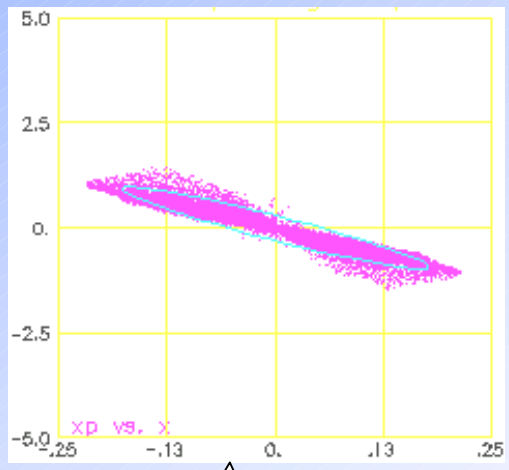

Energy=21.9, RMS(dkE)/kE=0.58%

σ_z = 1.24mm

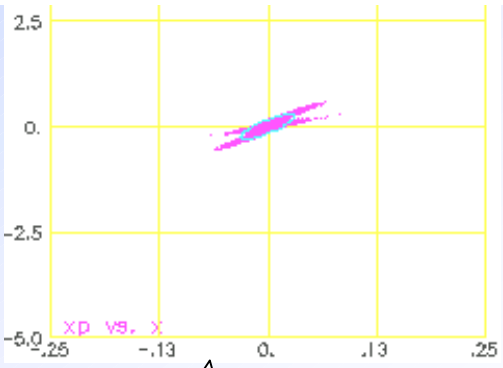

Gun exit

Linac entrance

Linac exit

2.5 cell with bunching cavities.

The bunching cavity is used for the purpose of bunching beam before entering linac. But by using 2.5 cell gun, beam energy is a little bit too high for bunching. In case E=2.35Mev, it needs 3% energy spread and 1m drift space to compress 1mm. So, this way may not be efficient. But it does work.

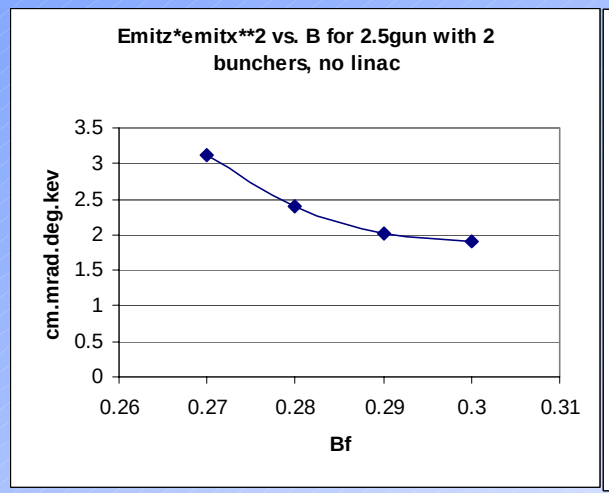

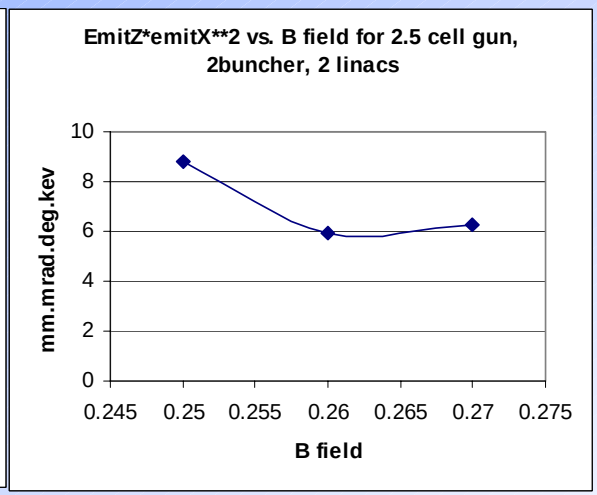

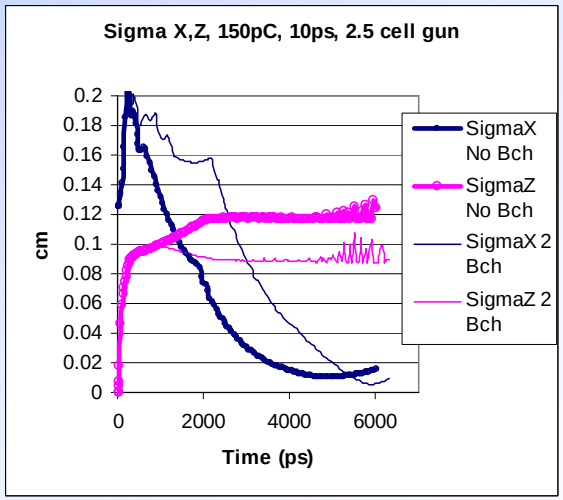

No linac

2 linacs

σ_z and σ_x

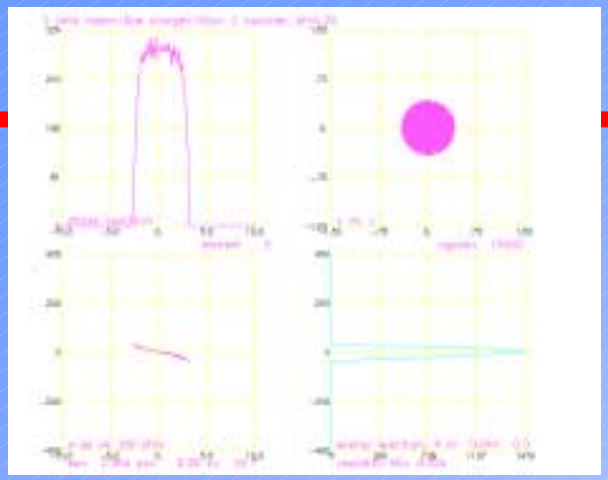

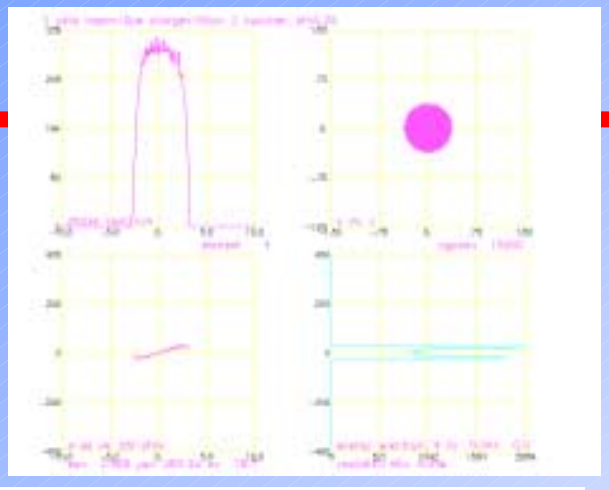

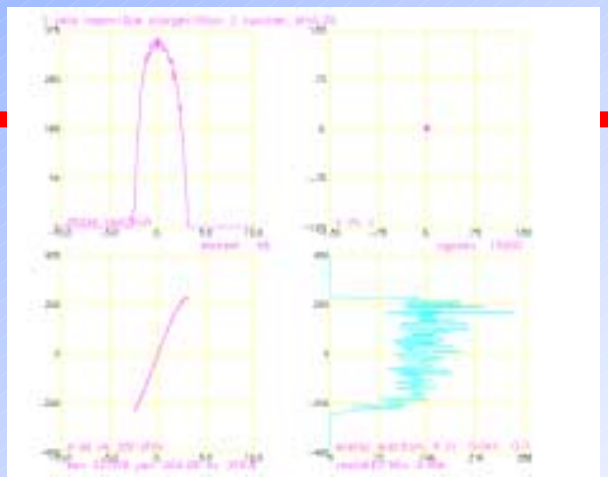

2.5 cell gun, 2 bunchers, 2 linacs

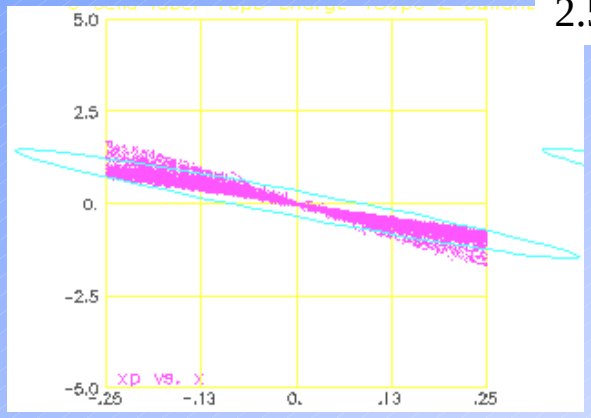

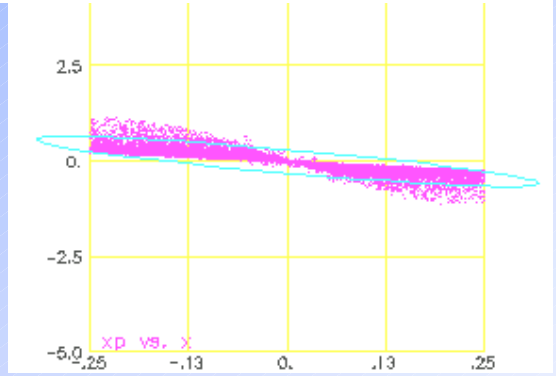

Energy=22.1, RMS(dkE)/kE=0.58%

σ_z = 0.891 mm

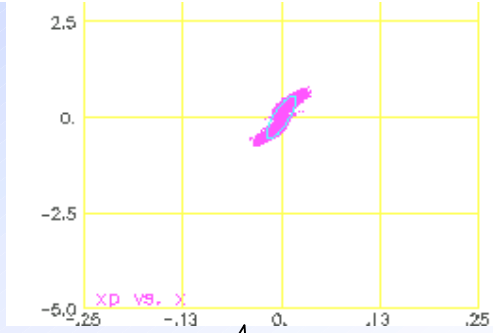

Gun exit

Buncher exit

Linac Exit

■ 75 pC, 7ps, 2.5 cell gun, no bunching cavity

As space charge becomes lower, performance is much better, $\varepsilon_z \times \varepsilon_x^2$ is 1/7 that of 150pc. σ_z = 0.828mm,

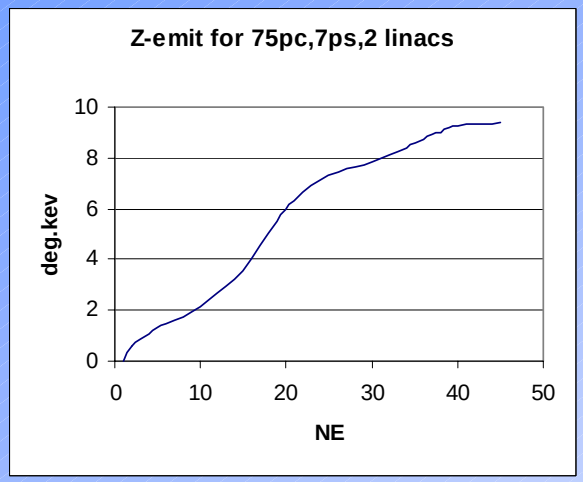

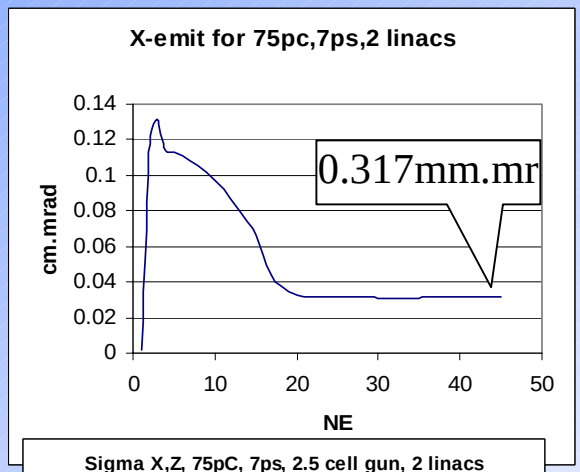

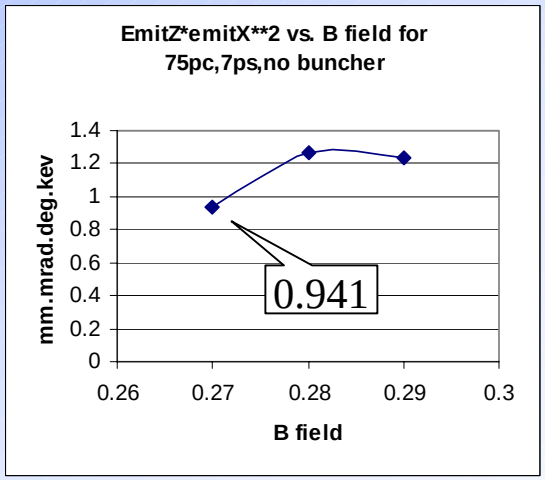

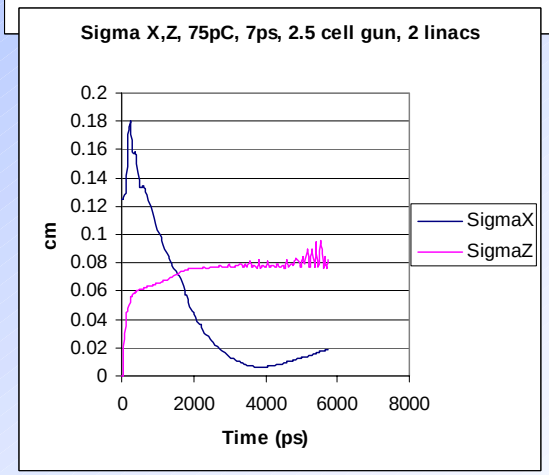

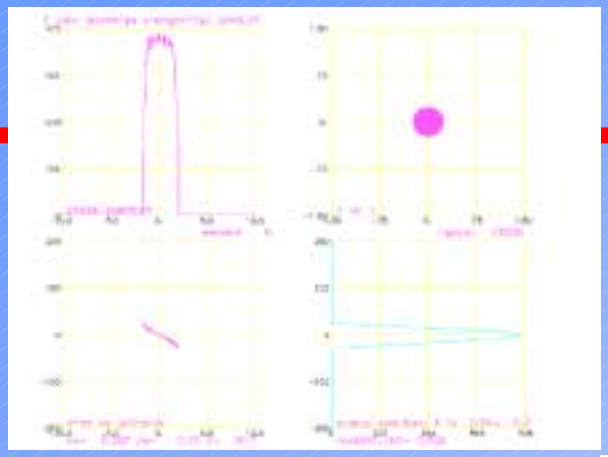

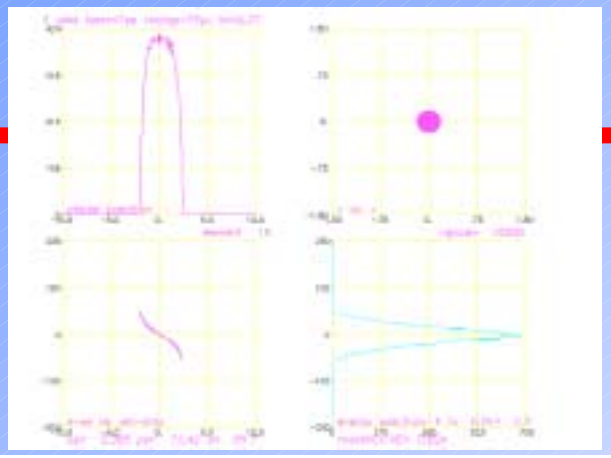

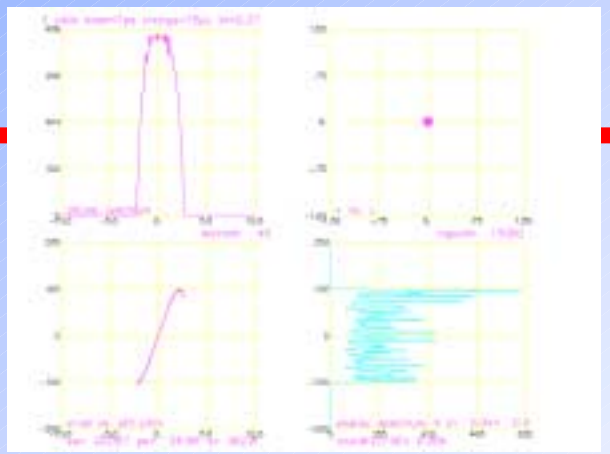

75pc,7ps,2.5 cell gun, 2 linacs

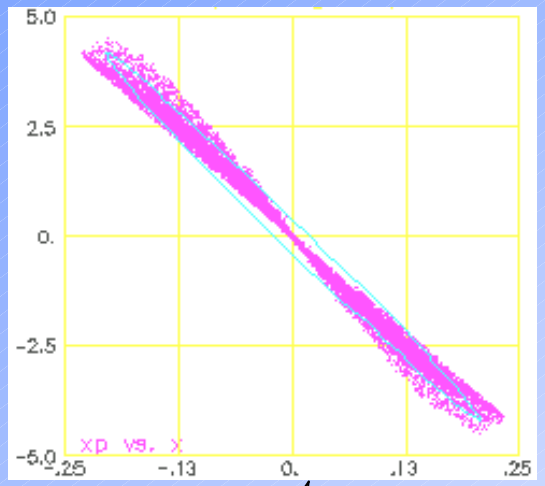

Gun exit

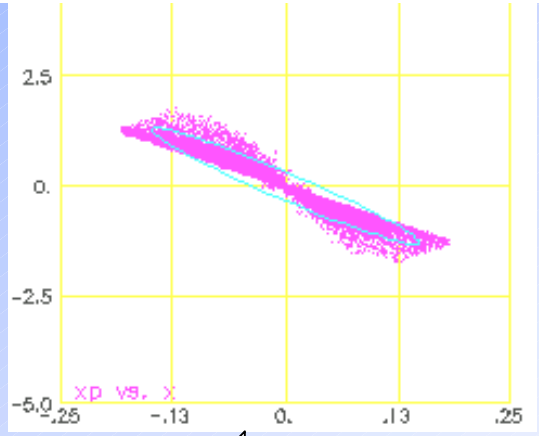

Linac entrance

Energy=22.1, RMS(dkE)/kE=0.28%

σ_z = 0.828mm

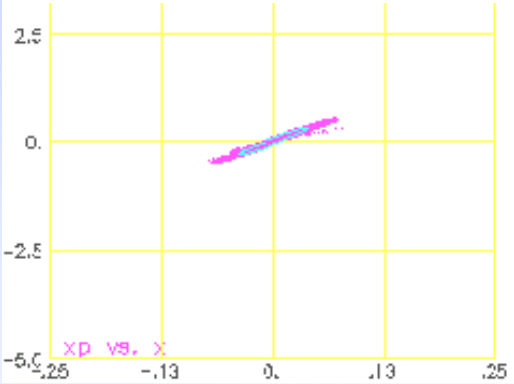

Linac exit

- 75 pC, 7ps, 2.5 cell gun, no bunching cavity, optimization

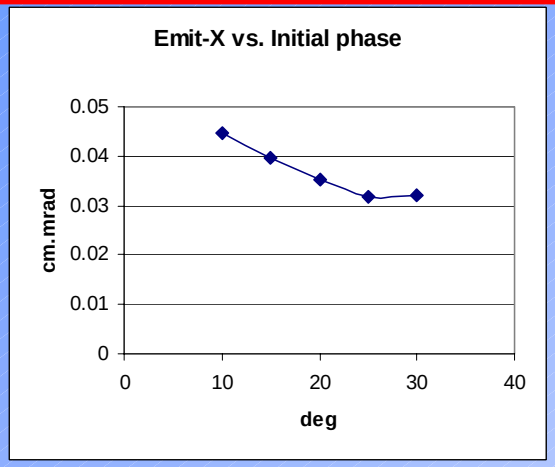

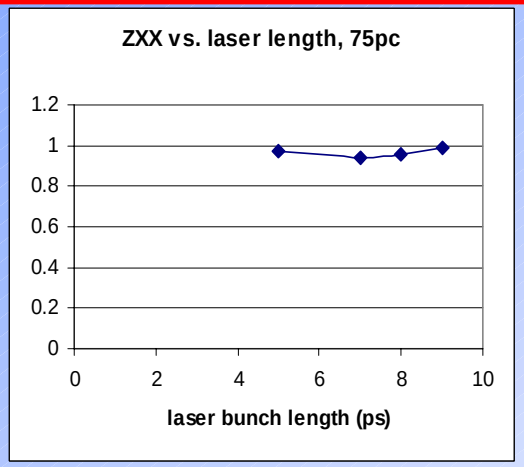

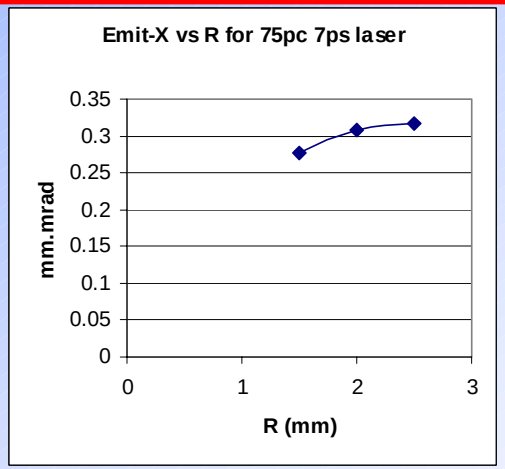

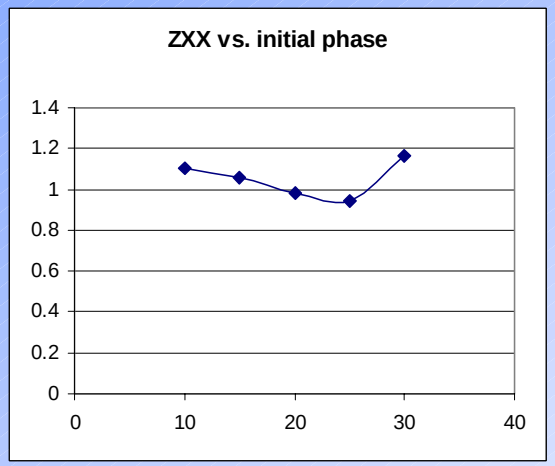

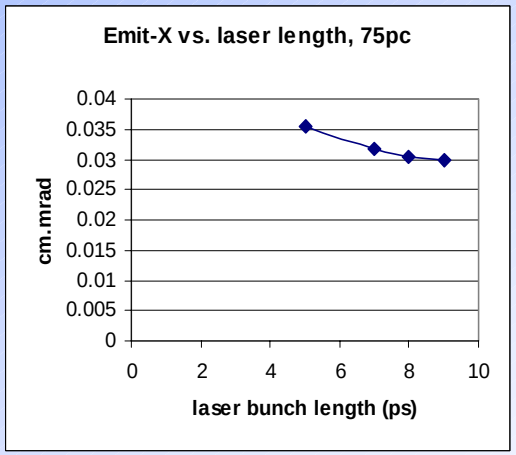

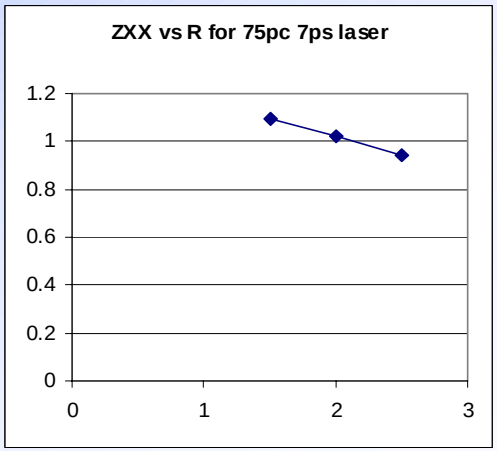

Initial Phase

Bunch Phase

R

75pc, Gaussian, FWHM 7ps, 2.5 cell gun

As the technique of shaping longitudinal laser distribution is difficult, using longitudinal Gaussian distribution can simplify the system and then improve system stability.

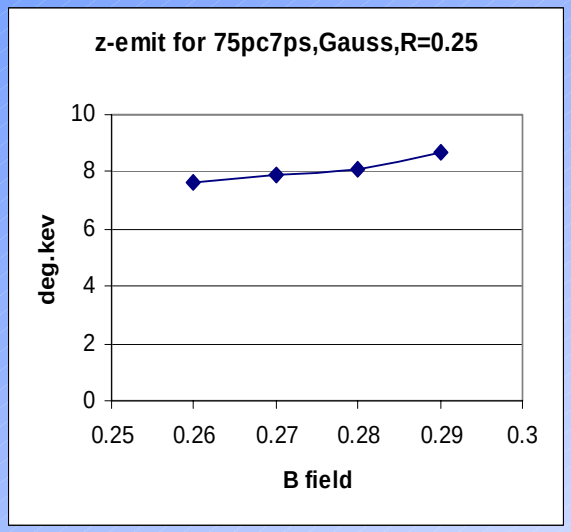

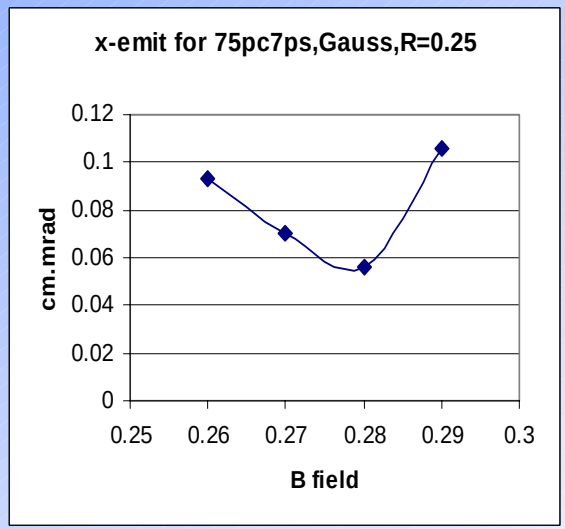

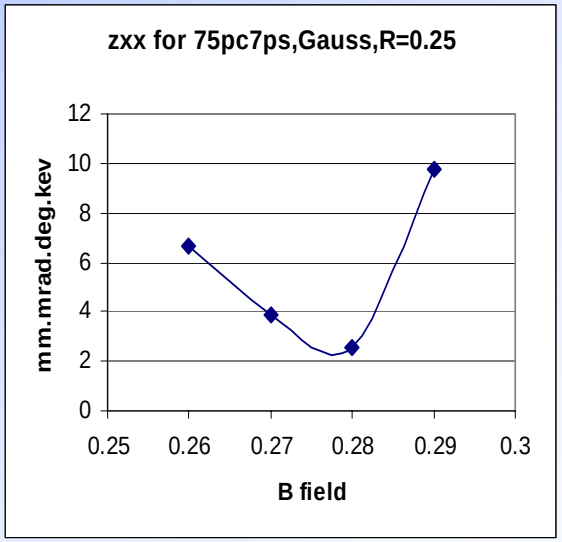

A typical case for 75pc Gaussian distribution

Optimization for 75pc, 7ps, Gaussian.

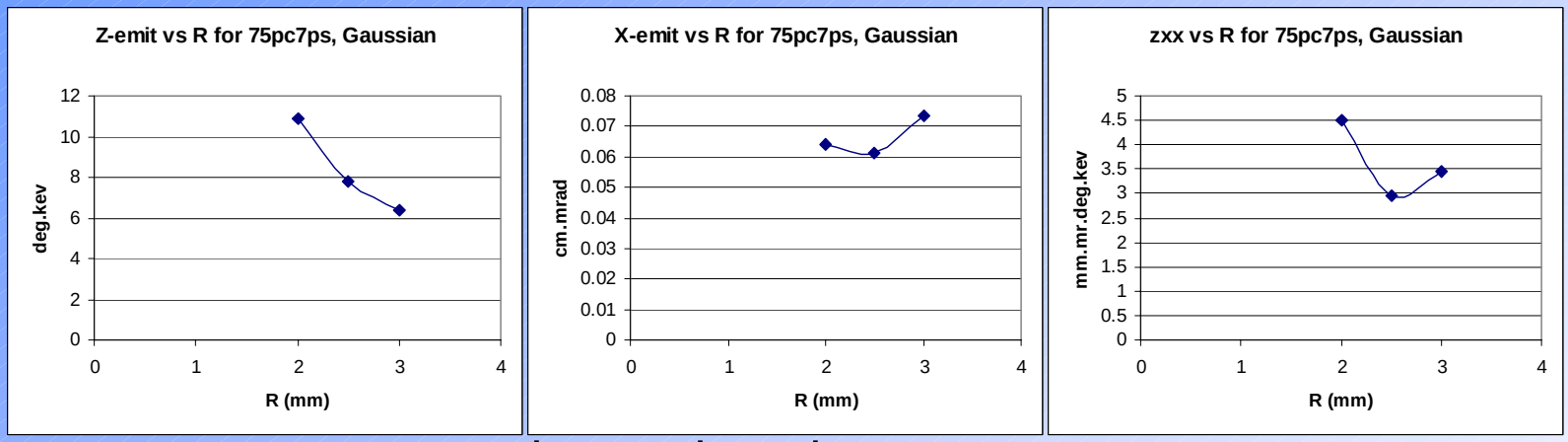

Z-emit,X-emit and ZXX vs. R

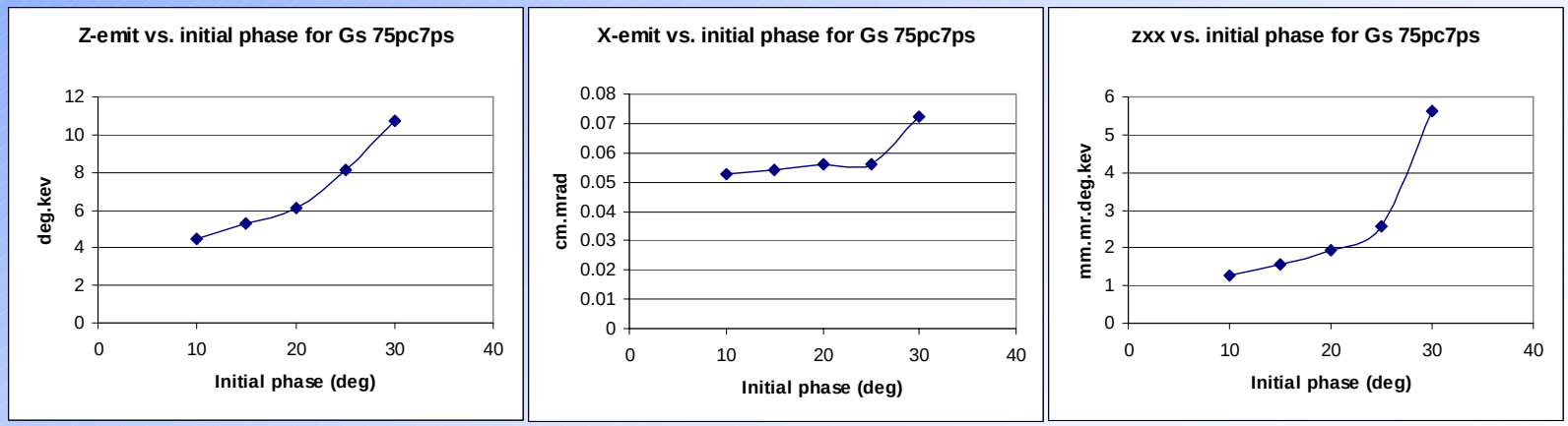

Z-emit,X-emit and ZXX vs. initial phase

- Higher order mode cavity.

By using a gun working at high mode can increase its size. The total power loss on wall increases 60%, but the power dissipation density on wall decreases 60%, which can relieve the heat handling problem. As the field distribution is almost the same as original gun, beam dynamics do not change much. The problem is it will be difficult to apply enough solenoid field in gun because the diameter becomes larger.

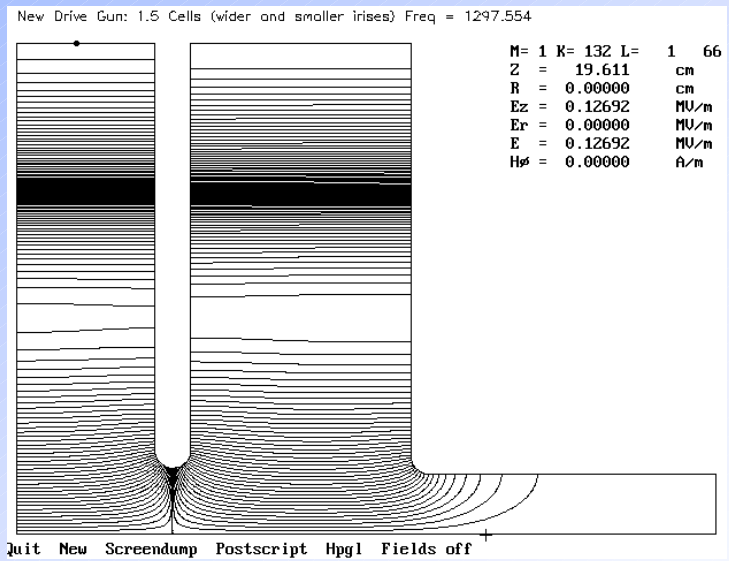

Conclusion and Summary

- **L-band photocathode RF gun is capable of producing PERL quality beam.**
- A 1.5 cell L-band with 25Mv/m can produce beam required by PERL.
- 2.5 cell gun is better than 1.5 cell gun. Assume the electric field on cathode we can achieved is 15Mv/m, by using the 2.5 cell gun, for charge =150pC, we can reach at least the following beam performance at linac exit:

  $Energy=21.9Mev,\ RMS(dkE)/kE=0.58\%,\ \sigma_z=1.24mm,$
  $\varepsilon_z=22.8deg.kev,\ \varepsilon_x=0.545mm.mrad,$
  $\varepsilon_z\times\varepsilon_x^2=6.775mm^2.mrad^2.deg.kev.$
- *For a 75pC charge, the performance is improved greatly.*
  $Energy=22.1Mev,\ RMS(dkE)/kE=0.28\%,\ \sigma_z=0.828mm,$
  $\varepsilon_z=9.364deg.kev,\ \varepsilon_x=0.317mm.mrad,$
  $\varepsilon_z\times\varepsilon_x^2=0.941mm^2.mrad^2.deg.kev.$
- To simplify the system and improve its stability performance, longitudinal Gaussian distribution laser is considered. We found that the lower the initial phase, the better the performance. When ϕ_l=10deg, $\sigma_z=0.673mm$
  $\varepsilon_z=4.464deg.kev,\ \varepsilon_x=0.529mm.mrad,$
  $\varepsilon_z\times\varepsilon_x^2=1.249mm^2.mrad^2.deg.kev.$

Conclusion and Summary

- Using higher mode cavity RF gun can reduce the power density on the gun cavity wall. More geometric optimization could lead to power reduction 10%.
- More studies need to be done, such as:

  A. Performance of higher order mode gun.

  B. Study the possibility of shaping the cathode to increase RF focusing near cathode.

  C. Parameter optimization.

  D. Thermal stress and heat flow calculation are needed

We would like to express our gratitude to Dr W. Gai and M. Conde for providing their gun input files.

Beam Dynamics Issues at PERL Injector

X.J. Wang
National Synchrotron Light Source

1. *Introduction.*
2. *Beam dynamics Major issues at PERL injector*

A. Space charge effect.

B. Longitudinal phase space.

C. Transverse phase space bifurcation.

D. Nonlinear longitudinal phase compensation.

E. Linear space charge compensation.

3. Summary

Introduction

The advantage of PERL over traditional light source is that, small transverse emittance couple with small longitudinal emittance. All beam dynamics issues addressed by Vitaly also exist in PERL injector, such as Wake field, BBU, but other issues even more important at injector:

1. Space charge effect.
2. Transverse phase space bifuracation caused by space charge effects.
3. Longitudinal phase.
4. Non-linearity in compensation in compressor by wake field or space charge effect.

Space charge effect

$$x''+k\ (s)x-\frac{2r_eN/\ell}{a^2\gamma^3}x=0$$

$$z'=\frac{\delta}{\gamma^2}$$

$$\delta'=\frac{3r_0N}{\gamma^3\beta^2{\ell_b}^3}\ f(a,b)z$$

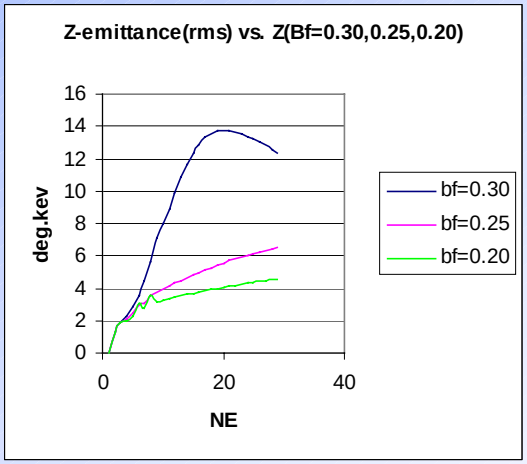

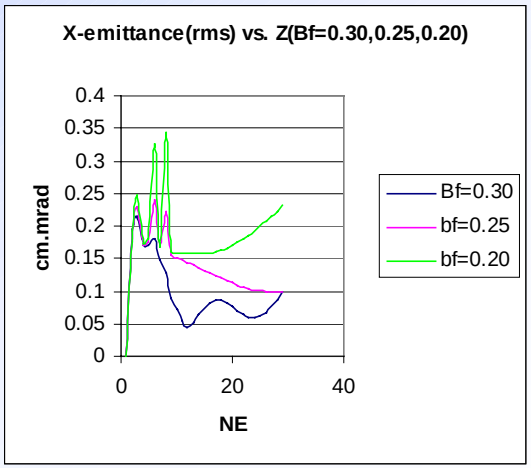

Energy is the most effective reduce space charge effect, asymmetry in transverse and longitudinal space charge effect must be kept in mind all time for PERL.

Transverse phase bifurcation

Studies were done at Jlab to understand transverse Phase Bifurcation due to space charge. We now observed at L-band injector studies. This could be important if beam will lost in later stage. We need to look into several solution on this problem:

1. Beam scrapper.
2. Reduce charge.
3. Modify the longitudinal beam distribution.

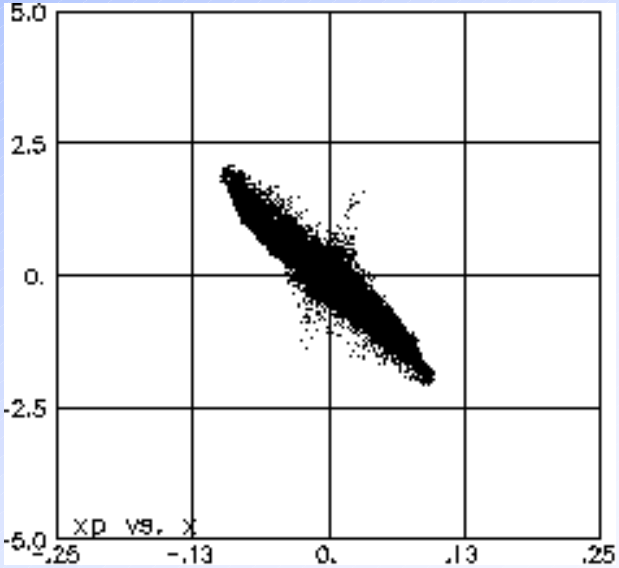

Longitudinal phase space compensation

H. Liu, NIM A (1997)

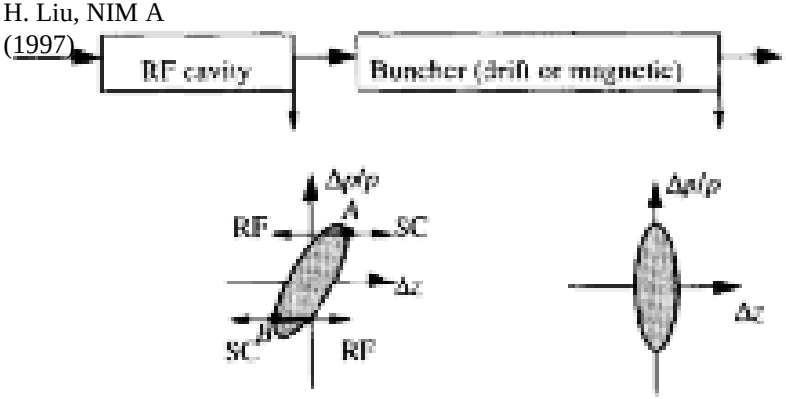

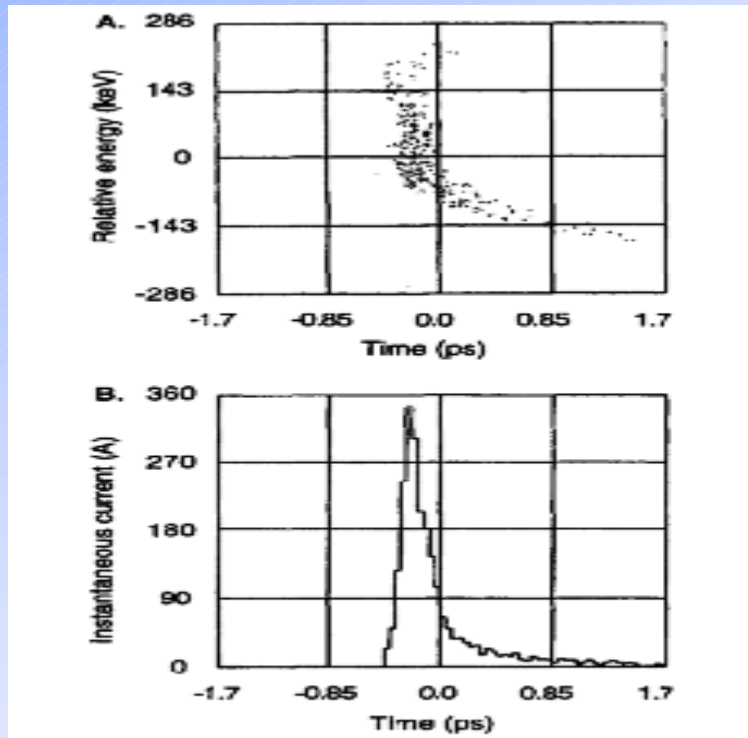

Fig. 5. PARMELA simulation results for a 0.1-nC bunch after compression to a FWHM of 0.22 ps. (a) Longitudinal phase space, showing residual quadratic curvature. (b) Instantaneous current profile.

B. Carlsten, NIM A (1996)

Longitudinal Emittance Compensation

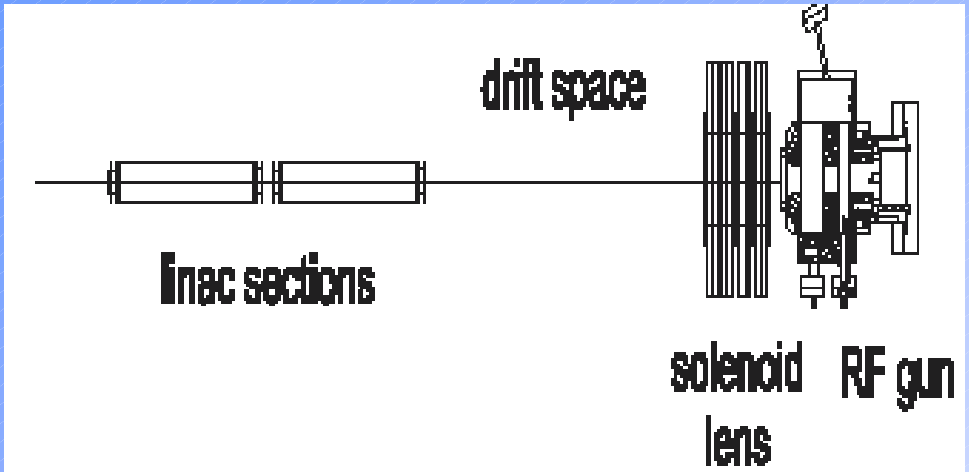

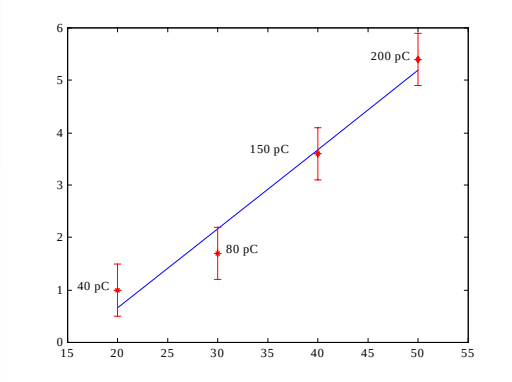

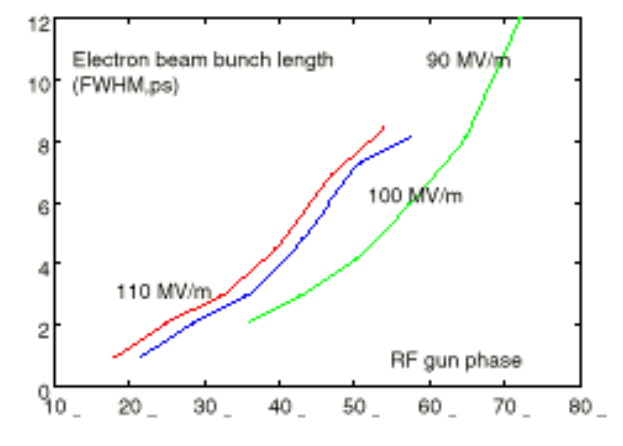

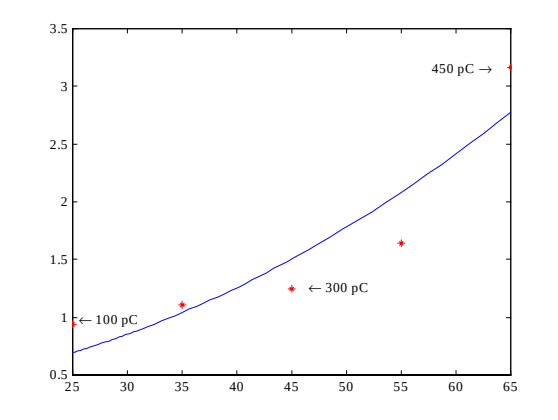

X.J. Wang et al, Phys Rev. E and PAC 97

RF Longitudinal Emittance

$$\varepsilon_z \propto \varphi^3$$

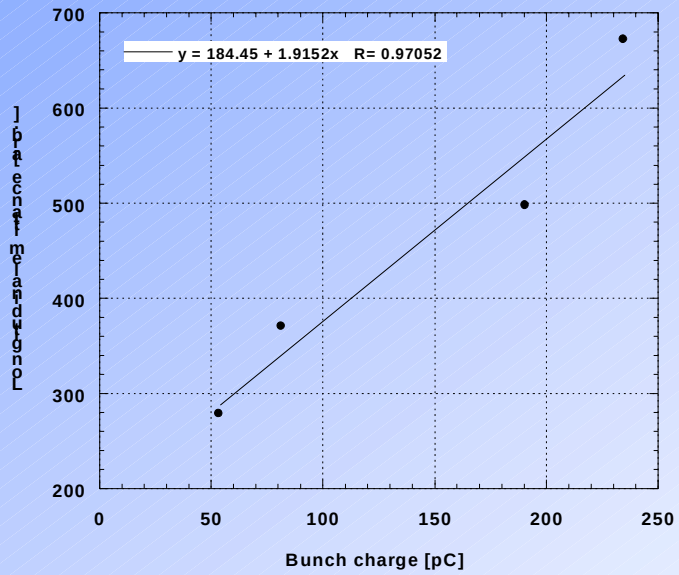

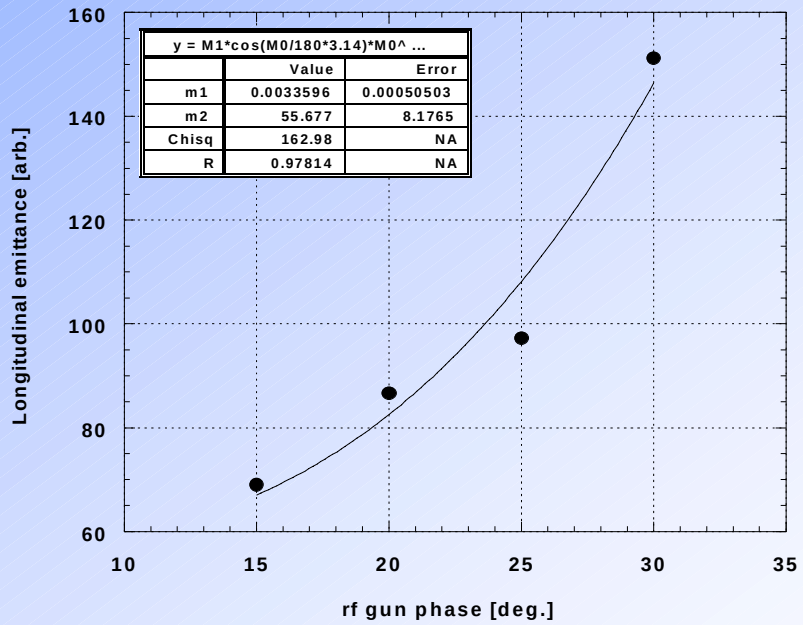

Linac 2000

Beam Instrumentation Consideration for PERL Injector
X.J. Wang

- *Introduction.*
- *Instrumentation consideration:*
  1. *Laser and optical system.*
  2. *Gun diagnostics.*
  3. *Boost linac.*
  4. *Beam characterization at 25 MeV.*
- *Issues and Summary*

Introduction

- Charge per bunch: 0.15 nC or 0.45 nC
- High rep rate: 1300 or 433 MHz *(200 mA)*
- Normalized RMS emittance: ~1 mm-mrad
- Longitudinal RMS emittance: 3 ps * 23.2 KeV @ 25 MeV
- *Uptime: 24 hrs/day, 25 days/month, 11 months/yea (Stability and reliability)*

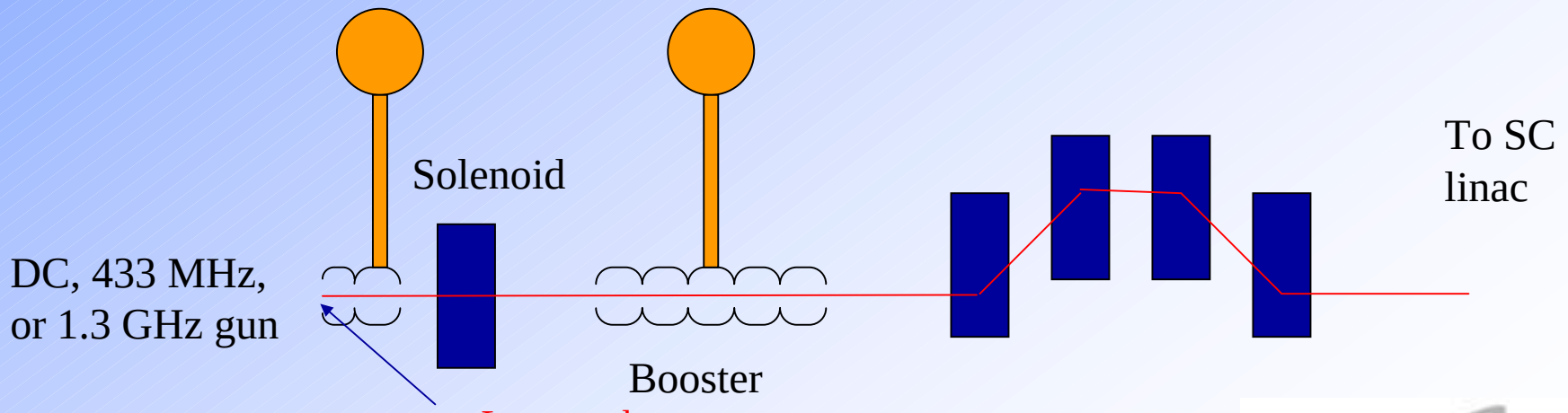

Introduction - continue

For high average current beams, identify methods to measure:

- Vertical and horizontal emittance.
- Energy and energy spread.
- Bunch length.
- Charge.
- Peak and average current.
- Bunch-to-bunch timing jitter.

Identify feedback systems required for laser and RF.

Special beam instrumentation issues for PERL injector:

- Laser and its transport optics.
- High average power.
- Safety interlock – loss monitoring.
- Beam characterization in 6-D.
- Space charge and relative low energy.
- Jitter – timing and position

PERL Injector instrumentation - Laser

Laser energy.

Profile and position.

Timing jitter

Cathode –QE and Uniformity

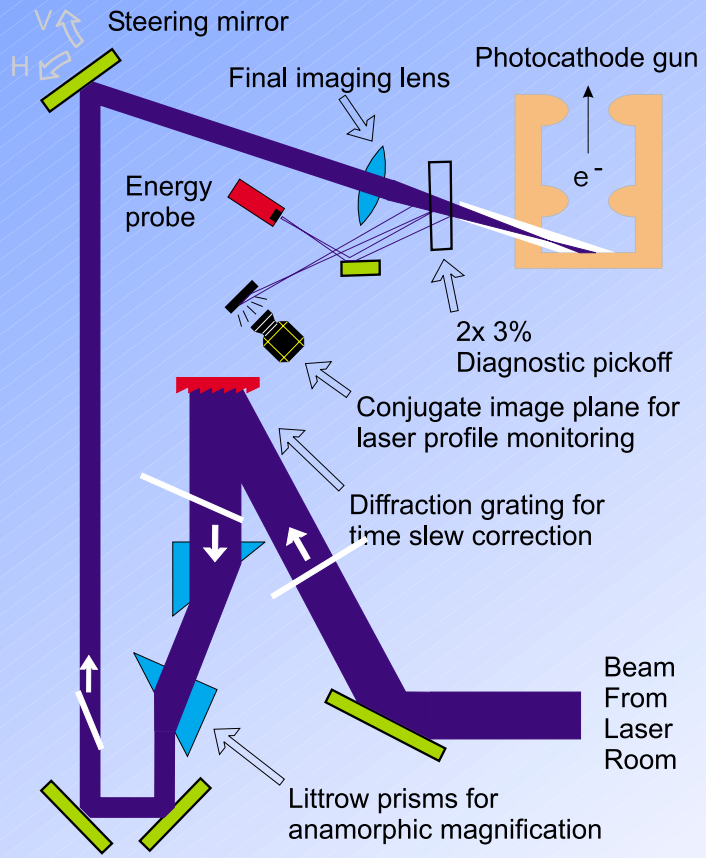

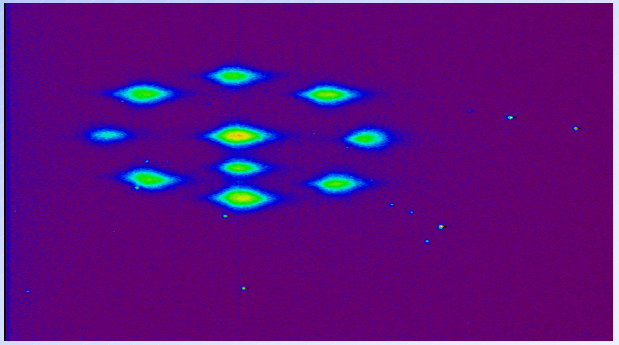

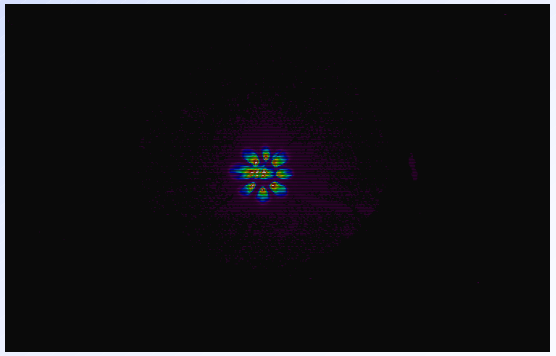

Special equipment: Streak Camera or gated CCD Camera.

PERL Injector instrumentation – ATF Laser

BNL ATF is the only multi-user facility based on the photocathode RF gun injector, it has demonstrated:

1. Good beam quality for users.
2. Delivery more 1000 year each year in the last two years.

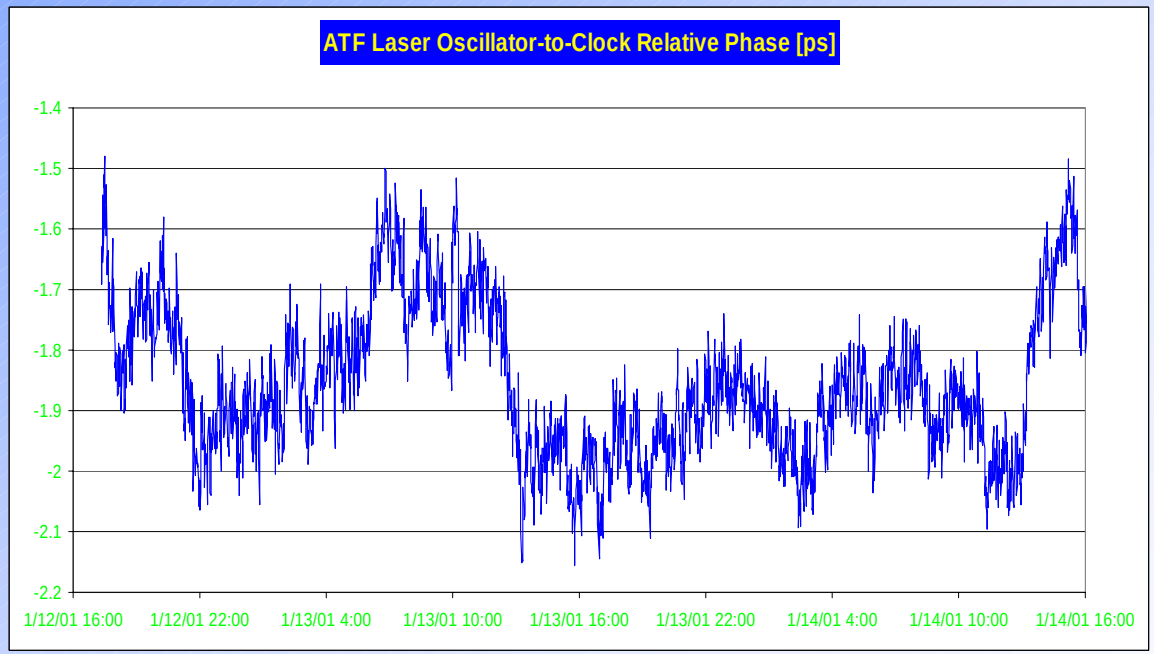

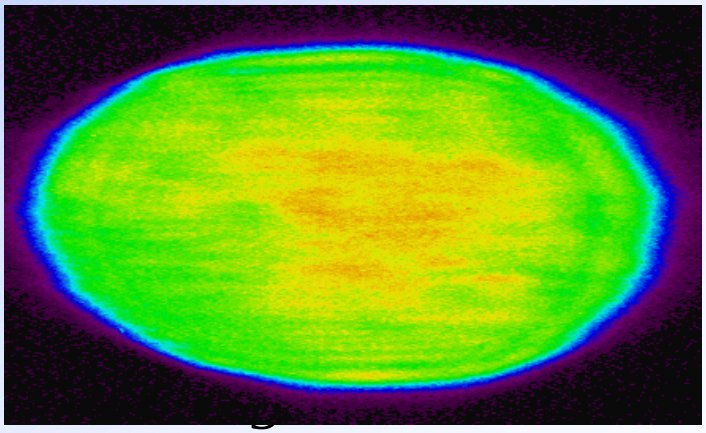

PERL Injector instrumentation - Gun

Charge.

Energy

RF gun phase

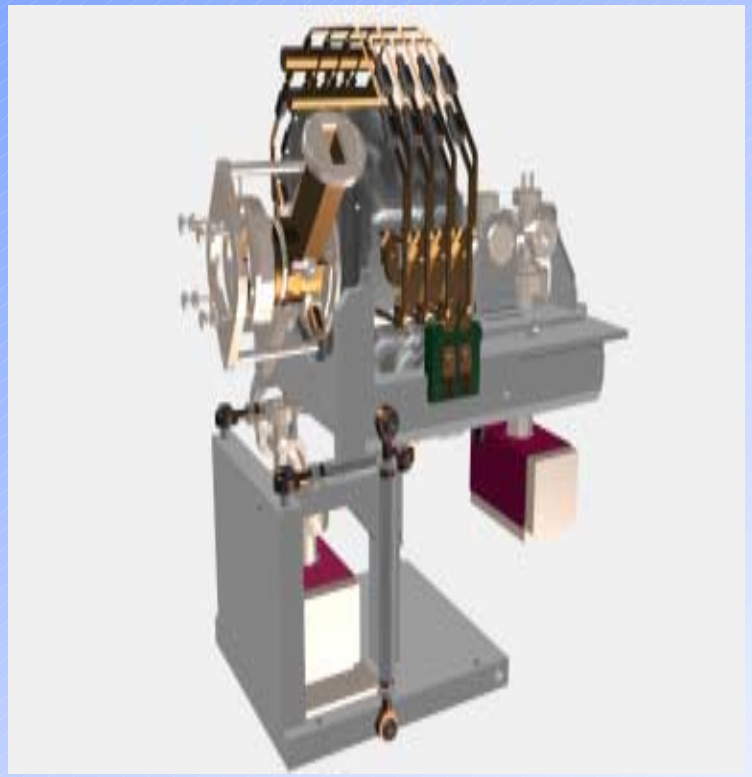

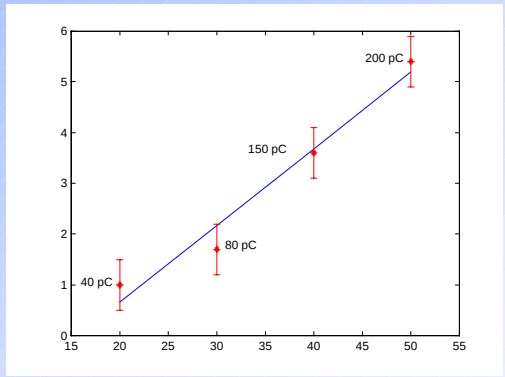

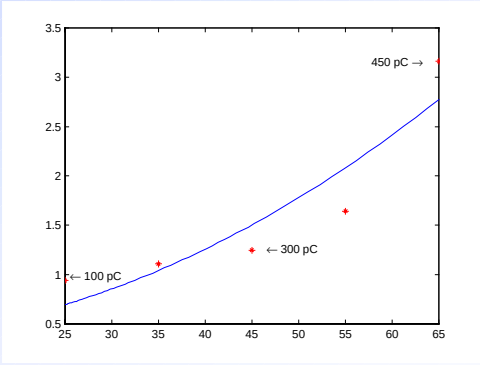

PERL Injector instrumentation – Gun cont.

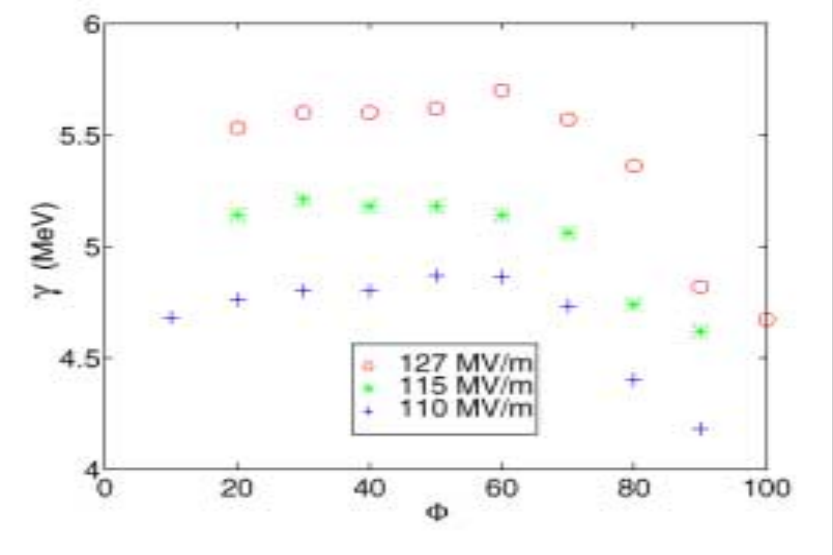

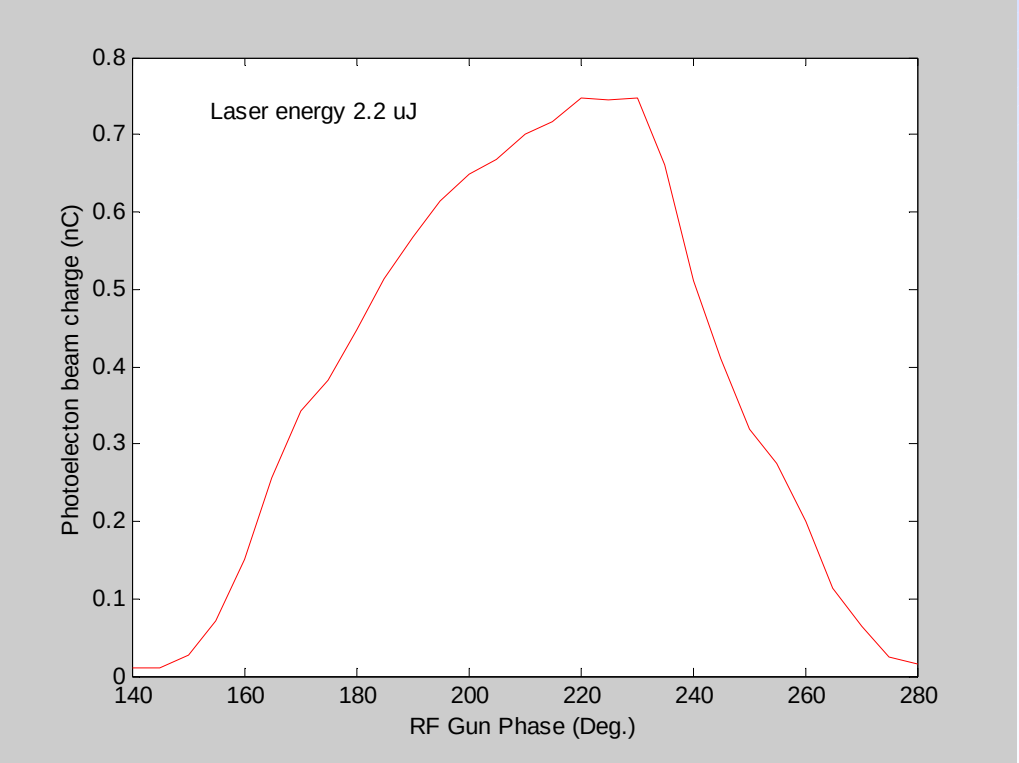

PERL Injector instrumentation – Timing jitter

$$V_{video} = V_{beam} x\ V_{local} \sin \varphi$$

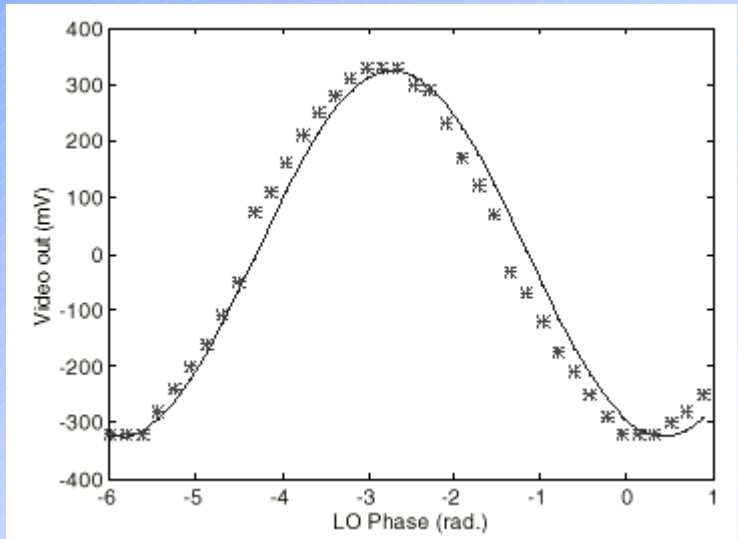

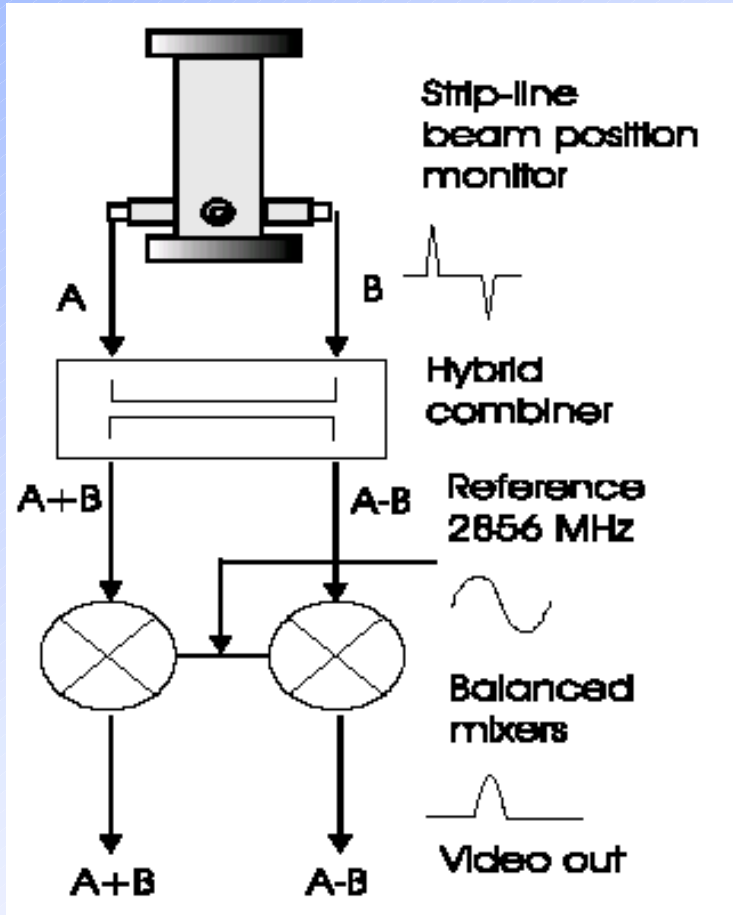

PERL Injector instrumentation – Boost Linac

Energy.

Positions before and after the linac.

Beam position inside the linac.

Beam profile after linac.

$$f = \frac{b \bullet g}{b + g}$$

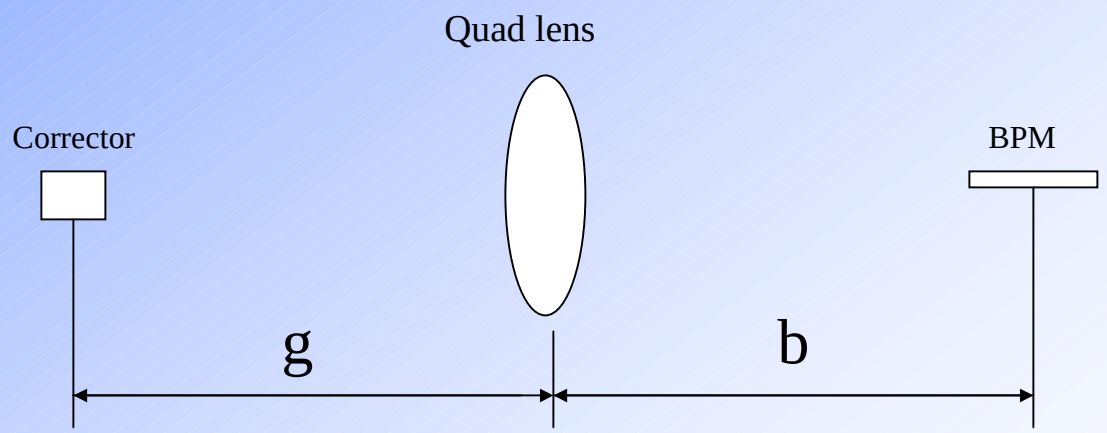

PERL Injector instrumentation – 25 MeV

Transverse emittance – pepper port, Q-scan, multi-monitors.

Bunch length, Energy spread – pick up cavity

Beam jitter – BPM for position and timing jitter

$$x'' + k\ (s)x - \frac{2r_e N/\ell}{a^2\gamma^3}x = 0$$

$$z' = \frac{\delta}{\gamma^2}$$

$$\delta' = \frac{3r_0 N}{\gamma^3\beta^2{\ell_b}^3}\ f(a,b)z$$

$$\Delta x = \sqrt{2}\frac{x}{a}[1-(3\frac{\sigma_x-\sigma_y}{a^2}+\frac{x^2-3y^2}{a^2})]$$

$$\Delta y = \sqrt{2}\frac{y}{a}[1-(3\frac{\sigma_y-\sigma_x}{a^2}+\frac{y^2-3x^2}{a^2})]$$

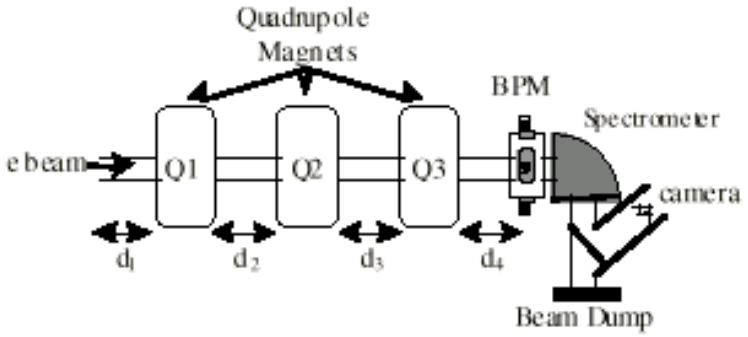

RF Pick up Cavity

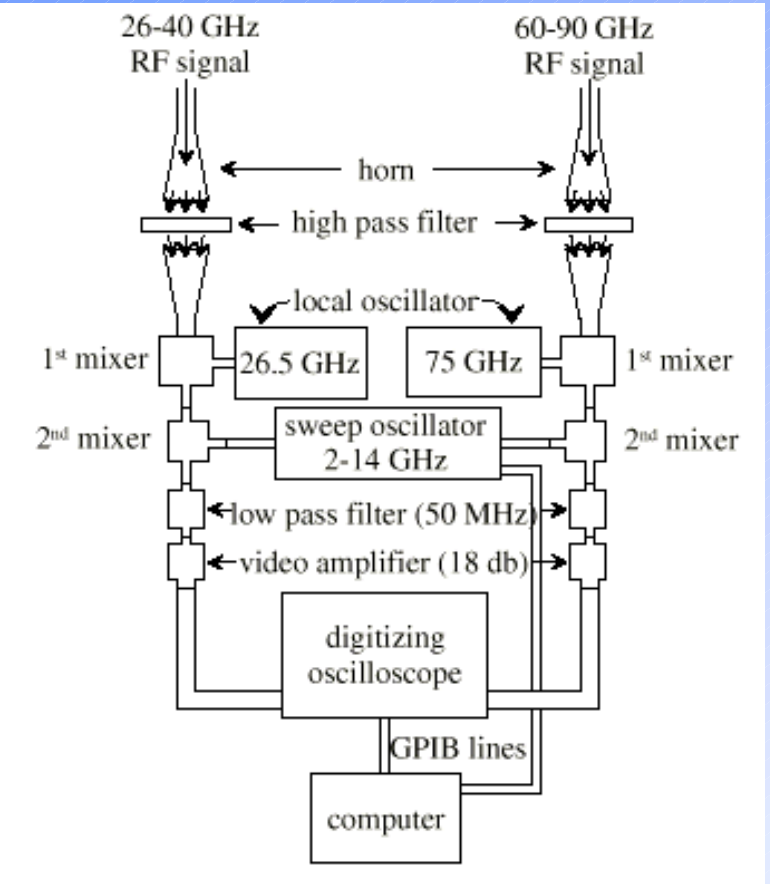

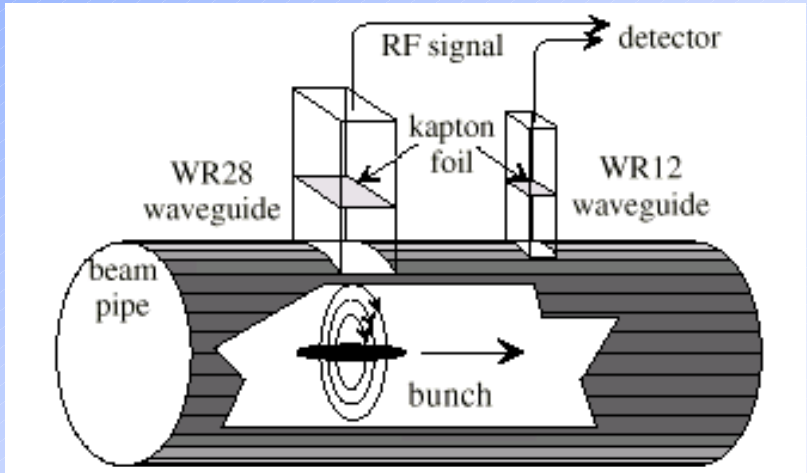

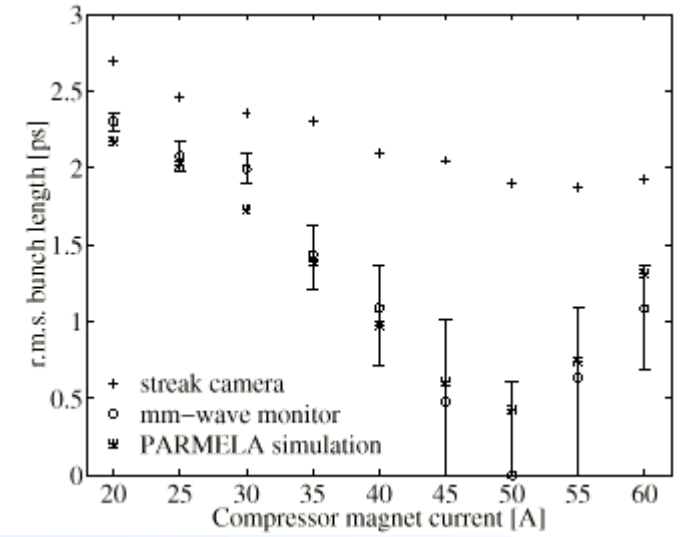

RF Transverse Kicker Cavity

- *Single shot.*
- *Time domain, and detail structure, large dynamic range due to the absence of space charge effects.*
- *Self calibration.*
- *Time Jitter measurements.*
- *Synchronized with beam.*
- *Slice emittance measurement*
- *Longitudinal phase space measurement combined with spectrometer*
- *Cost competitive if you already have RF source.*

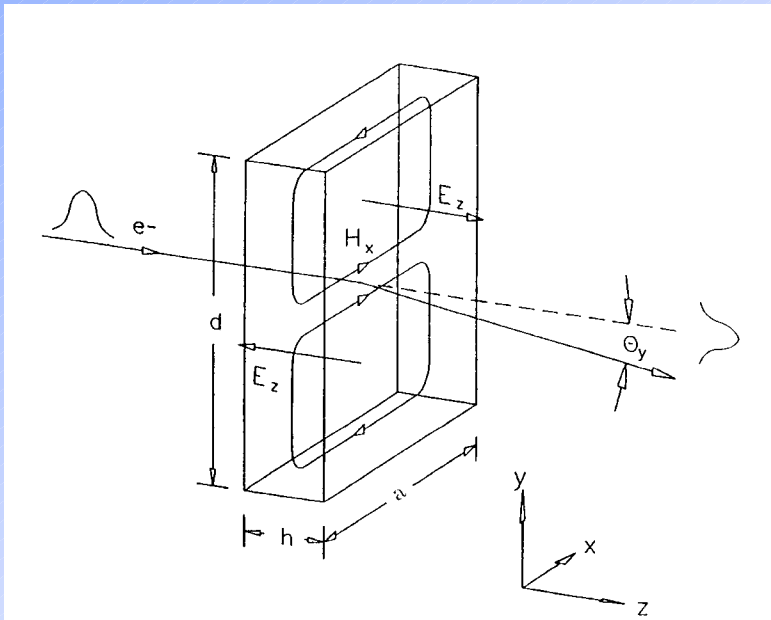

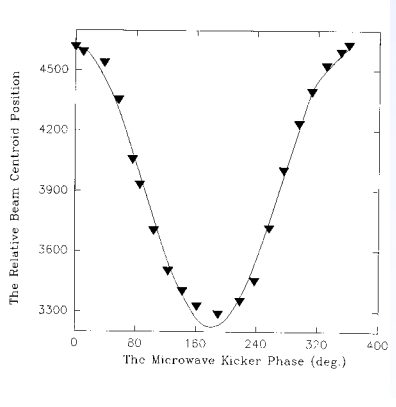

X.J. Wang, X-ray FEL and Linear collider applications, PAC99.

Transverse RF Cavity for Bunch Length and Slice-Emittance Measurements (J. Frisch, X.-J. Wang, ...)

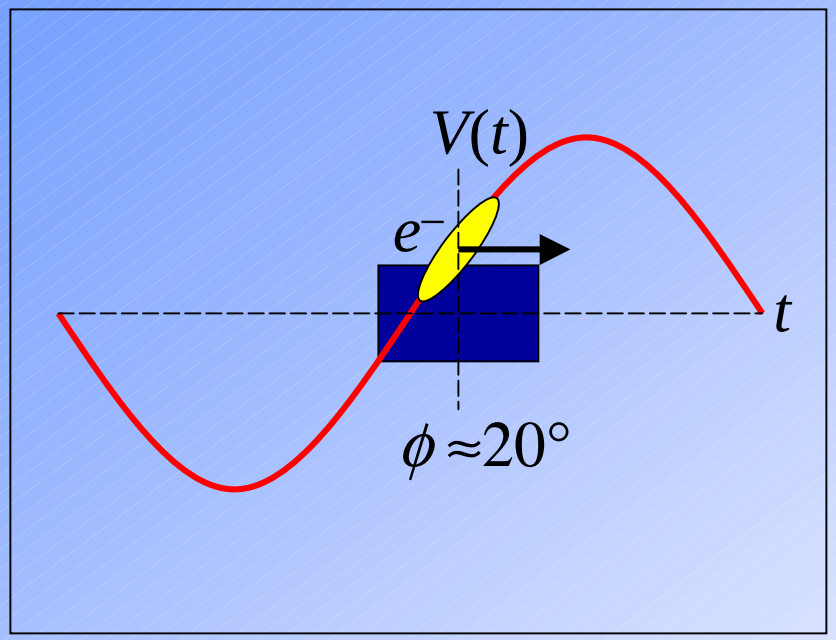

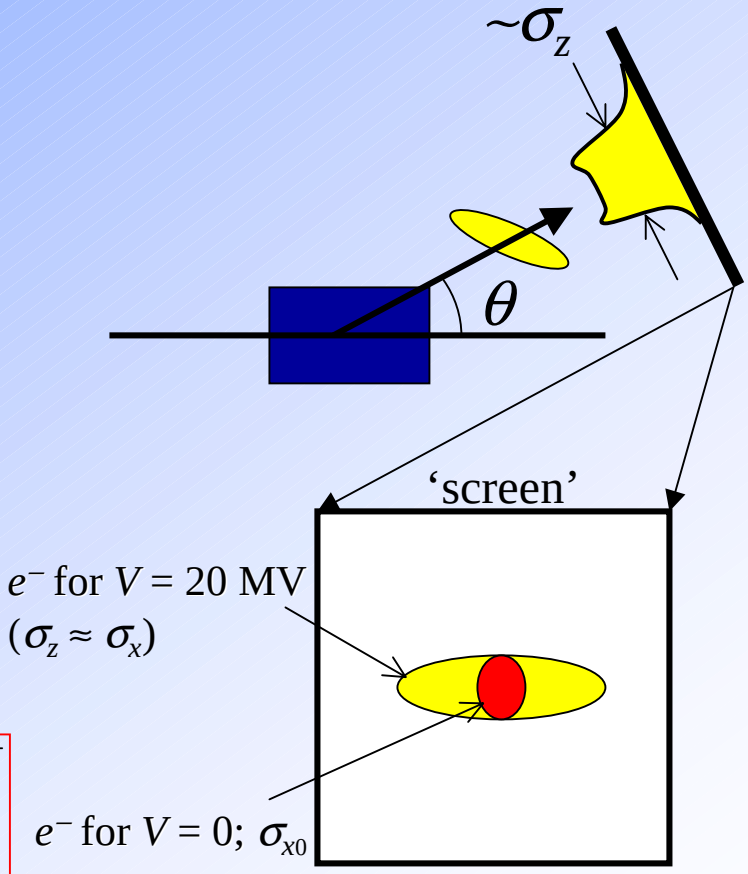

$$\sigma_z \approx \frac{\lambda E}{2\pi e V_0 \cos\varphi \sqrt{\beta_0 \beta_1} \sin\Delta\psi} \sqrt{\sigma_x^2 - \sigma_{x0}^2}$$

$V \approx 20$ MV at $\varphi \approx 20°$

RF kicker cavity for PERL Injector

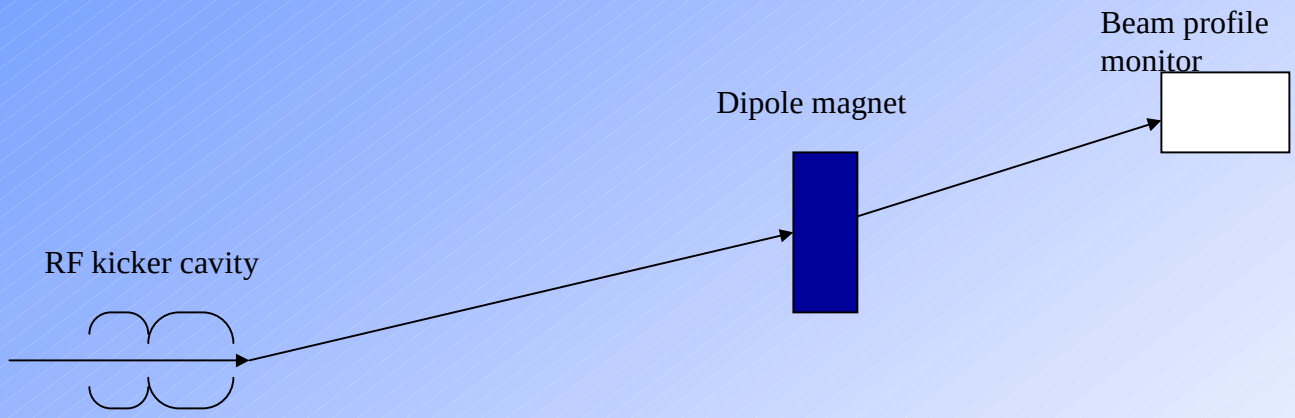

Both energy spread and bunch length.

Optical transition radiation

Semi-non-interceptive diagnostics.

Beam Profile

Energy

Emittance

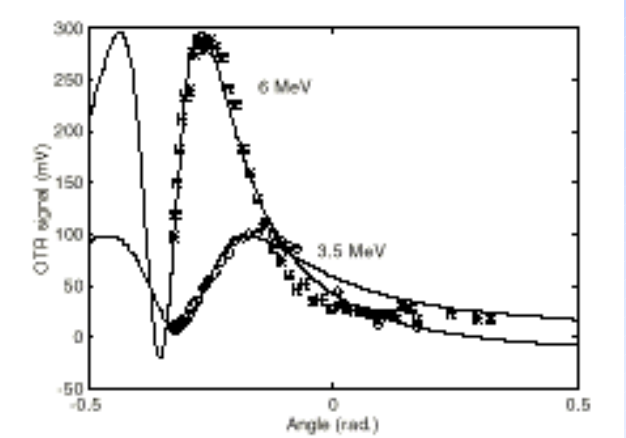

$$\frac{d^2 I_\perp}{d\omega\, d\Omega} = \frac{e^2}{\pi^2 c} \frac{\theta^2}{(\gamma^{-2} + \theta^2)^2}$$

Diamond

E-beam

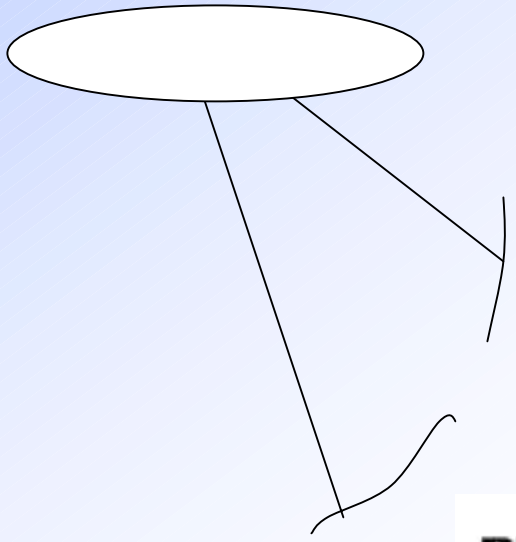

Summary

Beam instrumentation is the key for performance and stability and reliability. It must be addressed at early stage of R&D. Many issues are not addressed here, here is a personnel biased experience.

PERL Injector Workshop Laser and Cathode Working Group Summary

Marcus Babzien,
Brookhaven Accelerator Test Facility
NSLS, BNL
Upton, NY 11973

Introduction

In order to meet the general charge of developing the optimal electron source for a high average current, low emittance gun, the laser and photocathode must be considered together. The requirements set forth in these proceedings for a user facility specify beam stability and temporal shape, but it is the cathode material that determines the wavelength and power required from the drive laser. These fundamental quantities are the strongest determiners in choosing a laser system for PERL. For this reason, the laser and cathode are considered as one system by the working group. Therefore, design considerations of either the laser or the cathode will have direct consequences on the other.

Cathode Materials

The first task in developing a high average current electron source suitable for use in a DC or RF gun is to identify the various cathode materials and corresponding properties. These proceedings contain several talks on candidate materials, and a table of the most relevant parameters is shown below. This table provides a starting point from which to choose a cathode and make decisions on the laser systems that may illuminate them. To meet the goals of the meeting, it is necessary to make assumptions based on the experience of the participants, therefore the numbers shown in Figure 1 represent a best guess as to the state-of the-art performance of the different cathodes. Materials at much different levels of development are considered on an equal basis as far as basic parameters are concerned. Further conclusions taking into account the maturity of the different materials are presented at the end of this summary. The materials are broadly grouped into the Tellurides, Antimonides, Cesiated Gallium Arsenide, and a variety of lower quantum efficiency materials including Magnesium, Lanthanum Hexaboride, bonded, or other dispenser cathodes. Next, the required range of wavelengths at which the cathodes operate is given as a usable range, followed by lasers which can provide photons in this range, either directly or via harmonic generation. Typically, the variation in performance over these ranges is considered to be of secondary importance, although some of the wavelength dependence in emittance and quantum efficiency can be useful for optimizing performance. Next, the basic phenomena other than vacuum quality that affect the lifetime of the material are listed, but these are not very material specific. Other issues which deserve consideration are then listed for each material. These were issues that may limit the applicability of a cathode for PERL, but for which no good answers were known. Resolving some of these issues may require research and development. Next, the lifetime as demonstrated at initial fabrication and also more typical operating conditions are listed. Then, considering the wavelength and the PERL 200 mA current requirement, a the laser power for given quantum efficiency is given as a power*QE product. This demonstrates the basic advantage of the longer wavelength materials, especially GaAs. Expressed this way, an assumption in achievable quantum efficiency directly gives the amount of laser power required at the listed wavelength.

Some basic conclusions at this point are clear. The lowest quantum efficiency materials clearly involve a much larger effort to meet the PERL requirements than the other classes. This illustrates the tradeoff between cathode and laser, since the R&D effort required to produce a conventional, multi-100W UV laser system, which is beyond the current state-of-the-art, would be comparable to the effort required to incorporate either a parasitic or dedicated FEL amplifier to drive the photocathode. Such a conceptual design was presented at this workshop by A. Zholents. In addition, problems of laser heating, plasma formation, and cathode degradation may prove difficult to overcome for low quantum efficiency cathodes. As such, they should only be considered if other options fail.

Type	**Cs_2Te CsKTe**	**Cs_3Sb K_2CsSb**	**GaAs**	**Metal Bonded LaB6 Dispenser**
Usable Photon Wavelength	260-300	350-600	780	UV
Laser Sources	Nd * 4 Ti:Al_2O_3 * 3 Argon * 2	Nd * 3 Ti:Al_2O_3 * 2 Argon	Ti:Al_2O_3 Diode * 2 Nd * 2 Argon	Seeded FEL
Lifetime Limiting Phenomena	All:	Chemical preparation	Ion bombardment	Preparation technique
Outstanding Questions	Usable in DC gun? (large thermal emittance) Code available?	Coating?	Ion Bombardment Limit?	Laser heat removal?
Best QE, Lifetime	24% @ prep 2%, 1 year @ 10^{-8}	14%, hours @ 10^{-10}	13-15%, 1-1.2*10^5 C/cm^2 @ <10^{-11}	0.3%, months @ 10^{-10}
Power*QE product	90 W·%	45 W·%	30 W·%	90 W·%

The best overall performance at this time is from GaAs, since it has high quantum efficiency, and operates at the longer fundamental wavelengths generated from common lasers. The applicability of this material to an RF gun is in question, primarily because of the high vacuum requirement. In addition, the ion bombardment mechanism that currently limits GaAs lifetime may work differently in an RF gun than DC gun. Therefore, GaAs is best used in a DC gun at gradients around 10 MV/m. In order to extend lifetime further, the vacuum level should be improved approximately one order of magnitude. If this is possible, then a quantum efficiency of 10% should be sustainable for the several hour lifetime required in PERL.

The second material that was considered a candidate for PERL is K_2CsSb. It has demonstrated very high quantum efficiency under operating conditions, although with short lifetimes. The major reason that the lifetime was not considered a major flaw was that very little effort has been focused on producing longer lifetime cathodes. The type of improvements reported for CsTe by D. Nguyen at this workshop may be achievable with K_2CsSb, however, this involves R&D into cathode preparation. Currently, the quantum efficiency that would be achieved in a PERL photoinjector is estimated to be 1%, and this was the design number used in the following sections.

Laser Designs

When developing rough configurations for the drive laser, a target power level is chosen for a cathode based on the quantum efficiency that is likely to be achieved after 24 hours of continuos operation. This means that the injector can be taken out of operation daily to switch either to a fresh cathode in the same injector, or a duplicate injector with a fresh cathode already in place. The final choice will depend on the speed with which a particular cathode can be replaced, the expense of injector duplication, and the impact of daily beam interruption on user experiments. It was assumed that this is the minimum acceptable operating cycle for PERL, but may be too short for some users. This also requires that the laser power compensate for changes in quantum efficiency over the 24 hour operating cycle. Under such assumptions, the laser requirements for the two candidate materials above are 3W at 780nm for GaAs, and 45 W @ 350 nm for K_2CsSb. A further assumption was that temporal shaping should be used to produce a laser pulse with 3 ps rise and fall times, separated by a 10 ps flat period, as shown below:

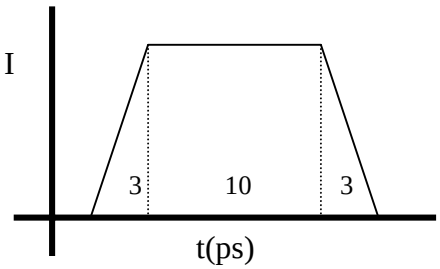

Also implicit in the following discussion is that any laser system will require feedback in intensity, phase and profile in order to meet the long term requirements for PERL. These feedback loops are not shown schematically, and would be expected to correct the long term drift as well as high frequency noise up to their bandwidth limit. The only parameter for which the feedback was deemed a possible weakness was in phase jitter. Although laser oscillators have demonstrated the required 200 fs rms value, no existing system has operated continuously and reliably at that level. Therefore it is considered to be at the limit of what can be achieved. For this reason, this requirement should be studied to determine if it presents a true limit for operation, or if slight degradation in laser performance is tolerable for some fraction of the time. Furthermore, some feedback systems may rely on instrumentation in the accelerator because sufficient sensitivity is not available from laser diagnostics located upstream of the photocathode.

Feedback is a necessary but not sufficient condition for satisfying the PERL stability requirements. The laser must be designed from the outset for highest possible stability. This includes environmental control for the laser room and all system components, power supplies and electronics. System performance should also rely as much as possible on physical mechanisms that maintain or enhance stability, such as gain or harmonic generation saturation. It is unlikely that a commercial vendor will have the experience necessary to design such a system. Although these considerations are as important as the choice of laser gain medium, they are assumed to be a critical part of the drive laser and will not be covered further.

GaAs Cathode

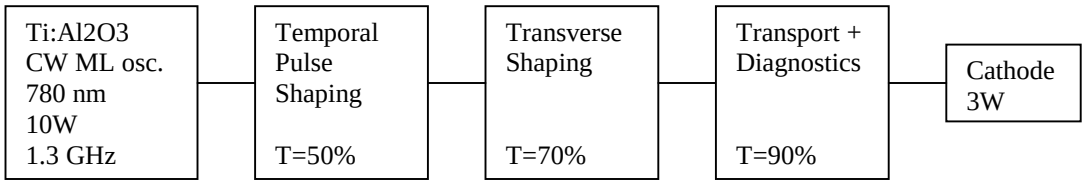

The first suggestion for a laser is to use a high power Ti:Al_2O_3 oscillator directly. A 5W oscillator was reported at the workshop, and GHz repetition rates have been demonstrated, but not simultaneously. It should therefore be a modest extension of existing technology to achieve 10W CW modelocked in a single unit. The short pulses could then be converted to quasi-flattops either by Fourier-plane phase modulation, or direct time-to-space shaping, both of which have been demonstrated to have sufficient control. Some loss is encountered in either scheme, which we estimate as 50%. A further consideration arises not from the drive laser, but the delayed emission from GaAs that would limit the falling edge of the electron bunch to at least a 10 ps fall time. Following the temporal shaping, a spatial flattop is generated either by random phase masks, aspheric optics, and/or active mirrors. This stage may have transmission up to 70% if properly designed. Finally, it is assumed that delivery to the cathode will include losses simply due to extended distances or the harsh environment around a photoinjector, as well as multiple splitting for laser diagnostics. This loss is estimated as 10%.

One concern with this simple arrangement is the lack of control over the pulse format because no high power electro-optic modulator exists with sufficient bandwidth to operate at 1.3 GHz. This means that the beam current ramp-up required for PERL starting conditions must be accomplished exclusively by changing the laser energy per pulse, not the duty cycle. If this is not acceptable, it would necessitate a more complex scheme using lower power, integrated-optic, Mach-Zender interferometers followed by post-amplification. Also, the PERL requirement for ion-clearing by blanking approximately 100 ns of the pulse train every 2 us will be difficult with a simple oscillator configuration. It may be possible to develop a high repetition rate Pockels cell for this function, but no participants were aware of demonstrated devices with this capability.

A second laser option for 780 nm was identified based on fiber oscillators already demonstrated.

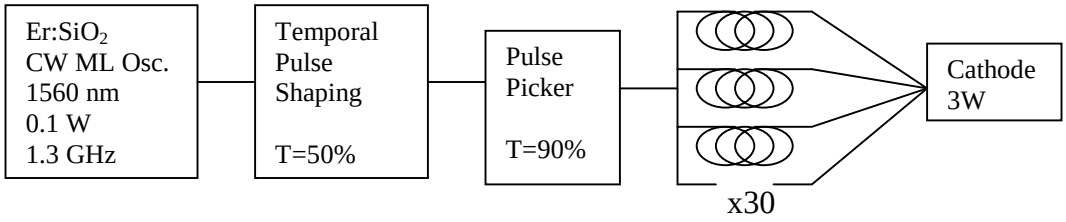

Such erbium-doped fiber oscillators are common in telecommunications applications, and are typically characterized by extreme phase and power stability. GHz repetition rates are achievable, with up to 100mW unamplified power. The temporal pulse shaping could be accomplished with the same techniques as above, and material bandwidth is sufficient for sub-picosecond shaping. There is some concern that shaping may be more complicated because of the non-gaussian gain spectrum when compared with $Ti:Al_2O_3$, and this may necessitate spectral filtering and reduced gain. Following temporal shaping, a GHz bandwidth pulse picker can be used to generate arbitrary trains to satisfy the PERL ramp-up and ion-clearing requirements. An assumption was made that high power fiber amplifiers may not be available, although greater than 10W has been demonstrated is research lasers. A conservative estimate of 200 mW per fiber would require over 30 individual amplifiers, assuming 50% conversion efficiency from 1560 to 780 nm. This conversion efficiency is routine using periodically poled lithium niobate. In this laser system, the total output of all the amplifiers could be angle-multiplexed onto the cathode. The beam profile achievable with such a configuration may be non-uniform, or depending on the geometry of the electron, may have too large a divergence angle to project to the cathode.

Another fiber-based scheme would start with a similar erbium oscillator, with the output Raman-shifted to 1.06 um. Such a system has been demonstrated with up to 1W, and higher powers are not limited by the fiber amplifier. Hence extrapolating to several watts should not be difficult. This would allow a single, diffraction limited output beam to be used for transport to the cathode.

K_2CsSb Cathode

The most attractive system for achieving the higher average power in this case may be the Raman-shifted fiber source, as it can be coupled to bulk amplifiers capable of multi-100 W output near 1060 nm. Frequency conversion would likely be the critical factor in deliverable power as efficiency may be limited by a combination of average and peak power crystal damage. At 1.3 GHz and 15 ps, the peak power enhancement would be a factor of 50, and very little data is available on damage thresholds in this regime. If it is possible to reach saturated conversion, third harmonic generation of 45W should be achievable. Reduced intensity and conversion efficiency could be overcome with higher amplification. Another option is be to use the second harmonic instead of the third. Although the quantum efficiency is about 30% higher at 350 nm compared with 530 nm, this may be offset by a higher doubling efficiency. Only by testing the different

nonlinear crystals involved, and the damage thresholds for the PERL pulse format, will data become available for selecting the best scheme.

Conclusions:

Because of the relatively small amount of effort that has gone into developing improved lifetime in K_2CsSb, the high quantum efficiency, and visible operating wavelength, this is a very promising candidate for further study. Techniques for extending lifetime are improving operating vacuum in the gun, and using cathode protective coatings. As demonstrated at Los Alamos, large improvements in cathode robustness are possible with a modest research and development effort. Therefore, cathode development appears to be the most fruitful area for further research. Should there be little or no improvement in lifetime, a greater effort could be placed into laser development to reach the necessary power. Finally, within the limitations noted above, the existing performance of GaAs indicates that it may already be a usable photocathode in a DC gun, and represents a fallback option.

Photocathode and DC Gun Summary

Charlie Sinclair
Jefferson Laboratory
12000 Jefferson Avenue, Newport News, VA 23606
Tel: 757-269-7679
E-mail: sinclair@jlab.org

Before discussing DC guns, it is necessary to provide some overview of the cathodes which would be used in these guns (or in RF guns for that matter). The first point is to recognize that only high quantum efficiency photocathodes can be considered to meet the PERL parameters. For any linear photoemitter, the following relation is true.

$$i(mA) = \frac{\lambda(nm)}{124} \bullet P_{laser}(W) \bullet Q.E.(\%)$$

There are three families of practical high quantum efficiency photocathodes – the alkali antimonides, the alkali tellurides, and the III-V semiconductors. The first two of these familes have positive electron affinity, while the III-V semiconductor cathodes are negative electron affinity. The importance of this distinction will become apparent later. One can make a simple summary of these three families, giving the typical operating wavelength, and the product of laser power and quantum efficiency necessary to reach the required 200 mA specification for PERL. This table makes it very clear that the lasers necessary are very demanding even for a 1% Q.E. photocathode. Photocathodes with Q.E.'s lower than about 1% are very unlikely suitable for application in a high average current PERL photoinjector.

Cathode Type	Operating Wavelength (nm)	P_{laser} x Q.E. (W - %)
NEA GaAs	780	31.8
K_2CsSb	532	46.6
KCsSb	266	93.2

It should be noted that the all of the above lasers are assumed to have an appropriate RF time structure (e.g. 1300 MHz), and that the P x QE numbers assume that every electron and every photon is useful. Thus, for example, if a Gaussian laser beam is truncated transversely to more closely approximate a "tophat" profile, or if some electrons are removed early in the injector, a higher P x QE product will be required.

One can inquire about the thermal emittance produced by each of the above cathode families. For our purposes, we write the normalized, rms emittance as:

$$\varepsilon_{n,rms} = \frac{r}{2}\sqrt{\frac{E_{thermal}}{mc^2}}$$

Thus, for example, if a cathode emits electrons from a Maxwell-Boltzmann distribution characterized by a temperature T, the thermal energy in the above expression is simply kT. The above expression is known to give a good description of the emittance from a thermionic cathode.

In the case of GaAs photocathodes, the absorption coefficient for light at ~ 780 nm is about 1.4/μ. This leads to a half absorption depth of about 500 nm. Electrons photoexcited into the conduction band of GaAs are very largely thermalized at the bottom of the conduction band by the time they diffuse to the surface of the cathode. Since GaAs is a negative electron affinity cathode, electrons at the bottom of the conduction band may energetically escape the cathode. Thus, the GaAs photocathode should produce an emittance characterized by a thermal energy close to the cathode temperature – i.e. room temperature in most cases. That this is indeed the case has been demonstrated by Bruce Dunham in his Ph.D. thesis, published in the proceedings of the 1995 PAC, p. 1030. Dunham measured that an emittance containing ~ 95% of the beam from a GaAs phtocathode was characterized by a thermal energy of about 35 meV (n.b. room temperature is 25 meV). Dunham's measurements were conducted with a tophat transverse laser profile at the cathode. His measurements were made for a number of spot sizes and illuminating wavelengths. It is worth mentioning that the negative electron affinity GaAs photocathode is being evaluated for e-beam lithography applications. In this application, the highest beam brightness is very important. A recent paper (Mankos et al., JVST B18, 3010 (2000)) reports an effective temperature of 0.05 +/- 0.02 eV, in agreement with Dunham's values. Also, measurements made on the injector for the CEBAF accelerator are in agreement with Dunham's values. In this latter case, the laser has an RF time structure (~ 45 psec duration pulses at 499 MHz repetition rate) and a Gaussian transverse profile.

Similar quality measurements of the emittance produced from alkali antimonide and alkali telluride photocathodes have not been made (to the best of this writer's knowledge). However, since these cathodes have positive electron affinity, it is not energetically possible for electrons thermalized at the bottom of the conduction band to escape. Thus photoemission from these materials is from a non-thermal electron

population. The optical absorption in these cathodes is much higher than in the case of GaAs – a typical absorption coefficient is about 30/μ. Thus, the half absorption depth is about 23 nm. One would expect that the photoemitted electrons would have a spectrum of energies ranging from about zero up to the energy difference between the exciting photon and the work function. Few measurements of this quantity have been reported, but there are numbers in the literature ranging between 200 and 600 meV for alkali antimonide cathodes. Alkali telluride cathodes have a smaller electron affinity than alkali antimonides, and thus might be expected to have a somewhat smaller effective thermal energy. At the workshop, numbers like 200 to 300 meV were mentioned.

For PERL applications, the emittance which matters is the geometric emittance at the insertion devices. This can be translated back to the emittance provided by the injector, which in turn is composed of two parts – the thermal emittance from the cathode and the space charge related emittance growth which occurs between the cathode and the beam energy where the electron bunches are sufficiently rigid that further emittance growth is negligible (assuming that effects like wakefields, coherent synchrotron radiation, etc. are limited or controlled). Once one has an injector design and understands the magnitude of the emittance growth, the maximum thermal emittance from the cathode can be specified. This number is directly related to the electric field that must be present at the cathode.

To hold space charge related emittance growth to tolerable levels, one can remove only a fraction of the charge stored at the cathode surface due to the cathode electric field. Thus, given a thermal emittance that cannot be exceeded, one knows the maximum cathode radius which can be illuminated. This, in turn, establishes the cathode field that must be present. The GaAs cathode, having the lowest value for the effective thermal energy, will allow the largest illuminated diameter, and thus may be operated at the lowest cathode fields. The positive electron affinity cathodes, having a higher effective thermal energy, will require a smaller illuminated spot, and thus a higher cathode field, to achieve the same thermal emittance.

At Jefferson Lab, we operate DC photoemission guns with GaAs cathodes for both the CEBAF accelerator, and the FEL. The CEBAF electron source operates at 100 kV with a maximum average current of about 200 μA, while the FEL operates at 320-350 kV with a maximum average current of 5 mA. Although the FEL gun has been processed to ~ 550 kV, it is operated at lower voltage due to field emission problems. This field emission is due to the fact that the cathode is prepared in situ in the gun. Cathode preparation involves the use of cesium, which lowers the work function of the cathode electrode structure. A gun re-design is underway which will eliminate this problem. An upgrade to the FEL is under development, and will involve

operation at 10 mA average current. We are confident that by eliminating the introduction of cesium into the gun structure, we will be able to operate this gun at its design value of 500 kV.

The operational lifetime of the GaAs cathodes used in the two guns above is limited only by ion back bombardment. These ions are produced in the cathode-anode gap by the beam, and accelerated back to the cathode, where they cause reduction in the QE by a variety of phenomena. Given that ion back bombardment is the lifetime limiting phenomenon, it makes far more sense to express the cathode life in terms of the number of coulombs delivered per unit illuminated area, rather than clock hours. Indeed, the 1/e lifetime of a GaAs cathode simply sitting in the static vacuum of one of the nuclear physics guns was measured to exceed 2.3 years. In service, the best 1/e operating lifetimes we have yet obtained are between 1 and 1.2 x 10^5 coulombs/cm^2. It should be noted that the ion back bombardment problem will be quite different, and probably much less severe, in an RF gun.

We have demonstrated that with a heat treatment and reactivation, we can fully recover the initial quantum efficiency of an ion-damaged GaAs cathode. How many times this operation can be successfully performed is not well known at present, but it is large. We have achieved further extensions of the practical cathode operational lifetime by illuminating a number of small area spots on a much larger area cathode. In the DC gun case, moving the laser beam spot on the cathode requires only a simple resteering of the electron beam, which is done by a fast, automatic routine on the CEBAF injector. This technique may not be so easy to employ in an RF gun, where one wants to operate with beam on the electromagnetic axis of the cavity.

In contrast to the GaAs cathode, which is formed by adding a single cesium – oxygen or cesium – fluorine monolayer to the GaAs surface, the alkali antimonide and alkali telluride cathodes are stochiometric chemical compounds. It is not unreasonable to assume that they might quite differently under ion back bombardment. Furthermore, since the light is absorbed in such a short depth in these cathodes, most of the damage done by ions is likely to be deeper in the cathode material than the region from which the photoemitted electrons originate. Indeed, Nguyen from Los Alamos reported an extrapolated lifetime of 8 x 10^6 coulombs/cm^2 – almost two orders of magnitude higher than the best numbers reported for GaAs.

It is possible to make high quantum efficiency cathodes from all three families. At the wavelengths indicated in the table above, quantum efficiencies between 10 and 20% have been reported for all cathode types. However, only the GaAs cathode has been used in DC guns, while the antimonide and telluride cathodes have been used in RF guns. These cathodes are prepared in chambers external to the RF gun structure, and then inserted into the RF gun with an in-vacuum transfer mechanism. While

these cathodes have good lifetimes in the static vacuum of the preparation chambers, they all lose quantum efficiency fairly rapidly on insertion into an RF gun. These cathodes appear to stabilize at quantum efficiencies between ½ and 2%, at which point they operate stably for extended periods of time. By contrast, the GaAs cathodes reported on are actually formed in situ in the gun, and their dark lifetime in the gun is excellent.

The difference in QE stability is no doubt largely due to the vacuum conditions in the gun. This is one area where a DC gun has an advantage. One has great freedom in choosing the vacuum wall material, the wall location, and the location of ports in a DC gun. In a RF gun, one has a limited choice of wall material, a wall geometry restricted by the realities of a resonant cavity, and great restrictions on the location and size of ports. Thus, it will likely always be true that it is much easier to establish an excellent vacuum in a DC gun, as opposed to a RF gun.

The limiting phenomenon in the cathode field strength and operating voltage of a DC gun is field emission. Field emitted electrons may collect on the ceramic insulator which holds off the primary gun voltage. Unless this charge is drained away, punch-through of the ceramic may occur. Even if the ceramic is protected from this problem, field emitted electrons striking metallic walls release gases through electron stimulated desorption. Such gases are harmful to the cathode lifetime, either through chemical poisoning of the cathode, or by providing a source of ions.

Recent developments have resolved both of these issues. First, an LBL/Jefferson Lab group has developed a metal ion implantation process which produces a high resistivity sheet resistance on the vacuum surface of large ceramic insulators (ref. F. Liu et al., PAC '97, p. 3752). Ceramics treated this way have been very successfully used in the Jefferson Lab FEL gun. More recently, a Jefferson Lab group has shown that plasma-source nitrogen ion implantation of large area metallic electrodes dramatically reduces the field emission up to quite high fields. Field emission as low as 0.5 pA/cm^2 has been observed at DC fields above 25 MV/m (ref. C. Sinclair et al, abstract submitted to PAC '01). With the benefits gained from these two separate ion implantation processes, it now appears to be within reach to build DC electron guns operating reliably with cathode fields above 20 MV/m.

A note regarding the drive laser for a GaAs gun is worth making. To produce the necessary RF time structure on the laser beam, some form of mode-locking is employed. In most mode-locking schemes, the optical cavity round-trip time must be equal to the desired RF period. At 1300 MHz, the resulting cavity length is impractical, leading to designs which use a lower mode-locked frequency followed by complicated schemes to produce the desired 1300 MHz pulse train. There are real issues of long term stability with such systems. Recently, a Ti:sapphire laser mode-

locked by gain modulation has been developed at Jefferson Lab (ref. Hovater and Poelker, NIM A 418, 280 (1998)). The fundamental frequency of this laser is typically about 225 MHz, but it is easy to obtain stable mode-locking at multiples fo the fundamental frequency up to several GHz (2.5 GHz has been demonstrated). The output power is independent of the RF frequency, and is quite high. A 2.5 W version of this laser has been demonstrated at Jefferson Lab, and we believe that this technique can be scaled to about 10W without significant problems. We also note that high average power amplification of a high frequency optical pulse train has been demonstrated at the 5.77 W level (Z. Liu et al., Appl. Phys. Lett. 76, 3182 (2000)). It appears that a ~ 10 W average power laser at 780 nm and 1300 MHz should be well within reach.

Another issue that should receive attention is that of energy deposition in the cathode material. For example, suppose we have a 2% QE Cs_2Te cathode illuminated at 266 nm. 46.6 W of laser power are required to deliver 200 mA average current. If we require a thermal emittance of 0.5 micron, and assume that we have a transverse "tophat" profile beam, the allowable illuminated radius is 1.43 mm. The absorption of Cs_2Te is about 30/μ, so that half the incident light is absorbed in a depth of only 23 nm. The power deposited in the cathode in this case is over 150 MW/cm^3. While it is clear that such a cathode would have to be formed on a thermally conductive substrate, this is a very prodigious power density, raising questions about the durability of the cathode.

In summary, we can say at the outset that the selection of the cathode type will have a very direct bearing on the design of the rest of the system. If a DC gun is chosen, there is at least a good opportunity to create a very excellent vacuum. In an RF gun, creating such a vacuum is more problematic, but it is not yet clear that much attention has been focussed in this issue. The primary problem with DC guns is field emission from the electrode structures. Recent developments in ion implantation have shown considerable promise in creating a highly resistive inner surface on the ceramic insulators, preventing charging from field emitted electrons, and on dramatically reducing the field emission from the electrode structures. It appears that DC electron guns operating with cathode fields in the 20 MV/m range may be developed in the near future. Such guns would be highly competitive with RF guns.

The GaAs cathode offers the prospect of very low thermal emittance, since the electrons originate from a thermal population at close to room temperature. At some stage in the development of very bright electron sources, the thermal emittance must be considered along with the emittance growth associated with space charge and other effects. Lasers with 1300 MHz RF structure and adequate power to provide 200 mA average current from a GaAs cathode are only a moderate extrapolation of

what has already been demonstrated. A GaAs cathode, operated in a state-of-the-art DC electron gun is surely a contender as a high brightness, high average current electron source for PERL type applications.

Conclusions of the 433 MHz / B-Factory Cavity Based RF Gun Working Group

D.H. Dowell, Chair
Working Group Members: R. Rimmer (LBNL), P. Piot (DESY), W. Gai (ANL), J-P. Carneiro (FNAL), I. Ben-Zvi (BNL), X.Y. Chang (BNL), H. Edwards (FNAL) J. Rose (BNL).
Since the 433 MHz working group had combined discussions with the 1300 MHz group, this summary includes comments related to the 1300 MHz photoinjector.

Executive Summary:

The 433 MHz photocathode gun technology is the most advanced of the three approaches discussed in this workshop. Essentially all the PERL photocathode gun performance requirements of high average current operation and beam quality are met either experimentally or by simulation. In addition, the overall architecture of the photoinjector up to injection into the SRF (approximately 25 MeV) is well-established. Therefore this approach has the lowest technical risk of the three photoinjectors being considered for PERL.

The 433 MHz gun working group, and the workshop participants in general, conclude the single disadvantage of the 433 MHz photoinjector is the high microbunch charge needed to generate 200 mA of average current. The charge is three times that of the 1300 MHz gun. Combined with the PERL specification for short, sub-ps microbunches, this high charge will strongly radiate in the high-energy bends, leading to significant degradation of the beam quality. However, it should be noted that the 1300 MHz photocathode gun has been operated only to 1% duty factor vs. 25% operation for the 433 MHz gun. In addition, the closely spaced microbunches (769 ps) of the 1300 MHz pulse train may experience more severe transverse wakes than the more widely separated (2.3 ns) 433 MHz pulse train. These and other issues require further study before deciding which frequency is best for PERL.

A concise list of the working group's recommendations follows:

1. Third-harmonic linearizer is required for either frequency.
2. Develop the high-QE K_2SbCs photocathode. Incorporate concepts presented in workshop for increasing cathode lifetime.
3. Further investigation of all wakes (CSR and resistive wall) is essential to decide between 433 and 1300 MHz approaches. It is preferable that the wakes be realistically included in the beam transport simulations.
4. Realistic simulation of entire 1300 MHz-based system. Include the much lower beam energy out of the cathode cell in the calculation. What can be used for the CW booster and 3.9 GHz linearizer accelerator sections? The single pass beam current is probably too high for a SRF booster.
5. Model energy recovery dynamics. Investigate RF-beam instabilities.
6. Review overall PERL architecture. Compare co-propagation vs. anti-propagation in energy recovery linacs to control beams with large energy differences.

Photoinjector Architecture

The photoinjector layout from the gun to injection into the SRF was show by D. Dowell. It consists of the RF gun, a 433 MHz booster, a 1300 MHz linearizer and a chicane compressor. Experimental results demonstrating improved compression with the third harmonic linearizer were shown.

In an earlier session, P. Piot discussed how the linearizer eliminates CSR-induced beam breakup, and pointed out that DESY is interested in collaborations to develop a 3.9 GHz. SRF linearizer cavity.

RF Design

R. Rimmer presented details of the 476 MHz B-factory cavities and how they could be adapted to 433 MHz for the gun and booster sections. These cavities have already demonstrated CW operation at the required beam currents, and present little technical risk.

D. Dowell presented details of the Boeing 433 MHz RF gun and APLE (Average Power Laser Experiment) booster cavities. The RF gun has successfully run at 25% duty factor, but will require some modification for CW operation. The CW APLE cavities are copper-plated aluminum and are available in 3-cell and 5-cell configurations.

A single Tesla SRF cavity can be used for the linearizer.

Photocathode

The photocathode choice has major implications for the drive laser. A high-power, UV drive laser, as required for Te_2Cs, is considered to be technically risky. GaAs is attractive from the drive laser's point of view, but requires the best vacuum of all the cathodes and has poor temporal response. Therefore the group decided that K_2SbCs is the only option for PERL.

Consider the following situation for PERL. The K_2SbCs cathode lifetime decays exponentially. Assume an initial QE_i of 12% (14% has been demonstrated) and that the drive laser power is sufficient to produce the required charge at a 1% final QE_f. Then the lifetime (LT) needed to operate T_{op} hours is given by,

$$LT = \frac{T_{op}}{\left(\ln \frac{QE_i}{QE_f} \right)} .$$

Therefore 24 hours of operation requires a lifetime of 9.6 hours. Lifetimes of 2.3 hours were demonstrated in the 1992 25% duty factor tests at Boeing. Therefore current technology is only a factor of five below PERL requirements, ignoring any improvements in the gun vacuum.

Techniques for greatly improving the lifetime were presented. These include coating with a thin protective layer of CsBr (presented by D. Nguyen, LANL in an earlier session) and operating the cathode at an elevated temperature to keep it clean. Experiments give a lifetime in excess of 20 hours for a cathode at 120 degrees C. in a poor vacuum, and therefore could easily meet the PERL specification. An automated, multi-cathode system incorporating these ideas should be considered.

To produce 0.5 nC of microbunch with a 1% QE cathode means the drive laser produces approximately 0.1 microjoule per microbunch at a repetition rate of 433 MHz or 43 watts CW at 527 nm. This should be possible. The drive laser developed by LANL for the 1992 Boeing 25% duty factor test operated with 0.47 microjoule per microbunch at 27 MHz. The 8.3 millisecond macropulse power was 12.7 watts, the average power was 3.2 watts.

Recommendations

The third harmonic linearizer is required at any photoinjector RF frequency. Detailed simulations of CSR and resistive wall wakes, both transverse and longitudinal, are needed since this will be a major factor in choosing between 433 and 1300 MHz guns. More effort is needed on the 1300 MHz injector to answer questions concerning the availability of a CW booster and a 3.9 GHz linearizer. The single-pass beam current maybe too high for a SRF booster.

The K_2SbCs cathode technology should be developed to allow the use of a visible wavelength drive laser. This effort should start soon since the cathode choice places major design requirements upon both the drive laser and the RF gun vacuum. In the longer term, an automated, multi-cathode should be developed.

In conclusion, the 433 MHz photoinjector is the most developed of the three injectors discussed in this workshop. Its sole disadvantage is the 200 mA average current requires the high-charge microbunches, which strongly radiate in the beam transport system when compressed to sub-ps bunches.

Summary of L-band Working Group

Wei Gai
ANL
Building 360,HEP
9700 South Cass Avenue
Argonne, IL 60439-4800

We have examined the L-band option for PERL in this working group. Some comparisons were made with 433 Mhz option. There were 4 talks given for preliminary design studies. The summary is given below.

The starting design point is the ANL 1 ½ cell L-band gun. With modified parameters, 1 ½ TM02 mode operation and 2 ½ cell options were also examined [X.Y. Chang]. From the beam dynamic point view, L-band would provide higher brightness beam at lower charge per pulse which is crucial for beam transport in bends (Coherent Synchrotron Radiation wakefield reduction). CSR can be very severe in beam transport, particularly beam pulse length compression using a chicane as experimentally verified by Ph. Piot. They observed beam energy bifurcation due to CSR at 130 MeV. It is believed that the six phase space parameters can be obtained using different L-band options as discussed above.

During the discussion, Bob Rimmer presented their work on the heat load at LBL. He suggests that 100 W/cm^2 is a limit for current operation. However, he also considered a few times of that maybe achievable. Another import result obtained through the discussions, is whether the L-band will be much worse than the 433 MHz structure. Bob Rimmer and Ilan Ben-zvi came to a conclusion that heat generation density in L-band is comparable to that of the 433 MHz using a scaling law.

We have also discussed the liquid nitrogen cooling option for the PERL gun. However, because there is no any experimental data available to date, we have to speculate how to cool the acceleration structure. Two options were discussed: 1) Single phase liquid cooling and 2) Two phases (liquid and gas) cooling. Advantages using liquid nitrogen as coolant are identified: 1) lower the RF power consumption; 2) increased heat conduction; 3) improved vacuum condition (no water residues) would improve cathode life time; and 4) sustain higher gradient in the gun than at normal temperature. Due to the attractive of liquid nitrogen option, we recommend some engineering research should be started right way.

Different RF photocathodes were considered, the conclusion is that we already have technologies may be not two far from the PERL requirements. Cathode lifetime and QE can be overcome by using hot standby spares. It was recommended by the working group that a lab should be setup to study the QE issues such as lifetime and vacuum conditions.

L-band RF power supply for 1 – 2 MW CW source is already available at Toshiba. We believe this is adequate for the PERL gun and booster applications.

One concern was raised and discussed but we were unable to get any answer is beam break up in the gun and booster. The average current in the PERL is 20 times higher than TESLA operation, therefore a serious beam break up problem may arise.

Workshop on Photo-injector for Energy Recovery Linac
January 22 & 23, 2001

Attendee List

Charlie Sinclair
Jefferson Laboratory
12000 Jefferson Avenue, Newport News, VA 23606
Tel: 757-269-7679
E-mail: sinclair@jlab.org

Manoel Conde
Argonne National Laboratory
9700 S. Cass Ave. Bldg. 362
Tel: 630-252-6099
E-mail: conde@anl.gov

Alexander Zholents
Lawrence Berkeley National Laboratory
1 Cyclotron Road, MS 71-259, Berkeley, CA 94720
Tel: (510)486-7533
E-mail: AAZholents@lbl.gov

Max Cornacchia
SLAC
2575 Sand Hill Rd, Menlo Park, CA 94025
Tel: (650) 926 3906
E-mail: cornacchia@ssrl.slac.stanford.edu

Marty Woodle
BNL
P.O. Box 5000, Bldg. 725C
Upton, NY 11973-5000
Tel: (631) 344-2521
E-mail: woodle1@bnl.gov

Thomas Tsang
BNL
P.O. Box 5000, Bldg. 535B
Upton, NY 11973-5000
Tel: (631) 344-2225
E-mail: Tsang@bnl.gov

Kwang-Je Kim
APS, ANL
9700 South Cass Ave, Buiding 401/C4265
Argonne, IL 60439
Tel:630 252 4647
E-mail:kwangje@aps.anl.gov

James Murphy
BNL
P.O. Box 5000, Bldg. 725C
Tel: (631) 344-5160
E-mail:jbm@bnl.gov

Feng Zhou
UCLA/BNL
B820M, BNL
Tel: 631-344-2042
E-mail:zhouf@sun2.bnl.gov

John Lewellen
Advanced Photon Source, ANL
9700 S. Cass Ave, 401/B2207
Argonne, IL 60439
Tel: 630-252-5252
E-mail:lewellen@aps.anl.gov

Philippe-Regis Piot
Deusches Elektronen Synchrotron DESY-Hamburg
MPY Group,
85, Notkestrasse
D-22603 HAMBURG, DEUTSCHELAND
Tel: +49-40-8998-2756
E-mail: philippe.piot@desy.de

Ivan Bazarov
CORNELL UNIV.
CHESS Wilson Lab, Cornell Univ., Ithaca, NY 15853
Tel: (607) 255-0678
E-mail: ib38@cornell.edu

Katsuyuki Kobayashi
Sumitomo Heavy Industries
c/o Aculight Corporation, 11805 North Creek Parkway
South, Bothell WA 98011
Tel: 425-482-1100, ext. 162
E-mail: kobayashi@aculight.com

Ilan Ben-Zvi
BNL
P.O. Box 5000, Bldg. 725C
Upton NY 11973-5000
Tel: (631) 344-5143
E-mail: ilan@bnl.gov

David Dowell
Boeing Physical Sciences Research Center
3116 NW 95th Street, Seattle, WA 98117
Tel: (206)782-6374 (home), (206)544-5409 (work)
E-mail: dowell@eskimo.com

Dinh Nguyen
Los Alamos National Laboratory
MS H851
Tel: 505-667-9385
E-mail: dcnguyen@lanl.gov

Marcus Babzien
BNL/ATF
P.O. Box 5000, Building 820M
Upton, NY 11973-5000
Tel: 631 344-5238
E-mail: babzien@bnl.gov

James Clendenin
SLAC
2575 Sand Hill Road, Menlo Park, CA 94025
Tel: 650/926-2962
E-mail: clen@slac.stanford.edu

Brian Sheehy
BNL
P.O. Box 5000,Bldg 725D
Upton, NY 11973-5000
Tel: x5491
E-mail: sheehy@bnl.gov

Michael Cole
Advanced Energy Systems Inc
27 Industrial Blvd., Suite E, Medford, NY 11763
Tel: (631) 345-6264, ext. 3004
E-mail: (631) 345-0458

Sal Pjerov
BNL
P.O. Box 5000, Bldg.725C
Tel: (631) 344-7080
E-mail:pjerov@bnl.gov

Vitaly Yakimenko
BNL
P.O. Box 5000, Bldg.725C
Upton, NY 11973-5000
Tel: (631)344 7830
E-mail: Yakimenko@bnl.gov

Donald Feldman
University Of Maryland
Institute for Plasma Research Bldg 223
College Park, MD 20742
Tel: 301-405-8484
E-mail: dfeldman@glue.umd.edu

Robert Rimmer
LBNL
MS 71-259
Berkeley CA 94720
Tel: 510 486 6243
E-mail: RARimmer@lbl.gov

John Galayda
ANL
Building 401
9700 South Cass Avenue
Argonne, IL 60439-4800
Tel:(630)252-7796
E-mail:deputy@aps.anl.gov

Timur Shaftan
BNL
P.O. Box 5000, Bldg.725C,
Upton, NY 11973-5000
Tel:(631)344 5144
E-mail:shaftan@bnl.gov

Wei Gai
ANL
Building 360,HEP
9700 South Cass Avenue
Argonne, IL 60439-4800
Tel: (630)252-6560
E-mail: wg@hep.anl.gov

Sam Krinsky
Brookhaven National Lab
P.O. Box 5000, Building 725B
Upton, NY 11973-5000
Tel: (631) 344-4740
E-mail: krinky@bnl.gov

Helen Edward
FNAL
E-mail: hedwards@fnal.gov

William S. Graves
BNL
P.O. Box 5000, Building 725D
Upton, NY 11973-5000
Tel: (631) 344-5353
E-mail: wsgraves@bnl.gov

David Robin
Lawrence Berkeley National Laboratory
1 Cyclotron Road, MS 80-101
Tel: 510 486 6028
E-mail: dsrobin@lbl.gov

Xiangyun Chang
IHEP, China
Mail Address: P.O. Box 752, Upton, NY 11973
Tel: (631)344-4730
E-mail:address:xychang@bnl.gov

Jean-Paul Carneiro
FNAL
E-mail: carneiro@waldo.fnal.gov

James Rose
BNL
P.O. Box 5000, Building 725C
Upton, NY 11973-5000
Tel: (631) 344-7079
E-mail: rose@bnl.gov

Frank Stephan
Deusches Elektronen Synchrotron DESY-Zeuthen
Photo injector test facility
Platanenallee 6,
D-15738 Zeuthen, DEUTSCHELAND
Tel: +49-33-762-77-338
E-mail: fstephan@mail.desy.de

Triveni Srinivasan-Rao
BNL
P.O. Box 5000, Bldg. 535B
Upton, NY 11973-5000
Tel: (631) 344-5072
E-mail: triveni@bnl.gov

Steve Milton
ANL,APS
Building 401
Argonne National Laboratory
9700 South Cass Avenue
Argonne, IL 60439-4800
Tel:(630) 252-9091
E-mail: milton@aps.anl.gov

Sandra Biedron
ANL, APS
Building 401
9700 South Cass Avenue
Argonne, IL 60439-4800
Tel:(630) 252-5703
E-mail: biedron@aps.anl.gov

Xijie Wang
BNL
P.O. Box 5000, Bldg. 725C
Upton, NY 11973-5000
Tel: (631) 344-5791
E-mail: xwang@bnl.gov

L.H. Yu
BNL
P.O. Box 5000, Bldg. 725C
Upton, NY 11973-5000
Tel: (631) 344-5012
E-mail: lhyu@bnl.gov

Aaron Tremaine
UCLA
Department of Physics and Astronomy
University of California, Los Angels
Los Angels, CA 90024
E-mail: tremaine@stout.physics.ucla.edu

Alex Murokh
UCLA
Department of Physics and Astronomy
University of California, Los Angels
Los Angels, CA 90024
E-mail: alex@stout.physics.ucla.edu

Juhao Wu,
Stony Brook/BNL
P.O. Box 5000, Bldg. 725C
Upton, NY 11973-5000
Tel: (631) 344-5072
E-mail: jhwu@bnl.gov

John Smedley
Stony Brook/BNL
P.O. Box 5000, Bldg. 535B
Upton, NY 11973-5000
Tel: (631) 344-7865
E-mail: Smedley@bnl.gov

Osgood, Jr Richard M
BNL
P.O. Box 5000, Bldg. 460
Upton, NY 11973-5000
Tel: (631) 344-3927
E-mail:osgood@bnl.gov

Takahashi, Hiroshi
BNL
P.O. Box 5000, Bldg. 475B
Upton, NY 11973-5000
Tel: (631) 344-4099
E-mail: takahash@bnl.gov

George Rakowsky
BNL
P.O. Box 5000, Bldg. 725D
Upton, NY 11973-5000
Tel: (631) 344-5298
E-mail: rakowsk1@bnl.gov